UNIVERSIDADE FEDERAL DE SANTA MARIA
CENTRO DE CIÊNCIAS DA SAÚDE
PROGRAMA DE PÓS-GRADUAÇÃO EM CIÊNCIAS FARMACÊUTICAS

Luana Mota Ferreira

SISTEMAS DE BASE NANOTECNOLÓGICA CONTENDO DISSELENETO DE DIFENILA PARA O TRATAMENTO DO MELANOMA E DO GLIOMA

Santa Maria, RS, Brasil, 2018

Luana Mota Ferreira

SISTEMAS DE BASE NANOTECNOLÓGICA CONTENDO DISSELENETO DE DIFENILA PARA O TRATAMENTO DO MELANOMA E DO GLIOMA

Tese de Doutorado apresentada ao Programa de Pós-Graduação em Ciências Farmacêuticas, Área de Concentração em Desenvolvimento e Avaliação de Produtos Farmacêuticos, da Universidade Federal de Santa Maria (UFSM, RS), como requisito para obtenção do grau de **Doutor em Ciências Farmacêuticas**.

Orientadora: Profª. Drª. Letícia Cruz

Coorientadora: Profª. Drª. Cristina Wayne Nogueira

Santa Maria, RS, Brasil, 2018

Ferreira, Luana Mota
SISTEMAS DE BASE NANOTECNOLÓGICA CONTENDO DISSELENETO DE DIFENILA PARA O TRATAMENTO DO MELANOMA E DO GLIOMA / Luana Mota Ferreira.- 2018.
197 p.; 30 cm

Orientadora: Letícia Cruz
Coorientadora: Cristina Wayne Nogueira
Tese (doutorado) - Universidade Federal de Santa Maria, Centro de Ciências da Saúde, Programa de Pós Graduação em Ciências Farmacêuticas, RS, 2018

1. Disseleneto de Difenila 2. Câncer 3. Nanocápsulas Poliméricas 4. Hidrogéis I. Cruz, Letícia II. Wayne Nogueira, Cristina III. Título.

Sistema de geração automática de ficha catalográfica da UFSM. Dados fornecidos pelo autor(a). Sob supervisão da Direção da Divisão de Processos Técnicos da Biblioteca Central. Bibliotecária responsável Paula Schoenfeldt Patta CRB 10/1728.

Universidade Federal de Santa Maria
Centro de Ciências da Saúde
Programa de Pós-Graduação em Ciências Farmacêuticas

A Comissão Examinadora, abaixo assinada, aprova a Tese de Doutorado

SISTEMAS DE BASE NANOTECNOLÓGICA CONTENDO DISSELENETO DE DIFENILA PARA O TRATAMENTO DO MELANOMA E DO GLIOMA

elaborada por
Luana Mota Ferreira

como requisito para a obtenção do grau de
Doutor em Ciências Farmacêuticas

COMISSÃO EXAMINADORA

Letícia Cruz, Drª.
(Presidente / Orientadora)

Marina Prigol, Drª (UNIPAMPA)

Ethel Antunes Wilhelm, Drª (UFPEL)

Cristiane de Bona da Silva, Drª (UFSM)

Cristiane Franco Codevilla, Drª, (UFSM)

Santa Maria, 31 de agosto de 2018

Dedico esta tese ao meu melhor amigo Marcel Henrique Marcondes Sari, que se tornou um irmão ao longo dos anos, fazendo-se presente nos melhores e piores momentos da minha vida.

"Quando imagino um anjo, logo desenho asas. Mas anjo é amigo, que abraça com gestos e palavras!"

Adriana Araujo Leal

AGRADECIMENTOS

Agradeço primeiramente à Deus e à todas as entidades pela oportunidade de vivenciar essa caminhada e por atender minhas orações, protegendo-me no decorrer de toda a vida até então.

Aos meus pais Mara e Jetúlio, que não estão mais presentes fisicamente, mas tenho certeza de que continuam me protegendo e me guiando pelo melhor caminho. Obrigada pela dedicação que tiverem comigo ao longo de suas vidas e por todos os momentos felizes que vivemos juntos. A saudade que sinto é imensurável, porém tenho certeza de que vocês estão sempre olhando por mim. Aos meus irmãos, Júlia e Deiverson, pelo amor incondicional e por me fazerem querer ser uma pessoa melhor a cada dia. Não menos importante, agradeço a minha madrasta Giovana pelo companheirismo, carinho, dedicação e amizade ao longo de todos os anos. Amo vocês!

Á minha família, tios, tias, primos e primas pelo companheirismo e por entender minha ausência em muitos momentos. Faço um agradecimento especial à tia Liliana, pelo apoio incondicional desde a infância até agora. Obrigada pelos momentos de desabafo e pelos conselhos.

Faço um agradecimento muito especial aos meus amigos Tatiana, Aline (Pixu), Joana, Tuane, Camila, Jamile, Juliana, Matheus, Francine e Mayara. Agradeço especialmente ao Marcel, à quem dedico esta tese, por tudo que fizestes por mim. Minha gratidão não cabe em palavras. À vocês meus amigos, família que tive a oportunidade de escolher, o meu muito obrigada! Pelo apoio e carinho incondicional, por estarem comigo durante toda essa caminhada, me lembrando sempre que eu tenho muitos motivos para levantar a cabeça e seguir em frente. Vocês são a minha base agora, e me incentivam a superar cada obstáculo e estão sempre ao meu lado, para o que der e vier.

À Profe Letícia, pelo carinho e companheirismo durante esses nove anos de convivência. Eu sou muito grata por tudo que fizestes por mim, principalmente pela paciência em entender os momentos difíceis que passei durante essa caminhada, nunca desistindo de "investir" em mim. Eu admiro muito a pessoa e a profissional que és, sempre atenciosa e dedicada com os alunos, pronta pra enfrentar qualquer desafio. Além disso, tenho muito carinho por ti Profe, e vou te levar no meu coração com uma gratidão enorme por tudo que representas pra mim. Agradeço a oportunidade de ter participado do grupo LabTec e pela confiança de depositastes em mim. Faço um agradecimento também a Profe Scheila Rezende

Schffazik pelos bons momentos vividos no laboratório, pelos ensinamentos e pelos conselhos ao longo desses anos.

Ao grupo LabTec, agradeço pelo convívio, colaboração e momentos de descontração. Foram nove anos de muito aprendizado e crescimento pessoal, onde pude conhecer pessoas especiais que se tornaram amigas e que hoje são essenciais para minha vida. À Verônica, Mailine, Alessandra, Marila, Felipe, Sara, Janaíne e Juliane muito obrigada pelo carinho e apoio durante os anos de laboratório e por hoje estarem do meu lado. Poder contar com vocês é muito importante.

À Professora Cristina Wayne Nogueira, pelo apoio desde o mestrado, pela dedicação do seu tempo para me orientar, por ceder o espaço de seu laboratório para realização dos meus experimentos e principalmente por ter me dado a honra de ter sua co-orientação. Estendo meus agradecimentos aos alunos do LASRAFTO, principalmente ao Vinícius, Bruna e Vanessa, os quais foram essenciais para o desenvolvimento desta tese.

Agradeço a Professora Michele Sagrillo e seus alunos pela ajuda nos experimentos de citotoxicidade realizados na Universidade Franciscana. Também ao professor Denis Rosemberg e seus alunos pela parceria nos experimentos com peixe-zebra. Ao professor Paulo Farago e à sua aluna Jéssica pela colaboração nas análises de caracterização das formulações. Por fim, agradeço a Professora Elizandra Braganhol e suas alunas Juliana e Elita, as quais tiveram um importante papel no desenvolvimento desta tese.

Aos colegas do Hospital da Brigada Militar e do Hospital de Caridade Dr. Astrogildo de Azevedo pela amizade e pelo apoio durante esse período.

Agradeço à Universidade Federal de Santa Maria e ao Programa de Pós-Graduação em Ciências Farmacêuticas pela oportunidade e à CAPES pelo suporte financeiro.

RESUMO

SISTEMAS DE BASE NANOTECNOLÓGICA CONTENDO DISSELENETO DE DIFENILA PARA O TRATAMENTO DO MELANOMA E DO GLIOMA

AUTORA: LUANA MOTA FERREIRA

ORIENTADORA: LETÍCIA CRUZ

COORIENDATORA: CRISTINA WAYNE NOGUEIRA

O câncer é atualmente uma das doenças com maior grau de mortalidade no Brasil e no mundo. As terapias convencionais apresentam na maioria dos casos uma baixa eficácia e elevada toxicidade. Sendo assim, o disseneleto de difenila [$(PhSe)_2$], um composto orgânico de selênio, vem sendo estudado por suas promissoras atividades farmacológicas, incluindo antitumoral. Porém, este composto apresenta elevada lipofilia e efeitos tóxicos, o que dificulta seu uso clínico. Nesse sentido, as nanocápsulas poliméricas tornam-se uma alternativa interessante para contornar as limitações do $(PhSe)_2$. Diante disso, este estudo teve como objetivo desenvolver nanocápsulas poliméricas para a incorporação do $(PhSe)_2$ e avaliar, de forma inédita, a sua atividade antitumoral contra o melanoma e o glioma, dois tipos de câncer de elevada agressividade. As suspensões de nanocápsulas de poli-Ɛ-caprolactona contendo $(PhSe)_2$ (NC $(PhSe)_2$) (5mg/mL) foram preparadas pelo método de deposição interfacial do polímero pré-formado e caracterizadas em relação ao tamanho médio de partícula, índice de polidispersão, potencial zeta, pH, teor do composto, eficiência de encapsulamento (EE), morfologia, estabilidade físico-química durante 30 dias e por análises térmicas (calorimetria diferencial exploratória e termogavimetria), interações entre os constituintes (raio-X e infravermelho) e fotoestabilidade. Foram observadas características compatíveis com sistemas nanoestruturados para liberação de fármacos, elevada estabilidade físico-química sem incompatibilidades entre os componentes e a formulação foi capaz de aumentar a fotoestabilidade do composto. Análises *in vitro* empregando os testes do MTT, iodeto de propidio e níveis de óxido nítrico foram utilizadas para avaliar o potencial citotóxico frente a células de melanoma humano A375 e SK-Mel-103 e células de glioma de rato C6. Além disso, o teste do MTT foi usado para determinar a citotoxicidade em células sanguíneas humanas, queratinócitos e astrócitos. Tanto o composto livre quanto o nanoencapsulado foram capazes de reduzir a viabilidade das células tumorais, sendo que as NC $(PhSe)_2$ tiveram efeito superior nas células SK-Mel-103 e C6. Além disso, foi observado que as suspensões de nanocápsulas causaram aumento nos níveis de óxido nítrico, sugerindo que a modulação desta via possivelmente esteja relacionada com o efeito antitumoral da formulação Em relação à citotoxicidade, as NC $(PhSe)_2$ não causaram toxicidade em nenhuma linhagem de células normais, enquanto que o composto livre foi citotóxico para os queratinócitos. A fim de propor um hidrogel como terapia adjuvante para o tratamento do melanoma, a suspensão de nanocápsula foi espessada com goma xantana. Os hidrogéis foram preparados utilizando pistilo e gral de vidro para espessar a suspensão de NC $(PhSe)_2$ e uma solução do composto livre (5 mg/g) e estas foram caracterizadas em relação ao tamanho médio de partículas, índice de polidispersão, pH, teor do composto, estabilidade físico-química, espalhabilidade, comportamento reológico e perfil de permeação *in vitro*. Ambas as formulações apresentaram características compatíveis com a aplicação tópica e o perfil de permeação cutânea demonstrou que as nanocápsulas favoreceram a permeação do composto até a derme em uma maior quantidade que a formulação contendo o composto livre. A fim de estudar a toxicidade da formulação nanoestruturada, dois protocolos foram conduzidos: o primeiro foi realizado empregando peixe-zebra como modelo animal e o teste do tanque novo para avaliar os efeitos da formulação (0,1 – 2 µM); o segundo protocolo utilizou ratos como modelo animal e análises bioquímicas plasmáticas e teciduais foram realizadas para determinar a toxicidade (5 mg/Kg – 1 mL/kg, durante 15 dias, uma vez ao dia, pela via intragástrica). No primeiro protocolo, as NC $(PhSe)_2$ não provocaram alterações comportamentais ou bioquímicas nos peixes e no segundo protocolo, tanto o composto livre quanto o nanoencapsulado, não causaram nenhuma alteração nos parâmetros bioquímicos avaliados. Por fim, um modelo pré-clínico de glioblastoma foi conduzido para determinar a atividade antitumoral do $(PhSe)_2$ e NC $(PhSe)_2$. Para isso, uma alíquota das células C6 foi injetada no cérebro dos ratos para o desenvolvimento do tumor. Após 5 dias, os animais foram tratados durante 15 dias (1 mg/Kg – 1 mL/kg, uma vez ao dia, pela via intragástrica). Foi observado que o composto, independente de estar na forma livre ou incorporado às nanocápsulas, foi capaz de reduzir o tamanho do tumor. Desta forma, o estudo realizado mostrou que nanocápsulas poliméricas, tanto em suspensão aquosa quanto em hidrogel, apresentam grande potencial como nanocarreadores do $(PhSe)_2$ em sistemas biológicos visando efeito antitumoral.

Palavras-chaves: Selênio; nanopartículas; câncer; hidrogel; toxicidade; permeação cutânea.

ABSTRACT
NANOTECHNOLOGICAL BASED-SYSTEMS CONTAINING DIPHENYL DISELENIDE INTENDING MELANOMA AND GLIOMA TREATMENT

AUTHOR: LUANA MOTA FERREIRA
ADVISOR: LETÍCIA CRUZ
CO-ADVISOR: CRISTINA WAYNE NOGUEIRA

Cancer is one of the diseases with the highest mortality in Brazil and worldwide. In addition, the conventional therapies present low efficacy and high toxicity. In this context, the diphenyl diselenide [$(PhSe)_2$], an organoselenium compound, has been investigated in view of its promising pharmacological properties, including the anti-tumoral effect. However, such molecule has some physicochemical (lipophilic) and toxicological issues, which limit its clinical application. The development of a nanocapsules formulation could be an interesting approach to overcome such restrictions and potentiates its pharmacological effects. Considering the aforementioned context, the current study aimed to develop a $(PhSe)_2$-loaded poly-Ɛ-caprolactone nanocapsules (NC $(PhSe)_2$) (5 mg/mL) formulation as well as to investigate the potential cytotoxicity against melanoma and glioma cell lines, which are both highly aggressive and prevalent cancers. The formulations were prepared by the interfacial deposition of preformed polymer method. A detailed physicochemical characterization was performed using the following parameters: average particle size, polydispersity index (PDI), zeta potential, pH, compound content, encapsulation efficiency, morphology, thermal behavior (thermogravimetric analysis and differential scanning calorimetry), X-ray diffractrometry and fourier-transform infrared spectroscopy. Stability studies were also carried out using a photodegradation assay and monitoring the formulations over a 30-day storage period. The obtained nanocapsules suspension had suitable physicochemical properties as well as adequate compatibility with the constituents and increased the compound stability. Different *in vitro* techniques (MTT assay, propidium iodide uptake and nitric oxide content) were applied to investigate the cytotoxic potential of the NC $(PhSe)_2$ against human melanoma cells lines (A375 and SK-Mel-103), rat glioma cells lines (C6) and healthy cells (human red blood cells and keratinocytes and rat astrocytes). Overall, the results demonstrated that the nanoencapsulation provided selective and superior cytotoxic effect against the tumoral cells in comparison to the free compound, which was also toxic to keratinocytes. The NC $(PhSe)_2$ caused an increase in the nitrite content to both SK-Mel-103 and C6 cells, suggesting that the oxide nitric mediated pathways could be associated with the cytotoxic potential of the formulation. Following, in order to develop an alternative adjuvant therapy to melanoma treatment, a hydrogel formulation was developed. A mortar and pestle were used to prepare the hydrogels by thickening the nanocapsules suspension or a solution of free compound, both at a final $(PhSe)_2$ concentration 5mg/g. Such formulations were characterized concerning average particle size, polydispersity index (PDI), pH, compound content, physicochemical stability, spreadability assessment, rheological behavior and cutaneous permeation profile (human skin). Both formulations had compatible characteristics intending cutaneous application and the nano-based hydrogel provided superior permeation of $(PhSe)_2$ to dermis layer in comparison to the free compound formulation. Regarding the toxicological potential of the nanostructured formulation, two different protocols were carried out to better understand such characteristic. The fist protocol evaluated the nanocapsules formulation effect in a Zebra-fish model by assessing many behavioral parameters; the second one was performed using a repeated administration schedule by the intragastric route in male adult Wistar rats (5 mg/Kg – 1 mL/Kg, once a day, during 15 days) in which theplasma biochemical markers of liver and kidney function as well as the oxidative status of different organs (brain, liver and kidney) were evaluated. The exposure of Zebra-fish to NC $(PhSe)_2$ did not trigger behavioral impairments or oxidative stress-related injuries in the samples of rats that received the repeated treatment. Finally, a preclinical model of glioblastoma multiforme was carried out. Male adult Wistar rats received an injection of C6 cells in the right striatum (1×10^6 cells/3 µL) for tumor developing. Five days after glioma implantation the animals were treated with free compound or NC $(PhSe)_2$ for 15 days (1 mg/Kg- 1 mL/Kg/once a day) by the intragastric route. At the end of the experiment, the groups that received the compound, free or nanoencapsulated, had a reduction in tumor size in comparison to the vehicle-treated groups. Therefore, as a conclusion, the results obtained herein showed the great biological potential of nanocapsule formulations containing $(PhSe)_2$ intending selective anti-tumoral effect.

Keywords: Selenium; nanoparticles; hydrogel; toxicity; cutaneous permeation.

LISTA DE FIGURAS

Introdução

Discussão geral

LISTA DE TABELAS

Introdução

SUMÁRIO

INTRODUÇÃO

1. Introdução

Segundo a Organização Mundial da Saúde (OMS) e o Instituto Nacional do Câncer José Alencar Gomes da Silva (INCA), o câncer é um problema de saúde pública, principalmente em países em desenvolvimento. O câncer é caracterizado como um conjunto de mais de 100 doenças, onde diversos processos complexos estão envolvidos, o que dificulta a eficácia das terapias (INCA, 2017). Nesse sentido, cada vez mais as pesquisas estão voltadas para a descoberta de novas terapias para o câncer, buscando uma maior eficácia e principalmente a redução dos efeitos adversos decorrentes do tratamento. Apesar das diversas campanhas de prevenção, o câncer ainda apresenta altos índices de morbidade e mortalidade no Brasil e no mundo (INCA, 2017; INCA, 2018). Para os anos de 2018-2019, o INCA estimou que 600.000 novos casos de câncer sejam diagnosticados, sendo os tumores de mama e próstata os mais prevalentes (INCA, 2018).

Tumores com elevada malignidade e altas taxas de metástase apresentam poucas chances de cura aos pacientes acometidos pela doença. Entre eles está o melanoma, um tipo de câncer de pele causado principalmente pela exposição excessiva à radiação solar (INCA, 2017; SIEGEL et al., 2018; WANG et al., 2001). O câncer de pele tipo melanoma apresenta baixa prevalência, no entanto, se diagnosticado em fase avançada, com presença de metástase, apresenta o pior prognóstico (INCA, 2017; RIGON et al., 2015; SIEGEL et al., 2018). Também com baixa prevalência e elevado índice de mortalidade podem ser mencionados os tumores do sistema nervoso central (SNC), os quais correspondem a cerca de 3% dos tumores malignos. Os gliomas são os tipos mais frequentes, representando de 40 a 60% dos tumores primários do cérebro, os quais são os mais comuns em pessoas adultas do sexo masculino (INCA, 2018).

Nesse contexto, a busca por terapias mais eficientes e menos agressivas cresce a cada ano. Um estudo publicado pela International Agency for Research on Cancer (IARC) relata que o consumo de selênio, um elemento traço essencial, pode ser uma estratégia para a prevenção do câncer do fígado (IARC 2016). Em humanos, o selênio é importante para regulação do sistema imune e estresse oxidativo, o qual está ligado ao desenvolvimento do câncer (IARC 2016; KHOSO et al., 2018). Os compostos orgânicos de selênio vêm sendo cada vez mais estudados nos últimos anos devido as potencialidades farmacológicas demonstradas tanto por estudos *in vitro*, quanto em modelos pré-clínicos (NOGUEIRA e ROCHA 2011). Entre estes compostos está o disseleneto de difenila [$(PhSe)_2$], o qual é empregado como intermediário em síntese orgânica e apresenta diversas atividades biológicas

relatadas: anti-inflamatória e antinociceptiva (LUCHESE et al., 2012; NOGUEIRA et al., 2003), hepatoprotetora (COSTA et al., 2013), neuroprotetora (BRUNING et al., 2012), antiulcerativa (SAVEGNAGO et al., 2006), entre outras. Além disso, já foi relatado para esse composto a atividade antitumoral, o qual mostrou ação frente a células de neuroblastoma (POSSER et al., 2011), adenocarcinoma de cólon humano (NEDEL et al., 2012) e câncer de mama (BARBOSA et al.,2008). Tal efeito pode ser atribuído à capacidade do $(PhSe)_2$ em modular a expressão de proteínas apoptóticas e pró-apoptóticas, interferindo no crescimento e na morte das céulas tumorais (DIAZ et al.,2018; NEDEL et al., 2012). Adicionalmente, as propriedades anti-inflamatórias e antioxidantes do composto contribuem para o efeito antitumoral, protegento ainda as células saudáveis dos danos ao DNA (MELO et al., 2013).

No entanto, apesar de suas potencialidades terapêuticas, o $(PhSe)_2$ apresenta efeitos tóxicos relacionados a sua dose/concentração. O composto é conhecido por oxidar grupos tióis os quais são essenciais para a atividade da enzima δ-aminolevulinato desidratase (δ-ALA-D) (BARBOSA et al., 1998; MACIEL et al., 2000; ROSA et al., 2007) envolvida na síntese do heme, e os níveis da glutationa reduzida (GSH), defesa antioxidante não-enzimática (ROSA et al., 2005; ROSA et al., 2007). Além disso, o composto é altamente lipofílico (PRIGOL et al., 2013), o que está relacionado a uma baixa biodisponibilidade oral (PRIGOL et al., 2012), por dificuldade de dissolução nos fluidos do trato gastrintestinal. A elevada lipofilia também dificulta a preparação de formulações aquosas para administração intravenosa. Tais limitações retardam a evolução dos estudos com o $(PhSe)_2$ para a etapa clínica e, sendo assim, os sistemas nanoestruturados são uma alternativa promissora para contornar esses problemas e explorar as atividades farmacológicas do composto.

Os investimentos em formulações empregando nanotecnologia vêm crescendo no Brasil e no mundo nos últimos anos (DIMER et al., 2013; FRANK et al., 2015). Os sistemas nanométricos apresentam vantagens frente às formulações convencionais, tais como: (i) tamanho reduzido; (ii) proteção frente à degradação química e enzimática; (iii) controle da liberação; (vi) facilidade de atravessar as barreiras biológicas; (v) melhora na penetração de moléculas na pele; e (vi) liberação sítio-específica (COUVREUR et al., 2002; COUVREUR E VAUTHIER, 2006; FRANK et al., 2015; GUTERRES et al.,2007; MARCATO E DURAN, 2008). Dentre os sistemas nanométricos, as nanocápsulas poliméricas destacam-se pela elevada eficiência em encapsular moléculas altamente lipofílicas. Tal sistema apresenta uma estrutura vesicular formada por um núcleo lipofílico circundado por uma camada de polímero. Estudos têm demonstrado as potencialidades das nanocápsulas para o tratamento de diversos

tipos de câncer (BERNARDI et al., 2013; CARLETTO et al., 2016; FRANK et al., 2015; KRAI et al., 2017; OURIQUE et al., 2010). Devido ao tamanho reduzido e composição, essas partículas são capazes de alcançar tumores sólidos com maior facilidade, modificar o volume de distribuição de fármacos antineoplásicos e reduzir a toxicidade em células saudáveis (BRIGGER et al., 2012; COUVREUR et al., 2006; FRANK et al., 2015).

Além das vantagens citadas, a aplicação tópica dos sistemas nanoestruturados pode servir como uma terapia adjuvante no tratamento do câncer de pele, principalmente no melanoma. No entanto, as suspensões de nanocápsulas são obtidas na forma líquida, o que dificulta a retenção no local de aplicação. Desta forma, a conversão das suspensões nanoestruturadas em formas semissólidas tem sido relatada como uma alternativa adequada para contornar este tipo de limitação. Tais formulações apresentam a propriedade de modular a permeação/retenção/liberação das moléculas ativas na pele. Esse efeito é atribuído ao tamanho reduzido das partículas, o que acarreta em uma elevada área superficial, facilitando o íntimo contato das nanoestruturas com o estrato córneo, sulcos e folículos pilosos (GUTERRES et al.,2007; ROBERTS et al.,2017).

Diante do exposto, esta tese de doutorado foi delineada no sentido de desenvolver suspensões de nanocápsulas contendo $(PhSe)_2$ e estudar, de forma inédita, o potencial deste composto para o tratamento do melanoma e do glioma. Visando a aplicação cutânea das nanocápsulas de $(PhSe)_2$ como forma adjuvante na terapia do melanoma, um hidrogel de goma xantana foi desenvolvido a partir das suspensões e a permeação do composto livre e nanoencapsulado foi avaliada em pele humana. Além disso, técnicas *in vitro* foram empregadas para demonstrar o efeito citotóxico das suspensões frente a diferentes linhagens de células de melanoma. A atividade antiglioma das suspensões de nanocàpsulas contento $(PhSe)_2$ foi avaliada com testes *in vitro* e também através de um modelo pré-clinico de glioblastoma empregando roedores. Além do efeito farmacológico, uma série de testes de toxicidade foram realizado a fim de demonstrar a segurança da aplicação das formulações desenvolvida. Na sequência, alguns assuntos serão abordados de maneira mais aprofundada, a fim de dar um embasamento teórico para esta tese.

1.1 Câncer: aspectos gerais

A palavra câncer origina-se do grego *karkínos*, que significa carangueijo (Figura 1), e foi utilizado pela primeira vez por Hipócrates, na era antes de Cristo. O câncer, em geral, é

definido como a proliferação desordenada de células, que invadem tecidos e órgãos. As células normais do organismo humano crescem, multiplicam-se e morrem de uma maneira ordenada e contínua. Por outro lado, as células cancerosas continuam crescendo em vez de morrerem no processo normal, formando outras novas células anormais que invadem tecidos e órgãos adjacentes (INCA, 2017; INCA, 2018; PEREZ-HERRERO E FERNANDEZ-MEDARDE, 2015).

Figura 1. Representação do símbolo do câncer

Fonte: http://cancer-informese.blogspot.com/

Esse crescimento celular pode ser controlado ou não (Figura 2); no primeiro caso, há um aumento localizado e autolimitado do número de células normais, podendo ser devido a estímulos fisiológicos ou patológicos, sendo na maioria das vezes benignos e reversíveis (hiperplasia, displasia e metaplasia). Já no crescimento não controlado, as células formam uma massa anormal de tecido, com desenvolvimento autônomo e persistente, sendo conhecidas como as neoplasias (câncer in situ e câncer invasivo), também denominadas na prática de tumores (INCA, 2017; INCA, 2018; NCI 2018; PEREZ-HERRERO E FERNANDEZ-MEDARDE, 2015).

Figura 2. Ilustração do crescimento celular desordenado

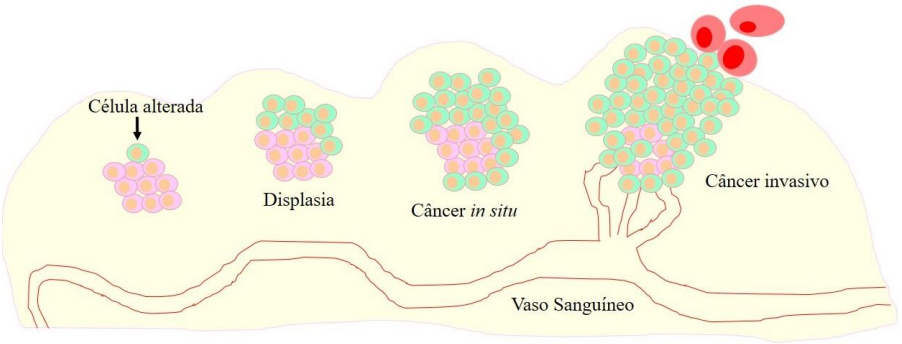

Fonte: adaptado de ABC do Câncer, 2017.

As causas do câncer são variadas, podendo envolver fatores externos e/ou internos ao organismo (Figura 3). As causas externas estão relacionadas aos hábitos e ao meio ambiente, enquanto que as causas internas estão ligadas a fatores genéticos e à capacidade do organismo em se defender de fatores externos (INCA, 2017; INCA, 2018; NCI 2018). Segundo o INCA, de 80 a 90% dos cânceres são causados por fatores externos, por exemplo, o cigarro é um fator determinante na formação de câncer de pulmão; exposição excessiva ao sol pode levar a tumores de pele; e alguns vírus podem levar ao aparecimento de leucemia (INCA, 2017; INCA, 2018). O processo de formação do câncer é denominado de carcinogênese ou oncogênese, o qual é composto por três estágios: I) Iniciação, II) Promoção e III) Progressão. Nesse processo, ocorre a exposição ao agente cancerígeno (externo ou interno) em uma determinada frequência e período de tempo, e o resultado depende da interação do agente cancerígeno com as céulas do organismo. Sendo assim, podem levar anos para que a célula cancerígena se prolifere e de origem a um tumor clinicamente visível (INCA, 2017; STEIN e PARDEE, 2004).

Figura 3. Principais causas do câncer

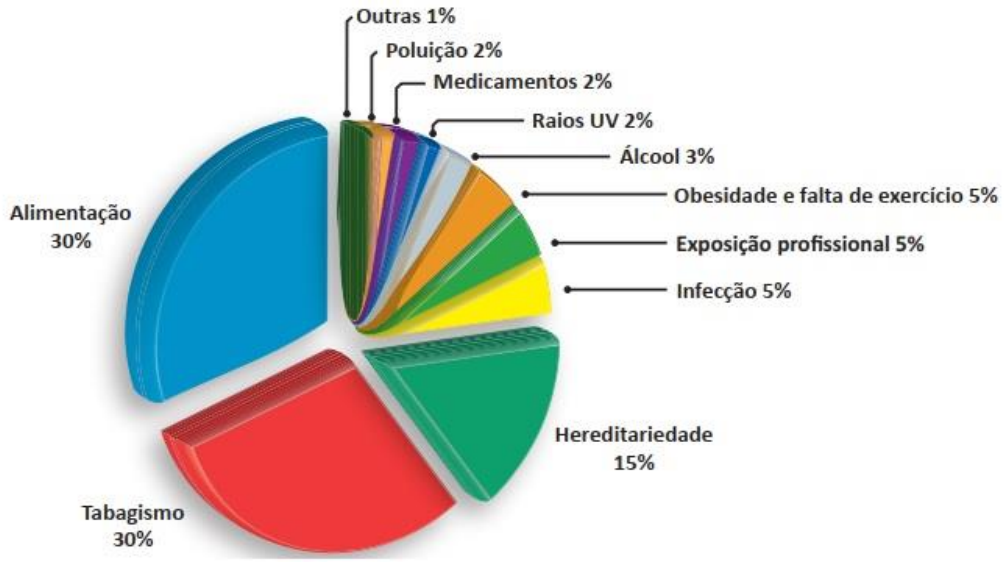

Fonte: ABC do Câncer, 2017.

A bioquímica e a biologia do câncer são muito complexas. Sabe-se que o microambiente tumoral leva a uma série de mudanças, como alterações de pH, presença de processos inflamatórios, presença de espécies reativas provocando estresse oxidativo, dano ao DNA das células, entre outros (MATTHEOLABAKIS et al., 2012; PEREZ-HERRERO e

FERNANDEZ-MEDARDE, 2015; POULSEN et al., 1998). Todos esses fatores fazem com que o câncer seja uma doença multifatorial, caracterizada como um conjunto de mais de 100 doenças, apresentando elevado índice de mortalidade e morbidade, e uma baixa eficácia de prevenção (INCA, 2017; INCA, 2018).

Atualmente, as terapias disponíveis para o tratamento do câncer são a intervenção cirúrgica, quimioterapia, radioterapia e terapias complementares como acunpultura, homeopatia e meditação. No entanto, em alguns casos a cirurgia não é recomendada e a quimioterapia e/ou radioterapia são as mais empregadas. Porém, os fármacos antineoplásicos desencadeiam uma série de efeitos adversos, o que leva a uma baixa eficácia na terapia, ou são de custo extremamente elevado. Muitas vezes, as medicações empregadas no tratamento atingem também as células saudáveis, deixando o paciente ainda mais debilitado (INCA, 2017; INCA, 2018; MEI et al., 2013). Diante disso, a busca por alternativas mais eficazes e menos tóxicas continua sendo muito relevante. Muitos estudos na literatura têm mostrado opções promissoras para o tratamento do câncer; entre elas está o emprego da nanotecnologia. Neste contexto, cabe mencionar que este trabalho está voltado para o desenvolvimento de formulações nanotecnológicas para o tratamento de melanoma e glioma, temas que serão abordados a seguir.

1.1.1 Melanoma

O melanoma maligno cutâneo é resultante da proliferação desordenada dos melanócitos presentes na epiderme (HAASS et al., 2005; INCA, 2017). É um tipo de tumor que acomete na sua maioria indivíduos caucasianos com mais de 50 anos. Segundo o INCA, o câncer de pele corresponde a aproximadamente 30 % dos casos de cânceres malignos do país, sendo que a região sul é a mais afetada. O câncer de pele tipo melanoma apesar de baixa prevalência, cerca de 4 %, apresenta alta letalidade pela alta taxa metastática (INCA, 2018). De acordo com a literatura, a incidência do melanoma deve-se aos hábitos de exposição solar excessiva, principalmente na infância e adolescência e também a mudanças na radiação solar (INCA, 2017; WANG et al., 2001). Além dos fatores externos, o fototipo de pele também pode levar uma predisposição ao desenvolvimento do tumor. Pessoas que se enquadram nos fototipos de pele I e II, ou seja, pele muito clara ou clara e com sardas apresentam um risco mais elevado de desenvolver o melanoma (RIGON et al., 2015).

Existem vários subtipos de melanoma: extensão superficial (60 – 70 %), nodular (15 – 30 %), lentigo maligno (5 – 15 %), acro-lentiginoso (5 – 10 %) e menos frequente, o

desmoplásico, spitzóide e o melanoma nevo azul. O subtipo mais comum é o de extensão superficial que acomete com maior frequência o tronco de homens e membros inferiores de mulheres com exposição solar excessiva (CLARK et al., 2007; NCI 2018; RIGON et al., 2015). O diagnóstico é feito basicamente pela observação da lesão em relação à assimetria, bordas, cor, diâmetro e evolução. Sinais como ulcerações e hemorragias sugerem um estado mais avançado (INCA, 2018; NCI 2018; RIGON et al., 2015). O tratamento de primeira escolha é a cirurgia, porém, a radio e/ou quimioterapia também são utilizadas. Os principais fármacos utilizados no tratamento do melanoma são dacarbazina, temozolomida, nitrosoureias, alcaloides da vinca, compostos de platina (Cisplatina), taxanos (Taxol, Docetaxel) e também a imunoterapia com citocinas, anticorpos monoclonais e inibidores do gene BRAF (GROSSMAN e ALTIERI, 2001; KAVANAGH et al., 2005; LI et al., 2015; RIGON et al., 2015; SCHREIBER et al., 1999). No caso de metástase, a chance de cura é praticamente zero, e o paciente entra em cuidados paliativos (INCA, 2018).

Diante da agressividade do melanoma torna-se relevante a busca por alternativas que proporcionem uma melhora na qualidade e no tempo de vida dos pacientes acometidos pela doença. Os sistemas nanoestruturados vêm sendo estudados como uma possibilidade no tratamento do melanoma. Na Tabela 1 estão citados alguns trabalhos mostrando o emprego da nanotecnologia para o tratamento do melanoma. A incorporação de agente antineoplásicos em sistemas nanoestruturados apresenta vantagens para o tratamento do melanoma por aumentar o tempo de circulação sanguínea, proporcionar seletividade, redução de dose e efeitos adversos (LI et al., 2015; RIGON et al., 2015).

Nos últimos anos, a literatura relata trabalhos onde fármacos utilizados no tratamento do melanoma são incorporados em formulações semissólidas com o objetivo de terapia adjuvante, podendo até reduzir a chance de metástases (RIGON et al., 2015; SINGH et al., 2017). Alguns exemplos podem ser citados como formulações de uso tópico contendo 5-fluorouracila, cremes com imiquimode, mebutato de ingenol, retinóides, doxorrubicina e até mesmo semissólidos contendo anti-inflamatórios como ibuprofeno e diclofenaco (CAPANEMA et al., 2018; REDPATH et al., 2009; RIGON et al., 2015; SINGH et al., 2017). Além disso, hidrogéis injetáveis também vêm sendo explorados e a aplicação subcutânea de hidrogéis contendo doxorrubicina (TAKEI et al., 2013), paclitaxel (RUEL-GARIEPY et al., 2004) e cisplatina (CASOLARO et al., 2011) têm mostrado bons resultados na regressão das lesões. Sendo assim, torna-se relevante o estudo de formulações de aplicação tópica contento

sistemas nanoestruturados incorporados como uma terapia adjuvante no tratamento do melanoma.

Tabela 1. Estudos recentes sobre o desenvolvimento de sistemas nanoestruturados para o tratamento do melanoma

Nanossistema	Ativo	Modelo	Referência
Nanocápsulas lipídicas	Ferrocifen	Células SK *in vivo* -de melanoma Mel28 e Modelo	(RESNIER et al., 2017)
Nanocápsulas poliméricas	Coenzima Q10	Células A375	(PEGORARO et al., 2017)
Nanocápsulas	Resveratrol	Modelo *in vivo* de melanoma	(CARLETTO et al., 2016)
Nanopartículas lipídicas	Acetileugenol	Modelo *in vivo* de melanoma	(DREWES et al., 2016)
Nanopartículas de ouro	----	Células B16-F10	(POON et al., 2015)
Gel contendo nanoemulsões	Leflunomida	Células A375	(PUND et al., 2015)
Nanopartículas lipídicas sólidas	Paclitaxel e microRNA	Células B16-F10	(SHI et al., 2014)
Lipossomas	Doxorrubicina	Células B16-F10	(MEI et al., 2014)
Nanocápsulas	Camptotecina	Modelo *in vivo* de melanoma	(GECIONI et al., 2007)

1.1.2 Glioma

Outro tipo de tumor com alta taxa de mortalidade são os tumores de cérebro. Os tumores primários do SNC representam uma das maiores causas de mortes por câncer antes dos 15 anos (NCI 2018; SIEGEL et al., 2018). Entre os tipos de tumores do SNC estão os gliomas, que representam um grupo de tumores geneticamente e histologicamente heterogêneos, caracterizados como neoplasias agressivas, com rápida invasividade e baixa resposta ao tratamento, apresentando alto índice de mortalidade e morbidade (BEHIN et al., 2003; LOUIS et al., 2016; OSTROM et al., 2014; PRADOS e LEVIN, 2000). Os gliomas são tumores de origem glial e são constituídos predominantemente de células como astrócitos, oligodentrócitos, células ependimais e uma mistura de vários tipos de células da glia (BEHIN et al., 2003; NCI 2018). A OMS classifica os gliomas em 4 graus de malignidade, de acordo com a morfologia celular, proliferação, atividade mitótica e necrose (BEHIN et al., 2003;

LOUIS et al., 2016). Os gliomas do tipo astrocitomas podem ser biologicamente benignos e facilmente retirados com cirurgia como o astrocitoma pilocítico (grau I). Já os astrocitomas de baixo grau (grau II) apresentem reduzida malignidade, porém podem infiltrar-se difusa e rapidamente no parênquima cerebral, dificultando a remoção cirúrgica. Os astrocitomas de grau III (astrocitoma anaplástico) são caracterizados por astrócitos fibrilares, com elevada proliferação e podem progredir rapidamente para glioblastoma. O glioblastoma multiforme (GBM) é um tumor de grau IV, com elevada letalidade e malignidade, apresentando proliferação vascular, necrose e resistência a radio/quimioterapia, levando o paciente a óbito em pouco tempo (BEHIN et al., 2003; LOUIS et al., 2016).

As terapias para o GBM são limitadas devido a sua agressividade; a cirurgia é a primeira escolha, no entanto a ressecção completa nem sempre é alcançada, pois pela elevada invasividade em tecidos saudáveis circundantes a taxa de recorrência é alta. Após a cirurgia, os pacientes são tratados com radio e/ou quimioterapia, porém, as terapias convencionais apresentam baixa eficácia devido à falta de especificidade dos fármacos e pela resistência intrínseca dos tumores. Os principais fármacos antineoplásicos empregados no tratamento do GBM são carmustina, procarbazina, lomustina, vincristina e a temozolomida como primeira escolha (LEVIN et al., 2000; WANG et al., 2017). No entando, a maioria dos fármacos tem dificuldade de ultrapassar a barreira sangue-cérebro, limitando a chegada no SNC, de modo que apenas fármacos com alta lipofilia, como a temozolomida, consigam atravessar e alcançar uma efetividade no tratamento (BEHIN et al., 2003; BRANDES et al., 2000; GROBBEN et al., 2002; MOUSSEAU et al., 1993).

A baixa eficácia das terapias convencionais para o tratamento de gliomas justifica a busca por alternativas promissoras para aumentar a resposta ao tratamento, bem como reduzir os efeitos adversos, aumentando assim o tempo de sobrevida dos pacientes. Nesse contexto, o desenvolvimento de sistemas nanoestruturados vem sendo explorado como uma tentativa de tratamento para o glioma. Na tabela 2 estão citados alguns trabalhos recentes empregando nanossistemas para o tratamento de gliomas.

Tabela 2. Estudos recentes relacionando nanotecnologia e glioma.

Nanossistemas	Ativo	Modelo	Referência
Nanopartículas (PLGA)	Curcumina	Modelo *in vivo* em ratos	(OAL RUNOGLU et al., 2017)
Nanocápsulas (Eudragit RS100®)	Indol-3-carbinol	Células de glioma de rato (C6)	(GAL EHRCKE et al., 2017)
Nanocápsulas (PCL)	Coenzima Q10	Células de glioma de rato (C6)	(PEGORARO et al., 2018)
Nanoemulsões (Óleo de romã)	-	Células de glioma de rato (C6)	(FERREIRA et al., 2016)
Nanopartículas lipídicas	Paclitaxel	Modelo camundongos *in vivo* em	(LOLLO et al., 2015)
Nanoemulsões estabilizadas com pullulan (Óleo de romã)	Cetoprofeno	Células de glioma de rato (C6)	(FERREIRA et al., 2015)
Nanopartículas (PLGA)	Carboplatina	Células de GBM humano (UPAB e SNB19)	(ARSHAD et al., 2015)
Nanopartículas (PCL)	Carboplatina	Células de glioma humano U87-MG	(KARANEM et al., 2015)
Nanopartículas (PLGA)	Camptotecina	Modelo camundongos *in vivo* em	(HOUSEHOLD et al., 2015)
Nanopartículas (Ácido hialurônico e quitosana)	Curcumina	Células de glioma de rato (C6)	(YANG et al., 2015)
Nanocápsulas (PCL)	Cetoprofeno	Modelo *in vivo* em ratos	(DAAL SILVEIRA et al., 2013)
Nanocápsulas (PCL)	Indometacina	Células de glioma de rato (C6) e humanos (U138-MG)	(BERNARDI et al., 2013)

1.2 Disseleneto de Difenila

O Selênio (Se) é um elemento não metálico da família dos calcogênios que foi descoberto em 1817 pelo químico sueco Jöns Jacob Berzelius (COMASSETO, 2010). Os primeiros relatos sobre este elemento são sobre sua toxicidade, principalmente da sua forma inorgânica (GE e YANG 1993; LI et al., 1985). No entanto, nos dias atuais sabe-se que o Se, em baixas doses, é um micronutriente essencial para as células do organismo. A Organização Mundial da Saúde (OMS) recomenda a ingestão diária de 34-35 μg para adultos (FAO/OMS, 2002). O Se constitui o sítio ativo de algumas enzimas, conhecidas como selenoenzimas e também está presente em aminoácidos como a selenocisteína. A glutationa peroxidase,

tioredoxina redutase e a 5’deiodinase são enzimas que participam ativamente no controle da formação de espécies reativas e apresentam o Se no seu sítio ativo (BEHNE et al., 1990; FLOHÉ et al., 1973; HOLMGREN 1985; NOGUEIRA e ROCHA 2011).

Diante das descobertas benéficas em relação ao elemento Se, os pesquisadores voltaram sua atenção para a síntese de compostos orgânicos de Se (COSe), buscando propostas inovadoras para seu uso terapêutico. Esses compostos, além de serem empregados como intermediários da síntese orgânica de outras moléculas apresentam diversas atividades biológicas. Na literatura são encontrados relatos de sua toxicidade e efeitos farmacológicos em diversos modelos animais. Além disso, estudos em humanos já foram conduzidos (NOGUEIRA e ROCHA 2012; NOGUEIRA e ROCHA 2011; NOGUEIRA et al., 2004). O disseleneto de difenila $(PhSe)_2$ (Figura 4) é um COSe da classe dos disselenetos de diorganoila de coloração amarela e odor característico. É de fácil obtenção e é utilizado como reagente eletrofílico intermediário na síntese orgânica (ROSA et al., 2007).

Figura 4. Estrutura química e características organolépticas do $(PhSe)_2$ (313,13 g/Mol).

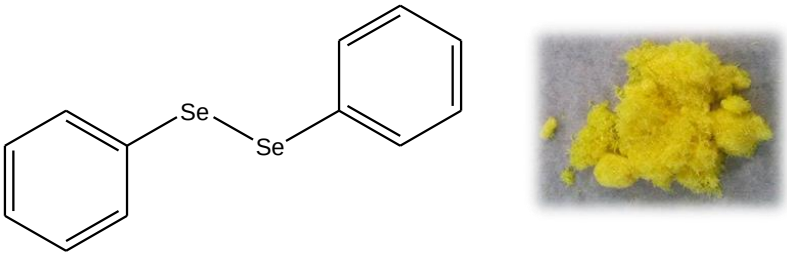

Essa molécula é conhecida por apresentar uma dupla face, ou seja, existe uma relação dose dependente entre os efeitos tóxicos e farmacológicos, como por exemplo, seus efeitos antioxidantes e pró-oxidantes, o que apresenta impacto em outras atividades relatadas para o composto (NOGUEIRA e ROCHA, 2010; ROSA et al., 2007). Diante disso, o $(PhSe)_2$ tornou-se alvo de muitos estudos, a fim de elucidar suas atividades terapêuticas e sua toxicidade. Na tabela 3 encontram-se os trabalhos considerados de maior relevância que mostram algumas atividades farmacológicas já relatadas do $(PhSe)_2$ em diferentes modelos animais.

Tabela 3. Atividades farmacológicas do $(PhSe)_2$

Atividade	Espécie animal	Referência
Antinociceptiva/ Anti-inflamatória	Rato/camundongo	(LUCHESE et al., 2012; NOGUEIRA et al., 2003; SAVEGNAGO et al., 2008; ZASSO et al., 2005)
Hepatoprotetora	Rato/camundongo	(BORGES et al., 2005; COSTA et al., 2013)
Gastroprotetora	Rato	(INEU et al., 2008; SAVEGNAGO et al., 2006)
Ansiolítica	Rato/Camundongo/Frangos com 6 dias de vida/Peixe zebra	(GHISLENI et al., 2008; IBRAHIM et al., 2014; PRIGOL et al., 2011; SAVEGNAGO et al., 2008)
Neuroprotetora	Rato	(BRUNING et al., 2012; DE FREITAS e ROCHA 2011; POSSER et al., 2008)
Antidepressiva	Camundongo	(ACKER et al., 2009; DIAS et al., 2014; ROCHA et al., 2012; SAVEGNAGO et al., 2008; WILHELM et al., 2010)
Memória	Rato	(CECHELLA et al., 2014)
Antihiperlipidemiante	Camundongo	(DA ROCHA et al., 2009)
Antihiperglicemiante	Rato	(ACKER e NOGUEIRA 2012; BARBOSA et al., 2006)
Antitumoral	Rato	(BARBOSA et al., 2008)

Além disso, os compostos de Se têm sido alvos de estudos e são promissores candidatos para quimioprevenção. Em geral, dependendo da sua estrutura química, esses compostos podem modular o desenvolvimento do processo tumoral, pelas seguintes ações: (I) atuação mimética aos fármacos antagonistas dos receptores androgênicos; (II) elevada atividade antioxidante, principalmente atuando na redução do estresse oxidativo com efeitos positivos nas enzimas glutationa peroxidase e tioredoxina redutase; (III) influência na reparação e prevenção de danos ao DNA das células pela modulação da expressão gênica; e (IV) regulação do processo de apoptose celular (SANMARTIN et al., 2008). Na literatura, até o momento, foram encontrados alguns relatos da atividade *in vitro* do $(PhSe)_2$ frente a células tumorais.

O efeito do $(PhSe)_2$ na indução de morte celular por apoptose já foi relatado por Posser e colaboradores (2011). Neste estudo foram investigadas a influência na viabilidade das células de neuroblastoma humano (SH-SY5Y) e o efeito nas proteínas quinases (ERK 1/2 e p38MAPK) após tratamento com o composto. Foi observada redução na viabilidade das células, mudanças morfológicas compatíveis com morte celular por apoptose e modulação da fosforilação de quinases, deixando as células mais susceptíveis ao efeito antimutagênico do

$(PhSe)_2$ (POSSER et al., 2011). Nedel e colaboradores (2012) demonstraram o efeito de disselenetos de diorganoila com diferentes substituintes frente a células de adenocarcinoma de cólon humano. Neste trabalho foram testados os compostos apresentados na figura 5, os quais demonstraram diferentes perfis de atividade. Os compostos I e II apresentaram efeito citotóxico na concentração de 80 µM, enquanto que os compostos III e IV mostraram efeito significativo a partir da concentração de 20 µM. Todos os compostos modularam a expressão dos genes Bax (pró-apoptótico) e Bcl-2 (anti-apoptótico) e da apoptose dependente das caspases 8 e 9 (NEDEL et al., 2012).

Figura 5. Representação dos disselenetos de diorganoilas.

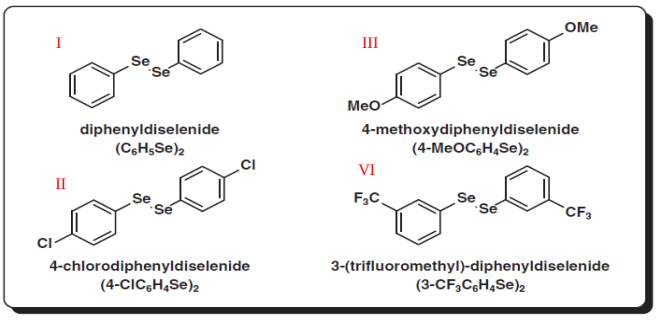

FONTE: Nedel et al., 2012.

Apesar das potencialidades terapêuticas do $(PhSe)_2$, sua toxicidade e problemas de solubilidade limitam o progresso dos estudos para a etapa clínica. Acredita-se que a toxicidade do $(PhSe)_2$ esteja relacionada ao processo de oxidação de grupos tióis endógenos de importância biológica, provenientes principalmente da glutationa reduzida (GSH), proteínas ou de sítio ativo de diferentes enzimas (NOGUEIRA e ROCHA, 2010; ROSA et al., 2007). O $(PhSe)_2$ desempenha um papel tóxico na δ-aminolevulinato desidratase (ALA-D), enzima que participa da segunda etapa da síntese do heme. A inibição da atividade da ALA-D leva ao acúmulo do ácido aminolevulínico, tóxico para a célula; além disso, a inibição da biosíntese do heme gera um distúrbio na produção do citocromo p450, essencial para a metabolização de xenobióticos e outras substâncias. O mecanismo está baseado principalmente na formação de um intermediário instável (selenol – selenoato) provocando a oxidação dos grupos sulfidrílicos (BARBOSA et al., 1998; MACIEL et al., 2000; ROSA et al., 2007). Outro alvo da toxicidade do $(PhSe)_2$ é o tripeptídeo glutationa reduzida (GSH), uma defesa antioxidante não enzimática, que apresenta em sua estrutura o aminoácido cisteína

dotado do grupamento tiol. O composto oxida os grupos sulfidrílicos formando um selenol e, dessa forma, reduz os níveis de GSH e, consequentemente, reduz o potencial antioxidante não enzimático (NOGUEIRA e ROCHA, 2010; ROSA et al., 2005; ROSA et al., 2007).

O $(PhSe)_2$ também já foi relatado por provocar efeitos citotóxicos, genotóxicos e mutagênicos em fibroblastos. No trabalho publicado por Rosa e colaboradores (2007) foi observado o "Efeito Janus" do composto, ou seja, em baixas concentrações não foram observados efeitos citotóxicos, danos ao DNA das células e houve redução nos níveis de peroxidação lipídica. Por outro lado, em altas concentrações, o composto apresentou uma atividade pró-oxidante nas células, sendo citotóxico, causando dano ao DNA, aumento da peroxidação lipídica e, ainda, houve depleção nos níveis de GSH. Nesse estudo fica clara a relação concentração dependente do composto e que o limite entre os efeitos tóxicos e farmacológicos é muito próximo (ROSA et al., 2007).

Além disso, o $(PhSe)_2$ também apresenta limitações físico-químicas e farmacocinéticas. Em 2013, Prigol e colaboradores publicaram um estudo mostrando o perfil bioquímico e físico-químico do $(PhSe)_2$. Este trabalho mostrou que a molécula é estável quimicamente frente aos meios gástrico e intestinal simulados, e biologicamente frente ao plasma humano e à albumina sérica bovina, não havendo produtos de degradação na análise por espectroscopia de massas. No entanto, os estudos de solubilidade e coeficiente de distribuição (Log D) mostraram que o $(PhSe)_2$ tem uma alta lipofilia, apresentando valores de solubilidade em tampão fosfato pH 7,4 de 0,98 µM e Log D de 3,13. Sabe-se que valores de Log D maiores de 3,0 indicam baixa solubilidade em água, dificultando a dissolução nos fluídos do trato gastrintestinal e, consequentemente, podendo levar a uma baixa biodisponibilidade oral (DELLIS et al., 2007; PRIGOL et al., 2013). Em estudo prévio, do mesmo autor, foi demonstrado que após a administração oral de 500 mg/Kg de $(PhSe)_2$ dissolvido em óleo de canola foram alcançadas concentrações máximas de apenas 13,1 e 10,1 µg/mL em ratos e camundongos, respectivamente. Além disso, grande quantidade de selênio foi quantificada nas fezes. Esses resultados indicam que o $(PhSe)_2$ apresenta uma baixa biodisponibilidade após administração oral (PRIGOL et al., 2012).

Diante dessas limitações, torna-se relevante a busca por alternativas que possam contornar a baixa solubilidade do $(PhSe)_2$, bem como reduzir seus efeitos tóxicos, em vista das diversas atividades biológicas relatadas para o composto. Nesse sentido, as nanocápsulas poliméricas têm sido estudadas para a incorporação do composto. Em 2014, Giordani e colaboradores desenvolveram nanocápsulas de poli(Ɛ-caprolactona) (PCL) empregando óleo

de canola como núcleo oleoso. As características físico-químicas das suspensões foram adequadas, com diâmetro médio entre 266 – 325 nm, índice de polidispersão abaixo de 0,2, potencial zeta de -29 a -19 mV, pH de 5,6 – 6,3, teor de $(PhSe)_2$ próximo ao teórico e eficiência de encapsulação maior que 95%. Na avaliação da distribuição biológica, o $(PhSe)_2$ foi quantificado em maior quantidade na urina do que nas fezes, sugerindo que as nanocápsulas modificaram a distribuição da molécula pela via intragástrica. Desses resultados vale ressaltar que o composto alcançou o cérebro, indicando que o sistema ultrapassou a barreira sangue-cérebro (GIORDANI et al., 2014). Na sequencia, Stefanello e colaboradores (2015) demonstraram que após a administração intraperitoneal em camundongos, estas mesmas formulações não foram tóxicas. Além disso, as nanocápsulas contendo $(PhSe)_2$ mostraram atividade antioxidante tanto *in vitro* quanto ex vivo (STEFANELLO et al., 2015).

1.3 Nanopartículas poliméricas

A nanotecnologia cada vez mais chama a atenção de pesquisadores e indústrias farmacêuticas pelas vantagens que apresenta frente às formulações convencionais. Países como os Estados Unidos, Japão e a Comunidade Européia são os maiores investidores em nanociência e nanotecnologia, gerando um investimento em torno de 160 bilhões de dólares até 2015 (DIMER et al., 2013; SHI et al., 2010). No Brasil, o investimento é menor, mas já existem iniciativas nacionais para o desenvolvimento de pesquisas em nanociência e nanotecnologia, buscando alternativas promissoras para o diagnóstico, prevenção e tratamento das doenças (DIMER et al., 2013). Os nanossistemas têm sido estudados para o tratamento de uma série de doenças e, segundo alguns autores, os principais alvos são o câncer, doenças cardiovasculares, inflamatórias, neurológicas e a imunodeficiência adquirida (AIDS) (DIMER et al., 2013; MARCATO e DURAN, 2008; MEI et al., 2013).

As principais características atribuídas aos sistemas nanométricos são o tamanho reduzido (10 – 1000 nm) e a capacidade de incorporação de moléculas hidro- e lipofílicas. Estes sistemas podem conferir vantagens como controle da liberação de fármacos, vetorização sítio-específica, maior distribuição no trato gastrintestinal, aumento de biodisponibilidade e redução de efeitos adversos (COUVREUR et al., 2002; COUVREUR e VAUTHIER, 2006; GUTERRES et al., 2007; MARCATO e DURAN, 2008; PEREZ-HERRERO e FERNANDEZ-MEDARDE, 2015). Essas vantagens podem ser exploradas em combinação ou, de acordo com a doença e o tipo de via de administração, podem ser estudadas isoladamente, através da utilização de diferentes condições de obtenção dos sistemas

nanoestruturados, tais como como método de preparação, tipo e concentração dos constituintes. Os principais sistemas nanométricos aplicados na terapêutica são os lipossomas, nanoemulsões, nanopartículas lipídicas sólidas, carreadores lipídicos nanoestruturados e as nanopartículas poliméricas.

As nanopartículas poliméricas diferem-se estruturalmente em nanoesferas e nanocápsulas, resultado das diferenças nas composições quali e quantitativas das formulações (Figura 6). As nanocápsulas são compostas por um núcleo oleoso, lipídico ou aquoso envolto por uma camada polimérica; o fármaco pode estar dissolvido e/ou disperso no núcleo e/ou adsorvido no polímero. Já as nanoesferas são sistemas poliméricos matriciais, onde o fármaco encontra-se disperso e/ou adsorvido na matriz (MORA-HUERTAS et al., 2010; OLIVEIRA et al., 2013; SCHAFFAZICK et al., 2003). O óleo, componente do núcleo oleoso das nanocápsulas, pode ser sintético, como triglicerídeos de cadeia média (SANTOS et al., 2013) e óleo de silicone (FERREIRA et al., 2015), ou de origem vegetal, como o óleo de coco (SANTOS et al., 2014), óleo de rosa mosqueta (CHASSOT et al., 2015; GEHRCKE et al., 2017), óleo de arroz (RIGO et al., 2015), óleo de semente de uva (ALMEIDA et al., 2010), óleo de borragem (WEBER et al., 2016), óleo de romã (MARCHIORI et al., 2017), entre outros. Os polímeros mais empregados no preparo destes sistemas são os poliésteres, como a poli(Ɛ-caprolactona) (CHASSOT et al., 2015; FERREIRA et al., 2015; GEHRCKE et al., 2017; PEGORARO et al., 2018; WEBER et al., 2016) e o poli(lactídeo-co-glicolídeo) (PLGA) (GUO et al., 2011); os derivados do ácido metacrílico, os Eudragit's, como o Eudragit® RS100 (GEHRCKE et al., 2018; SANTOS et al., 2013; SANTOS et al., 2014), Eudragit RL® 100 (VERMA et al., 2013) e Eudragit® S100 (YOO et al., 2011); e os derivados da celulose, como a etilcelulose (CHASSOT et al., 2015; MARCHIORI et al., 2017).

Figura 6. Estrutura e forma de associação do fármaco às nanopartículas poliméricas: (a) nanocápsula com o fármaco dissolvido no núcleo oleoso e/ou adsorvido na parede polimérica e (b) nanoesfera com o fármaco disperso em toda a matriz polimérica.

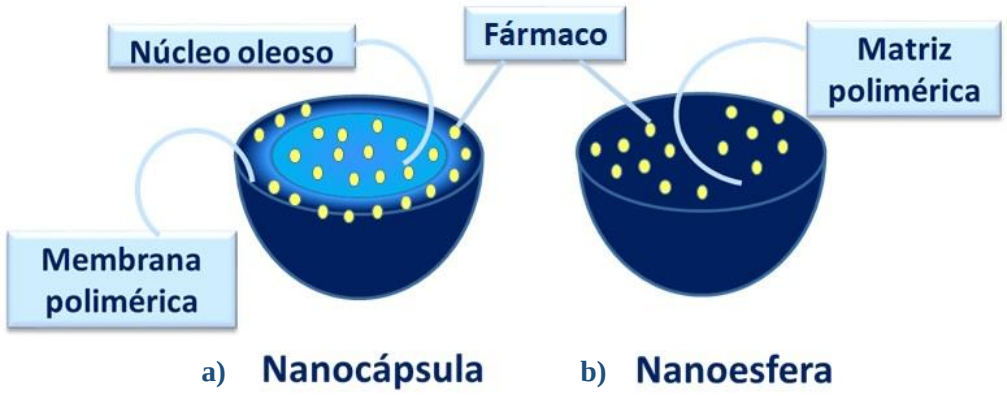

Fonte: o próprio autor

Os principais métodos de preparação das nanopartículas poliméricas são a nanoprecipitação, para formação de nanoesferas, e a deposição interfacial de polímero pré-formado, para as nanocápsulas. Os métodos baseiam-se na preparação de duas fases, uma orgânica e uma aquosa; a fase orgânica contendo um solvente miscível em água (acetona ou etanol), tensoativo de baixo equilíbrio hidrofílico – lipofílico (EHL), polímero, óleo (no caso nas nanocápsulas) e o fármaco é vertida em uma fase aquosa contendo tensoativo de alto EHL. Quando o solvente orgânico difunde na água inicia-se o processo de precipitação do polímero hidrofóbico, formando a estrutura casca-núcleo para as nanocápsulas e a matriz polimérica para as nanoesferas. Esse processo tem seu término após a evaporação total do solvente orgânico, permanecendo apenas uma suspensão aquosa de nanopartículas (FESSI et al., 1989; MORA-HUERTAS et al., 2010; MORA-HUERTAS et al., 2012; SCHAFFAZICK et al., 2003).

Alguns fatores importantes dos métodos de preparação podem modificar as características finais das partículas como, por exemplo, a viscosidade das fases, uma vez que quanto mais viscosa for a fase, mais lenta será a difusão do solvente e, consequentemente, maior será o tamanho de partícula; o pH das fases pode interferir na carga de superfície ou, ainda, interferir na estrutura do polímero, podendo levar à hidrólise; o tipo e a concentração dos tensoativos devem ser determinados para que se tenha uma redução da tensão interfacial e com isso a estabilização e formação da suspensão, além de também interferir na viscosidade. Além disso, parâmetros como temperatura e velocidade de evaporação também podem

modificar as características finais da formulação (COUVREUR et al., 2002; MORA-HUERTAS et al., 2010). A caracterização do sistema é de extrema importância, para que se tenha um controle maior do desempenho da formulação no organismo. Na tabela 4 encontram-se as principais avaliações que devem ser feitas nos sistemas nanométricos após sua preparação.

A determinação do perfil de liberação *in vitro* do fármaco a partir das nanoestruturas tem sua relevância no sentido não só de mostrar um possível comportamento *in vivo*, mas também de fornecer informações da forma de associação do fármaco à partícula. Modelos matemáticos são empregados para elucidar o mecanismo de liberação, bem como supor o mecanismo de associação do fármaco. Diferentes cinéticas de liberação são esperadas quando o fármaco está dissolvido no núcleo oleoso ou está adsorvido na parede polimérica. As técnicas empregadas para avaliação do perfil de liberação *in vitro* são a difusão em sacos de diálise (EL-SAMALIGY et al., 1986), difusão reversa em sacos de diálise (ARAÚJO et al., 2011; MAGALHAES et al., 1991), ultracentrifugação ou a ultrafiltração-centrifugação (GUTERRES et al., 1995; MAGENHEIM e BENITA 1991).

Tabela 4. Caracterização físico-química das nanopartículas

Característica	Técnica
Morfologia	As microscopias eletrônicas de varredura (MEV) e de transmissão (MET) permitem obter informações sobre a estrutura e tamanho da partícula, bem como mostram a presença de cristais de fármaco na superfície. Além disso, a microscopia de força atômica também pode ser empregada (SCHAFFAZICK et al., 2003).
Tamanho e distribuição de tamanho	A espectroscopia de correlação de fótons (PCS) determina o raio hidrodinâmico das partículas em suspensão e fornece informações a respeito de sua distribuição, indicando o perfil de homogeneidade do tamanho. Outra técnica é a difração a laser, pela a qual se obtém informações de partículas em uma faixa de tamanho de 0,01 a 3000 µm, o que permite excluir a presença de micropartículas na formulação nanométrica. Além disso, a utilização das microscopias também demonstra a faixa de tamanho das partículas (MORA-HUERTAS et al., 2010; SCHAFFAZICK et al., 2003).
Potencial zeta	A microeletroforese permite avaliar o potencial zeta, o qual reflete a carga de superfície da partícula. As nanopartículas usualmente apresentam valores diferentes de zero, o que indica baixa tendência à agregação. O potencial zeta geralmente é decorrente da natureza do polímero e dos grupos funcionais presentes em sua estrutura (MORA-HUERTAS et al., 2010; SCHAFFAZICK et al., 2003).
pH	Através do monitoramento do pH das suspensões durante um período de tempo pode-se ter informações sobre a estabilidade da formulação, uma vez que mudanças de pH podem ser indicativo de hidrólise do polímero ou dos ácidos graxos presentes no óleo, no caso das nanocápsulas. O pH é determinado diretamente nas suspensões com potenciômetro calibrado (MORA-HUERTAS et al., 2010; SCHAFFAZICK et al., 2003).
Teor de fármaco e eficiência de encapsulação	A determinação do teor total de fármaco é feita pela dissolução das nanopartículas em solvente adequado e posterior quantificação por método analítico. Para determinar a fração de fármaco encapsulado utilizam-se as técnicas de ultrafiltração-centrifugação ou ultracentrifugação, nas quais ocorre a separação do fármaco livre do encapsulado (MORA-HUERTAS et al., 2010; SCHAFFAZICK et al., 2003).

Uma vez preparados e caracterizados, um passo muito importante é a avaliação da toxicidade dos sistemas nanoestruturados. Apesar de suas vantagens e da biocompatibilidade dos seus constituintes, a compreensão da interação dessas partículas com biomoléculas do organismo humano é, todavia, relevante. Apesar das diversas vantagens que as nanoestruturas apresentam frente às formulações convencionais e da biocompatibilidade de seus constituintes, ainda se tem uma preocupação em entender a interação dessas partículas com as biomoléculas no organismo humano (ADABI et al., 2017; AULA et al., 2015). Parâmetros como o tamanho reduzido, forma e superfície podem modificar as características dos materiais utilizados, assim como as do principio ativo, podendo ter efeitos indesejáveis no organismo (ADABI et al., 2017). Muitas abordagens experimentais são empregadas atualmente para a determinação da toxicidade dos sistemas nanoestruturados (figura 7), partindo de análises *in vitro*, utilizando células e organismos monocelulares, até estudos pré-clínicos utilizando comumente roedores. Nos últimos anos, o peixe-zebra (*Danio rerio*) tem sido empregado como modelo animal para avaliar os possíveis efeitos tóxicos de nanoformulações (CHAKRABORTY et al., 2016). O peixe-zebra apresente semelhaças genéticas e fisiológicas com o organismo humano, sendo um protocolo rápido, simples e de baixo custo, uma vez que a reprodução dos peixes se da em poucos dias, além de ser um animal pequeno e fácil de manusear (KALUEFF et al., 2016; KALUEFF et al., 2013). Assim, cada vez mais é possível realizar o panorama completo de toxicidade dos sistemas nanoestruturados, iniciando com organismos menos complexos até aqueles que apresentam maior proximidade com o organismo humano.

Figura 7. Representação da evolução de escala para a determinação da toxicidade dos sistemas nanoestruturados.

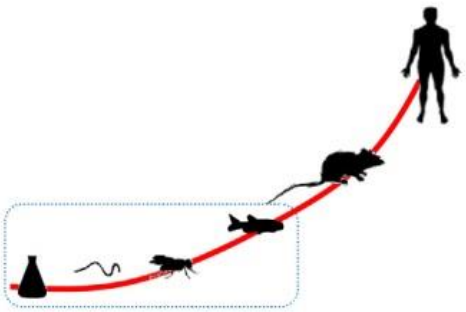

Fonte: adaptado de Kalueff et al., 2015

Após a fase de otimização dos sistemas, estudos in vtiro e/ou *in vivo* são conduzidos para avaliar as potencialidades farmacológicas, de acordo com o fármaco incorporado. Neste sentido os sistemas nanométricos são muito estudados para o tratamento do câncer pela capacidade de atingir um alvo específico, reduzindo os efeitos adversos das terapias convencionais. A liberação sítio-específica proporcionada pelas nanopartículas pode ocorrer pelo aumento de permeação e retenção vascular do fármaco nos tecidos tumorais sólidos (figura 8) (FANG et al., 2011; PEREZ-HERRERO e FERNANDEZ-MEDARDE, 2015).

Figura 8. Ilustração do transporte passivo e ativo das nanopartículas ao tumor.

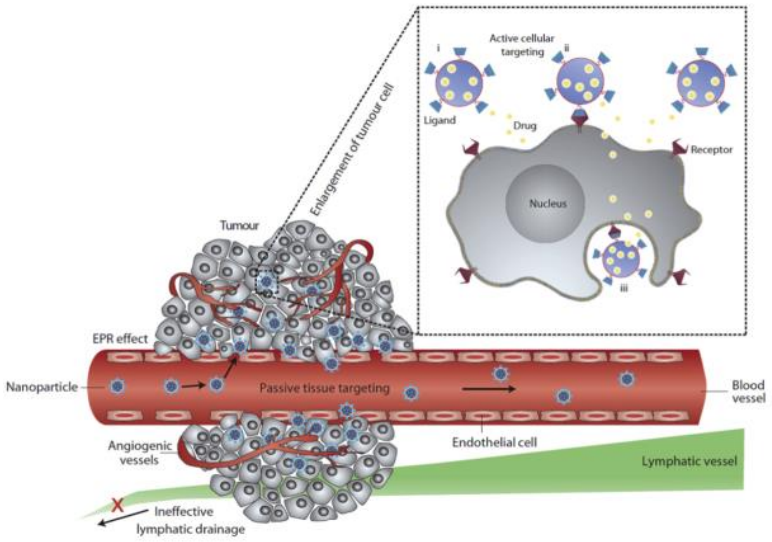

Fonte: Pérez-Herrero e Fernández-Medarde, 2015.

A rede microvascular tumoral é complexa e faz com que se tenha um aumento da permeabilidade do endotélio e uma redução da drenagem linfática. Isso faz com que as nanopartículas alcancem essa área com mais facilidade, através do transporte passivo e, ainda ocorre um acúmulo das partículas, liberando o fármaco com uma velocidade controlada e promovendo uma melhor eficácia da formulação (COUVREUR et al., 2006; PEREZ-HERRERO e FERNANDEZ-MEDARDE, 2015). Os nanocarreadores também podem vetorizar os fármacos de maneira ativa através de ligantes em sua estrutura que favoreçam o direcionamento da formulação para o microambiente tumoral e promovam sua captação. A modificação da superfície das partículas pode ocorrer pela adsorção ou ligação covalente de polímeros hidrofílicos, como os polietilenoglicóis, tornando as partículas furtivas, ou seja,

invisíveis ao sistema fagocitário monocítico (MATTHEOLABAKIS et al., 2012; PEREZ-HERRERO e FERNANDEZ-MEDARDE, 2015).

Além disso, as nanopartículas podem ser incorporadas em formulações semissólidas para aumentar a permeação cutânea dos fármacos para as camadas mais profundas da pele, ou ainda promover uma maior retenção da formulação na pele, favorecendo um efeito local mais prolongado. Essa propriedade pode ser interessante para o tratamento de tumores de pele, pois desempenha um efeito local sem que ocorram efeitos adversos sistêmicos (GUTERRES et al., 2007). No caso do tratamento do melanoma, hidrogéis contendo nanopartículas são uma alternativa promissora por promover um acúmulo ou uma manutenção de altos níveis do fármaco utilizado no local do tumor (RIGON et al., 2015). Para o tratamento tópico do câncer de pele, o fármaco deve atravessar o estrato córneo para atingir as camadas de pele normalmente acometidas pelos tumores. No entanto, o estrato córneo é a principal barreira para a penetração de substâncias na pele, por ser formado por queratinócitos localizados em uma matriz lipídica organizada. Para contornar essa limitação, a incorporação de fármacos em formulações semissólidas contendo nanopartículas tem sido estudada. Devido ao tamanho reduzido, os nanocarreadores aumentam a área de contato com a pele e promovem uma maior penetração para as camadas mais profundas. Além disso, essas formulações liberam o fármaco de maneira controlada, evitando efeitos tóxicos na pele e pelas propriedades de oclusão, restauram a hidratação natural do órgão (FONTANA et al., 2011; GUTERRES et al., 2007; OURIQUE et al., 2011).

Usualmente, polímeros sintéticos como o Carbopol Ultrez® (BEBER et al., 2016; FLORES et al., 2015; MARCHIORI et al., 2013; MELERO et al., 2014; RIGO et al., 2015), Carbomer Ultrez® (DE ANDRADE et al., 2015) e Pemulen TR1® (DE LIMA et al., 2017) são os mais utilizados para o desenvolvimento de formulações semissólidas com nanocarreadores incorporados. Recentemente, nosso grupo de pesquisa tem desenvolvido hidrogéis a base de suspensões de nanocápsulas pelo simples espessamento das formulações com polissacarídeos naturais (MARCHIORI et al., 2017; PEGORARO et al., 2017). Em ambos os trabalhos, a goma gelana foi empregada para espessar as suspensões de nanocápsulas para obtenção de uma formulação semissólida. Tais formulações apresentaram características adequadas, como tamanho médio de partícula na faixa nanométrica, pH compatível com a pele, teor de fármaco próximo ao teórico, perfil de espalhabilidade e comportamento reológico favorável para aplicação tópica. Nesse contexto, para o desenvolvimento dos hidrogéis nesse trabalho, a

goma xantana foi escolhida como um novo agente formador de gel. A goma xantana é um polissacarídeo aniônico, produzido pela bactérica Xanthomonas campestris, e tem sido empregada na indústria farmacêutica e de alimentos como agente espessante e estabilizante (KUMAR et al., 2018; PRAJAPATI et al., 2013). Alguns estudos já têm demonstrado a potencialidade deste polissacarídeo para obtenção de hidrogéis com sistemas nanoestruturados incorporados. Estas formulações apresentam características adequadas para aplicação tópica e proporcionaram liberação controlada dos ativos incorporados (JUNYAPRASERT et al., 2009; MISHRA et al., 2018; POPLE e SINGH 2006; SHAH et al., 2007). Porém, cabe ressaltar que a goma xantana ainda não foi empregada como agente formador de gel pelo simples espessamento de uma suspensão de nanocápsulas.

OBJETIVOS

2. Objetivos

2.1 Objetivo Geral

O presente trabalho objetivou o desenvolvimento de suspensões e hidrogéis a nanocápsulas contendo disseleneto de difenila, bem como estudar o potencial antitumoral destas formulações contra o melanoma cutâneo e o glioblastoma e avaliar a toxicidade destas em linhagens celulares e modelos animais.

2.2 Objetivos Específicos

• Preparar suspensões de nanocápsulas de poli(Ɛ-caprolactona) contendo disseleneto de difenila;

• Caracterizar as formulações quanto ao diâmetro médio de partícula, índice de polidispersão, potencial zeta, pH, teor de disseleneto de difenila e eficiência de encapsulação, morfologia, interações/incompatibilidades entre os contituíntes e estabilidade térmica;

• Estudar a estabilidade das suspensões de nanocápsulas pelo período de 30 dias;

• Determinar da fotoestabilidade do disseleneto de difenila associado ou não às nanocápsulas poliméricas;

• Elucidar a citotoxicidade das suspensões de nanocápsulas e do composto livre frente a células sanguíneas humanas, queratinócitos e astrócitos;

• Estudar a toxicidade das suspensões de nanocápsulas contendo disseleneto de difenila em peixe zebra através de análises comportamentais e estresse oxidativo no cérebro dos animais;

• Avaliar a toxicidade do disseleneto de difenila livre e associado às suspensões de nanocápsulas após administração intragástrica em ratos através de análises bioquímicas plasmáticas e teciduais;

• Determinar o potencial antitumoral *in vitro* das formulações em células de melanoma (A375, SKMel – 103, SK-Mel-28 e B16F10) e glioma (C6);

• Desenvolver hidrogéis pelo espessamento das nanocápsulas de disseleneto de difenila com goma xantana;

• Caracterizar os hidrogéis quanto ao tamanho médio de partícula, pH, teor do composto, espalhabilidade e comportamento reológico;

• Avaliar o perfil de permeação/penetração cutânea dos hidrogéis contendo o composto livre e nanoencapsulado;

• Demonstrar o efeito antitumoral *in vivo* do disseleneto de difenila livre e nanoencapsulado em um modelo pré-clínico de glioblastoma após administração intragástrica.

CAPÍTULO 1: Desenvolvimento de nanocápsulas poliméricas contendo $(PhSe)_2$, avaliação da atividade antimelanoma *in vitro* e incorporação em hidrogéis a base de goma xantana.

3. Capítulo 1: Desenvolvimento de nanocápsulas poliméricas contendo $(PhSe)_2$, avaliação da atividade antimelanoma *in vitro* e incorporação em hidrogéis a base de goma xantana.

Apresentação

O primeiro capítulo desta tese demonstra a preparação e caracterização de sistemas de base nanotecnológica contendo o disseleneto de difenila, sua citotoxicitade em células normais e seu efeito antitumoral *in vitro* frente a diferentes tipos de células de melanoma. Neste capítulo encontra-se o **artigo 1**, publicado na revista "*Materials Science and Engineering C*", o qual contempla os resultados da caracterização da suspensão de nanocápsulas contendo o composto, o efeito citotóxico do $(PhSe)_2$, livre e nanoencapsulado, frente a células senguíneas humanas e queratinócitos, e sua ação antitumoral frente a células de melanoma humano (A375). Na sequência, apresenta-se o **manuscrito 1**, onde se realiza a determinação do efeito antimelanoma da suspensão de nanocápsulas frente a células resistentes de melanoma, empregando-se diferentes técnicas *in vitro*. Adicionalmente, este estudo reporta a preparação e caracterização de um hidrogél formado pelo espessamento da suspensão de nanocápsulas com goma xantana e seu perfil de permeação cutânea utilizando pele humana.

3.1 Artigo 1

Materials Science & Engineering C 91 (2018) 1–9

Contents lists available at ScienceDirect

Materials Science & Engineering C

journal homepage: www.elsevier.com/locate/msec

Diphenyl diselenide loaded poly(ε-caprolactone) nanocapsules with selective antimelanoma activity: Development and cytotoxic evaluation

Luana Mota Ferreira[a], Verônica Ferrari Cervi[a], Marcel Henrique Marcondes Sari[a,b], Allanna Valentini Barbieri[a], Andiara Prates Ramos[c], Priscila Marquezan Copetti[c], Gerson Fernandes de Brum[c], Kátia Nascimento[c], Jessica Mendes Nadal[d], Paulo Vitor Farago[d], Michele Rorato Sagrillo[c], Cristina Wayne Nogueira[b], Letícia Cruz[a,*]

[a] Laboratório de Tecnologia Farmacêutica, Programa de Pós-graduação em Ciências Farmacêuticas, Centro de Ciências da Saúde, Universidade Federal de Santa Maria, Santa Maria, RS, Brazil
[b] Laboratório de Síntese, Reatividade e Avaliação Farmacológica e Toxicológica de Organocalcogênios, Centro de Ciências Naturais e Exatas, Universidade Federal de Santa Maria, Santa Maria, RS, Brazil
[c] Curso de Biomedicina, Universidade Franciscana, Santa Maria, Brazil
[d] Programa de Pós-graduação em Ciências Farmacêuticas, Universidade Estadual de Ponta Grossa, PR, Brazil

1. Introduction

Malignant cutaneous melanoma is a result of the melanocytes disordered proliferation in the epidermis and is considered the most severe skin cancer because of its high metastatic rate [1]. The first-choice approach is the surgical removal of the tumor, but the treatment with radio and/or chemotherapy is also used. In cases of metastasis occurrence, the cure chances are practically zero, and the therapies are just palliative care [2]. The most chemotherapeutic agents employed for melanoma treatment are dacarbazine, temozolomide, nitrosoureas, vinca alkaloids, platinum compounds and taxanes (Taxol, Docetaxel) [2–4]. Besides, immunotherapy with cytokines is also used as well as antibodies and BRAF inhibitors (BRAFV600E is a gene expressed in melanoma) [2,5–7]. Unfortunately, these therapies can cause severe side effects and some of them may even cause other primary cancers [2]. Thus, in view of the melanoma aggressiveness and the complications of therapy, the search for alternatives to improve the melanoma treatment becomes relevant.

Selenium (Se) is recognized as an essential micronutrient for the human body. Considering such beneficial discovery about the Se atom, researchers turned their attention to the organoselenium compounds synthesis searching for innovative proposals focusing on their therapeutic use. Among them, diphenyl diselenide [$(PhSe)_2$] stands out for the several *in vitro* and *in vivo* pharmacological activities already reported [8,9]. Of particular importance, it was previously demonstrated the $(PhSe)_2$ effectiveness against tumor cells (human neuroblastoma, human colon adenocarcinoma, and breast cancer cells) and in animal models of cancer [10–13]. However, up to now, there is no report about the $(PhSe)_2$ effect on melanoma cells line. This compound seems to exert the antitumor action by disrupting the cell cycle (apoptosis) [12,13], reducing the tumor growth, and increasing the cancer onset latency [10]. Despite this, $(PhSe)_2$ has a double face profile due to its contrasting behavior that depends on the conditions of exposure and other factors. A wide range of evidence supports that the interaction of $(PhSe)_2$ with thiols seems to play a central role in its toxicity; Such interaction can oxidize thiol groups that are essential for some enzyme activities such as δ-aminolevulinate enzyme dehydratase (δ-ALA-D) [9], decrease the reduced glutathione content [8,9,14] and also promoting oxidative imbalance, which can cause toxic effects as neurotoxicity and impaired hepatic and renal functions. Besides, $(PhSe)_2$ is a very lipophilic compound, suggesting low oral bioavailability and hindering the preparation of parenteral solutions [15,16]. Both toxicity issues and physicochemical restrictions represent a barrier to $(PhSe)_2$ clinical application. An alternative to circumvent these limitations could be its association into nanocarrier systems, such polymeric nanocapsules.

The last decades have been marked by a true research explosion in the nanotechnology field [17–19]. Polymeric nanocapsules are widely studied drug nanocarriers and are defined as nanovesicular systems, in which an oil core is surrounded by a polymeric shell [20,21]. The oily core confers high drug loading capacity, labile drug protection and burst release reduction [22]. Furthermore, they have been used to treat several diseases and the main targets are cancer, cardiovascular and neurological diseases as well as inflammation related to pathologies and to acquired immune deficiency [17,18,23,24].

Although, the studies about organoselenium compounds incorporation into nanocarriers systems are rare, some authors have already demonstrated that such association triggered many advantages considering their biological potential and biodistribution profile [25–29]. In view of these data, the current study aimed to prepare and characterize a nanocapsule suspension loaded with $(PhSe)_2$, as well as

* Corresponding author at: Programa de Pós-Graduação em Ciências Farmacêuticas, Universidade Federal de Santa Maria, Santa Maria 97105-900, Brazil.
E-mail address: leticiacruz@smail.ufsm.br (L. Cruz).

https://doi.org/10.1016/j.msec.2018.05.014
Received 20 September 2017; Received in revised form 10 April 2018; Accepted 2 May 2018
Available online 04 May 2018
0928-4931/

to investigate its cytotoxic potential against human melanoma A375 cells line. Additionally, the formulation toxicity in keratinocytes (HaCaT) and human blood cells was assessed.

2. Material and methods

2.1. Material

Poly(ε-caprolactone) (PCL) (MW: 80 kDa), Span 80® (sorbitan monooleate), dimethylsulphoxide (DMSO), 3(4-5-dimethyl)-2-5diphenyl tetrazolium bromide (MTT) and Histopaque-1077® were acquired from Sigma Aldrich (Brazil). Tween80® (polysorbate 80) and MCT (medium chain triglycerides) were furnished by Delaware (Brazil). Blue colouring trypan and hydrogen peroxide were furnished by Nuclear® (Brazil). Culture claw 25 cm^2 was obtained from TPP (USA) and RPMI culture medium from Vitrocell (Brazil). All other chemicals had analytical grade and were obtained from standard commercial suppliers.

2.2. Compound

The $(PhSe)_2$ was synthesized following the method described by Paulmier [30]. The ^1H and ^{13}C nuclear magnetic resonance as well as gas chromatography were employed to confirm the compound chemical structure and to determine its purity (99.9%), respectively.

2.3. Analytical procedures

The $(PhSe)_2$ quantification was performed on a LC-10A HPLC system (Shimadzu, Japan) equipped with a LC-20AT pump, a UV-VIS SPD-M20A detector, a CBM-20A system controller and a SIL-20A HT valve sample automatic injector. Separation was achieved at room temperature using a Gemini C_{18} Phenomenex column (150 mm × 4.60 mm, 5 μm; 110 Å) coupled to a C_{18} guard column. The isocratic mobile phase consisted of methanol and water (80:20, v/v) at 1 mL/min of flow rate. The $(PhSe)_2$ was detected at 243 nm. The method for the $(PhSe)_2$ quantification in nanocapsules was validated in agreement with the International Conference on Harmonization (ICH) guidelines. The methodology was linear ($r = 0.997$), specific, accurate (96.36 to 104.60%) and precise (relative standard deviation ≤ 2.22%) in a concentration range of 5.0–25.0 μg/mL.

2.4. Nanocapsule suspensions preparation

Nanocapsule suspensions were prepared by interfacial deposition of preformed polymer method, described by Fessi and collaborators [31]. An organic phase containing PCL (0.1 g), Span 80® (0.077 g), MCT (330 μL), acetone (27 mL) and $(PhSe)_2$ (0.05 g) was kept under magnetic stirring at 40 °C for 60 min. After total constituents solubilization, the organic phase was injected into a Tween 80® (0.077 g) aqueous dispersion (53 mL) and kept for 10 min under magnetic stirring. Next, the organic solvent was eliminated by evaporation under reduced pressure to achieve a final volume of 10 mL, which corresponds to a $(PhSe)_2$ concentration of 5.0 mg/mL (NC $(PhSe)_2$). For comparison purposes, formulations without $(PhSe)_2$ were also prepared (NC B). All samples were performed in triplicate.

2.5. Nanocapsules characterization

The following basic characteristics were evaluated on the nanocapsule suspensions: granulometric distribution, average diameter, polydispersity index (PDI), zeta potential, pH, $(PhSe)_2$ content and encapsulation efficiency. For morphological (microscopy), spectroscopic (X-ray diffraction and fourier-transform infrared spectroscopy) and thermal analyses (thermogravimetric and differential scanning calorimetry), the NC $(PhSe)_2$ and NC B were freeze-dried using 10% lactose (w/v) as cryoprotectant. For this, lactose powder was dispersed in NC $(PhSe)_2$ and NC B and, subsequently, the formulations were frozen for 24 h and subjected to dehydration in a freeze-dryer (LIOTOP L 101, Liobras, Brazil) at −55 °C during 24 h and then used to analyzes. Moreover, for X-ray diffraction (XRD), Fourier-transform infrared spectroscopy (FTIR), Thermogravimetric (TGA) and Differential scanning calorimetry (DSC) analyses, a physical mixture of $(PhSe)_2$ and PCL (1:1, w/w) was also evaluated. Accordingly, these techniques have a high resolution and detection limit, which allows that compounds/materials can be detected at 1% concentration in the samples [32].

2.5.1. Granulometric distribution

Granulometric distribution was performed by laser diffraction (Mastersizer® 3000E, Malvern Instruments, United Kingdom) after diluting the samples in distilled water until reach a laser obscuration of 15%. A refractive index of 1.59 was used to perform the measurement.

2.5.2. Average diameter, polydispersity index and zeta potential

Average diameter and PDI were determined by photon correlation spectroscopy (Zetasizer Nanoseries®, Malvern Instruments, United Kingdom) after diluting the samples in ultrapure water (1:500). Zeta potential analyses were performed using the same instrument after the samples dilution in 10 mM NaCl (1:500). These analyses were performed at room temperature.

2.5.3. pH determination

The pH values were determined using a calibrated potentiometer (Model pH 21, Hanna Instruments, Brazil) by its direct immersion in the nanocapsules suspension.

2.5.4. $(PhSe)_2$ content and encapsulation efficiency (EE)

The total $(PhSe)_2$ content in nanocapsules was determined by the HPLC method described above (Section 2.3). For this, 30 μL of nanocapsule suspensions were diluted in 10 mL of acetonitrile and acetone (1:1, v/v), sonicated for 15 min, filtered through a 0.45 μm membrane and injected into the HPLC system. For the EE determination, a formulation aliquot was placed in a 10,000 MW centrifugal device (Amicon® Ultra, Millipore) and the free compound was separated by ultrafiltration/centrifugation technique (10 min at 2200*g*). The difference between the total and the free $(PhSe)_2$ concentrations, determined in the nanocapsules suspensions and in the ultrafiltrate, respectively, was defined as nanocapsules encapsulation efficiency.

2.5.5. Morphology

Scanning electron microscopy with field emission guns (FEG-SEM) was used to determine the morphological characteristics of pure and nanoencapsulated $(PhSe)_2$. The samples were mounted on aluminum stubs, sputtered with gold (IC-50 Ion Coater, Shimadzu, Kyoto, Japan) and subsequently analyzed through FEG-SEM equipment (TESCAN, model MIRA3, Brno, Czech Republic) at an accelerating voltage of 10 kV with different magnifications.

2.5.6. X-ray diffraction analysis (XRD)

XRD patterns of pure $(PhSe)_2$, PCL, physical mixture (PM), lactose, NC B and NC $(PhSe)_2$ were obtained by a wide-angle X-ray diffractometry, which were carried out using a Shimadzu X-ray diffractometer (Shimadzu XRD-6000, Kyoto, Japan). The 2θ value was increased from 3° to 80° at a scan rate of 2°/min using a Cu-Kα source ($\lambda = 1.5418$ Å) at 40 kV and 40 mA.

2.5.7. Fourier-transform infrared spectroscopy (FTIR)

The FTIR spectra for $(PhSe)_2$, PCL, PM, lactose, NC B and NC $(PhSe)_2$ were recorded from 4000 to 400 cm^{-1} using a Shimadzu IR Prestige-21 spectrophotometer (Kyoto, Japan) with potassium bromide pellets with 32 scans and a resolution of 4 cm^{-1}.

2.5.8. Thermogravimetric analysis (TGA)

The pure substances, PM and nanocapsules were analyzed by thermogravimetry using a thermobalance (STA 6000, Perkin Elmer, Waltham, MA, USA). The thermogravimetric curves were obtained at a temperature range of 20–600 °C, using platinum crucibles with 5.0 ± 0.1 mg of sample under dynamic N_2 atmosphere (flow rate: 50 mL/min) and heat flow of 10 °C/min. The equipment was previously calibrated with copper sulfate pentahydrate.

2.5.9. Differential scanning calorimetry (DSC)

The DSC analyses were carried out in a DSC-60 calorimeter (Shimadzu, Kyoto, Japan) using aluminum crucibles with 2.5 ± 0.1 mg of sample under dynamic N_2 atmosphere (flow rate: 50 mL/min). The temperature range was 20–300 °C with a heating rate of 10 °C/min. An empty aluminum pan was used as reference. The DSC cell was calibrated with indium (m.p. = 156.45 °C; ΔH_{fusion} = 28.54 J/g) and zinc (m.p. = 419.45 °C).

2.6. Stability studies

Nanocapsule suspensions were packaged in amber glass flasks and stored at room temperature. After 30 days, average diameter, PDI, zeta potential, pH and compound content in the formulations were evaluated as previously described (Section 2.5).

The photostability study was performed using a mirrored chamber (1 m × 25 cm × 25 cm) coupled with an ultraviolet lamp (Phillips TUV lamp–UVC long life, 30 W), which emits ultraviolet radiation C over 300 min. Aliquots (700 µL) of NC $(PhSe)_2$ or $(PhSe)_2$ methanolic solution (MS $(PhSe)_2$–5 mg/mL) were individually placed in plastic cuvettes with covers and kept 14 cm of distance from the light source. At predetermined intervals, aliquots of 30 µL were withdrawn and the $(PhSe)_2$ remaining percentage was evaluated as described in Section 2.5.4 and determined by the HPLC method. Aiming at discarding thermal degradation, dark controls were simultaneously assessed.

2.7. In vitro tests

2.7.1. Cells culture and blood collection

The human malignant melanoma (A375) and keratinocytes (HaCaT) cell lines were obtained from the American Type Culture Collection (ATCC). The cells were grown and maintained in RPMI 1640 medium containing 1% of antibiotic, supplemented with 10% of fetal bovine serum (FBS) and kept at 37 °C in a humidified atmosphere with 5% CO_2. After the cells reached a confluency of 90% they were submitted to trypsinization and counted in a Neubauer chamber, after seeding 2×10^5 cells per 96 well plates. These plates were kept at 37 °C in a humidified atmosphere of 5% CO_2 for 24 h, and then they were used for tests.

The formulations cytotoxicity was also evaluated using human blood cells, which were obtained from School Laboratory of Clinical Analyses of Franciscan University, under the approval of the Ethics Committee for Research with Human Beings Institution (CAAE: 31211214.4.0000.5306). Blood samples were collected from healthy volunteers by venous puncture, using a Vacutainer® (BD Diagnostics, Plymouth, United Kingdom) and heparin tubes. Histopaque-1077® density gradient was used to separate red blood cells and mononuclear cells using 4 mL of blood samples. After separation, mononuclear cells with a 2×10^5 initial density were standardized to perform the assay.

2.7.2. Cytotoxic effect against human A375 melanoma cells

The plates containing A375 cells were incubated with NC $(PhSe)_2$ and free $(PhSe)_2$ at the concentrations of 10, 25, 50 and 100 µM. The concentrations were selected based on previous studies about the cytotoxic effect of $(PhSe)_2$ and other structural analogs. To achieve such concentrations, 10-fold serial dilutions were made using RPMI culture medium from the $(PhSe)_2$ nanocapsules suspension or the stock solution of free $(PhSe)_2$, which was dissolved in DMSO (10%). Cells treated with DMSO (10%) or NC B were used for comparison purposes. The 3(4-5-dimethyl)-2-5diphenyl tetrazolium bromide (MTT) salt reduction assay was performed after 24, 48 or 72 h of incubation in A375 cells, following the methodology described by Rosa and collaborators [9,48]. Briefly, after the incubation period, the cells were washed twice with sodium phosphate buffer (SPB) before adding 150 µL of yellow tetrazolium salt MTT solution to the 96 well plate containing the sample treatments. Then, the plates were incubated at 37 °C for 3 h and under light protection until it was observed the presence of violet formazan crystals. Subsequently, the spectrophotometric absorbance was measured and the results were expressed by cell viability (%) in comparison to the negative control. Negative, RPMI culture medium, and positive, hydrogen peroxide at concentration 1%, controls were carried out. All observations were validated by at least three independent experiments, and for each experiment the analyses were performed in triplicate.

2.7.3. Cytotoxicity studies on keratinocytes and human blood cell

Keratinocytes and human mononuclear cells were treated with NC $(PhSe)_2$, NC B or $(PhSe)_2$ dissolved in DMSO, at 10, 25, 50 and 100 µM concentrations and incubated for 72 h at 37 °C in a 5% humidified CO_2 atmosphere. With the purpose of discarding any possible $(PhSe)_2$ vehicle interference, the cells were treated with DMSO at a maximum concentration of 10%. RPMI culture medium was used as negative control and hydrogen peroxide as the positive control. The cell viability was assessed by MTT reduction as previously describes at Section 2.7.2 and it was expressed as percentage (%) of living cells.

2.8. Statistical analysis

Formulations were prepared and analyzed in triplicate and the results were expressed as mean ± S.E.M. The GraphPad Prism® version 6 software was used to perform the Student's *t*-test and variance analyses one-way (ANOVA) followed by post-hoc Tukey's test. Values of $p < 0.05$ were considered statistically significant. The IC_{50} values were calculated by linear regression.

3. Results

3.1. $(PhSe)_2$-loaded polymeric nanocapsules characterization

3.1.1. Granulometric distribution, average diameter, PDI, zeta potential, pH, compound content and EE

After preparation, the formulations showed a macroscopic "milk-like" homogeneous appearance without any visible precipitation. The NC $(PhSe)_2$ had a slight yellow color due to the compound incorporation into the nanostructures. The results of the characterization as soon as prepared are expressed at Table 1. The NC $(PhSe)_2$ had an average diameter in the nanometric range (240 ± 52 nm) and PDI value of 0.15 ± 0.06. Corroborating with these data, the laser diffractometry technique (Supplementary Material; Fig. S1) demonstrated nanoparticles with a narrow size distribution and the absence of particles in the micrometer range ($D_{0.5}$ = 0.276 ± 0.019 µm and SPAN = 1.678 ± 0.148). Negative values of zeta potential were obtained (−10.9 ± 2.2 mV) and the pH values were in the neutral range (7.4 ± 0.1). The total $(PhSe)_2$ content in nanocapsules suspension was 99.01 ± 2.20%, close to the theoretical value (5 mg/mL), and EE was around 98.0%. The NC B suspension had average diameter of 240 ± 29 nm, PDI values lower than 0.2 (0.19 ± 0.08), negative zeta potential (−11.5 ± 1.11 mV) and pH value of 6.9 ± 0.07. The statistical analysis performed using Student's *t*-test showed no significant difference between the NC $(PhSe)_2$ and NC B ($p > 0.05$).

3.1.2. Morphology

Morphological characteristics of pure $(PhSe)_2$ and NC $(PhSe)_2$ obtained by FEG-SEM are depicted in Fig. 1. The organoselenium

Table 1
Stability study of the NC $(PhSe)_2$ and NC B during 30 days of storage and photostability study of $(PhSe)_2$ methanolic solution (MS $(PhSe)_2$) and NC $(PhSe)_2$ after UVC radiation exposure.

Stability study					
Samples	Average diameter (nm)	PDI	Zeta potential (mV)	pH	Compound content (%)
NC $(PhSe)_2$					
T0	240 ± 52	0.151 ± 0.06	−10.9 ± 2.21	7.4 ± 0.1	99.01 ± 2.20
T30	245 ± 47	0.166 ± 0.17	−13.2 ± 4.91	5.9 ± 0.2*	91.56 ± 3.98
NC B					
T0	240 ± 29	0.190 ± 0.08	−11.5 ± 1.11	6.9 ± 0.1	–
T30	236 ± 25	0.173 ± 0.05	−11.4 ± 0.94	6.2 ± 0.2*	–

Photostability study		
Time (min)	MS $(PhSe)_2$ (%)	NC $(PhSe)_2$ (%)
0	100.00 ± 2.39	99.01 ± 2.20
30	95.43 ± 0.74	100.10 ± 4.01
60	95.76 ± 1.60*	101.20 ± 0.78
120	87.58 ± 7.50*#	101.90 ± 2.94
180	87.99 ± 2.06*#	98.97 ± 1.85
240	86.00 ± 6.28*#	100.10 ± 2.73
300	82.09 ± 4.19*#	100.50 ± 2.30

The results are expressed by mean with S.E.M. of triplicate. For the stability study the asterisks denote the significant difference (*) $p < 0.05$ by paired Student's *t*-test between T0 and T30. For photostability comparisons, the asterisks denote significant difference (*) $p < 0.05$ between MS $(PhSe)_2$ and NC $(PhSe)_2$ at a specific time analyzed by paired Student's *t*-test. Sharps denote the significant difference in comparison to the respective initial time (0 min) analyzed by One-way ANOVA of repeated measures, followed by Tukey's test.

compound $(PhSe)_2$ had irregular surface and shape (Fig. 1A), while NC $(PhSe)_2$ showed spherical shape and smooth surface (Fig. 1B). Besides, FEG-SEM images confirmed that the formulation of NC $(PhSe)_2$ had average diameter in the nanometric range (< 500 nm). In the supplementary material is showed the morphological characteristics of NC B (Supplementary material, S2).

3.1.3. X-ray diffraction analysis

The XRD patterns are presented in Fig. 2. The PCL X-ray diffraction pattern showed peaks at 21.54° (main peak) and 23.90°, while pure $(PhSe)_2$ presented crystalline peaks at 7.18°, 11.35° (main peak), 21.32°, 22.56° and 32.61°. The PM demonstrated a diffractogram with the same peaks of the pure. The compound nanoencapsulation modified the diffraction pattern in comparison to its free form. The $(PhSe)_2$ main peak it was no longer detected regardless some peaks related to the lactose (main peak at 19.94°). The NC B had a similar diffraction pattern of NC $(PhSe)_2$. The diffractograms for each substance and formulation are available in the supplementary material (Supplementary material; Fig. S3).

3.1.4. Fourier-transform infrared spectroscopy

The FTIR spectra for PCL, $(PhSe)_2$, PM, lactose as well as nanocapsule formulations are depicted in Fig. 3. The PCL spectrum showed characteristic bands of C=O stretching vibrations at 1736 cm^{-1}, CH_2 bending modes at 1466 cm^{-1} and CH_2 asymmetric stretching at 2921 cm^{-1} and symmetric stretching at 2852 cm^{-1}. Besides, the C–O–C stretching vibrations yield bands around 1000 and 1200 cm^{-1}. The $(PhSe)_2$ spectrum exhibited absorption bands at 1565, 1466 and 1426 cm^{-1} which are referring to C=C vibration presented in phenyl group; at 1014 cm^{-1} it is related to the aromatic C–H stretching

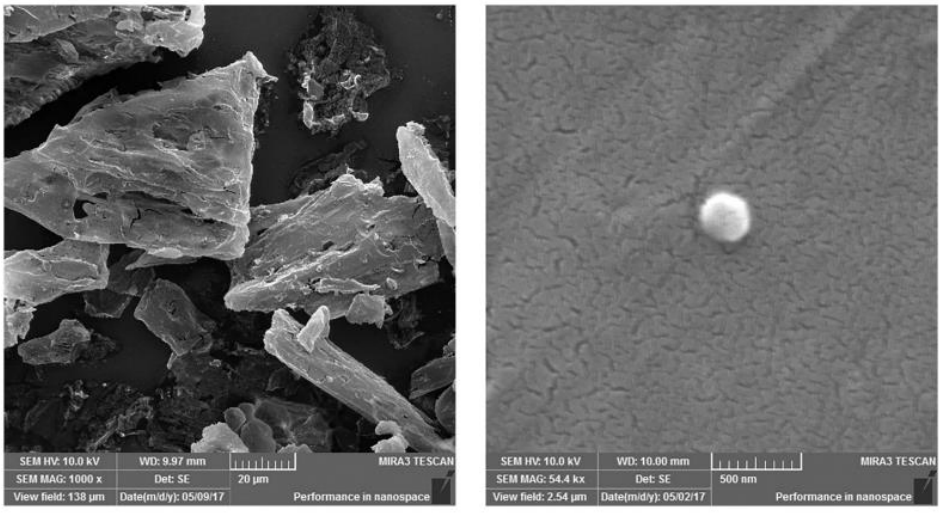

Fig. 1. FEG-SEM micrographs of pure $(PhSe)_2$ (A) and (B) and NC $(PhSe)_2$. Experimental condition: accelerating voltage: 10 kV.

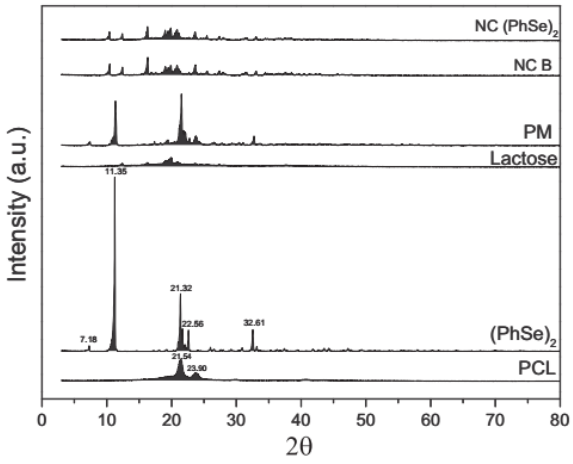

Fig. 2. X-ray diffraction patterns of NC $(PhSe)_2$, NC B, physical mixture, lactose, bulk $(PhSe)_2$ and PCL determine by wide-angle X-ray diffractometry. Experimental conditions: 2θ: 3–80 °C; scan rate 2 °C/min; Source: Cu-Kα (λ = 1.5418 Å); tube voltage: 40 kV; current: 40 mA.

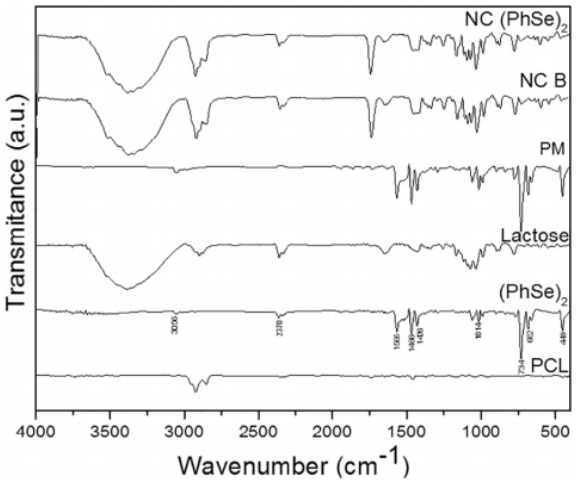

Fig. 3. FTIR spectra of NC $(PhSe)_2$, NC B, physical mixture (PM), lactose, bulk $(PhSe)_2$ and PCL determine from 4000 to 400 cm^{-1} with potassium bromide pellets with 32 scans and a resolution of 4 cm^{1}.

vibrations in the plan and at 734 cm^{-1} it is related to aromatic C—H out of plane. At 682 cm^{-1}, it linked to the band characteristic of aromatic C═C out of the plane. Lactose presented a broad band at 3394 cm^{-1} assigned to O—H stretching vibration. Physical mixture spectrum was corresponded to FTIR $(PhSe)_2$ and PCL superposition suggesting no interaction between these components. In general, the spectrum of NC $(PhSe)_2$ showed typical infrared absorption bands of raw materials, mainly from PCL and lactose. Besides, the $(PhSe)_2$ characteristics absorption bands are not observed. NC B showed a similar profile that formulation containing the organoselenium compound. The spectrum of each substance and formulation is available in the supplementary material (Supplementary material; Fig. S4).

3.1.5. Thermogravimetric analysis (TGA)

The steps of weight loss observed to raw materials, PM and nanocapsules are showed in Fig. 4. PCL showed only one event of weight loss ranging from 366 to 460 °C as previously reported [33]. The $(PhSe)_2$ had one event of weight loss from 160 to 275 °C, which confirms its high purity. Lactose showed a first stage of thermal degradation at 152 °C related to the loss of water of crystallization. The other steps could be associated to lactose degradation. The PM showed two events of weight loss. The first event started at 160 °C as observed to pure organoselenium compound, while the second one occurred between 280 and 355 °C. The thermal degradation patterns of nanocapsules displayed a three-stage of thermal decomposition profile. The first stage of weight loss was associated with water evaporation and began at 100 °C; the second and third steps were attributed to a mixture of $(PhSe)_2$ and polymer chain degradations (220–345 °C) and their decomposition products volatilization (345–440 °C), respectively.

3.1.6. Differential scanning calorimetry (DSC)

DSC curves for PCL, $(PhSe)_2$, lactose, PM, and nanocapsules are summarized in Fig. 5. PCL demonstrated the melting temperature at 60.2 °C. The pure $(PhSe)_2$ showed endothermic events at 76 °C, which corresponds to its melting temperature, and at 215 °C that could be associated with its decomposition. Lactose as monohydrate revealed two endothermic events at 163 °C induced by dehydration and the melting endotherm at 234 °C. As expected, PM had the thermal events attributed to both polymer and $(PhSe)_2$. However, the typical melting event of $(PhSe)_2$ was not observed in DSC nanocapsules curve. Nanoformulations presented a low endothermic event at 55 °C related to PCL, an endothermic event between 90 and 110 °C due to water loss and an endotherm around 234 °C corresponding to the melting of β-lactose.

3.2. Stability studies

After 30 days of storage at room temperature and protected from light, formulations showed the same macroscopic appearance without any visible alterations. Furthermore, no statistical difference was observed to average diameter, PDI, zeta potential, and drug content in comparison to the initial time ($p > 0.05$). However, there was a slight decrease in pH values for NC B and NC $(PhSe)_2$ ($p < 0.05$) as can be seen in Table 1.

After 300 min of UVC radiation exposure, NC $(PhSe)_2$ presented no statistical significant change in compound content ($p < 0.05$), while the $(PhSe)_2$ methanolic solution showed a reduction in the remaining content (around of 82% after 300 min) ($p < 0.05$) (Table 1). Moreover, degradation products were not detected by HPLC analysis (data not shown).

3.3. Cytotoxic effect against human A375 melanoma cells

The cytotoxic effect of NC $(PhSe)_2$ was expressed by cell viability percentage (Fig. 6A and B). After 48 h of exposure it is possible to observe a reduction on cell viability caused by NC $(PhSe)_2$ (Fig. 6A) at all concentrations tested (10–100 μM) ($p < 0.05$) and the IC_{50} was 76.40 μM. The $(PhSe)_2$ at 25, 50 and 100 μM concentrations reduced the melanoma cell viability ($p < 0.05$) with an IC_{50} 65.29 μM. The highest viability reduction was achieved after 72 h of incubation (Fig. 6B) at 50 and 100 μM concentrations ($p < 0.05$) for both free and nanoencapsulated compound. The IC_{50} was 48.30 and 43.56 μM for NC $(PhSe)_2$ and $(PhSe)_2$, respectively. NC B did not reduce cell viability regardless the time and concentrations tested ($p > 0.05$). The results of melanoma cell viability after 24 h of treatment are shown in the supplementary material (Supplementary material; Fig. S5). At this time of treatment neither NC $(PhSe)_2$ nor $(PhSe)_2$ had cytotoxic effect.

3.4. Cytotoxicity studies on keratinocytes and human blood cell

The HaCaT keratinocytes cell line was used as non-transformed cell model to determine the formulations safety and selectivity (Fig. 6C). After 72 h of incubation, the free $(PhSe)_2$ caused a cytotoxic effect by reducing the HaCaT cells viability to 75.38, 75.05, 71.87 and 57.83% at

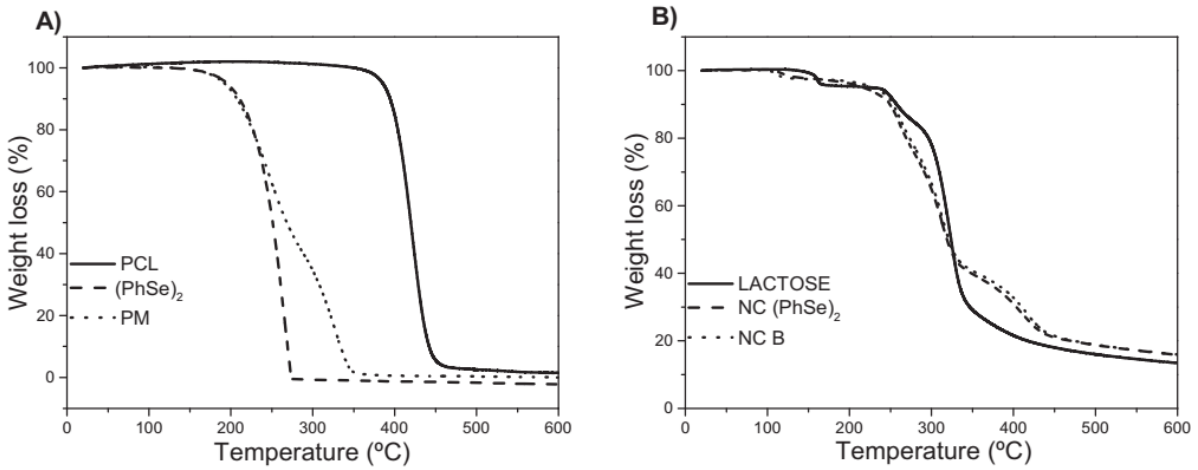

Fig. 4. Thermal degradation profiles assessed through thermogravimetric curves: A) PCL, $(PhSe)_2$ free and physical mixture (PM) and B) lactose, NC $(PhSe)_2$ and NC B. Experimental conditions: temperature range: 20–600 °C; atmosphere: N_2; flow rate: 50 mL/min; heat flow: 10 °C/min.

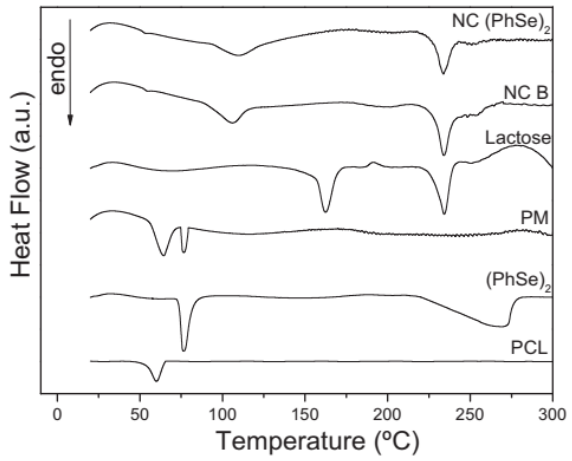

Fig. 5. DSC curves of PCL, pure $(PhSe)_2$, physical mixture (PM), lactose, NC B and NC $(PhSe)_2$. Experimental conditions: temperature range: 20–300 °C; atmosphere: N_2; flow rate: 50 mL/min; heating flow: 10 °C/min.

10, 25, 50 and 100 μM, respectively ($p < 0.05$). On the other hand, NC $(PhSe)_2$ did not cause cytotoxicity at all concentrations tested ($p > 0.05$). The NC B induced a slight decrease in cell viability at all concentrations tested of approximately 20% ($p > 0.05$).

The cytotoxicity studies were also carried out inhuman mononuclear cells (Fig. 6D). The statistical analyses revealed no significant differences in the cell viability among the experimental groups ($p > 0.05$). All samples and concentrations tested kept the cell viability around 100%.

4. Discussion

The search for ways to circumvent solubility and toxicity issues has shown that the nanotechnology approach can be a promising alternative. The nanocapsules suspensions are versatile system that can be administered by different routes, such as oral, ocular, vaginal, cutaneous and parenteral one [21]. The nanocapsules oil core confers high lipophilic substances entrapment, modified release, enhanced protection against photo or chemical degradation, and increased interaction with cells and tissues and drug targeting to specific sites [18]. A previous study [26] reported the development of $(PhSe)_2$ nanocapsules using PCL as polymeric shell and canola oil as oily core. On the other hand, the $(PhSe)_2$ nanocapsules suspension described by the current study, employed MCT as the oil core of the nanovesicular system, a material that is widely used in formulations for parenteral use, especially for intravenous administration. Besides promoting an increase in the compound stability, the $(PhSe)_2$ nanoencapsulation provided a selective and superior cytotoxic effect against the human melanoma A375 cell line in comparison to free compound.

The characteristics of the $(PhSe)_2$ nanoformulations are in accordance with other studies that applied the same nanocapsules composition, PCL and MCT [34–37]. The results demonstrated the absence of micrometer particles and a unimodal distribution (Supplementary material, Fig. S1), which is adequate for drug delivery nanosystems. Besides, the mean particle size was around 240 nm and is in agreement with other reports that showed the incorporation of organoselenium compounds into nanostructures [26,28]. The zeta potential evaluation demonstrated negative values, which is attributed to the PCL and polysorbate 80 density of charge [28,38]. The pH values were around the neutral range, which is suitable for nanocapsules suspensions of PCL and MCT. Besides, the compound content into the nanostructures was close to the theoretical value (100% — 5 mg/mL) and the EE was 98%, suggesting that the $(PhSe)_2$ is confined inside the particle, which was expected due to the $(PhSe)_2$ high lipophilic character, favoring the compound solubilization in the oil core. A high encapsulation efficiency can promote many advantages such as: superior stability of the compound, sustained and controlled drug release, side effects reduction, favored absorption, and improved bioavailability and, consequently, biological effect [18,21].

A complete nanocarrier characterization is important considering the influence of such parameters in biological effects. Besides, the nanoencapsulation process could cause physical modifications in the incorporated molecule, for instance, changing the crystalline form to an amorphous state [25,33]. The morphological images of NC $(PhSe)_2$ demonstrated that the particles had spherical shape, smooth surface and, confirm the nanometric size (around 250 nm), while the raw compound showed a crystalline character. The pure substances (PCL and $(PhSe)_2$) showed well defined peaks in XRD patterns, which represents a crystalline form of them; after the nanoencapsulation process, the $(PhSe)_2$ profile of peaks was not observed, only PCL and lactose characteristics, corroborating the hypothesis of $(PhSe)_2$

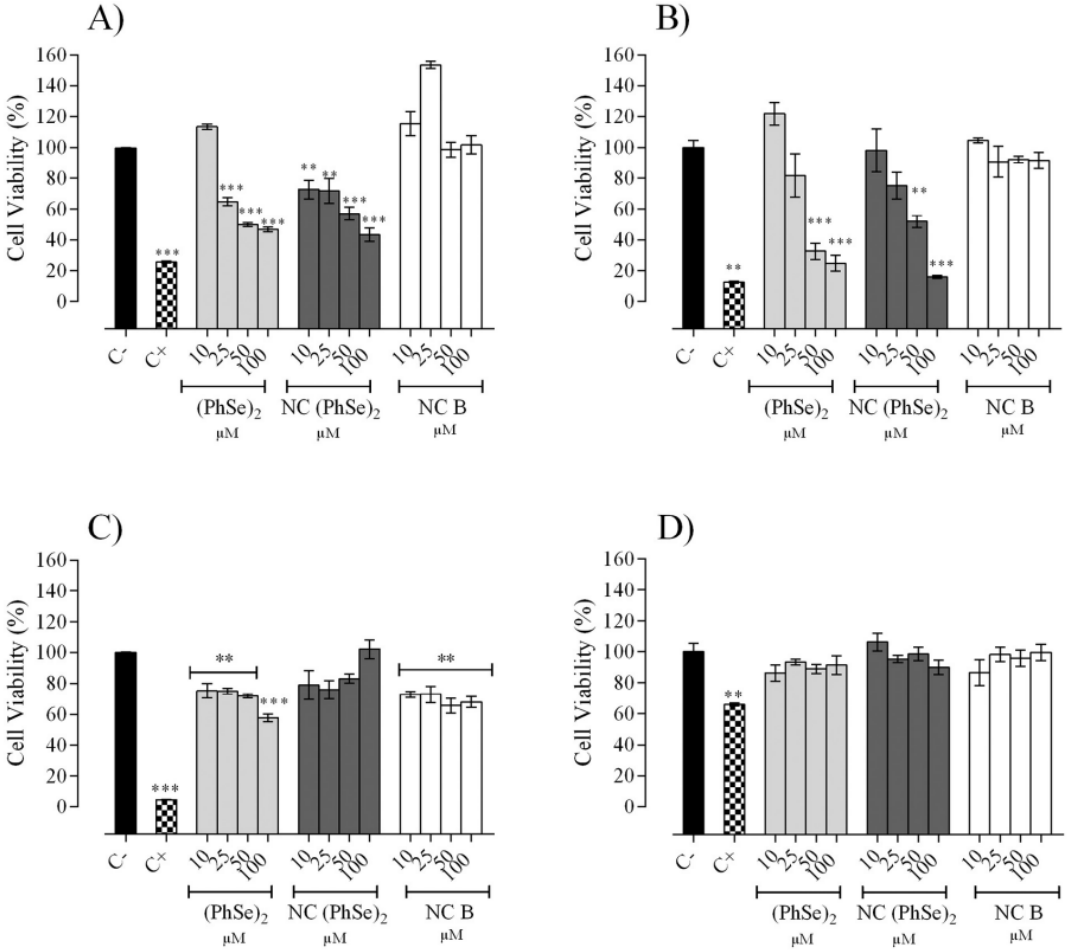

Fig. 6. Cytotoxic effect of $(PhSe)_2$ and NC $(PhSe)_2$ against A375 human melanoma cells after 48 h (A) and 72 h (B) of treatment and cytotoxicity evaluation on keratinocytes HaCaT (C) and mononuclear human cells after 72 h (D) of treatment. NC B was used as comparison purposes while RPMI culture medium were used negative control and hydrogen peroxide was used as positive control. Each column represents the mean with S.E.M. of triplicate. Asterisks denote the significance levels (***) $p < 0.0001$, (**) $p < 0.01$ compared to negative control, by one-way ANOVA, Tukey's *post hoc* test.

solubilization in the oil core. Reinforcing these data, the DSC technique showed no endothermic event to $(PhSe)_2$ after its nanoencapsulation.

The FTIR elucidate the chemical groups in molecules and is a useful tool to study possible chemical interactions among nanocapsule constituents. It was observed no chemical bonds formed between $(PhSe)_2$ and PCL because their main absorption infrared bands remained in the spectra of nanocapsules formulation and physical mixture. The $(PhSe)_2$ bands could be masked by the polymeric matrix and this also can be explained by the ratio between PCL:$(PhSe)_2$ used to prepare the nanocapsules. Besides, $(PhSe)_2$ can also be overlapped by the lactose bands. Regarding the scientific literature, similar results of XRPD, DSC and FTIR were demonstrated by Antunes and collaborators [25] and in our recent study [28]. In the first study, the authors reported a physical interaction between the compound and poly(lactic acid), suggesting that $(PhSe)_2$ is dispersed in the polymeric matrix of nanoparticles; on the other hand, we suggested that these results indicate that organoselenium compound was dissolved in the oil core, with no chemical interaction among the components.

After 30 days of storage no changes were observed in the macroscopic appearance, average diameter, PDI, zeta potential and $(PhSe)_2$ content. Despite this, a slight reduction in pH values were observed independent of the $(PhSe)_2$ presence, which could be explained by PCL chains relaxation, leading to carboxylic terminal group exposure [35,36]. Recently, Antunes and collaborators [25] showed that the aqueous suspensions of $(PhSe)_2$ poly(lactic acid) nanoparticles presented an increase in particle sizes and PDI after few days of storage, suggesting inferior stability than the nanocapsules developed in the current study. In order to expand the studies concerning the compound stability, the $(PhSe)_2$ photodegradation profile was evaluated through its exposure to UVC radiation. After 120 min of exposure, there was a significant decrease in the $(PhSe)_2$ content in the methanolic solution, while nanocapsules kept the compound content unaltered. This effect has already been reported to PCL nanocapsules due to reflection and/or scattering ultraviolet light, as recently stated by our group [38,39]. Additionally, the nanometric size can contribute to radiation scattering and to photostability improvement [40]. Furthermore, reinforcing these data, the thermogravimetric results demonstrated distinct degradation profiles of the pure substances and nanocapsule suspensions. The first stage of nanocapsules degradation was registered around 100 °C, which is earlier then pure substances. However, nanocapsules presented an inferior loss weight than $(PhSe)_2$ and PCL at the same temperature, suggesting that the nanostructured systems have superior thermal

stability than the raw materials. These results are in accordance with our recent study [28], which demonstrated that $(OMePhSe)_2$-loaded PCL nanocapsules are more stable then bulk substances. Therefore, the $(PhSe)_2$ nanoencapsulation provided superior stability to the compound, and, to the best of our knowledge, this is the first study that focuses on the $(PhSe)_2$-loaded nanocapsules stability.

The melanoma is responsible for most of skin cancer-related death, due to its aggressiveness, high metastasis susceptibility and drug resistance [1–3]. In general, the main problems of the conventional cancer therapy are the selectivity lack and drug resistance, based on the cellular and non-cellular mechanisms [41,42]. Usually, antitumor drugs have an elevate distribution volume, which leads to toxicity both tumor and normal cells, triggering serious side effects and limiting the maximum allowable dose of the drugs [24,41,42]. The nanocarriers systems are useful tools to circumvent these limitations and improve the cancer therapy since they can modify the drugs distribution profile, favor the drug accumulation in tumor microenvironment and reduce its dose. These changes can lead to an improvement of therapy efficacy and a side effects reduction [24,41–43].

Covering lines of evidence suggest that organoselenium compounds are promising candidates for chemoprevention due to their many biological effects [44]. In fact, the literature presents some studies reporting the *in vitro* antitumor effect of $(PhSe)_2$ against human neuroblastoma cell [13], human colon adenocarcinoma cells [12], breast cancer cells [11] and an *in vivo* study demonstrating the chemopreventive property of $(PhSe)_2$ by dietary supplementation [10]. The reports mentioned above demonstrated the $(PhSe)_2$ potential towards the cancer treatment. In front of this, we focused our efforts to investigate the $(PhSe)_2$ antimelanoma effect instead of other structural analogs such as the $(OMePhSe)_2$. Nevertheless, due to the $(PhSe)_2$ lipophilic character, this compound presents low oral bioavailability, high plasmatic protein binding, elevate adipose tissue accumulation and its intravenous administration is a challenge [15,16]. These limitations could provide low therapeutic efficacy and toxicity in health cells. In such context, this is the first report about the $(PhSe)_2$ antitumor effect against human melanoma cells (A375 cell line). Despite our findings demonstrate that both compound forms had similar IC_{50} values, the $(PhSe)_2$-loaded nanocapsules formulation was less toxic for keratinocytes, which highlights the potential to be used in further studies as an alternative therapy for melanoma management.

Nowadays, as alternative approach to study the potential toxicity of any molecule/formulation are the *in vitro* tests. These assays allow performing a detailed toxicity evaluation minimizing the animal model usage. Cytotoxicity evaluations support a better nanostructure systems characterization mainly because of the many factors that may influence in nanotoxicology such as size, shape, surface charge, among others [45,46]. The results of cytotoxicity on keratinocytes demonstrate that the free $(PhSe)_2$ caused a decrease in the cell viability, indicating a nonselective toxic effect. On the other hand, the NC $(PhSe)_2$ formulation did not modify the viability of keratinocyte cells, which suggests that the compound incorporation into the nanocapsules reduces compound toxicity and also promotes a selectivity to tumor cells. As a complementary *in vitro* evaluation, human blood cells were used as cytotoxicity parameter. In the experimental conditions used in this study, any cytotoxic effect was detected. However, Bueno and collaborators [47], using the trypan blue exclusion method, demonstrated a significant lymphocyte viability reduction of about 20% after 3 h of incubation with free $(PhSe)_2$, at 50 μM concentration [47]. In other study, the MTT reduction assay was used in comparison with other methods to determine the free $(PhSe)_2$ effect in V79 cell viability Chinese lung fibroblast. After incubation, a significant decrease in cell viability was observed. However, for the MTT test, free $(PhSe)_2$ treatment was considerably less toxic [48], suggesting that this compound has low toxicity to mitochondria. Besides that, this study has some weaknesses that need to be acknowledged for proper interpretation. In this regard, we do recognize that the MTT technique has some limitations and an appropriate experimental design would apply more assays in order to provide a complete comprehension regarding the effect on living cells. Even devoid additional *in vitro* tests, the nanoencapsulation promoted a selective and superior cytotoxic effect of $(PhSe)_2$ against the human melanoma A375 cell line in comparison to free compound, which was successfully demonstrated using the MTT assay. Further studies have been carried out to investigate the possible mechanisms underlying such action, using more sensitive and selective methods than the MTT assay. Thus, we demonstrate, for the first time, the development and characterization of $(PhSe)_2$-loaded nanocapsules formulation in addition to its promising antimelanoma potential.

5. Conclusion

In conclusion, polymeric nanocapsules containing $(PhSe)_2$ employing PCL as polymeric shell and MCT as oil core were successfully developed. The $(PhSe)_2$ NC formulations presented characteristics of a colloidal drug delivery system and superior chemical stability. Furthermore, the formulation had a potential cytotoxic effect against A375 melanoma cells without causing any toxicity to health cells (keratinocyte and blood cells). Therefore, our results show that the polymeric nanocapsules containing $(PhSe)_2$ could be considered a promising alternative for melanoma treatment due to its higher chemical stability and lack of toxicity in comparison to the free compound. Following up on this study, studies with more sensitive methods should be carried out to better understand the $(PhSe)_2$ and NC $(PhSe)_2$ antimelanoma effect.

Conflict of interest

The authors report no conflict of interests.

Acknowledgements

We thank Coordenação de Aperfeiçoamento de Pessoal de Nível Superior (CAPES) - Brazil for the scholarship (L. M. Ferreira) and C.B. Silva for the zetasizer access.

Appendix A. Supplementary data

Supplementary data to this article can be found online at https://doi.org/10.1016/j.msec.2018.05.014.

References

[1] N.K. Haass, K.S.M. Smalley, L. Li, M. Herlyn, Adhesion, migration and communication in melanocytes and melanoma, Pigment Cell Res. 18 (2005) 150–159.
[2] R.B. Rigon, M.H. Oyafuso, A.T. Fujimura, M.L. Gonçalez, A.H.D. Prado, M.P.D. Gremião, M. Chorilli, Nanotechnology-based drug delivery systems for melanoma antitumoral therapy: a review, Biomed. Res. Int. 2015 (2015) 1–22.
[3] D. Grossman, D.C. Altieri, Drug resistance in melanoma: mechanisms, apoptosis, and new potential therapeutic targets, Cancer Metastasis Rev. 20 (2001) 3–11.
[4] D. Kavanagh, A.D.K. Hill, B. Djikstra, R. Kennelly, E.M.W. McDermott, N.J. O'Higgins, Adjuvant therapies in the treatment of stage II and III malignant melanoma, Surgeon 3 (2005) 245–256.
[5] S. Schreiber, E. Kampgen, E. Wagner, D. Pirkhammer, J. Trcka, H. Korschan, A. Lindemann, R. Dorffner, H. Kittler, F. Kasteliz, Z. Kupcu, A. Sinski, K. Zatloukal, M. Buschle, W. Schmidt, M. Birnstiel, R.E. Kempe, T. Voigt, H.A. Weber, H. Pehamberger, R. Mertelsmann, E.-B. Brocker, K. Wolff, G. Stingl, Immunotherapy of metastatic malignant melanoma by a vaccine consisting of autologous interleukin 2-transfected cancer cells: outcome of a phase I study, Hum. Gene Ther. 10 (1999) 983–993.
[6] R.W. Dubois, S.M. Swetter, M. Atkins, K. McMasters, R. Halbert, S.J. Miller, R. Shiell, J. Kirkwood, Developing indications for the use of sentinel lymph node biopsy and adjuvant high-dose interferon alfa-2b in melanoma, Arch. Dermatol. 137 (2001).
[7] V.K. Sondak, G.T. Gibney, Indications and options for systemic therapy in melanoma, Surg. Clin. N. Am. 94 (2014) 1049–1058.
[8] C.W. Nogueira, J.B.T. Rocha, Diphenyl diselenide a janus-faced molecule, J. Braz. Chem. Soc. 21 (2010) 2055–2071.
[9] R.M. Rosa, R. Roesler, A.L. Braga, J. Saffi, J.A.P. Henriques, Pharmacology and toxicology of diphenyl diselenide in several biological models, Braz. J. Med. Biol.

Res. 40 (2007) 1287–1304.
[10] N.B. de Vargas Barbosa, C.W. Nogueira, T.N. Guecheva, M. de Lourdes Bellinaso, J.B.T. Rocha, Diphenyl diselenide supplementation delays the development of *N*-nitroso-*N*-methylurea-induced mammary tumors, Arch. Toxicol. 82 (2007) 655–663.
[11] M.T. Melo, I.M. de Oliveira, I. Grivicich, T.N. Guecheva, J. Saffi, J.A.P. Henriques, R.M. Rosa, Diphenyl diselenide protects cultured MCF-7 cells against tamoxifen-induced oxidative DNA damage, Biomed Pharmacother 67 (2013) 329–335.
[12] F. Nedel, V.F. Campos, D. Alves, A.J.A. McBride, O.A. Dellagostin, T. Collares, L. Savegnago, F.K. Seixas, Substituted diaryl diselenides: cytotoxic and apoptotic effect in human colon adenocarcinoma cells, Life Sci. 91 (2012) 345–352.
[13] T. Posser, M.T. de Paula, J.L. Franco, R.B. Leal, J.B.T. da Rocha, Diphenyl diselenide induces apoptotic cell death and modulates ERK1/2 phosphorylation in human neuroblastoma SH-SY5Y cells, Arch. Toxicol. 85 (2010) 645–651.
[14] R. Moreira Rosa, R.B. de Oliveira, J. Saffi, A.L. Braga, R. Roesler, F. Dal-Pizzol, J.C. Fonseca Moreira, M. Brendel, J.A. Pêgas Henriques, Pro-oxidant action of diphenyl diselenide in the yeast *Saccharomyces cerevisiae* exposed to ROS-generating conditions, Life Sci. 77 (2005) 2398–2411.
[15] M. Prigol, C.A. Brüning, F. Martini, C.W. Nogueira, Comparative excretion and tissue distribution of selenium in mice and rats following treatment with diphenyl diselenide, Biol. Trace Elem. Res. 150 (2012) 272–277.
[16] M. Prigol, C.W. Nogueira, G. Zeni, M.R. Bronze, L. Constantino, Physicochemical and biochemical profiling of diphenyl diselenide, Appl. Biochem. Biotechnol. 169 (2013) 885–893.
[17] F.A. Dimer, R.B. Friedrich, R.C.R. Beck, S.S. Guterres, A.R. Pohlmann, Impactos da nanotecnologia na saúde: produção de medicamentos, Quím. Nova 36 (2013) 1520–1526.
[18] L.A. Frank, R.V. Contri, R.C.R. Beck, A.R. Pohlmann, S.S. Guterres, Improving drug biological effects by encapsulation into polymeric nanocapsules, Wiley Interdiscip. Rev. Nanomed. Nanobiotechnol. 7 (2015) 623–639.
[19] J. Shi, A.R. Votruba, O.C. Farokhzad, R. Langer, Nanotechnology in drug delivery and tissue engineering: from discovery to applications, Nano Lett. 10 (2010) 3223–3230.
[20] W. Badri, R. Eddabra, H. Fessi, A. Elaissari, Biodegradable polymer based nanoparticles: dermal and transdermal drug delivery, J. Colloid Sci. Biotechnol. 3 (2014) 141–149.
[21] C.E. Mora-Huertas, H. Fessi, A. Elaissari, Polymer-based nanocapsules for drug delivery, Int. J. Pharm. 385 (2010) 113–142.
[22] P. Couvreur, G. Barratt, E. Fattal, P. Legrand, C. Vauthier, Nanocapsule technology: a review, Crit. Rev. Ther. Drug Carrier Syst. 19 (2002) 99–134.
[23] P.D. Marcato, N. Durán, New aspects of nanopharmaceutical delivery systems, J. Nanosci. Nanotechnol. 8 (2008) 2216–2229.
[24] L. Mei, Z. Zhang, L. Zhao, L. Huang, X.-L. Yang, J. Tang, S.-S. Feng, Pharmaceutical nanotechnology for oral delivery of anticancer drugs, Adv. Drug Deliv. Rev. 65 (2013) 880–890.
[25] O. dos Reis Antunes Junior, E. Antônio, R.M. Mainardes, N.M. Khalil, Preparation, physicochemical characterization and antioxidant activity of diphenyl diselenide-loaded poly(lactic acid) nanoparticles, J. Trace Elem. Med. Biol. 39 (2017) 176–185.
[26] C.F.A. Giordani, D. de Souza, L. Dornelles, C.W. Nogueira, M.P. Alves, M. Prigol, O.E.D. Rodrigues, Diphenyl diselenide-loaded nanocapsules: preparation and biological distribution, Appl. Biochem. Biotechnol. 172 (2013) 755–766.
[27] M.H. Marcondes Sari, L.M. Ferreira, V.A. Zborowski, P.C.O. Araujo, V.F. Cervi, C.A. Brüning, L. Cruz, C.W. Nogueira, *p,p′*-Methoxyl-diphenyl diselenide-loaded polymeric nanocapsules are chemically stable and do not induce toxicity in mice, Eur. J. Pharm. Biopharm. 117 (2017) 39–48.
[28] M.H.M. Sari, L.M. Ferreira, V. AngonesiZborowski, P.C.O. Araujo, J.M. Nadal, P.V. Farago, L. Cruz, C.W. Nogueira, *p,p′*-Methoxyl-diphenyl diselenide incorporation into polymeric nanocapsules improves its antinociceptive action: physicochemical and behavioral studies, Colloids Surf. B: Biointerfaces 157 (2017) 464–472.
[29] F. Soares, S.T. Stefanello, F. Dobrachinski, N.R. Carvalho, G.P. Amaral, R.P. Barcelos, V.A. Oliveira, C.S. Oliveira, C.F.A. Giordani, M.E. Pereira, O.E.D. Rodrigues, Free radical scavenging in vitro and biological activity of diphenyl diselenide-loaded nanocapsules: DPDS-NCS antioxidant and toxicological effects, Int. J. Nanomedicine (2015), http://dx.doi.org/10.2147/ijn.s87190(2015)5663.
[30] C. Paulmier, Selenoorganic functional groups. Selenium reagents and intermediates in organic synthesis, Angew. Chem. 100 (1986) 25–51.
[31] H. Fessi, F. Puisieux, J.P. Devissaguet, N. Ammoury, S. Benita, Nanocapsule formation by interfacial polymer deposition following solvent displacement, Int. J. Pharm. 55 (1989) R1–R4.
[32] R. Kumari, A. Sahai, N. Goswami, Effect of nitrogen doping on structural and optical properties of ZnO nanoparticles, Prog. Nat. Sci. Mater. Int. 25 (2015) 300–309.
[33] J.B.E. Mendes, M.K. Riekes, V.M. de Oliveira, M.D. Michel, H.K. Stulzer, N.M. Khalil, S.F. Zawadzki, R.M. Mainardes, P.V. Farago, PHBV/PCL microparticles for controlled release of resveratrol: physicochemical characterization, antioxidant potential, and effect on hemolysis of human erythrocytes, Sci. World J. 2012 (2012) 1–13.
[34] R. Beck, M. Fontana, A. Beckenkamp, A. Buffon, Controlled release of raloxifene by nanoencapsulation: effect on in vitro antiproliferative activity of human breast cancer cells, Int. J. Nanomedicine (2014), http://dx.doi.org/10.2147/ijn.s62857(2014)2979.
[35] M.C. Fontana, K. Coradini, S.S. Guterres, A.R. Pohlmann, R.C. Beck, Nanoencapsulation as a way to control the release and to increase the photostability of clobetasol propionate: influence of the nanostructured system, J. Biomed. Nanotechnol. 5 (2009) 254–263.
[36] R.B. Friedrich, M.C. Fontana, R.C.R. Beck, A.R. Pohlmann, S.S. Guterres, Development and physicochemical characterization of dexamethasone-loaded polymeric nanocapsule suspensions, Quím. Nova 31 (2008) 1131–1136.
[37] A.F. Ourique, A.R. Pohlmann, S.S. Guterres, R.C.R. Beck, Tretinoin-loaded nanocapsules: preparation, physicochemical characterization, and photostability study, Int. J. Pharm. 352 (2008) 1–4.
[38] N.S. Pegoraro, J. Mattiazzi, E.F. da Silveira, J.H. Azambuja, E. Braganhol, L. Cruz, Improved photostability and cytotoxic effect of coenzyme Q10 by its association with vitamin E acetate in polymeric nanocapsules, Pharm. Dev. Technol. (2018), http://dx.doi.org/10.1080/10837450.2017.1332641(2017)1-7.
[39] M. Gehrcke, L.M. Giuliani, L.M. Ferreira, A.V. Barbieri, M.H.M. Sari, E.F. da Silveira, J.H. Azambuja, C.W. Nogueira, E. Braganhol, L. Cruz, Enhanced photostability, radical scavenging and antitumor activity of indole-3-carbinol-loaded rose hip oil nanocapsules, Mater. Sci. Eng. C 74 (2017) 279–286.
[40] P. Perugini, S. Simeoni, S. Scalia, I. Genta, T. Modena, B. Conti, F. Pavanetto, Effect of nanoparticle encapsulation on the photostability of the sunscreen agent, 2-ethylhexyl-p-methoxycinnamate, Int. J. Pharm. 246 (2002) 37–45.
[41] I. Brigger, C. Dubernet, P. Couvreur, Nanoparticles in cancer therapy and diagnosis, Adv. Drug Deliv. Rev. 54 (2002) 631–651.
[42] G. Mattheolabakis, B. Rigas, P.P. Constantinides, Nanodelivery strategies in cancer chemotherapy: biological rationale and pharmaceutical perspectives, Nanomedicine 7 (2012) 1577–1590.
[43] P. Couvreur, R. Gref, K. Andrieux, C. Malvy, Nanotechnologies for drug delivery: application to cancer and autoimmune diseases, Prog. Solid State Chem. 34 (2006) 231–235.
[44] C.W. Nogueira, J.B.T. Rocha, Toxicology and pharmacology of selenium: emphasis on synthetic organoselenium compounds, Arch. Toxicol. 85 (2011) 1313–1359.
[45] M. Adabi, M. Naghibzadeh, M. Adabi, M.A. Zarrinfard, S.S. Esnaashari, A.M. Seifalian, R. Faridi-Majidi, H. Tanimowo Aiyelabegan, H. Ghanbari, Biocompatibility and nanostructured materials: applications in nanomedicine, Artif. Cells Nanomed. Biotechnol. 45 (2016) 833–842.
[46] S. Aula, S. Lakkireddy, K. Jamil, A. Kapley, A.V.N. Swamy, H.R. Lakkireddy, Biophysical, biopharmaceutical and toxicological significance of biomedical nanoparticles, RSC Adv. 5 (2015) 47830–47859.
[47] D. Caeran Bueno, D.F. Meinerz, J. Allebrandt, E.P. Waczuk, D.B. dos Santos, D.O.C. Mariano, J.B.T. Rocha, Cytotoxicity and genotoxicity evaluation of organochalcogens in human leucocytes: a comparative study between ebselen, diphenyl diselenide, and diphenyl ditelluride, Biomed. Res. Int. 2013 (2013) 1–6.
[48] R.M. Rosa, J.D.N. Picada, J. Saffi, J.A.P. Henriques, Cytotoxic, genotoxic, and mutagenic effects of diphenyl diselenide in Chinese hamster lung fibroblasts, Mutat. Res. Genet. Toxicol. Environ. Mutagen. 628 (2007) 87–98.

SUPPLEMENTARY MATERIAL

Diphenyl diselenide loaded poly(Ɛ-caprolactone) nanocapsules with selective antimelanoma activity: development and cytotoxic evaluations

Luana Mota Ferreira[a], Verônica Ferrari Cervi[a], Marcel Henrique Marcondes Sari[b], Allanna Valentini Barbieri[a], Andiara Prates Ramos[c], Priscila Marquezan Copetti[c], Gerson Fernandes de Brum[c], Kátia Nascimento[c], Jessica Mendes Nadal[d], Paulo Vitor Farago[d], Michele Rorato Sagrillo[c], Cristina Wayne Nogueira[b], Letícia Cruz[a*].

Abstract

Diphenyl diselenide [$(PhSe)_2$] is a widely studied organoselenium compound with promising antitumor effects. However, $(PhSe)_2$ has low water solubility and bioavailability limiting its clinical application. Due to these unfavorable characteristics, polymeric nanocapsules emerge as a promising nanotechnological approach to overcome such limitations. This study aimed to develop polymeric nanocapsules containing $(PhSe)_2$ and to investigate their cytotoxic potential against melanoma cells line. Nanocapsule suspensions were prepared by the interfacial deposition of preformed polymer method andevaluatedby means of physicochemical, morphological, spectroscopic and thermal characteristics. The antimelanoma effect of $(PhSe)_2$ nanocapsules (10 – 100 µM) was evaluated against A375 human melanoma cellsline. Cytotoxicity of $(PhSe)_2$ nanocapsules (10 – 100 µM) was also determined in keratinocytes and in human blood cells. The nanocapsules had an average diameter of 240 ± 52 nm, polydispersity index of 0.15 ± 0.06, zeta potential of -10.9 ± 2.21 mV, pH 7.4 ± 0.1, $(PhSe)_2$ content of 99.01 ± 2.20 % and encapsulation efficiency around 98%. Besides, the $(PhSe)_2$ nanocapsules were spherical in shape, presented no chemical interaction among the components, and showed higher thermal stability than the raw materials. Both nanoencapsulated and free $(PhSe)_2$ reduced the viability of A375 human melanoma cells with IC_{50} 48.30 and 43.50 µM, respectively. Cytotoxicity studies showed that $(PhSe)_2$-loaded nanocapsules did not cause toxicity on keratinocytes, while the free compound at 100 µM reduced the cell viability to approximately 50%. No cytotoxicity was observed for the human mononuclear cells after the incubation with $(PhSe)_2$, independent of its form. Therefore, the $(PhSe)_2$–loaded nanocapsule suspensionscan be considered a promising formulation for the melanoma treatment.

KEYWORDS: Nanoparticles, organoselenium compounds, melanoma, antitumor.

Figures

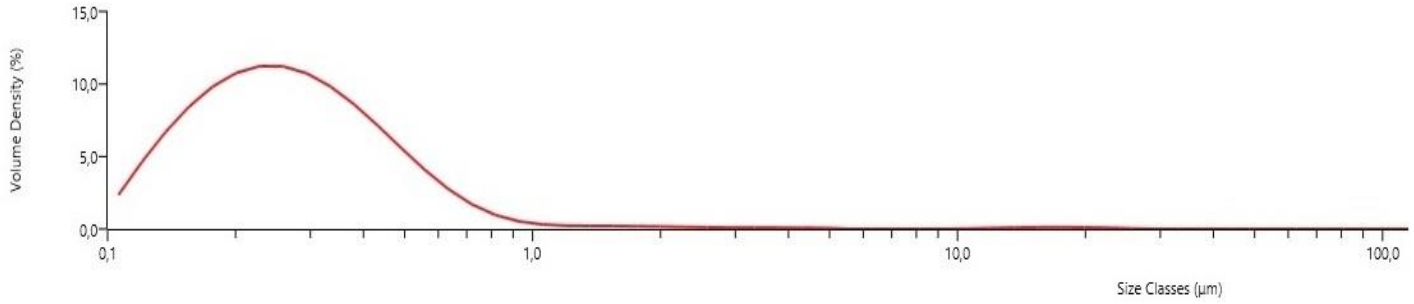

Figure 1. Granulometric distribution by laser diffraction (Mastersizer® 3000E, Malvern Instruments, UK). Refractive index: 1.59.

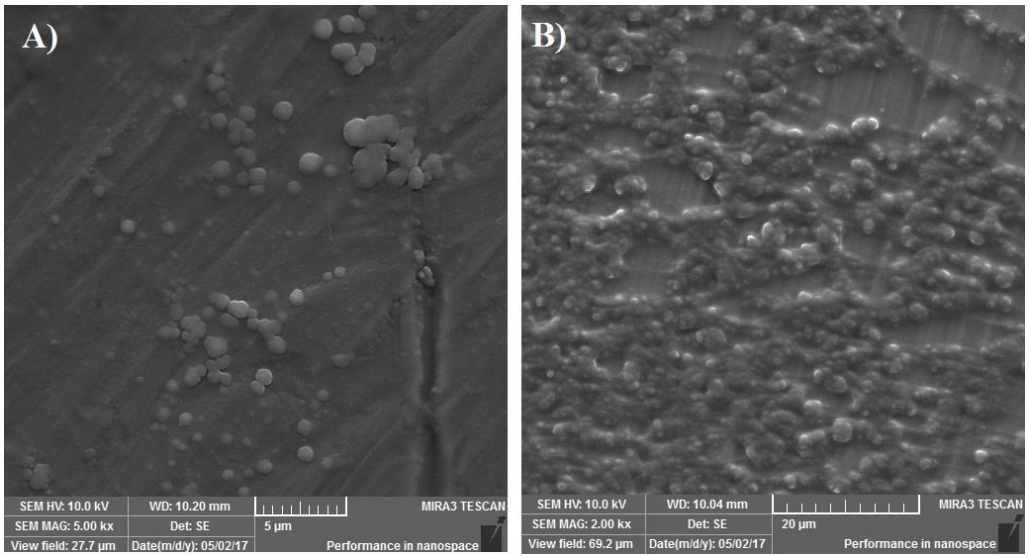

Figure 2. FEG-SEM micrographs of NC $(PhSe)_2$ (A) and NC B (B). Experimental condition: accelerating voltage: 10 kV.

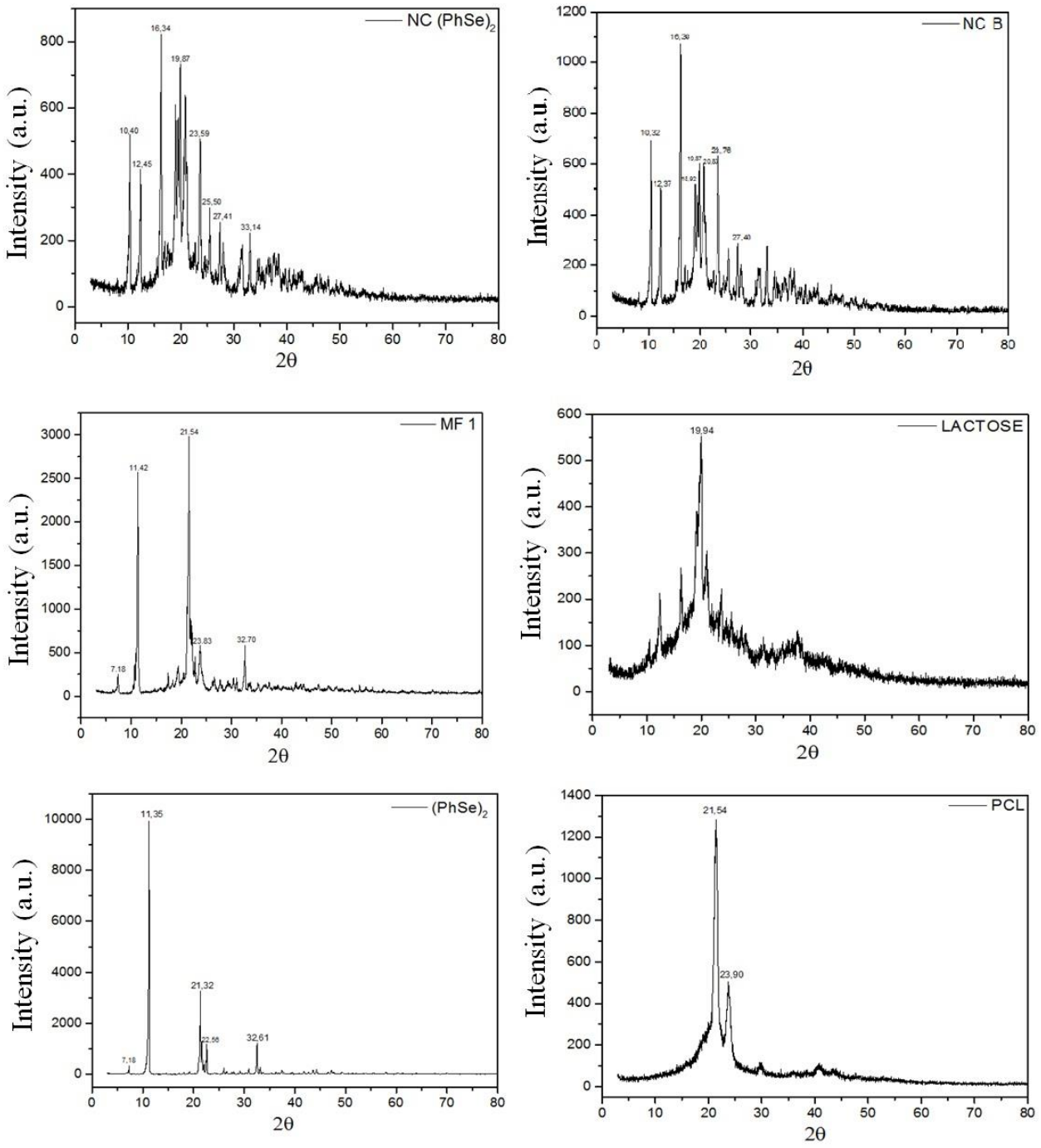

Figure 3. X-ray diffraction spectrum of NC $(PhSe)_2$, NC B, PM, Lactose, $(PhSe)_2$ and PCL.

The pure substance and formulation physical state was evaluated through wide-angle X-ray diffraction analysis using a Shimadzu X-ray diffractometer (Shimadzu XRD-6000, Kyoto, Japan). The 2θ value was increased from 5º to 80º at a scan rate of 2º/min using a Cu-Kα source (λ = 1.5418 Å) at 40 kV and 40 mA.

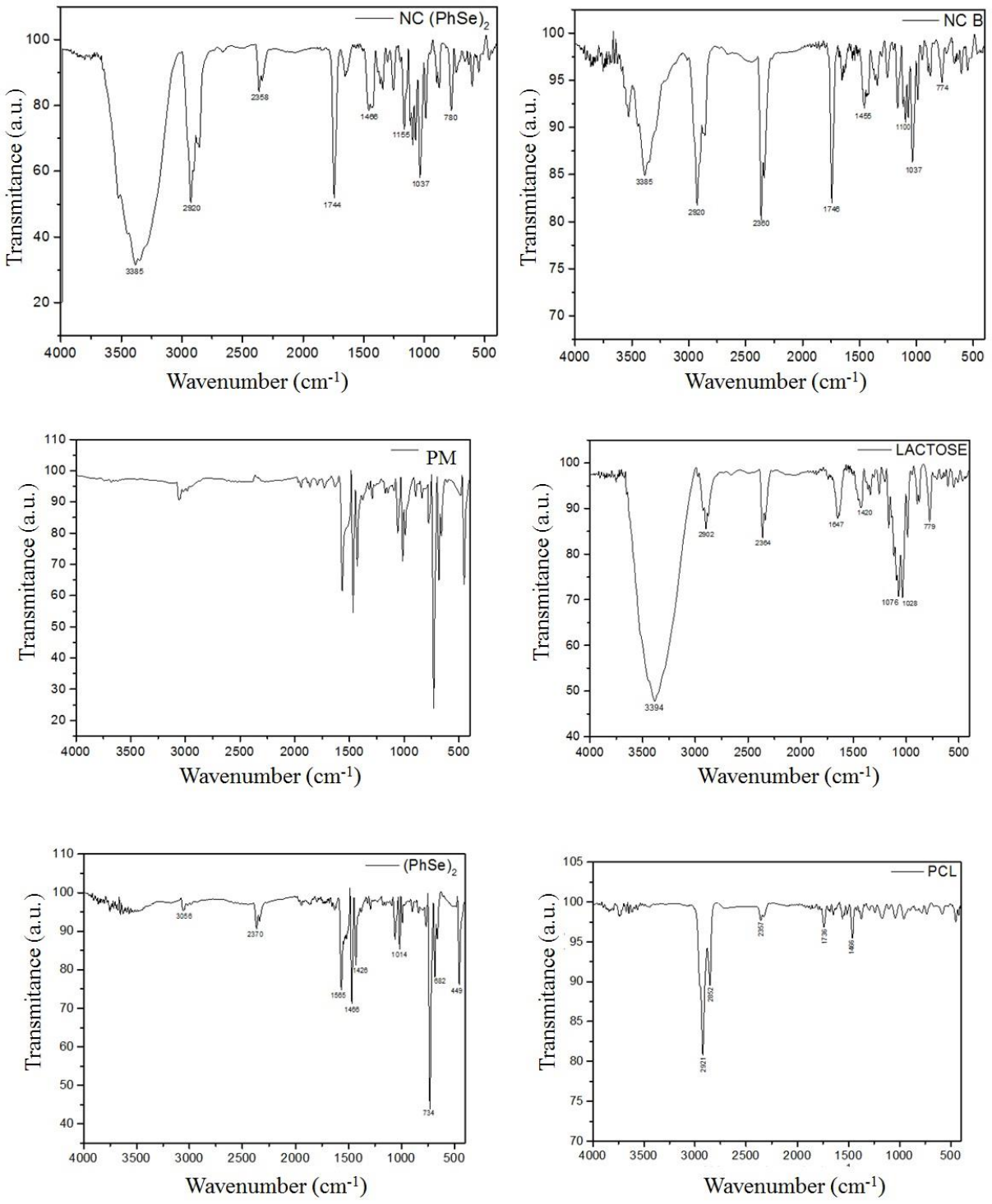

Figure 4. The FTIR spectra of NC $(PhSe)_2$, NC B, PM, Lactose, $(PhSe)_2$ and PCL. The Fourier-transformed infrared (FTIR) spectra of raw materials and nanocapsules were recorded

from 4000 to 400 cm^{-1} using a Shimadzu IR Prestige-21 spectrophotometer (Kyoto, Japan) with KBr pellets with 32 scans and a resolution of 4 cm^{-1}.

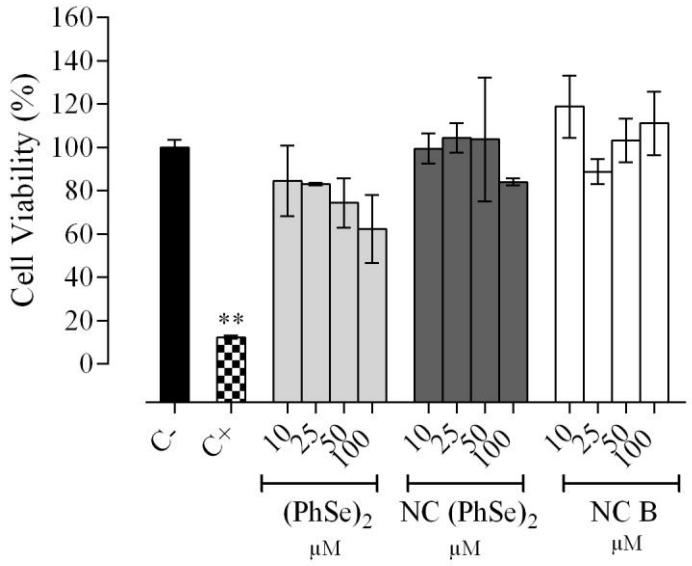

Figure 5. Cytotoxic effect of $(PhSe)_2$ and NC $(PhSe)_2$ against A375 human melanoma cells after 24 h. NC B was used as comparison purposes while RPMI culture medium were used negative control and hydrogen peroxide was used as positive control. Each column represents the mean with S.E.M. of triplicate. Asterisks denote the significance levels (**) $p<0.01$ compared to negative control, by one-way ANOVA, Tukey's post hoc test.

3.2 Manuscrito 1

Xanthan gum-based hydrogel containing nanocapsules for topical diphenyl diselenide delivery in melanoma therapy

Luana Mota Ferreira[a], Marcel Henrique Marcondes Sari[a,d], Juliana Hofstatter Azambuja[b], Elita Ferreira da Silveira[c], Verônica Ferrari Cervi[a], Marila Crivellaro Lay Marchiori[a], Marcia Rosângela Wink[b], Cristina Wayne Nogueira[d], Elizandra Braganhol[b,c], Letícia Cruz[a*].

[a]Laboratório de Tecnologia Farmacêutica, Programa de Pós-graduação em Ciências Farmacêuticas, Centro de Ciências da Saúde, Universidade Federal de Santa Maria, Santa Maria, RS, Brazil

[b]Programa de Pós-Graduação em Biociências, Universidade Federal de Ciências da Saúde, Porto Alegre 90050-170, Brazil.

[c]Programa de Pós-Graduação em Bioquímica e Bioprospecção, Centro de Ciências Químicas, Farmacêuticas e de Alimentos, Universidade Federal de Pelotas, Pelotas 96010- 900, Brazil.

[d]Laboratório de Síntese, Reatividade e Avaliação Farmacológica e Toxicológica de Organocalcogênios, Centro de Ciências Naturais e Exatas, Universidade Federal de Santa Maria, Santa Maria, RS, Brazil

*Corresponding author

Letícia Cruz, Programa de Pós-Graduação em Ciências Farmacêuticas, Universidade Federal de Santa Maria, Santa Maria, 97105-900, Brazil.

Phone: +55 55 3220 9373

E-mail: leticiacruz@smail.ufsm.br

Abstract

Melanoma is the most aggressive skin cancer and is usually refractory to conventional therapies. The diphenyl diselenide [$(PhSe)_2$] is an organoselenium compound that has antitumor effect but it presents some limitations regarding its physicochemical characteristics and toxicological issues. In this sense, its incorporation into polymeric nanocapsules has been a useful tool to circumvent its limitations and enhance its pharmacological effect. Besides, nanocarriers could be incorporate in hydrogels and they can improve the actives permeation in inner layers of skin becoming a promising alternative for topical melanoma management. Concerning that, this study aimed to evaluate $(PhSe)_2$-loaded polymeric nanocapsules (NC $(PhSe)_2$) antimelanoma effect against a resistant cell line (SK-Mel-103). In sequence, it was developed a xanthan gum-based hydrogel containing the nanocapsules and the determination of $(PhSe)_2$ permeation profile in human skin was performed. For the cytotoxic effect evaluation the cells were treated with free $(PhSe)_2$ or NC $(PhSe)_2$ (0.7 - 200 µM) and after 48 h incubation the assessment was carried out using the MTT method and such effect was further confirmed by propidium iodide uptake (necrosis marker) and the nitrite levels estimation. The *in vitro* assay demonstrated an antimelanoma effect for $(PhSe)_2$ free or nanoencapsulated. The NC $(PhSe)_2$ had a superior effect presenting a IC50 value of 47.43 µM, while the free compound had 65.05 µM. After that, the hydrogels were developed by thickening the nanocapsules suspension or $(PhSe)_2$ solution with xanthan gum and characterized in terms of average diameter, polydispersity index, pH, drug content, spreadability, rheological behavior and *in vitro* permeation. All hydrogels had pH around 7, drug content close to the theoretical value and mean diameter in the nanometric range. Besides, formulations had non-Newtonian flow with pseudoplastic behavior and suitable spreadability factor. Skin permeation studies revealed that nano-based hydrogel increased the compound content in the dermis layer demonstrating that a superior permeation was achieved by the compound encapsulation. In conclusion, the xanthan gum-based hydrogel containing NC $(PhSe)_2$ could be suggested as an adjuvant formulation in melanoma therapy.

Keywords: nano-based hydrogels, nanoparticles, cutaneous delivery, skin cancer, organoselenium compound, SK-Mel-103.

1. Introduction

Melanoma is the most aggressive skin cancer and it is responsible for the majority of deaths. The high incidence rates are linked with excessive sun exposure especially during childhood and adolescence, and with the solar radiation changes caused by the ozone layer depletion [1, 2]. The statistics are not encouraging; the number of melanoma cases has been rising over the last 30 years and according to the World Health Organization approximately 132,000 melanoma skin cancers globally occur each year [3] and around 91,210 new cases were estimated in United States for 2018 [1]. The available therapeutic approaches, which include surgical excision (initial stages), chemotherapy, radiotherapy and immunotherapy, have a high cost and cause several undesirable effects [4-6]. Furthermore, melanoma cancer is usually refractory to such conventional treatments mainly because of drug resistance by apoptosis downregulation [7]. Thus, the search for novel and improved therapies focused on a better prognostic to this disease is urgent and relevant.

A remarkable spectrum of pharmacological properties was already assigned to the class of organoselenium molecules [8, 9] and one of the most studied compounds is the diphenyl diselenide [$(PhSe)_2$] [8]. Such molecule has the simplest chemistry synthesis and diversified biological effects, including the anticancer action. Importantly, the *in vitro* $(PhSe)_2$ effectiveness against different tumor cells (human neuroblastoma, human colon adenocarcinoma and breast cancer cells) as well as in animal models of mammary cancer was previously demonstrated, supporting the hypothesis of its potential application towards cancer treatment [10-13]. However, some toxicity issues [8] and physicochemical limitations, for instance: poor aqueous solubility, high Log D values and elevated plasma protein binding rates [14], negatively counterbalance $(PhSe)_2$ biological applications in a way that delays the development of more advanced studies.

In this sense, the nanotechnology field has received special attention because of the benefits that are achieved by encapsulating molecules [15-17]. Among the most studied nanocarrier systems, nanocapsules are vesicular colloidal structures composed by an oil core surrounded by a polymer layer [18]. In addition, such nanostructures have been widely studied for cancer management due to their advantages in comparison to conventional approaches [15, 16, 19]. The application of this pharmaceutical tool becomes an interesting alternative to overcome the aforementioned physicochemical limitations. In fact, some studies regarding the $(PhSe)_2$ incorporation into polymeric nanocapsules have shown a

general improvement in its tissue biodistribution and biological effects [20, 21]. Moreover, in our recent study the $(PhSe)_2$-loaded polymeric nanocapsules effectiveness against human melanoma cells (A375) was demonstrated, for the first time, using *in vitro* assays. The nanoformulation had adequate physicochemical characteristics and was not toxic to keratinocytes cells whereas free $(PhSe)_2$ reduced the keratinocytes viability [22]. These characteristics reinforce the positive impact of the $(PhSe)_2$ encapsulation and encourages further studies regarding the formulation application in the cancer management.

Despite their advantages, nanocapsules are obtained as a liquid suspension, which complicates its adequate cutaneous application. Considering melanoma management, in recent years topical treatment is emerging as an adjuvant therapy for patients who refuse surgery or in cases where this procedure is not recommended. Some Food and Drug Administration (FDA) approved drugs are being employed as topical therapy for skin cancer, as 5-fluoruracil and imiquimod creams, and besides that, some common anti-inflammatory drugs, such diclofenac and ibuprofen, were used as a complementary treatment [6, 23-25]. Regarding the literature, the incorporation of nanocapsule suspensions in semisolid vehicles can benefit topical treatments. The nanostructures can increase the drug retention time in the stratum corneum, furrows, pores and hair follicles, modulating the drug release and improving the local pharmacological effect. Additionally, due to the small size, the topical formulations containing nanocarriers can increase the drug penetration/permeation in deeper skin layers consequently reaching the bloodstream what can play a role as a transdermal system [26, 27].

The synthetic polymers as Carbopol Ultrez® [28-32], Carbomer Ultrez® [33] and Pemulen TR1® [34] are the most used materials to prepare semisolid formulations containing nanocarriers. Recently, our research group reported the polysaccharides potential properties to form hydrogels from liquid nanocapsule suspensions intended to cutaneous application. The simple thickening of nanocapsules suspension with the gellan gum, a natural polysaccharide, produced a hydrogel that had adequate physicochemical and rheological characteristics as well as improved biological effects in comparison to the formulations with non-encapsulated active [35, 36]. In a similar approach, in this study xanthan gum, which is an anionic polysaccharide produced by the bacteria Xanthomonas campestris [37], was applied as a new thickening agent for $(PhSe)_2$-loaded nanocapsule suspensions.

Taking all of this into account, the current study evaluated the $(PhSe)_2$-loaded nanocapsules antimelanoma effect against a resistant malignant melanoma cells line (SK-Mel-103). Besides, to propose a final formulation intending to melanoma adjuvant treatment, a xanthan gum-based hydrogel containing $(PhSe)_2$ nanocapsules was developed and the permeation profile of $(PhSe)_2$ in human skin was investigated.

2. Material and Methods

2.1 Material

Poly(Ɛ-caprolactone) (PCL) (MW: 80 KDa) and Span 80® (sorbitan monooleate) were acquired from Sigma Aldrich (Brazil). Tween 80® (polysorbate 80) and Medium Chain Triglycerides (MCT) were furnished by Delaware (Brazil). Dulbecco's modified Eagle's medium (DMEM), Fungizone, penicillin/streptomycin, 0.25% trypsin/EDTA solution and fetal bovine serum (FBS) were obtained from Gibco (Gibco BRL, Carlsbad, CA, USA). All other chemicals and solvents were obtained from standard commercial suppliers with analytical grade standard and were used as received.

2.2 Compound

The $(PhSe)_2$ was obtained following the method previously described by Paulmier [38]. Chemical purity of the compound (99.9 %) was assessed by gas chromatography-mass spectrometry and high-performance liquid chromatography (Shimadzu QP2010PLUS GC/MS). The ^{1}H and ^{13}C nuclear magnetic resonance spectra were obtained at 400 MHz (Bruker AvanceTM III HD) and showed analytical and spectroscopic data in full agreement with the assigned structure.

2.3 Nanocapsules suspension

Nanocapsules suspension containing $(PhSe)_2$ were prepared by the interfacial deposition of preformed polymer methodology [18] and characterized (average diameter, polidispersity index, zeta potential, pH, $(PhSe)_2$ content and encapsulation efficiency) as described in our previous report [22]. Briefly, an organic phase composed by PCL (0.1 g), Span 80® (0.077 g), MCT (330 µL), acetone (27 mL), and $(PhSe)_2$ (0.05 g) was magnetically stirred at 40 °C for 60 min to solubilize the constituents. Following, the organic phase was injected into a Tween 80® (0.077 g) aqueous

dispersion (53 mL) and this mixture was magnetically stirred for 10 min longer at room temperature. Next, the solvent was eliminated by evaporation under reduced pressure to achieve 10 mL of final volume, which corresponds to a $(PhSe)_2$ concentration of 5.0 mg/mL in the formulation (NC $(PhSe)_2$). For comparison purposes, nanocapsules without $(PhSe)_2$ were also formulated (NC B).

2.4 In vitro antimelanoma effect

2.4.1 General Cell Culture Procedures

The melanoma cell lines SK-Mel-103 were purchased from American Type Culture Collection (ATCC - Rockville, MD, USA). As a complementary analysis, the NC $(PhSe)_2$ antimelanoma effect was also determined in SK-Mel-28 (human) and B16F10 (murine) cells line, which were also obtained from ATCC. The genetic profile of human melanoma cell lines is shown in Table 1. The melanoma cell lines SK-Mel-103, SK-Mel-28 and B16F10 were growth in DMEM containing 0.1% Fungizone and 100 U/L penicillin/streptomycin and supplemented with 5% (v/v) fetal bovine serum (FBS). After the cultures reached confluency, the cells were released by trypsinization in the cultivation bottle. The cells were seeded in 96 well plates, which were maintained at 37 °C in a humidified atmosphere of 5% CO_2 for 24 h before the experiments. The plates containing SK-Mel-103 cells were incubated with NC $(PhSe)_2$ and free $(PhSe)_2$, at the concentration range of 0.7 - 200 µM for 48h. The SK-Mel-28 and B16F10 cells were treated with samples at concentrations of 10 - 100 µM and incubated for 48h. To achieve such concentrations, 10-fold serial dilutions were made using RPMI culture medium from the $(PhSe)_2$ nanocapsules suspension or the stock solution of free $(PhSe)_2$, which was dissolved in DMSO (10 %). Cells treated with DMSO (10 %) or NC B were used for comparison purposes.

2.4.2 Cell viability measurement by 3(4-5-dimethyl)-2-5diphenyl tetrazolium bromide (MTT) salt reduction assay

The test was carried out according to the methodology described in our previous study [22]. After the incubation with the respective treatments, the cells were washed twice with sodium phosphate buffer and an amount of the yellow tetrazolium salt MTT solution (1 mg/mL) was added to the 96 well plate. Then, the plates were incubated at

37 °C for 3 h and under light protection until it was observed the presence of violet formazan crystals. Subsequently, the solution was removed and the plates were shaken with DMSO for 30 min. The optical density of each well plate was measured at 492 nm and the results were expressed by cell viability (%) in comparison to the DMEM culture medium, which was used as the negative cell death control.

2.4.3 Microscopic images of SK-Mel-103 cells

After the incubation, SK-Mel-103 cells density was evaluated using an inverted microscope (Olympus IX71, Tokyo, Japan).

2.4.4 Nitrite content determination

The Griess reaction was used to estimate the nitrite (NO_2^-) levels, as a nitric oxide (NO) marker, in the culture medium [39] after SK-Mel-103 cells incubation with $(PhSe)_2$, free and nanoencapsulated. Briefly, culture supernatant was mixed with sulfanilamide in 5% phosphoric acid, followed by an incubation at room temperature during 10 min. Then, n-1l-napthylethylenediamine (NED) 0.1% was added to the samples and incubated protected from light for 10 min to complete the reaction. The absorbance was determined in a spectrophotometer at 540 nm. The amount of nitrite in the supernatant was determined using a sodium nitrate standard curve and the results were expressed as μM of NO_2^-.

2.4.5 Propidium iodide assay

SK-Mel-103 cell damage was assessed by fluorescent imaging of propidium iodide (PI) uptake. At the end of the treatments, cells were gently washed with calcium -magnesium free (CMF) buffer and incubated with PI (7.5 μM) for 1 h. PI fluorescence was excited at 515-560 nm using an inverted microscope (Olympus IX71, Tokyo, Japan) equipped with a standard rhodamine filter. The images were captured with a digital camera connected to microscope.

2.5 Hydrogels preparation

Hydrogels (HG) were prepared using mortar and pestle by directly adding the formulation (10 mL) in 0.3 g of xanthan gum (HG NC $(PhSe)_2$) to obtain around 10 g

of HG [35, 36]. For the HG containing free $(PhSe)_2$ (HG $(PhSe)_2$), the compound was prior solubilized in a mixture of MCT (330 µL) and DMSO (670 µL). Following, it was added to a previously prepared xanthan gum dispersion (3 %) in water (9 mL). Both HG presented a final $(PhSe)_2$ concentration of 5 mg/g. HGs containing the vehicles, NC B (HG NC B) and a xanthan gum dispersion (3%) containing a mixture of MCT and DMSO (HG V), were concomitantly prepared and characterized for comparison purposes.

2.6 Hydrogels characterization

The following parameters were used to characterize the HGs: nanocapsules average diameter, polydispersity index, pH and $(PhSe)_2$ content.

2.6.1 Average diameter and polydispersity evaluations

The nanocapsules average diameter in hydrogels was determined using ZetaSizer Nano Series Malvern Instruments (UK), by photon correlation spectroscopy method. For this, an aliquot of HGs (0.1 g) was dispersed in 50 mL ultrapure water (1:500) and than filtered to performed the analyze. The measurements were conducted at room temperature.

2.6.2 pH measurements

The pH values were evaluated using a previous calibrated potentiometer (Model pH 21, Hanna Instruments, Brazil) by the direct immersion of the electrode in an aqueous dispersion of each hydrogel (10%, w/v).

2.6.3 $(PhSe)_2$ content in hydrogels

The $(PhSe)_2$ content in the hydrogels was determined by HPLC employing the analytical methodology described in our previous study [22]. For this, an amount of HGs (0.05 g) was dispersed in 25 mL of acetonitrile:acetone (1:1, v/v), submitted to 30 min of magnetic stirring followed by 30 min of sonication. Then, samples were filtered through a 0.45 µm membrane and injected into the equipment. Brief, the compound quantification was performed on a LC-10A HPLC system (Shimadzu, Japan) equipped with a LC-20AT pump, a UV-VIS SPD-M20A detector, a CBM-20A system controller

and a SIL-20A HT valve sample automatic injector. Separation was achieved at room temperature using a Gemini C18 Phenomenex column (150 mm x 4.60 mm, 5 μm; 110 Å) coupled to a C18 guard column. The $(PhSe)_2$ was detected at a wavelength of 243 nm and a mixture of methanol and water (80:20, v/v) was used as isocratic mobile phase at a flow rate of 1 mL/min.

2.7 Stability evaluation

Aiming to evaluate the stability of the formulations, the HGs were stored in plastic containers at room temperature (25 °C). At predetermined time intervals (0, 15 and 30 days), the average diameter, PDI, pH, and compound content in the HGs were assessed as previously described in *section 2.6.*

2.8 Spreadability determination

The spreadability of HGs was evaluated according to Rigo and coworkers [40] based on the parallel plate method. An amount of each HGs was placed in a central hole (1 cm diameter) of a mold glass plate, which was positioned on the scanner surface (HP Officejet, model 4500 Desktop). The mold plate was carefully removed and the sample was subsequently pressed with glass plates of known weights, during an interval of 1 min to each added plate. To determine the spreadability profile, an image of each spreading area was captured employing the desktop scanner and the respective area of the images were quantified using the software ImageJ (Version 1.49q, National Institutes of Health, USA). The spreadability factor (Sf) was calculated using the Eq. (1). Such parameter represents the spreading capacity on a smooth horizontal surface when one gram of weight is added to it.

$$Eq\ (1)\ Sf = A/W$$

where Sf is the spreadability factor (mm^2/g), A is the maximum spread area (mm^2) after addition of the total number of plates, and W is the total weight added (g).

2.9 Rheological behavior

To determine the rheological behavior a Brookfield viscometer (RVDV-IPRIME model, Brookfield, USA) was employed using a RV06 spindle. An amount of

approximately 30 g of HG NC $(PhSe)_2$ or HG $(PhSe)_2$ was submitted to a speed range from 2 to 100 rpm at room temperature (25 ± 1 ˚C). Besides, to better understanding the rheological behavior of the HGs, the experimental data was fitted to the mathematical models of Bingham (*Eq.2*), Casson (*Eq.3*) and Ostwald (*Eq.4*) [35].

$$Eq.\ (2)\ \tau = \tau^0 + \eta\gamma$$

$$Eq\ (3)\ \tau^{0.5} = \tau^{00.5} + \eta^{0.5}\,\gamma^{0.5}$$

$$Eq.\ (4)\ \tau = \kappa\gamma^n$$

where τ0 is the yield stress, η is the viscosity, *n* is the index of flow, K is the index of consistency, τ is the shear stress and γ is the shear rate.

2.10 In vitro skin permeation studies

2.10.1 Skin sample preparation

Skin samples were obtained from a healthy female patient who had undergone to abdominal plastic surgery. The protocol was approved by the committee for research with humans of Federal University of Santa Maria with no identifying data (CAEE: 552200016.3.0000.5346). The subcutaneous fat was carefully removed and the skin was cut in circles. Following, the tissue was wrapped in aluminum foil and stored at -20 ºC until it uses.

2.10.2 Permeation experiments

The study of the compound permeation profile from the HGs was carried out using vertical Franz-type diffusion cells applying human skin as barrier (surface area of 3.14 cm^2). The skin explants were harvested and mounted on the diffusion cells with the stratum corneum facing upwards to the donor compartment (in contact with the HG) and the dermis in contact with the receptor media. The receptor compartment was filled with phosphate buffer pH 5.5, at 32 ± 0.5 °C and magnetically stirred. An amount of HGs (HG NC $(PhSe)_2$ and HG $(PhSe)_2$) corresponding to 0.5 g of $(PhSe)_2$ (infinite dose) was spread on the skin surface. After 8 h, the HG was removed from the skin surface and the tissue and the receptor media were collected. The skin was dissected in its layers prior the compound determination. The stratum corneum (SC) was separated

by the tape stripping technique with 18 tapes (Adelbras®) and the viable epidermis (VE) and dermis (DE) were separated by heating the tissue in a water bath at 60 ºC for 45 s [27]. The compound was extracted from the skin layers with methanol (4 mL for SC, 1 mL for the VE and 2 mL for DE) followed by vortex mixing (2 min) and sonication (15 min). Each sample was filtered (0.45 µm membrane) and the $(PhSe)_2$ was quantified by the previously described HPLC method (section *2.6.3*). The method was previously validated to determine the $(PhSe)_2$ recovery (%) and specificity. The recovery was performed using a system containing tape samples (Adelbras®) and pieces of full skin, which was contaminated with a compound solution (15 µg/mL) and subjected to the same experimental protocol described above. The specificity was tested following the same protocol but without the $(PhSe)_2$ contamination. The recovery percentages were 96.82 ± 4.70 %, indicating that the Adelbras® tape was considered an adequate material for tape strips. Furthermore, no interference in the $(PhSe)_2$ chromatogram was observed.

2.11 Statistical analysis

Formulations were prepared and analyzed in triplicate and the results were expressed as mean ± S.E.M. The GraphPad Prism® version 6 software was used to perform the Student's *t* test and variance analyses one-way (ANOVA) followed by post-hoc Tukey's test. Values of $p<0.05$ were considered statistically significant. The IC50 values were calculated by linear regression using the GraphPad Prism® version 6.

3. Results

3.1 In vitro antimelanoma effect by MTT assay

In order to determine the $(PhSe)_2$ antitumor effect against resistant melanoma cells (SK-Mel-103) a concentration curve was performed (0.7 - 200 µM; Fig. 1). Both $(PhSe)_2$ and NC $(PhSe)_2$ reduced the SK-Mel-103 cell viability ($p<0.05$ by One-way ANOVA followed by Tukey's test), but the NC $(PhSe)_2$ had superior cytotoxicity effect than $(PhSe)_2$ at minor concentrations (6 µM and 12 µM, reducing cell viability to 55.49 ± 20.27 % and 40.28 ± 12.08 %, respectively; $p<0.05$ by One-way ANOVA followed by Tukey's test). The NC B caused no alteration in the cell viability ($p>0.05$ by Oneway ANOVA followed by Tukey's test). The IC50 values showed that NC $(PhSe)_2$ had

higher antitumor effect than free compound (47.43 µM and 65.05 µM to NC $(PhSe)_2$ and $(PhSe)_2$, respectively).

As a complementary analysis, the antitumor effect against other melanoma cell lines was also determined by MTT assay. The cytotoxic effect of nanocapsules suspension against B16F10 melanoma cells was demonstrated in supplementary material (Fig. S1 A). The NC $(PhSe)_2$ had cytotoxic effect at all concentrations (10 - 100µM) ($p<0.05$ by One-way ANOVA followed by Tukey's test) decreasing the cell viability to 59.05 ± 13.39 % (100µM). There was no statistical difference among the NC $(PhSe)_2$ concentrations ($p<0.05$). Besides, free $(PhSe)_2$ reduced cell viability at concentration range 25 - 100 µM ($p<0.05$ by One-way ANOVA followed by Tukey's test), reaching a maximum effect at 100 µM (68.49 ± 11.39 %). NC B and DMSO did not cause any significant alteration in cell viability ($p>0.05$ by One-way ANOVA followed by Tukey's test).

Figure S1 B depicts the cytotoxic effect of $(PhSe)_2$ against human malignant melanoma cell line (SkMel-28). The NC $(PhSe)_2$ had cytotoxic effect at all concentrations (10 - 100µM) ($p<0.05$ by One-way ANOVA followed by Tukey's test) decreasing the cell viability to 58.10 ± 6.79 %. Concerning the free $(PhSe)_2$, it was observed a decrease in cell viability around 56.34 ± 4.50 % at concentration range 25 - 100 µM ($p<0.05$ by One-way ANOVA followed by Tukey's test). The NC B reduced the cell viability around 75 % independently of the concentration tested (10 - 100µM) ($p<0.05$ by One-way ANOVA followed by Tukey's test). DMSO did not have any effect in cell viability.

3.2 Microscopic images of SK-Mel-103 cells

Complementing the results of MTT assay, the microscopic images of the SKMel-103 cell after incubations with $(PhSe)_2$, NC $(PhSe)_2$ and NC B are depicted in figure 2. It was possible to observe that the incubation with free $(PhSe)_2$ or its nanoencapsulated form reduced the cell density, while NC B did not promote cell death.

3.3 Nitrite content determination

Following the antitumor effect, our data demonstrated that NC $(PhSe)_2$ and NC B (50, 100 and 200 µM) increased the NO_2^- levels (Fig. 3; $p<0.05$ by One-way ANOVA

followed by Tukey's test). Interestingly, free $(PhSe)_2$ did not modify the NO_2^- levels ($p<0.05$ by One-way ANOVA followed by Tukey's test).

3.4 Propidium iodide measurement

Additionally, the possible occurrence of necrosis induced by the treatment was assessed using the PI incorporation by SK-Mel-103 cells. Supporting the MTT assay, the results demonstrated that the incubation of SK-Mel-103 cell with free $(PhSe)_2$ and NC $(PhSe)_2$ at 100 µM promoted PI incorporation as well as caused cell morphological alterations and density reduction (Fig. 4). No modifications were observed in SK-Mel-103 exposed to NC B.

3.5 Hydrogels characterization

The HGs macroscopic characteristics are demonstrated in figure 5. All HGs had homogeneous aspect, without lumps or precipitates. The HG V (Fig. 5A) was colorless and transparent while HG NC B (Fig. 5C) had a white milky appearance. Both HGs containing the $(PhSe)_2$ had a yellow color, but HG $(PhSe)_2$ was bright yellow (Fig. 5B) while HG NC $(PhSe)_2$ presented an opaque aspect (Fig. 5D). The HGs physicochemical characteristics are depicted in table 2. The measure of average diameter demonstrated that the nanocapsules in HGs had nanometric size (280 ± 39 nm and 306 ± 15 nm, for HG NC $(PhSe)_2$ and HG NC B, respectively; $p>0.05$ by paired Student's *t* test). PDI values of HG NC $(PhSe)_2$ was 0.282 ± 0.079 and for HG NC B was 0.380 ± 0.008 ($p<0.05$ by paired Student's *t* test). The pH values of HGs were around the neutral range 7.1 ± 0.7 for HG NC $(PhSe)_2$, 8.1 ± 0.5 for HG NC B, 7.5 ± 0.1 for HG $(PhSe)_2$ and 8.3 ± 0.1 for HG V ($p>0.05$ by One-way ANOVA followed by Tukey's test). Lastly, the compound content was 100.55 ± 7.42 % for HG NC $(PhSe)_2$ and 101.71 ± 4.51 % to HG $(PhSe)_2$, ($p>0.05$ by paired Student's *t* test).

3.6 Stability evaluation

The results of stability study are demonstrated in table 2. After 15 days of storage the HG V and HG NC B had instabilities phenomena as fungal growth (Fig. S1 supplementary material), thus no further analyzes were carried out with these formulations. On the other hand, the HGs containing $(PhSe)_2$ maintained the initial macroscopic appearance 30 days after their preparation (Fig. S2, supplementary

material). The stability results of physicochemical parameters demonstrated an increase in the average diameter and polydispersity index of HG NC $(PhSe)_2$ over the days ($p<0.05$ by one-way ANOVA, followed Tukey's test). The pH values of HG NC $(PhSe)_2$ decreased after 15 and 30 days of storage ($p<0.05$ by one-way ANOVA, followed Tukey's test) except for the HG $(PhSe)_2$ that did not show any alteration. The compound content remained unaltered during the entire storage period for both formulations ($p>0.05$).

3.7 Spreadability determination

HGs spreadability profiles were demonstrated in figure 6. The results showed that the spreadability area of all HGs increased as higher was the plates weight. The repeated One-way measures, followed by Tukey' test revealed no significant difference among the profiles. The HGs Sfs were also determined and are depicted in table 2, which showed that the values were similar for all HGs ($p>0.05$, one-way ANOVA followed Tukey's test).

3.8 Rheological properties

The HGs rheological evaluation indicated a non-Newtonian flow because a decrease in viscosity was observed when the shear rate was increased. The HG NC $(PhSe)_2$ showed a superior viscosity in comparison to HG $(PhSe)_2$ ($p<0.05$; Fig. 7). Following, the rheograms were mathematical modeled using different equations to establish the best rheological behavior (plastic or pseudoplastic). According to the regression coefficients, the HG NC $(PhSe)_2$ rheogram fitted better to Ostwald model, indicating a pseudoplastic behavior, while the HG $(PhSe)_2$ rheogram fitted better to Casson model, suggesting a plastic behavior (table 3). Besides, the flow index (*n*) and consistency index (K) of HGs are depicted in table 3. By paired Student's *t* test it was possible to demonstrate a significant difference between the HGs consistency index, indicating a higher viscosity of HG NC $(PhSe)_2$ ($p<0.05$).

3.9 Hydrogels in vitro skin permeation studies

To investigate the penetration/ permeation rate of $(PhSe)_2$ from HGs, the human skin was used as biological membrane. The amount of $(PhSe)_2$ in each skin layer and in

receptor compartment is demonstrated in figure 8. The results demonstrated that the highest quantity of $(PhSe)_2$ was detected in the SC layer regardless the formulation ($p<0.0001$ by One-Way ANOVA analyze), 281.76 ± 52.60 μg/cm^2 and 340.19 ± 186.30 μg/ cm^2 for HG NC $(PhSe)_2$ and HG $(PhSe)_2$, respectively ($p>0.05$ by paired Student's *t* test). Regarding the epidermis, a higher amount of $(PhSe)_2$ was determined to the HG with free compound form (8.00 ± 1.85 μg/cm^2) in comparison to the HG NC $(PhSe)_2$ (5.23 ± 0.87 μg/cm^2) ($p<0.05$ by paired Student's *t* test). However, in DE layer the $(PhSe)_2$ content was 1.07 ± 0.11 μg/cm^2 for HG NC $(PhSe)_2$ and 0.59 ± 0.32 μg/cm^2 for HG $(PhSe)_2$ after topical administration ($p>0.05$ by paired Student's *t* test). The smallest $(PhSe)_2$ concentration was determined in receptor compartment, indicating a permeation rate, but the content found was similar for both HG (2.69 ± 2.00 and 4.40 ± 4.00 μg/mL for HG NC $(PhSe)_2$ and HG $(PhSe)_2$, respectively).

4. Discussion

The cancer biology is complex and during the tumor development there is an interplay of multiple processes such as inflammation and oxidative stress [41]. Among them, the melanoma is one of most aggressive skin cancers; it has high proliferation and elevate metastasis rates, which considerably reduces the chance of cure [6, 42]. Due to its aggressiveness, mainly of the metastatic one, it is relevant the research for improved therapies for the melanoma management. In this sense, the $(PhSe)_2$ is a potential candidate to further investigations concerning a novel treatment for cancer.

Considering our previous results [22] $(PhSe)_2$ showed antimelanoma effect against A375 cells and its nanoencapsulation abolished the toxicity to keratynocytes cells, suggesting that the incorporation into nanocapsules provided a selective action against tumoral cells. In this study, it was investigated the $(PhSe)_2$ antitumor effect when it is incorporated into polymeric nanocapsules against a resistant line of melanoma cells. Usually, the common therapeutic protocol to melanoma management had intervals between administration cycles, which stimulates drug resistance development, favoring the disease progression [7, 43]. The current study demonstrated that the incubation with free or nanoencapsulated $(PhSe)_2$ reduced the SK-Mel-103 cell viability and density and NC B did not promote cell death. Furthermore, the NC $(PhSe)_2$ had a superior effect in reducing cell viability at minor concentrations and showed

lower values of IC50 than the free compound. The improvement of *in vitro* and *in vivo* biological effects by incorporating molecules was already reported by several authors [6, 15, 30, 44].

To complement the MTT and microscopic evaluations, the nitrite content was also determined. Nitric oxide (NO) is an inorganic free radical, which plays an important role in cancer biology [45, 46]. The NO role in cancer is complex (pro tumorogenic and anti-tumorogenic effects) and is dependent on its source and concentration in the tumor area. Cell proliferation, migration and invasion or stimulation of apoptosis and angiogenesis are some of the biological effects that could be triggered by NO. The literature reports that high levels of NO produced by iNOS (inducible nitric oxide synthase) can contribute to apoptosis induction, cellular DNA damage, oxidative stress and cytotoxicity of tumor cells [45, 46]. Concerning that, our results are in accordance with these reports, once the NC $(PhSe)_2$ increased the NO_2^- levels as well as NC B. Drewes and coworkers reported that blank lipid core nanocapsules increased the NO_2^- levels even without cytotoxic effect on melanoma cells. Besides, this study also demonstrated that the NO_2^- levels augmentation was linked with the acetyleugenol-loaded lipid core nanocapsules antimelanoma effect [44]. Thus, the incorporation of $(PhSe)_2$ into the nanocapsules promoted superior effect against SK-Mel-103 cells and it is possibly mediated by an increase in the NO_2^- levels. To corroborate the MTT, microscopic and nitrite content results, a possible mechanics involved in cellular death was determined by PI incorporation. The results demonstrated that incubation with free or nanoencapsulated $(PhSe)_2$ triggered the PI incorporation by cells, suggesting that the antimelanoma effect of $(PhSe)_2$ may be mediated by necrosis. However, it is important to recognize that the involvement of other cell death pathways in the $(PhSe)_2$ antimelanoma effect cannot be excluded. Further studies should be carried out to better elucidate the exact mechanisms associated with such effect.

The skin is the most important protective barrier of human body and is composed by three layers: epidermis, dermis and hypodermis. The cutaneous route can be an alternative route for systemically administered drugs with the advantages of reducing the effective doses and side effects [26, 47]. In the last decade, the use of nanocarriers for cutaneous application have emerged as a more effective way for the treatment of skin disorders [26, 27, 29, 30, 34]. In this regard, hydrogels stand out for

their pleasant sensorial aspects, which are related to its aqueous character without leaving an oily sensation on the skin and also promoting skin hydration [47].

Nanobased hydrogels have been explored in the last years aiming at the treatment of cutaneous disorders [30, 31, 35, 36, 48]. Due to their high surface contact area, nanoformulations facilitate the drug penetration/permeation in viable skin. Besides, the particles may accumulate in hair follicles and provide a prolonged drug release and, consequently, achieving a superior pharmacological effect [26, 47]. After confirming the NC $(PhSe)_2$ effectiveness against resistant melanoma cells line, we developed a HG by thickening the nanocapsules suspension with xanthan gum. This simple and low-cost method can be considered a suitable tool to prepare adequate hydrogels for topical applications. Xanthan gum is a sugar-like compound widely applied in food and pharmaceutical industry due to its thickener and stabilizer properties [37, 49]. In this context, the scientific literature reports the use of xanthan gum to prepare HGs containing nanocarriers. These studies demonstrated that the obtained formulations had adequate physicochemical characteristics and sustained drug release, reinforcing its potential as a gelling agent in nanostructured hydrogels [50-52].

The physicochemical characterization demonstrated that HGs containing nanocapsules had average diameter in the nanometric range, which is in accordance to our previous study that demonstrated the nanocapsules diameter in suspension [22]. Such result suggests that the thickening process cause no negative impact on the physicochemical characteristics. Regarding PDI, a slight increase in its values was observed for the HGs containing NC in comparison to the NC $(PhSe)_2$ and NC B suspensions (0.151 ± 0.06 and 0.190 ± 0.08, respectively; $p<0.05$) [22]. These results are in accordance with those observed for the gellan gum nanobased-hydrogels prepared by our group [35, 36]. However, the pH values found in this study are slightly higher than the pH values demonstrated by the gellan gum nanobased-hydrogels [35, 36]. Considering that the method employed to prepare the HGs was the same, such difference could be attributed to the gum characteristic (gellan gum *versus* xanthan gum) and/or the nanocapsules composition. Finally, the compound content was around 100%, which was close to the theoretical value (5 mg/g), indicating no compound degradation during the samples preparation.

The stability study results showed that HG NC $(PhSe)_2$ had an augmentation in average diameter and PDI values, which is probably due to the particle aggregation. These results are in accordance with the study of Junyaprasert and coworkers [53], that reported the same physicochemical modification in xanthan gum hydrogels based on coenzyme Q10-loaded nanostructured lipids carriers and nanoemulsions. According to Cevc and Vierl [47], particles bigger than 750 nm cannot permeate the intact skin, suggesting that even considering such modification, the formulation still has an adequate particle size for transdermal delivery. The HGs pH values containing NC decreased over the storage days, which is probably due to the PCL chain relaxation, triggering the exposure of carboxylic terminal groups and decreasing the pH values. Lastly, it is important to highlight that no microbiological growth was observed for HGs containing $(PhSe)_2$ during the stability study. On the other hand, formulations without the compound showed evident fungal growth during this period. The $(PhSe)_2$ antifungal and antibacterial properties were already reported [8, 54], suggesting that the microbiologic stability is due to the compound presence acting as a preservative agent.

Easy spreadability and cutaneous biocompatibility are essential properties to develop drug delivery systems intended for treatment of skin disorders [30, 40]. Besides, Sfs can be a long-term parameter of hydrogels stability [40, 55]. The therapeutic efficacy may be related to the ease of spreading the formulation in the skin [35, 56]. The Sf values found in this study are slightly higher than some reports about HG composed by nanoformulations. Rigo and coworkers [30] prepared Carbopol Ultrez® hydrogels containing rice bran oil lipid core nanocapsules and achieved values of Sf less than 3.5 mm^2/g. Pegoraro and coworkers demonstrated values of Sf around 4 mm^2/g for HGs developed by thickening of nanocapsules containing coenzyme Q10 and vitamin E acetate using gellan gum [35]. Besides, Lima and coworkers showed Sfs values less than 3 mm^2/g for pemulen/pullulan blended HGs containing cationic nanocapsules [34]. The results of Sfs demonstrated in this study suggest that SFF formed by $(PhSe)_2$-nanocapsules thickened with xanthan gum had adequate skin coverage.

The rheological behavior is an indicative of required force for HG application in skin [56]. Additionally, the knowledge about formulations viscosity is important to determine the spreadability, stability and flow properties [28, 32, 55, 56]. Trough

mathematical models the HG NC $(PhSe)_2$ rheogram represents a pseudoplastic behavior, while the HG $(PhSe)_2$ had a plastic behavior. Plastic and pseudoplastic behaviors are desirable for topical application, since the viscosity decreases during the high shear process of spreading in skin [28, 32]. Our results are in agreement with previous studies that demonstrated the plastic and pseudoplastic behaviors for HG containing nanocapsules suspension [30, 32, 35].

The *in vitro* permeation results demonstrated in this study are in accordance with previous reports that showed an improvement in drug penetration/ permeation by preparing HGs with nanostrucutured systems [27, 32, 57]. Contri and coworkers fabricated HGs of chitosan by incorporating capsaicinoids-loaded nanocapsules, which increased drug skin residence time and provided superior permeation of capsaicinoids to the dermis in comparison to a HG with the free active [57]. Furthermore, Beber and coworkers reported that the skin penetration and permeation of dexamethasone from HG to viable epidermis was superior to the formulation containing the active incorporated in cationic nanocapsules [32].

In this sense, the narrow particle size and high superficial area of nanostructured systems can contribute to increase the residence time in skin layers and achieve a better drug distribution to deeper layers of this tissue, which could be an explanation for the higher $(PhSe)_2$ quantity determined in dermis after HG NC $(PhSe)_2$. Besides, stratum corneum and epidermis are both more lipophilic than dermis due to the composition of such layers [27], which could justify the higher amount of $(PhSe)_2$ quantified in these layers.

Melanoma is associated with malignance of melanocytes, which are located at dermis and epidermis junction or between the keratinocytes of the epidermis basal layer. Initially, the disordered growth of malignant melanocytes is restricted to the epidermis; however, over the years, the neoplastic cells infiltrate the collagen fibers and reach the dermis layer, leading to the worst prognostic [6, 24, 58]. In this sense, the results of permeation studies suggest that HG NC $(PhSe)_2$ could be a potential formulation for topical melanoma treatment as an adjuvant approach, because it provided superior amount of compound retained in stratum corneum and also improved the permeation/ penetration to viable epidermis and dermis.

5. Conclusion

In this study the feasibility to prepare HGs by thickening nanocapsules suspensions with xanthan gum were demonstrated. Besides, for the first time the $(PhSe)_2$ incorporation in a topical formulation as an alternative for the melanoma treatment were assessed. The $(PhSe)_2$ nanocapsules suspension exhibited higher cytotoxicity effect than free compound against resistant malignant melanoma cell line SK-Mel-103, murine (B16F10) and human (SkMel-28) melanoma cell lines. The developed HGs had adequate physicochemical characteristics, good stability as well as appropriate spreadability and rheological behavior for cutaneous application. The HG prepared with NC $(PhSe)_2$ provided superior compound permeation to dermis, which could be interesting to the topical melanoma treatment considering the potential antimelanoma effect exerted by $(PhSe)_2$. Therefore, the HGs fabricated by the simple nanocapsules suspension thickening with xanthan gum can be an effective adjuvant therapy for the melanoma treatment and could increase effectiveness of the actual intravenous drugs used to melanoma management.

Acknowledgments

We thank Coordenação de Aperfeiçoamento de Pessoal de Nível Superior (CAPES) - Brazil for the scholarship (L. M. Ferreira), Dra. Cristiane de Bona Silva for the zetasizer access and Dra. Silvia Stuchi Maria-Engler (Faculdade de Farmácia da USP) for the the murine cell line B16F10 and human cell lines SK-Mel-103 and SK-Mel-28 donation.

References

[1] R.L. Siegel, K.D. Miller, A. Jemal, Cancer Statistics, 2018, Ca-Cancer J Clin 68(1) (2018) 7-30.

[2] S.Q. Wang, R. Setlow, M. Berwick, D. Polsky, A.A. Marghoob, A.W. Kopf, R.S. Bart, Ultraviolet A and melanoma: A review, J Am Acad Dermatol 44(5) (2001) 837-846.

[3] W.H. Organization, Skin Cancers, (2017).

[4] D. Kavanagh, A.D.K. Hill, B. Djikstra, R. Kennelly, E.M.W. McDermott, N.J. O'Higgins, Adjuvant therapies in the treatment of stage II and III malignant melanoma, Surg-J R Coll Surg E 3(4) (2005) 245-256.

[5] V.K. Sondak, G.T. Gibney, Indications and Options for Systemic Therapy in Melanoma, Surg Clin N Am 94(5) (2014) 1049-+.

[6] R.B. Rigon, M.H. Oyafuso, A.T. Fujimura, M.L. Goncalez, A.H. do Prado, M.P.D. Gremiao, M. Chorilli, Nanotechnology-Based Drug Delivery Systems for Melanoma Antitumoral Therapy: A Review, Biomed Res Int (2015).

[7] D. Grossman, D.C. Altieri, Drug resistance in melanoma: Mechanisms, apoptosis, and new potential therapeutic targets, Cancer Metast Rev 20(1-2) (2001) 3-11.

[8] C.W. Nogueira, J.B.T. Rocha, Toxicology and pharmacology of selenium: emphasis on synthetic organoselenium compounds, Arch Toxicol 85(11) (2011) 1313-1359.

[9] R.M. Rosa, R. Roesler, A.L. Braga, J. Saffi, J.A.P. Henriques, Pharmacology and toxicology of diphenyl diselenide in several biological models, Braz J Med Biol Res 40(10) (2007) 1287-1304.

[10] N.B.D. Barbosa, C.W. Nogueira, T.N. Guecheva, M.D. Bellinaso, J.B.T. Rocha, Diphenyl diselenide supplementation delays the development of N-nitroso-Nmethylurea-induced mammary tumors, Arch Toxicol 82(9) (2008) 655-663.

[11] T. Posser, M.T. de Paula, J.L. Franco, R.B. Leal, J.B.T. da Rocha, Diphenyl diselenide induces apoptotic cell death and modulates ERK1/2 phosphorylation in human neuroblastoma SH-SY5Y cells, Arch Toxicol 85(6) (2011) 645-651.

[12] F. Nedel, V.F. Campos, D. Alves, A.J.A. McBride, O.A. Dellagostin, T. Collares, L. Savegnago, F.K. Seixas, Substituted diaryl diselenides: Cytotoxic and apoptotic effect in human colon adenocarcinoma cells, Life Sci 91(9-10) (2012) 345-352.

[13] M.T. Melo, I.M. de Oliveira, I. Grivicich, T.N. Guecheva, J. Saffi, J.A.P. Henriques, R.M. Rosa, Diphenyl diselenide protects cultured MCF-7 cells against tamoxifen-induced oxidative DNA damage, Biomed Pharmacother 67(4) (2013) 329-335.

[14] M. Prigol, C.W. Nogueira, G. Zeni, M.R. Bronze, L. Constantino, Physicochemical and Biochemical Profiling of Diphenyl Diselenide, Appl Biochem Biotech 169(3) (2013) 885-893.

[15] L.A. Frank, R.V. Contri, R.C.R. Beck, A.R. Pohlmann, S.S. Guterres, Improving drug biological effects by encapsulation into polymeric nanocapsules, Wires Nanomed Nanobi 7(5) (2015) 623-639.

[16] M. Basha, Nanotechnology as a Promising Strategy for Anticancer Drug Delivery, Curr Drug Deliv 15(4) (2018) 497-509.

[17] S. Friberg, A.M. Nystrom, Nanotechnology in the war against cancer: new arms against an old enemy - a clinical view, Future Oncol 11(13) (2015) 1961-1975.

[18] H. Fessi, F. Puisieux, J.P. Devissaguet, N. Ammoury, S. Benita, Nanocapsule Formation by Interfacial Polymer Deposition Following Solvent Displacement, Int J Pharmaceut 55(1) (1989) R1-R4.

[19] I. Brigger, C. Dubernet, P. Couvreur, Nanoparticles in cancer therapy and diagnosis, Adv Drug Deliver Rev 54(5) (2002) 631-651.

[20] C.F.A. Giordani, D. de Souza, L. Dornelles, C.W. Nogueira, M.P. Alves, M. Prigol, O.E.D. Rodrigues, Diphenyl Diselenide-Loaded Nanocapsules: Preparation and Biological Distribution, Appl Biochem Biotech 172(2) (2014) 755-766.

[21] S.T. Stefanello, F. Dobrachinski, N.R. de Carvalho, G.P. Amaral, R.P. Barcelos, V.A. Oliveira, C.S. Oliveira, C.F.A. Giordani, M.E. Pereira, O.E.D. Rodrigues, F.A.A. Soares, Free radical scavenging *in vitro* and biological activity of diphenyl diselenideloaded nanocapsules: DPDS-NCS antioxidant and toxicological effects, Int J Nanomed 10 (2015).

[22] L.M. Ferreira, V.F. Cervi, M.H.M. Sari, A.V. Barbieri, A.P. Ramos, P.M. Copetti, G.F. Brum, K. Nascimento, J.M. Nadal, P.V. Farago, M.R. Sagrillo, C.W. Nogueira, L. Cruz, Diphenyl diselenide loaded poly(ε-caprolactone) nanocapsules with selective antimelanoma activity: Development and cytotoxic evaluation, Mat Sci Eng C-Mater 91 (2018) 1-9.

[23] M. Redpath, C.M.G. Marques, C. Dibden, A. Waddon, R. Lalla, S. MacNeil, Ibuprofen and hydrogel-released ibuprofen in the reduction of inflammation-induced migration in melanoma cells, Brit J Dermatol 161(1) (2009) 25-33.

[24] J. Li, Y.J. Wang, R.J. Liang, X.J. An, K. Wang, G.X. Shen, Y.T. Tu, J.T. Zhu, J. Tao, Recent advances in targeted nanoparticles drug delivery to melanoma, NanomedNanotechnol 11(3) (2015) 769-794.

[25] A. Sisti, G. Sisti, C.M. Oranges, Topical treatment of melanoma skin metastases with Imiquimod: a review, Dermatol Online J. 21(2) (2015) 1-9.

[26] S.S. Guterres, M.P. Alves, A.R. Pohlmann, Polymeric nanoparticles, nanospheres and nanocapsules, for cutaneous applications, Drug Target Insights 2 (2007) 147-157.

[27] M.P. Alves, A.L. Scarrone, M. Santos, A.R. Pohlmann, S.S. Guterres, Human skin penetration and distribution of nimesulide from hydrophilic gels containing nanocarriers, Int J Pharmaceut 341(1-2) (2007) 215-220.

[28] M.C.L. Marchiori, R.H. Rascovetzki, A.F. Ourique, L.A. Rigo, C.B. Silva, R.C.R. Beck, Improved tretinoin photostability in a topical nanomedicine replacing original liquid suspension with spray-dried powder with no loss of effectiveness, Drug Dev Ind Pharm 39(4) (2013) 579-586.

[29] A. Melero, A.F. Ourique, S.S. Guterres, A.R. Pohlrnann, C.M. Lehr, R.C.R. Beck, U. Schaefer, Nanoencapsulation in Lipid-Core Nanocapsules Controls Mometasone Furoate Skin Permeability Rate and Its Penetration to the Deeper Skin Layers, Skin Pharmacol Phys 27(4) (2014) 217-228.

[30] L.A. Rigo, C.R. da Silva, S.M. de Oliveira, T.N. Cabreira, C.D. da Silva, J. Ferreira, R.C.R. Beck, Nanoencapsulation of rice bran oil increases its protective effects against UVB radiation-induced skin injury in mice, Eur J Pharm Biopharm 93 (2015) 11-17.

[31] F.C. Flores, J.A. de Lima, C.R. da Silya, D. Benvegnu, J. Ferreira, M.E. Burger, R.C.R. Beck, C.M.B. Rolim, M.I.U.M. Rocha, M.L. da Veiga, C.D. da Silya, Hydrogels Containing Nanocapsules and Nanoemulsions of Tea Tree Oil Provide Antiedematogenic Effect and Improved Skin Wound Healing, J Nanosci Nanotechno 15(1) (2015) 800-809.

[32] T.C. Beber, D.F. de Andrade, P.D. Chaves, A.R. Pohlmann, S.S. Guterres, R.C.R. Beck, Cationic Polymeric Nanocapsules as a Strategy to Target Dexamethasone to Viable Epidermis: Skin Penetration and Permeation Studies, J Nanosci Nanotechno 16(2) (2016) 1331-1338.

[33] D.F. de Andrade, M.C. Fontana, A.R. Pohlmann, S.S. Guterres, R.C.R. Beck, Nanoencapsulation of Clobetasol Propionate Decreases Its Penetration to Skin Layers Without Changing Its Relative Skin Distribution, J Nanosci Nanotechno 15(1) (2015) 875-879.

[34] J.A. de Lima, T.C. Paines, M.H. Motta, W.B. Weber, S.S. dos Santos, L. Cruz, C.D. da Silva, Novel Pemulen/Pullulan blended hydrogel containing clotrimazole

loaded cationic nanocapsules: Evaluation of mucoadhesion and vaginal permeation, Mat Sci Eng C-Mater 79 (2017) 886-893.

[35] N.S. Pegoraro, A.V. Barbieri, C. Camponogara, J. Mattiazzi, E.S. Brum, M.C.L. Marchiori, S.M. Oliveira, L. Cruz, Nanoencapsulation of coenzyme Q10 and vitamin E acetate protects against UVB radiation-induced skin injury in mice, Colloid Surface B 150 (2017) 32-40.

[36] M.C.L. Marchiori, C. Rigon, C. Camponogara, S.M. Oliveira, L. Cruz, Hydrogel containing silibinin-loaded pomegranate oil based nanocapsules exhibits antiinflammatory effects on skin damage UVB radiation-induced in mice, J Photoch Photobio B 170 (2017) 25-32

[37] A. Kumar, K.M. Rao, S.S. Han, Application of xanthan gum as polysaccharide in tissue engineering: A review, Carbohydr Polym. 180 (2018) 128-144.

[38] C. Paulmier, Selenoorganic functional groups. Selenium reagents and intermediates in organic synthesis, Angew. Chem. 100 (1986) 25-51.

[39] D.J. Stuehr, C.F. Nathan, Nitric-Oxide - a Macrophage Product Responsible for Cytostasis and Respiratory Inhibition in Tumor Target-Cells, J Exp Med 169(5) (1989) 1543-1555.

[40] L.A. Rigo, J. Weber, C.B. Silva, R.C.R. Beck, Evaluation of the Spreadability of Pharmaceutical or Cosmetic Semisolid Formulations Using Scanned Images, Lat Am J Pharm 31(10) (2012) 1387-1391.

[41] H.E. POULSEN, H. PRIEME, S. LOFT, Role of oxidative DNA damage in cancer initiation and promotion.,Eur J Cancer Prev. 7 (1998) 9-16.

[42] N.K. Haass, K.S.M. Smalley, L. Li, M. Herlyn, Adhesion, migration and communication in melanocytes and melanoma, Pigm Cell Res 18(3) (2005) 150-159.

[43] A.K. Brys, R. Gowda, D.B. Loriaux, G.P. Robertson, P.J. Mosca, Nanotechnologybased strategies for combating toxicity and resistance in melanoma therapy, Biotechnol Adv 34(5) (2016) 565-577.

[44] C.C. Drewes, L.A. Fiel, C.G. Bexiga, A.C.C. Asbahr, M.K. Uchiyama, B. Cogliati, K. Araki, S.S. Guterres, A.R. Pohlmann, S.P. Farsky, Novel therapeutic mechanisms determine the effectiveness of lipid-core nanocapsules on melanoma models, Int J Nanomed 11 (2016) 1261-1279.

[45] D. Fukumura, S. Kashiwagi, R.K. Jain, The role of nitric oxide in tumour progression, Nat Rev Cancer 6(7) (2006) 521-534.

[46] K. Yarlagadda, J. Hassani, I.P. Foote, J. Markowitz, The role of nitric oxide in melanoma, Bba-Rev Cancer 1868(2) (2017) 500-509.

[47] G. Cevc, U. Vierl, Nanotechnology and the transdermal route A state of the art review and critical appraisal, J Control Release 141(3) (2010) 277-299.

[48] M.C. Fontana, J.F.P. Rezer, K. Coradini, D.B.R. Leal, R.C.R. Beck, Improved efficacy in the treatment of contact dermatitis in rats by a dermatological nanomedicine containing clobetasol propionate, Eur J Pharm Biopharm 79(2) (2011) 241-249.

[49] V.D. Prajapati, G.K. Jani, N.G. Moradiya, N.P. Randeria, Pharmaceutical applications of various natural gums, mucilages and their modified forms, Carbohydr Polym. 92(2) (2013) 1685-1699.

[50] K.A. Shah, A.A. Date, M.D. Joshi, V.B. Patravale, Solid lipid nanoparticles (SLN) of tretinoin: Potential in topical delivery, Int J Pharmaceut 345(1-2) (2007) 163-171.

[51] P.V. Pople, K.K. Singh, Development and evaluation of topical formulation containing solid lipid nanoparticles of vitamin A, Aaps Pharmscitech 7(4) (2006).

[52] B. Mishra, S.K. Sahoo, S. Sahoo, Liranaftate loaded Xanthan gum based hydrogel for topical delivery: Physical properties and ex-vivo permeability, Int J Biol Macromol 107 (2018) 1717-1723.

[53] V.B. Junyaprasert, V. Teeranachaideekul, E.B. Souto, P. Boonme, R.H. Müller, Q10-loaded NLC versus nanoemulsions: Stability, rheology and *in vitro* skin permeation, Int J Pharmaceut 377 (2009) 207-214.

[54] I.B. Rosseti, J.B.T. Rocha, M.S. Costa, Diphenyl diselenide (PhSe)(2) inhibits biofilm formation by Candida albicans, increasing both ROS production and membrane permeability, J Trace Elem Med Bio 29 (2015) 289-295.

[55] G. Netto, J. Jose, Development, characterization, and evaluation of sunscreen cream containing solid lipid nanoparticles of silymarin, J Cosmet Dermatol 1 (2017) 1-11.

[56] A. Garg, D. Aggarwal, S. Garg, A.K. Singla, Spreading of Semisolid Formulations. An Update, Pharm Technol. 1 (2002) 84-105.

[57] R.V. Contri, T. Katzer, A.F. Ourique, A.L.M. da Silva, R.C.R. Beck, A.R. Pohlmann, S.S. Guterres, Combined Effect of Polymeric Nanocapsules and Chitosan

Hydrogel on the Increase of Capsaicinoids Adhesion to the Skin Surface, J Biomed Nanotechnol 10(5) (2014) 820-830.

[58] S. Singh, A. Zafar, S. Khan, I. Naseem, Towards therapeutic advances in melanoma management: An overview, Life Sci 174 (2017) 50-58.

Table 1. Molecular characteristics of the human melanoma cell lines

Cell lines	p53	p53 induced	p14 (mRNA)	p16 (mRNA)	B-RAF (V599E)	N-RAS (éxon 3)	Apaf-1 (prot)	Casp.8 (prot)	Bcl-2 (prot)	Bcl-xL (prot)	Mcl-1
SK-Mel-28	wt	+	+	+	wt	Q61R	-	+	++	+++	+++
SK-Mel-103	R273H	-	ND	+	Mutant	wt	-/+	++	++	++	++

wt: wild type
ND: not detected
Prot: protein

Table 2. Physicochemical characteristics of semisolid formulations.

Physicochemical evaluations					
		0 days			
Semisolid	**Average diameter (nm)**	**PDI[a]**	**pH**	**Compound content (%)**	**Sf[b] (mm_2/g)**
HG NC $(PhSe)_2$	280 ± 39	0.28 ± 0.08*	7.1 ± 0.7	100.55 ± 7.42	6.7 ± 1.3
HG NC B	306 ± 15	0.38 ± 0.01	8.1 ± 0.5	-	5.4 ± 2.2
HG $(PhSe)_2$	-	-	7.5 ± 0.1	101.71 ± 4.51	8.3 ± 0.7
HG V	-	-	8.3 ± 0.1	-	7.6 ± 0.7
Stability study					
Semisolid	**Average diameter (nm)**	**PDI[a]**	**pH**	**Compound content (%)**	
		15 days			
HG NC $(PhSe)_2$	381 ± 91#	0.47 ± 0.07#	5.3 ± 0.8#	101.88 ± 7.44	
HG $(PhSe)_2$	-	-	6.7 ± 0.5	91.33 ± 3.77	
		30 days			
HG NC $(PhSe)_2$	402 ± 132#	0.47 ± 0.02#	5.0 ± 0.5#@	97.08 ± 1.09	
HG $(PhSe)_2$	-	-	8.1 ± 0.1	99.78 ± 8.92	

The results are expressed by mean with S.E.M. of triplicate. For physicochemical evaluations asterisks denote the significant difference (*) $p<0.05$ by paired Student's t test between HG NC $(PhSe)_2$ and HG NC B. For stability study the sharp denote the significant difference (#) $p<0.05$ of same formulation between 0 day/15 days and 0 day/30 days and arroba denote significant difference (@) $p<0.05$ between HG NC $(PhSe)_2$ and HG $(PhSe)_2$, both by One-Way ANOVA followed by Tukey's test.

a – Polydispersity index
b – Spreadability factor

Table 3. Regression coefficients (r^2) for mathematical modeling in shear rate-shear stress curves to models of Ostwald, Casson and Bingahan and Flow index (*n*) and consistency index (*K*) of SSFs.

	HG $(PhSe)_2$	**HG NC $(PhSe)_2$**
Ostwald	0.985 ± 0.005	0.993 ± 0.002
Casson	0.995 ± 0.001	0.983 ± 0.012
Bingahan	0.955 ± 0.011	0.941 ± 0.031
Flow index (*n*) and consistency index (*K*) of SSFs		
***n* (mPas)**	0.151 ± 0.007	0.149 ± 0.021
K	171.11 ± 1.16	180.43 ± 3.43*

The results are expressed by mean with S.E.M. of triplicate. The asterisks denote the significant difference (*) $p<0.05$ by paired Student's *t* test between K of HG NC $(PhSe)_2$ and HG $(PhSe)_2$.

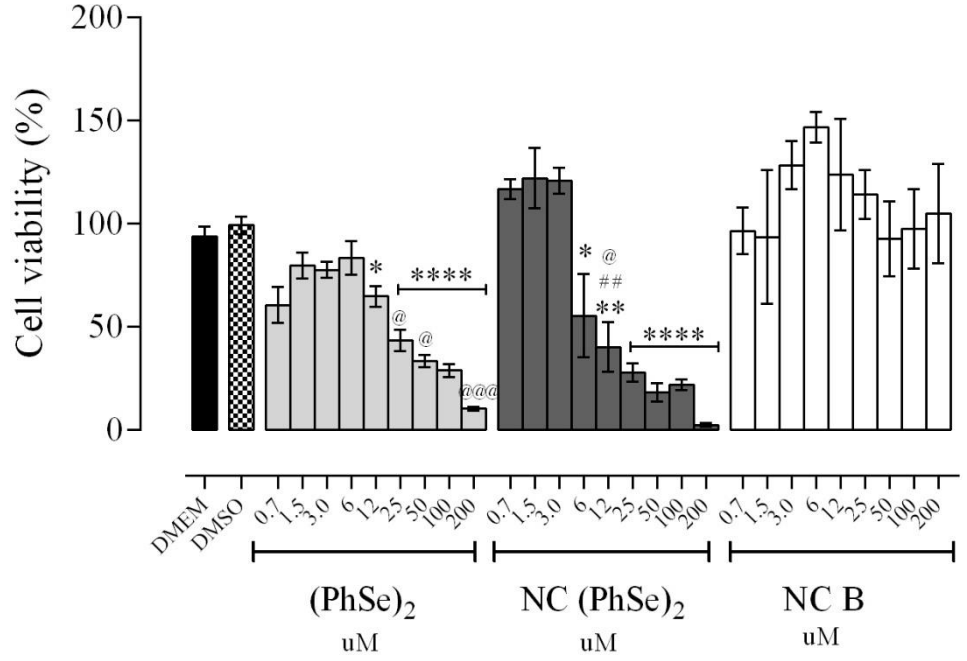

Figure 1. Cytotoxic effect of NC $(PhSe)_2$ and free $(PhSe)_2$ against SK-Mel-103 cells after 48 h of incubation assessed by MTT assay. The concentrations screening was in the range of 0.7 – 200 µM. NC B and DMSO were used for comparison purposes, while DMEM culture medium were used negative control. Each column represents the mean ± S.E.M. of triplicate. Asterisks denote significant differences (** $p<0.01$ and **** $p<0.0001$) in comparison to the negative control group and sharps ($^{\#\#}$ $p<0.01$) denotes the differences among the concentrations the same group, by one-way ANOVA, followed by Tukey's post hoc test. Arroba symbol ($^{@}$ $p<0.05$, $^{@@}$ $p<0.01$ and $^{@@@}$ $p<0.001$) denotes significant differences between the same concentrations of different groups by Unpaired Student's *t* test.

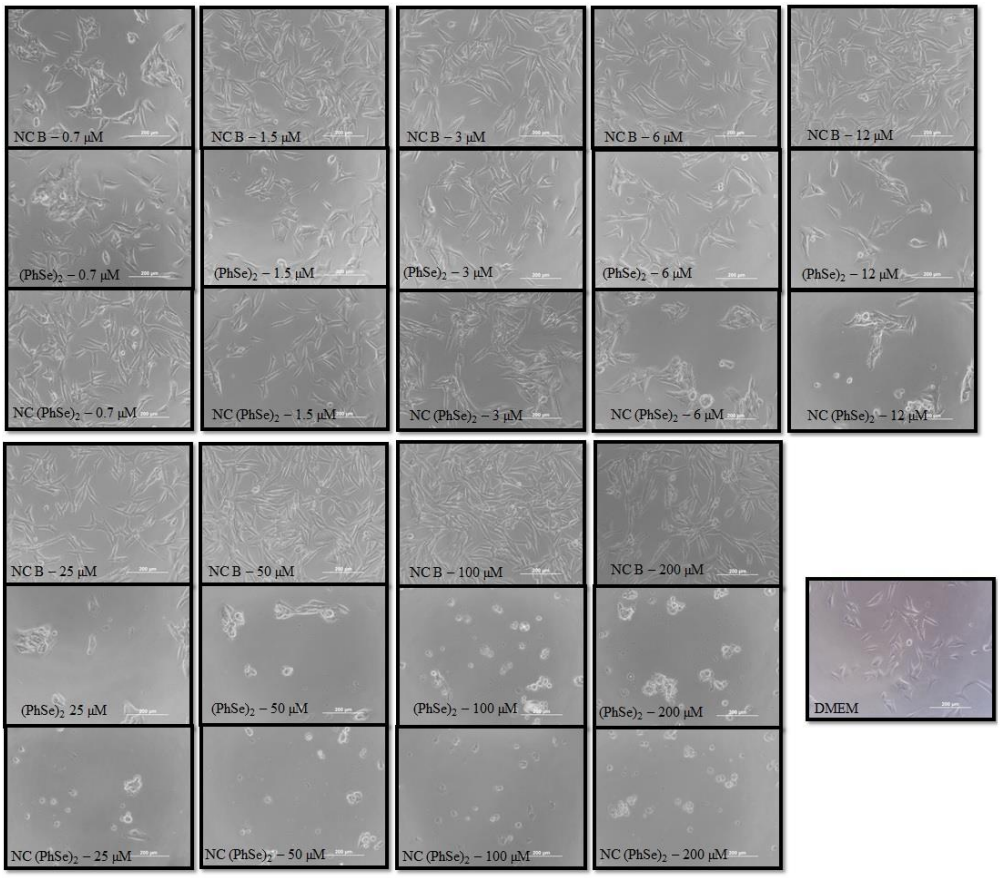

Figure 2. Representative images of SK-Mel-103 cells density and morphology after 48 h of incubation with different concentration of NC B, free $(PhSe)_2$ and NC $(PhSe)_2$.

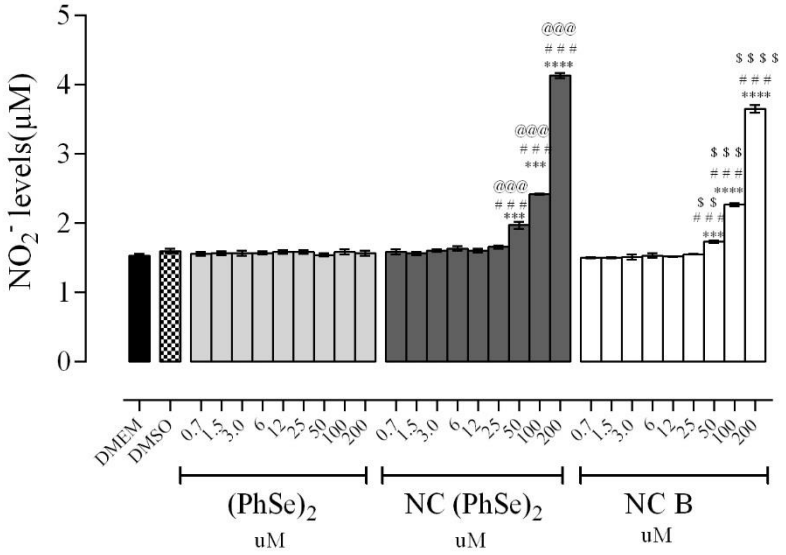

Figure 3. Nitrite (NO_2^-) levels was determined in SK-Mel-103 cells supernatant. Each column represents the mean ± S.E.M. of triplicate. Asterisks denote significant differences (*** $p<0.001$ and **** $p<0.0001$) in comparison to the negative control group and sharps ($^{###}$ $p<0.001$) denotes the differences among the concentrations the same group, by one-way ANOVA, followed by Tukey's post hoc test. Arroba symbol ($^{@@@}$ $p<0.001$) denotes significant differences between the same concentrations of NC $(PhSe)_2$ and $(PhSe)_2$ while cipher ($^{\$\$}$ $p<0.01$, $^{\$\$\$}$ $p<0.001$ and $^{\$\$\$\$}$ $p<0.0001$) means significant differences between the same concentrations of NC B and NC $(PhSe)_2$ by Unpaired Student's *t* test.

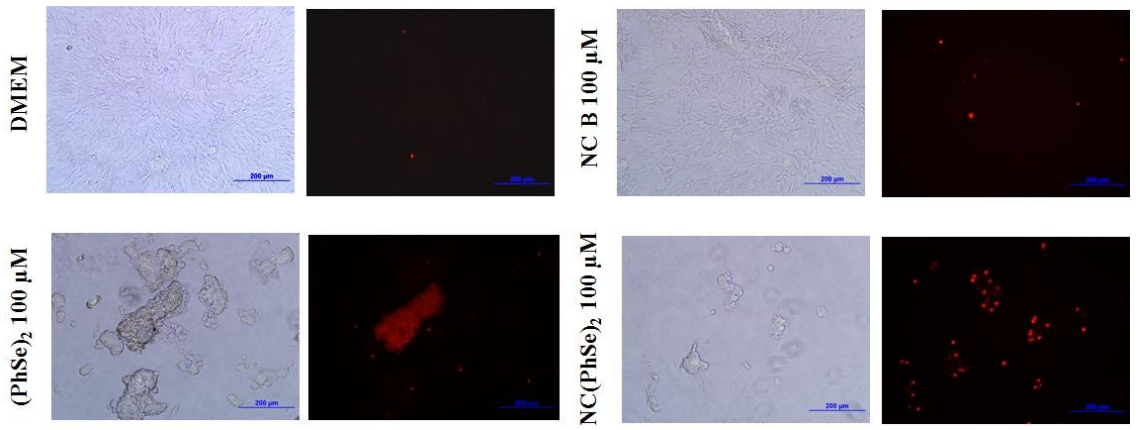

Figure 4. Propidium iodide (PI) incorporation in SK-Mel-103 cell following 48 h of incubation with $(PhSe)_2$, free or nanoencapsulated. DMEM and NC B were used as comparative purposes.

Figure 5. Macroscopic appearance of hydrogels: A) HG V; B) HG $(PhSe)_2$; C) HG NC B; D) HG NC $(PhSe)_2$.

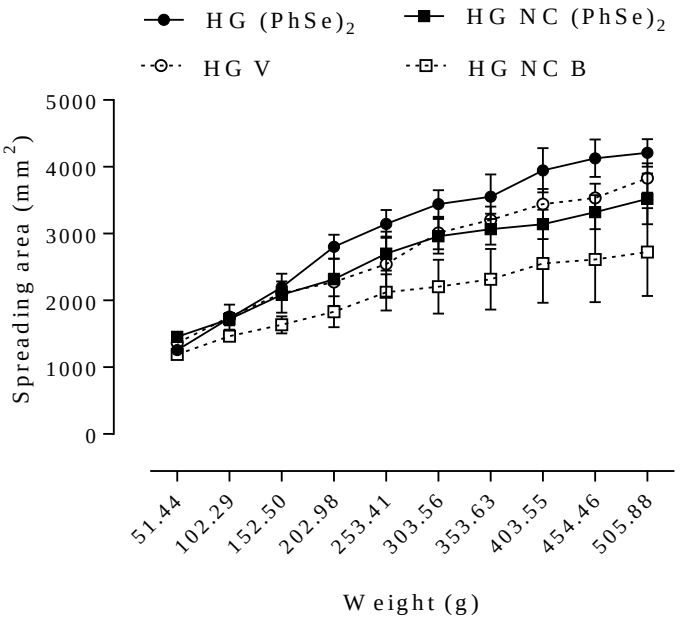

Figure 6. Spreadability profiles (mm^2) of xanthan gum hydrogels: HG V, HG $(PhSe)_2$, HG NC B and HG NC $(PhSe)_2$. The results were evaluated by One-way analyze of repeated measures, followed by Tukey' test (p>0.05).

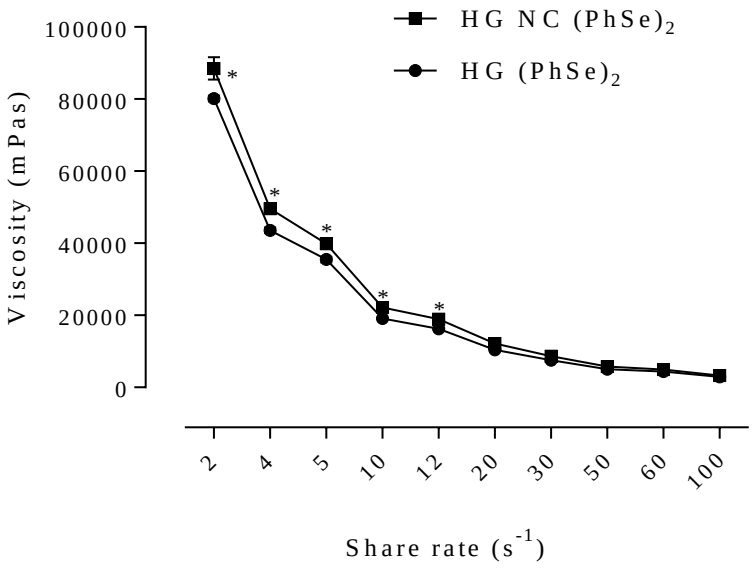

Figure 7. Viscosity determination by Brook-field viscometer of semisolids containing $(PhSe)_2$ in its free (HG $(PhSe)_2$) or nanoencapsulated form (HG NC $(PhSe)_2$). Asterisk denotes the difference (*) p<0.05 between HG $(PhSe)_2$ and HG NC $(PhSe)_2$ by One-way of repeated measures, followed by Tukey' test.

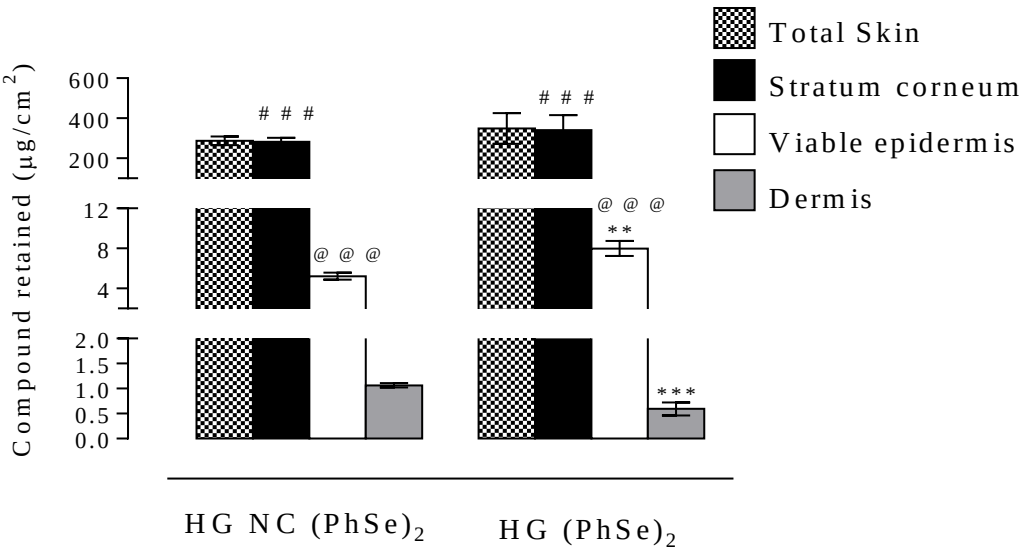

Figure 8. Cumulative amount of $(PhSe)_2$ in skin layers after 8 h of incubation with HG $(PhSe)_2$ or HG NC $(PhSe)_2$. Each column represents the mean ± S.E.M. of *n=6*. One-way ANOVA analyzes followed by Tukey's test was used to determine the statistical differences among the layers to each formulation. Sharps denote statistical differences between compound content in SC with VE or DE ($^{###}$) $p<0.001$. Arroba denotes significant differences between $(PhSe)_2$ amount quantified in VE and DE ($^{@@@}$) $p<0.001$. By unpaired Student's t test asterisks denote the significance levels (*) $p<0.05$, (**) $p<0.01$ comparing the $(PhSe)_2$ content in VE and DE after skin application of HG $(PhSe)_2$ or HG NC $(PhSe)_2$. Abbreviations: stratum corneum (SC), viable epidermis (VE) and dermis (DE).

SUPPLEMENTARY MATERIAL

Xanthan gum-based hydrogel containing nanocapsules for topical diphenyl diselenide delivery in melanoma therapy

Luana Mota Ferreira[a], Marcel Henrique Marcondes Sari[a,d], Juliana Hofstatter Azambuja[b], Elita Ferreira da Silveira[c], Verônica Ferrari Cervi[a], Marila Crivellaro Lay Marchiori[a], Marcia Rosângela Wink[b], Cristina Wayne Nogueira[d], Elizandra Braganhol[b,c], Letícia Cruz[a*].

Figures

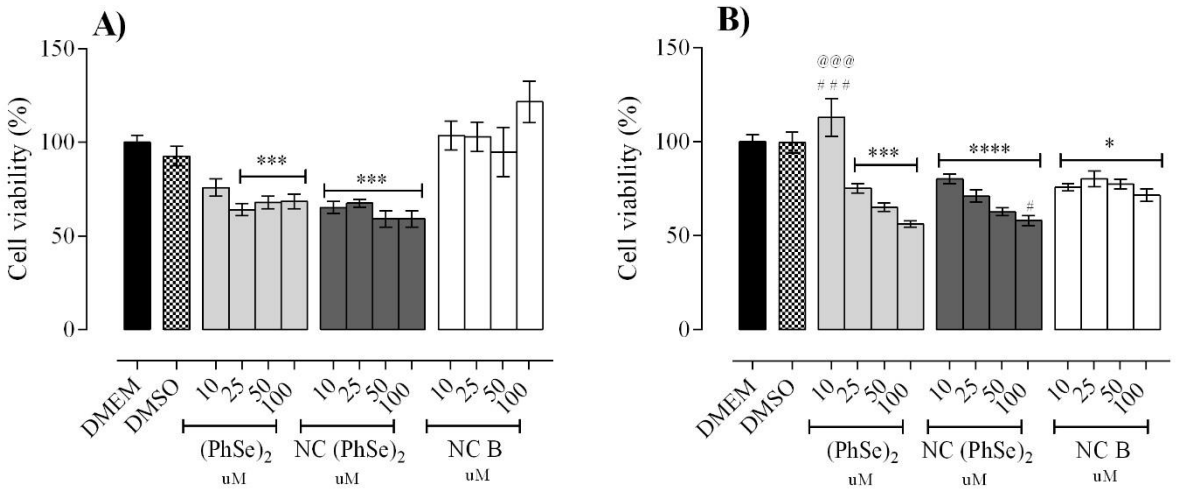

Figure 1. Cytotoxic effect of NC $(PhSe)_2$ and free $(PhSe)_2$ against B16F10 (A) and SK-Mel-28(B) cells after 48 h of incubation assessed by MTT assay. NC B and DMSO were used for comparison purposes, while DMEM culture medium were used negative control. Each column represents the mean ± S.E.M. of triplicate. Asterisks denote significant differences (* $p<0.05$, *** $p<0.001$ and **** $p<0.0001$) in comparison to the negative control group and sharps ($^{\#}$ $p<0.5$ and $^{\#\#\#}$ $p<0.001$) denotes the differences among the concentrations the same group, by one-way ANOVA, followed by Tukey's post hoc test. Arroba symbol ($^{@@@}$ $p<0.001$) denotes significant differences between the same concentrations of different groups by Unpaired Student's *t* test.

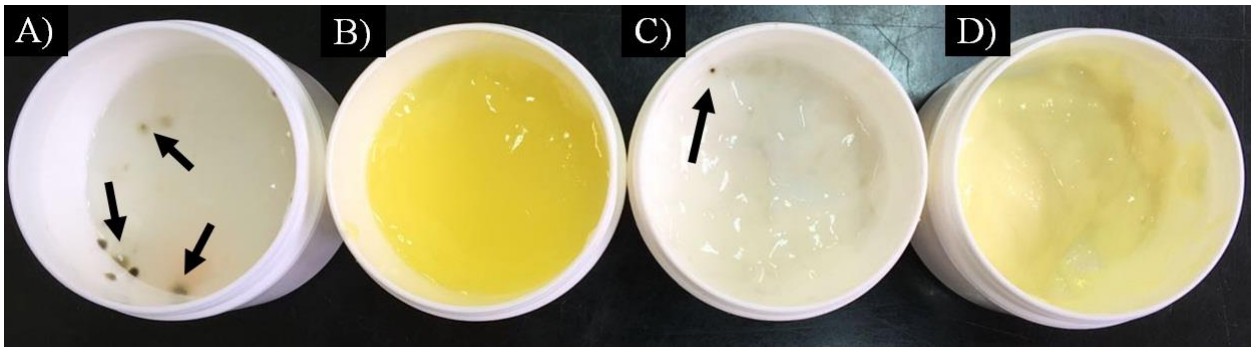

Figure 2. Semisolid formulations macroscopic appearance: A) HG V; B) HG $(PhSe)_2$; C) HG NC B; D) HG NC $(PhSe)_2$ after 15 days of storage at room temperature (25°C)

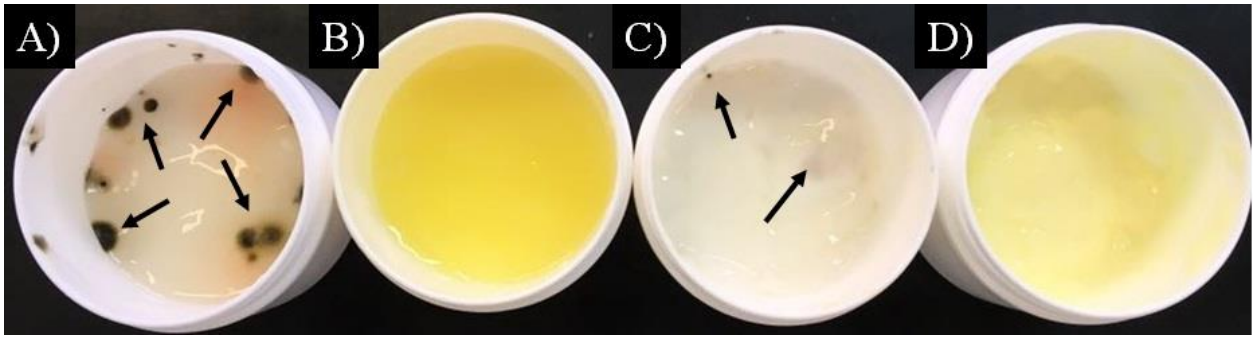

Figure 3. Semisolid formulations macroscopic appearance: A) HG V; B) HG $(PhSe)_2$; C) HG NC B; D) HG NC $(PhSe)_2$ after 30 days of storage at room temperature (25°C)

CAPÍTULO 2: Avaliação da toxicidade *in vivo* das nanocápsulas contendo $(PhSe)_2$ e determinação da atividade antitumoral em um modelo pré-clínico de glioblastoma.

4. Capítulo 2: Avaliação da toxicidade *in vivo* das nanocápsulas contendo $(PhSe)_2$ e determinação da atividade antitumoral em um modelo pré-clínico de glioblastoma.

Apresentação

No presente capítulo estão agrupados os resultados da avaliação da toxicidade *in vivo* e do efeito antiglioma *in vitro* e *in vivo* em um modelo pré-clínico de glioblastoma. O **manuscrito 2** relata a exposição aguda de peixe-zebra às nanocápsulas contendo o disseleneto de difenila e os efeitos no comportamento dos animais, bem como o balanço oxidativo no cérebro dos peixes. Na sequência, o **manuscrito 3** contempla os resultados do efeito antitumoral do composto livre e nanoencapsulado frente a células de glioma de rato (C6) e sua toxicidade em astrócitos. Além disso, finalizando a avaliação toxicológica das formulações, um experimento de toxicidade *in vivo* em ratos foi conduzido. Por fim, neste trabalho também estão descritos os resultados da atividade antitumoral *in vivo* utilizando um modelo pré-clínico de glioblastoma em ratos.

4.1 Manuscrito 2

Zebrafish exposure to diphenyl diselenide-loaded polymeric nanocapsules caused no behavioral impairments and brain oxidative stress

Luana Mota Ferreira[a], Luíz Vinícius Costa da Rosa[b], Talise Ellwanger Müller[b], Charlene Menezes[b], Marcel Henrique Marcondes Sari[a,b], Vania Lucia Loro[b], Cristina Wayne Nogueira[b], Denis B. Rosemberg[b], Letícia Cruz[a*].

[a]Laboratório de Tecnologia Farmacêutica, Programa de Pós-Graduação em Ciências Farmacêuticas, Centro de Ciências da Saúde, Universidade Federal de Santa Maria, Santa Maria, RS, Brazil

[b]Programa de Pós-Graduação em Bioquímica Toxicológica, Centro de Ciências Naturais e Exatas, Universidade Federal de Santa Maria, Santa Maria, RS, Brazil

*Corresponding author

Letícia Cruz, Programa de Pós-Graduação em Ciências Farmacêuticas, Universidade Federal de Santa Maria, Santa Maria, 97105-900, Brazil.

Phone: +55 55 3220 9373

E-mail: leticiacruz@smail.ufsm.br

Abstract

Previous findings showed that nanoencapsulation of diphenyl diselenide, an organoselenium compound, provided superior biological activity and lower toxicological potential than its free form *in vitro*. However, few studies reported the behavioral and biochemical effects of this nanocapsules formulation *in vivo*. Zebrafish (*Danio rerio*) has emerged as a useful animal model to determine the pharmacological and toxicological effects of nanoparticules. Here, we evaluated the behavioral and brain oxidative effects after zebrafish exposure to $(PhSe)_2$-loaded nanocapsules. Formulations were prepared by the interfacial deposition of preformed polymer method and after tested in zebrafish at concentrations ranging from 0.1 – 2.0 µM. Both locomotor and exploratory activities were assessed in the novel tank diving test. Moreover, brain oxidative status were determined by measuring thiobarbituric acid-reactive substance levels, glutathione peroxidase, glutathione redutase and glutathione S-transferase activities. $(PhSe)_2$-loaded nanocapsules did not alter distance travelled, immobility, and erratic swimming, suggesting the absence of behavioral impairments. Interestingly, the higher concentration tested had anxiolytic-like effects, since animals spent more time in the top area and showed a decreased thigmotaxis. Biochemical analysis showed that the tested concentrations did not affect oxidative stress-related parameters in brain samples, reinforcing the low toxicological potential of the formulation. In conclusion, exposure to $(PhSe)_2$-loaded nanocapsules caused no locomotor impairments as well as did not modify the oxidative status of zebrafish brain, suggesting the safeness of the formulation and that future pharmacological studies are worthy.

Key words: Organoselenium compounds, nanoparticles, nanotoxicology, zebrafish, novelty paradigm

1. Introduction

Selenium (Se) is an essential micronutrient for human body and it is particularly important in modulating the homeostasis of oxidative status because it contributes to endogenous antioxidant systems [1-3]. The Se biological importance motivated further studies concerning the element and its potential application as a therapeutic tool. Diphenyl diselenide [$(PhSe)_2$] is an organoselenium molecule, which has antioxidant, anti-inflammatory, antinociceptive, antitumor, neuro and hepatoprotective, antidepressant-like and anxiety-like actions [2, 4]. Nevertheless, its high lipophilicity difficults the preparation of aqueous parenteral solutions and reduces its complete dissolution in gastrointestinal tract and, consequently, its oral bioavailability [5, 6]. In addition, this molecule has a double character due to its contrasting behavior in biological systems that depends on the conditions of exposure and other factors (dose, administration route, animal specie) [2, 4, 7], which negatively counterbalance its therapeutic application.

Over the last years, the nanotechnology field has been considered an important tool in the pharmaceutical research [8, 9]. Undesired characteristics of active molecules such as high water insolubility and toxic effects can be masked and/or avoided by their incorporation into nanocarriers. Besides, the nanometric size promotes advantages such as drug targeting, controlled release, ease of crossing biological barriers and improved pharmacokinetics [9, 10]. Furthermore, these systems can be administered by different routes (e.g., oral, intravenous, ocular, ophthalmic and cutaneous) [11]. Among the nanocarriers, the polymeric nanocapsules have been studied for the encapsulation of lipophilic drugs due to their structural organization: a reservoir system wherein an oil core is surrounded by a polymeric wall and the drug can be adsorbed onto the polymeric surface and/or dissolved in the oil [10, 12]. Of particular importance, the scientific literature has some studies regarding the $(PhSe)_2$ incorporation into nanocapsules [13, 14]. Recently, in a previous study of our research group, $(PhSe)_2$-loaded nanocapsules were prepared using biocompatible materials such as medium chain triglycerides (MCT) and poly(ε-caprolactone) (PCL) and showed selective antimelanoma activity in a preliminary *in vitro* evaluation as well as no cytotoxic effects in human blood and keratinocytes cells [15].

The nanocarriers toxicology is still a challenge field for their pharmaceutical applications and represents an obstacle toward the clinical studies of nanoformulations. The main aspects regarding such condition are the possible unknown interaction with biological

molecules due to their nanometric size scale, shape and surface charge of the particles [16, 17]. There are several experimental approaches to estimate nanoparticles toxicity, including *in vitro* analyses as well as cellular assays and multi-cellular organisms, and *in vivo* models employing different animal species, mainly rodents [16, 17]. In this context, zebrafish (*Danio rerio*) has become an alternative animal model in the last years [18, 19]. This species exhibits genetic and physiologic similarities with human organism, which reinforces its application as an experimental tool. Importantly, protocols using zebrafish models are rapid and have low cost due to their small size, high reproducibility and quick development [18]. Interestingly, behavior evaluations are the most important parameters to identify toxic effects mainly because chemical toxicity can modify the swimming and exploratory activity [19, 20]. Moreover, zebrafish specie has been used as animal model to assay the safety, toxicity and/or biological effects of nanocarriers [20]. Considering the advantages of this animal model, the present study was designed to evaluate whether the acute exposure of zebrafish to $(PhSe)_2$-loaded polymeric nanocapsules alters locomotor and exploratory behaviors as well as influences some oxidative stress-related parameters in brain samples.

2. Materials and Methods

2.1 Materials

PCL (MW: 80 KDa), Span 80® (sorbitan monooleate) were acquired from Sigma Aldrich (Brazil). Tween 80® (polysorbate 80) and MCT (medium chain triglycerides) were furnished by Delaware (Brazil). All other were obtained from standard commercial suppliers. All other solvents and reagents were analytical grade and used as received.

2.2 Compound

$(PhSe)_2$ was obtained by the method described by Paulmier [21]. Chemical purity was determined by hydrogen and carbon nuclear magnetic resonance and gas chromatography (99.9 %).

2.3 Diphenyl diselenide-loaded polymeric nanocapsules

Nanocapsule suspensions containing $(PhSe)_2$ were prepared by interfacial deposition of preformed polymer method [22] and characterized in terms of average diameter, polydispersty index, zeta potential, drug content and encapsulation efficiency according to

Ferreira and co-workers [15]. Briefly, an organic phase composed by PCL (0.1 g), Span 80® (0.077 g), MCT (330 μL) and $(PhSe)_2$ (0.05 g) was prepared in acetone (27 mL), which was magnetically stirred until solubilize the components. Then, this phase was injected into a Tween 80® (0.077 g) aqueous dispersion (53 mL) and was magnetically stirred for 10 min longer. Next, the organic solvent and the excess of water were eliminated by evaporation under reduced pressure to achieve 10 mL of final volume, which corresponds to a $(PhSe)_2$ concentration at 5.0 mg/mL (NC $(PhSe)_2$). For comparison purposes, formulations without $(PhSe)_2$ were also prepared (NC B).

2.4 Animals

Adult zebrafish (*Danio rerio*) of mixed genders (50:50 male:female ratio) of 4 to 6 months old from a heterogeneous wild-type stock, weighing 0.6 ± 0.1 g and measuring 3.0 ± 1.0 cm in length were obtained from a local commercial supplier (Hobby Aquários, RS, Brazil) and housed in 50-L aquariums (80–100 fish per aquarium) for at least 2 weeks prior to the experiments. All tanks were filled with non-chlorinated water that was previously treated with 132 μL/L AquaSafe (Tetra, VA, USA) and maintained under mechanical and chemical filtration at 26 ± 2 °C. Water temperature, pH, and conductivity were set at 26 ± 2ºC, 7.0-8.0, and 1500–1600 μS/cm, respectively. The room illumination was provided by ceiling-mounted fluorescent lamps on a 14/10 light/dark photoperiod (lights on at 7:00 a.m.) and animals were fed twice a day with a commercial flake fish food (Alcon BASIC, Alcon, Brazil), which is recommended by the National Institutes of Health Guide for the Care and Use of Laboratory Animals. The animals were used in compliance with the Council for Control of Animal Experiments (CONCEA) and in accordance with the NIH Guide for the Care and Use of Laboratory Animals and approved by Ethics Committee for the Use of Animals-CEUA from the Federal University of Santa Maria (protocol number: 2301271116/2017). All efforts were made to minimize the number of animals used in the experiments and their stress.

2.5 Experimental design

Animals were randomly assigned to different groups (n = 8 to 12/group) for behavioral experiments and biochemical assays. Fish were randomly handled, removed from their home tanks, and individually transferred to beakers filled with the nanocapsule suspensions. Based on the study of free $(PhSe)_2$ conducted by Ibrahim and co-workers [23], fish were individually

exposed to different NC $(PhSe)_2$ concentrations (0.1, 0.25, 0.5, 1.0 and 2.0 µM) during 30 min. To discard some effect from the formulation constituents, other group was exposed to NC B at the same volume that was used to prepare the NC $(PhSe)_2$ at 2 µM. The NC formulations were further diluted in water to achieve the desired concentrations. Additionally, a control group was concomitantly carried out (without any exposure). For each exposure, a single fish was placed in each solution, and the solution was not used in subsequent experiments. To maintain the same experimental conditions all experiments were performed from 9:00 a.m. to 4:00 p.m.

2.6 Locomotor and exploratory evaluations by novel tank test

Thirty minutes after NCs exposure, animals were individually placed in a rectangular tank (23.9 cm along the bottom × 28.9 cm at the top, 15.1 cm in height) filled with home system water to perform the locomotor and exploratory evaluations [23-25]. A webcam (Microsoft LifeCam 1.1 with Auto-Focus) connect to a laptop was placed in front and on the top of the novel tank to monitoring the location and swimming activity of zebrafish during a 360-seconds trial [26]. The apparatus was virtually divided in two horizontal sections (bottom and top) to assess the vertical exploration, number of entries and time spent in bottom or in top area. Distance travelled was used to measure motor pattern. Anxiety- like behaviors were determined by measuring the number of freezing episodes and erratic swimming. Behavioral parameters were automatically measured at a rate of 30 frames/s using appropriate video-tracking software (ANY-maze, Stoelting CO, USA) and analyzed by different observers. To minimize handling stress and external influences, animals were gently moved from home tanks to beakers (exposure procedure) or to the novel tank. All experimental procedures were performed on a stable surface with the environmental distractions kept to a minimum. Each experimental group comprised individuals from multiple batches, and the tank water was replaced with clean system water for each trial.

2.7 Biochemical assays

2.7.1 Tissue preparation

After behavioral experiments, zebrafish were anesthetized with 0.25 g/L tricaine [27] and euthanized by punching the spinal cord behind the opercula. Brain samples were dissected out in ice, transferred to microtubes, and stored at - 80ºC. To perform the biochemical

analyses, samples were homogenized in 150 µL of Tris-HCl 50 mM pH 7.4 buffer and then centrifuged (3,000 g for 10 min, - 4ºC) to obtain the supernatant (S1), which was used for the assays. All experiments were performed in duplicate.

2.7.2 Protein determination

Protein was determined in the S1 by the Coomassie blue method using bovine serum albumin as analytical standard. Absorbance of samples was measured at 595 nm [28].

2.7.3 Lipid peroxidation

Thiobarbituric acid-reactive substance (TBARS) levels was the protocol used to estimate the lipid peroxidation [29]. Briefly, an aliquot of S1 was added to NaOH 3 M and incubated at 60 ºC for 30 min. After, phosphoric acid 6% and thiobarbituric acid (TBA) 0.8% were added to the system and the mixture was heated at 90 °C for 2h. A volume of 10% sodium dodecyl sulfate (SDS) and n-butanol was then added to extract the TBA-malondialdehyde (MDA) adduct, which was analyzed on Shimadzu® HPLC equipment. The analytical procedure was composed by a column Phenomenex® ODS-2 C18 reverse-phase (250 mm x 4.6 mm, 5 µm; 100 Å, Allcrom, BR) and a mobile phase constituted by ultrapure water and methanol (50:50; v/v). The HPLC analyses were performed under isocratic conditions at a 0.6 mL/min flow rate and UV detector set at 532 nm with a 20 µL sample volume injection [30]. Results were expressed as nmol MDA/mg protein.

2.7.4 Glutathione peroxidase (GPx)

GPx activity was assessed by spectrophotometric analysis following the rate of nicotinamide adenine dinucleotide phosphate (NADPH) oxidation at 340 nm by the coupled reaction with glutathione reductase [31]. The system consisted of potassium phosphate buffer (100 mM, pH 7.0), NaN_{31} mM, reduced glutathione1 mM, NADPH0.15 mM and 20 µL of S1 (40-60 µg of protein). The reaction was started by the addition of H_2O_2 0.4 mM (30 µL). The GPx activity was expressed as nmol/min/mg of protein.

2.7.4 Glutathione reductase (GR)

GR activity was based on the consumption of NADPH and it was spectrophotometrically measured at 340 nm. The 120 µL of S1 (40-60 µg of protein) was

added to 250 µL of a system (TFK 0.15 M and NADPH 0.15 mM). The reaction was started by the addition of 30 µL of GSSG (oxidized glutathione substrate). The GR activity was determined using the extinction coefficient of 6.22 mM/cm and expressed as nmol/min/mg protein [32].

2.7.5 Glutathione S-transferase (GST)

GST activity was carried out according to Habig and co-workers [33]. Samples were consisted of 1-chloro-2, 4-dinitrobenzene (CDNB) 1 mM in ethanol, glutathione reduced 10 mM, potassium phosphate buffer (20 mM; pH 6.5) and 20 µL of S1 (40-60 µg of protein). The enzyme activity was calculated by the changes in absorbance at 340 nm using a molar extinction coefficient of 9.6 mM/cm. One unit GST activity was defined as the amount of enzyme required to catalyze the conjugate 1 mol CDNB with GSH/min at 25 ºC. The activity was expressed as µmol GS-DNB/min/mg protein.

2.8 Statistical analysis

Data were expressed as mean ± standard error of the mean (S.E.M.) and analyzed by one-way ANOVA, followed by the Student-Newman-Keuls multiple comparison test whenever necessary. The significance level was set at $p \leq 0.05$. Since NC B results were compared with control data by t test and no significant differences were revealed data obtained with the NC B exposure were used to perform statistical evaluation with the different NC $(PhSe)_2$ concentrations.

3. Results and discussion

Over the last years, the zebrafish emerges as a versatile model in behavioral neuroscience and toxicology [18]. When compared to mammals, this species shares evolutionarily conserved brain structures, neurotransmitters, receptors and hormones, suggesting its utility in preclinical toxicological screenings [18]. Moreover, due to their intermediate position between *in vitro* cell-based tests and *in vivo* mammalian models, the use of zebrafish in basic research reduces the existing gap between invertebrates and mammalian model systems [20, 34]. The novel tank test has been employed as an experimental protocol to determine possible alterations in the normal behavioral activity of zebrafish to estimate the pharmacological and/or toxicological effects of substances [18, 24, 25]. Some parameters,

such as distance traveled, number of immobile episodes, and erratic swimming are considered indicative of locomotor activity, while thigmotaxis and vertical activity (bottom and top areas) were used as exploratory endpoints [19, 24].

The effects of free $(PhSe)_2$ in zebrafish was investigated elsewhere [23]. Similarly, the novel tank test was also employed to evaluate spatiotemporal behavior, locomotor parameters, vertical exploration, and homebase formation. The $(PhSe)_2$ was used at a concentration ranging from 0.1 – 1.0 µM and anxiolytic-like effects were observed at 0.25 µM. However, beyond the pharmacological effects, the high concentrations tested (0.5 and 1.0 µM) caused severe side effects. Here, we evaluated for the first time the effects of nanoencapsulated $(PhSe)_2$ on zebrafish, using the behavioral assessment as a potential indicative of toxicological effects. After the exposure to NCs formulation, brain oxidative status was determined to further investigate the actions of NC $(PhSe)_2$ on oxidative stress-related biomarkers.

Fig. 1 depicts the results of number of immobile episodes and erratic swimming after the NC exposure. These behaviors are indicative of high stress situations and/or anxiety during habituation to novelty [19]. There were few episodes of immobility and erratic swimming (figure 1A and 1B) and no statistical differences were revealed among groups. Importantly, fish exposed to free $(PhSe)_2$ at 1 µM had an increase in number of immobility episodes [23], a similar side effect when compared to benzodiazepines, such as diazepam and chlordiazepoxide [35]. Conversely, the nanoencapsulation abolished this negative effect, reinforcing the advantages of incorporating molecules [10].

Fig. 2A shows the results of distance traveled in the novel tank test. Alterations on distance traveled may reflect hyper/hypoactivity and/or loss of motor patterns [19]. Here, none of the NC $(PhSe)_2$ concentrations tested modified the distance traveled in comparison to NC B ($p>0.05$). In comparison to the study conducted by Ibrahin and co-workers, the zebrafish exposure to free compound caused a significant reduction in distance traveled at 0.5 and 1.0 µM, which represent an undesired side effect of lethargy [23]. These results indicate that nanoencapsulation reduces adverse effects on locomotion.

The habituation and the gradual exploration of novel environments depend on anxiety-like behaviors, which can be measured by the time spent in each horizontal sections and vertical areas of tank [19]. Moreover, thigmotaxis refers to a behavioral preference by tank edge/sides, in which animals avoid the central areas [19]. Fig. 2B shows that animals exposed to NC $(PhSe)_2$ at concentrations 0.1, 0.25, 0.5 and 1.0 µM had a similar thigmotaxis when compared

to NC B ($p > 0.05$), suggesting that no behavioral impairments concerning the aquarium spatial preference were observed. Nevertheless, 2.0 µM NC $(PhSe)_2$ decreased the time in the peripheral area ($p<0.05$), suggesting the absence of toxic effects and an increased exploratory activity, which is an indicative of anxiolytic-like behavior. Reinforcing such hypothesis, this behavioral modification was already reported in zebrafish exposed to escitalopram, which is a well-recognized anxiolytic compound [36].

Usually, non-treated fish has a tendency of homebase formation by establishing a safe place at a specific tank area, in which animals repeatedly returns after exploring other tank areas [19, 23, 37]. In this sense, the spatiotemporal behavior of zebrafish exposed to a range of NC $(PhSe)_2$ concentrations were also determined. Fig. 3A shows that the highest concentration tested (2.0 µM) caused a reduction in the time spent at bottom area ($p<0.05$). Furthermore, zebrafish exposed to 2.0 µM NC $(PhSe)_2$ had a significant increase in time spent at top area as demonstrated in Fig. 3B ($p<0.05$). The other NC $(PhSe)_2$ concentrations did not change the respective parameters ($p>0.05$). Figs. 4C and 4D show the number of transitions to top area and the latency to enter the top, respectively. No statistical differences were found among the groups ($p>0.05$). In the study of Ibrahim and co-workers, the group of animals exposed to 1.0 µM $(PhSe)_2$ spent less more time in the top area of the aquarium, suggesting anxiolytic-like effects. However, the same concentration that promoted this potential pharmacological action also triggered undesirable effects [23].

Our data suggest that the differently than observed to free $(PhSe)_2$ [23], NC $(PhSe)_2$ had no potential toxicological effects in such parameters evaluated. The respective study did not test $(PhSe)_2$ concentrations upper to 1 µM due to the low water solubility of the compound at higher concentrations. On the other hand, we showed the behavioral and biochemical effects of 2 µM, which was possible due to the aqueous character of NC suspension. Importantly, both $(PhSe)_2$ forms (free and nanoencapsulated) elicited anxiolytic-like effects in zebrafish. However, while the free compound caused such effect at 0.25 µM, the NC $(PhSe)_2$ triggered anxiolytic-like effects only at 2.0 µM. This difference could be attributed to the $(PhSe)_2$ controlled release conferred by nanocapsules. Such characteristic is an advantageous property that prevents the abrupt exposure of the organism to the selenium compound, reducing its toxicity. Moreover, such nanocapsules property is well demonstrated by the scientific reports, especially in formulations prepared with the components used here [10, 38, 39].

Biochemical markers of oxidative status were assessed in brain samples of the animals after zebrafish exposure to NC $(PhSe)_2$. Fig. 4 depicts the MDA levels (A) and the activity of GPx (B), GR (C) and GST (D). One-way ANOVA analysis revealed that regardless the NC $(PhSe)_2$ concentration tested, the parameters remained unchanged. The oxidative stress is an important mechanism associated with the toxicity triggered by nanostructures [40]. The small size could facilitate nanoparticles uptake by cells, promoting superior interaction between the formulation and cellular components, which may cause oxidative injury by overproduction of reactive species [40, 41]. In addition, the brain is the most organ susceptible to oxidative stress, main because of the high oxygen consumption [42]. Based on the current results, it is possible to suggest that the exposure of zebrafish to NC $(PhSe)_2$ did not trigger neither behavioral impairments nor brain oxidative imbalance.

Conclusion

In summary, the nanoencapsules formed by PCL and MCT reduced the $(PhSe)_2$ apparent toxicity in zebrafish, broadening the perspective of its therapeutic application. In this sense, the nanocapsules suspension containing $(PhSe)_2$ may be considered a promising formulation for future studies of pharmacological action.

Conflict of interest

The authors report no conflicts of interest.

Acknowledgements

L. M. Ferreira acknowledges the grant from CAPES.

References

[1] G. Mugesh, W.W. du Mont, H. Sies, Chemistry of biologically important synthetic organoselenium compounds, Chem Rev 101(7) (2001) 2125-79.

[2] R.M. Rosa, R. Roesler, A.L. Braga, J. Saffi, J.A.P. Henriques, Pharmacology and toxicology of diphenyl diselenide in several biological models, Braz J Med Biol Res 40(10) (2007) 1287-1304.

[3] J.V. Comasseto, Selenium and tellurium chemistry: historical background, J Brazil Chem Soc 21 (2010) 2027-2031.

[4] C.W. Nogueira, J.B.T. Rocha, Diphenyl Diselenide a Janus-Faced Molecule, J Brazil Chem Soc 21(11) (2010) 2055-2071.

[5] M. Prigol, C.W. Nogueira, G. Zeni, M.R. Bronze, L. Constantino, Physicochemical and Biochemical Profiling of Diphenyl Diselenide, Appl Biochem Biotech 169(3) (2013) 885-893.

[6] M. Prigol, C.A. Bruning, F. Martini, C.W. Nogueira, Comparative Excretion and Tissue Distribution of Selenium in Mice and Rats Following Treatment with Diphenyl Diselenide, Biol Trace Elem Res 150(1-3) (2012) 272-277.

[7] N.B.V. Barbosa, J.B.T. Rocha, G. Zeni, T. Emanuelli, M.C. Beque, A.L. Braga, Effect of organic forms of selenium on delta-aminolevulinate dehydratase from liver, kidney, and brain of adult rats, Toxicol Appl Pharm 149(2) (1998) 243-253.

[8] F.A. Dimer, R.B. Friedrich, R.C.R. Beck, S.S. Guterres, A.R. Pohlmann, Impactos da nanotecnologia na saúde : produção de medicamentos, Quim. Nova 36(10) (2013) 1520-1526.

[9] S.G. Bhokare, R.P. Marathe, M.T. Gaikwad, P.B. Salunke, Biodegradable Polymer Based Nanoparticles: A Novel Approach, Int. J. Pharm. Sci. Rev. Res. 35(1) (2015) 43-52.

[10] L.A. Frank, R.V. Contri, R.C.R. Beck, A.R. Pohlmann, S.S. Guterres, Improving drug biological effects by encapsulation into polymeric nanocapsules, Wires Nanomed Nanobi 7(5) (2015) 623-639.

[11] C.E. Mora-Huertas, H. Fessi, A. Elaissari, Polymer-based nanocapsules for drug delivery, Int J Pharmaceut 385(1-2) (2010) 113-142.

[12] C. Vauthier, K. Bouchemal, Methods for the preparation and manufacture of polymeric nanoparticles, Pharm Res 26(5) (2009) 1025-58.

[13] C.F.A. Giordani, D. de Souza, L. Dornelles, C.W. Nogueira, M.P. Alves, M. Prigol, O.E.D. Rodrigues, Diphenyl Diselenide-Loaded Nanocapsules: Preparation and Biological Distribution, Appl Biochem Biotech 172(2) (2014) 755-766.

[14] S.T. Stefanello, F. Dobrachinski, N.R. de Carvalho, G.P. Amaral, R.P. Barcelos, V.A. Oliveira, C.S. Oliveira, C.F.A. Giordani, M.E. Pereira, O.E.D. Rodrigues, F.A.A. Soares, Free radical scavenging *in vitro* and biological activity of diphenyl diselenide-loaded nanocapsules: DPDS-NCS antioxidant and toxicological effects, Int J Nanomed 10 (2015).

[15] L.M. Ferreira, V.F. Cervi, M.H.M. Sari, A.V. Barbieri, A.P. Ramos, P.M. Copetti, G.F. Brum, K. Nascimento, J.M. Nadal, P.V. Farago, M.R. Sagrillo, C.W. Nogueira, L. Cruz, Diphenyl diselenide loaded poly(ε-caprolactone) nanocapsules with selective antimelanoma activity: Development and cytotoxic evaluation, Mat Sci Eng C-Mater 91 (2018) 1-9.

[16] S. Aula, S. Lakkireddy, K. Jamil, A. Kapley, A.V.N. Swamyd, H.R. Lakkireddy, Biophysical, biopharmaceutical and toxicological significance of biomedical nanoparticles, Rsc Adv 5 (2015) 47830–47859.

[17] M. Adabi, M. Naghibzadeh, M.A. Zarrinfard, S.S. Esnaashari, A.M. Seifalian, R. Faridi-Majidi, H. Tanimowo Aiyelabegan, H. Ghanbari, Biocompatibility and nanostructured materials: applications in nanomedicine, Artificial cells, nanomedicine, and biotechnology 45(4) (2017) 833-842.

[18] A.V. Kalueff, D.J. Echevarria, S. Homechaudhuri, A.M. Stewart, A.D. Collier, A.A. Kaluyeva, S. Li, Y. Liu, P. Chen, J. Wang, L. Yang, A. Mitra, S. Pal, A. Chaudhuri, A. Roy, M. Biswas, D. Roy, A. Podder, M.K. Poudel, D.P. Katare, R.J. Mani, E.J. Kyzar, S. Gaikwad, M. Nguyen, C. Song, Zebrafish neurobehavioral phenomics for aquatic neuropharmacology and toxicology research, Aquat Toxicol 170 (2016) 297-309.

[19] A.V. Kalueff, M. Gebhardt, A.M. Stewart, J.M. Cachat, M. Brimmer, J.S. Chawla, C. Craddock, E.J. Kyzar, A. Roth, S. Landsman, S. Gaikwad, K. Robinson, E. Baatrup, K. Tierney, A. Shamchuk, W. Norton, N. Miller, T. Nicolson, O. Braubach, C.P. Gilman, J. Pittman, D.B. Rosemberg, R. Gerlai, D. Echevarria, E. Lamb, S.C. Neuhauss, W. Weng, L. Bally-Cuif, H. Schneider, Towards a comprehensive catalog of zebrafish behavior 1.0 and beyond, Zebrafish 10(1) (2013) 70-86.

[20] C. Chakraborty, A.R. Sharma, G. Sharma, S.S. Lee, Zebrafsh: A complete animal model to enumerate the nanoparticle toxicity, J Nanobiotechnol 14(65) (2016) 1-13.

[21] C. Paulmier, Selenoorganic functional groups. Selenium reagents and intermediates in organic synthesis, Angew. Chem. 100 (1986) 25-51.

[22] H. Fessi, F. Puisieux, J.P. Devissaguet, N. Ammoury, S. Benita, Nanocapsule Formation by Interfacial Polymer Deposition Following Solvent Displacement, Int J Pharmaceut 55(1) (1989) R1-R4.

[23] M. Ibrahim, B.H. Mussulini, L. Moro, A.M. de Assis, D.B. Rosemberg, D.L. de Oliveira, J.B. Rocha, R.S. Schwab, P.H. Schneider, D.O. Souza, E.P. Rico, Anxiolytic effects of diphenyl diselenide on adult zebrafish in a novelty paradigm, Prog Neuropsychopharmacol Biol Psychiatry 54 (2014) 187-94.

[24] D.B. Rosemberg, E.P. Rico, B.H.M. Mussulini, A.L. Piato, M.E. Calcagnotto, C.D. Bonan, R.D. Dias, R.E. Blaser, D.O. Souza, D.L.d. Oliveira, Differences in spatio-temporal

behavior of zebrafish in the open tank paradigm after a short-period confinement into dark and bright environments. , Plus One 6(5) (2011) e19397; 1-11.

[25] J. Cachat, A. Stewart, L. Grossman, S. Gaikwad, F. Kadri, K.M. Chung, N. Wu, K. Wong, S. Roy, C. Suciu, J. Goodspeed, M. Elegante, B. Bartels, S. Elkhayat, D. Tien, J. Tan, A. Denmark, T. Gilder, E. Kyzar, J. Dileo, K. Frank, K. Chang, E. Utterback, P. Hart, A.V. Kalueff, Measuring behavioral and endocrine responses to novelty stress in adult zebrafish, Nature protocols 5(11) (2010) 1786-99.

[26] R. Gerlai, M. Lahav, S. Guo, A. Rosenthal, Drinks like a fish: zebra fish (*Danio rerio*) as a behavior genetic model to study alcohol effects, Pharmacol Biochem Behav. 67 (2000) 773-782.

[27] J.M. Wilson, R.M. Bunte, A.J. Carty, Evaluation of rapid cooling and tricaine methanesulfonate (MS222) as methods of euthanasia in zebrafish (*Danio rerio*), J Am Assoc Lab Anim Sci 48 (2009) 785-789.

[28] M.M. Bradford, A rapid and sensitive method for the quantitation of microgram quantities of protein utilizing the principle of protein-dye binding, Anal. Biochem 79 (1976) 248-254.

[29] H. Ohkawa, N. Ohishi, K. Yagi, Assay for lipid peroxides in animal tissues by thiobarbituric acid reaction, Anal Biochem 95(2) (1979) 351-8.

[30] D. Grotto, L.D. Santa Maria, S. Boeira, J. Valentini, M.F. Charao, A.M. Moro, P.C. Nascimento, V.J. Pomblum, S.C. Garcia, Rapid quantification of malondialdehyde in plasma by high performance liquid chromatography-visible detection, J Pharm Biomed Anal 43(2) (2007) 619-24.

[31] D.E. Paglia, W.N. Valentine, Studies on the quantitative and qualitative characterization of erythrocyte glutathione peroxidase, The Journal of laboratory and clinical medicine 70(1) (1967) 158-69.

[32] I. Carlberg, B. Mannervik, Glutathione reductase, Methods Enzymol 113 (1985) 484-90.

[33] W.H. Habig, M.J. Pabst, G. Fleischner, Z. Gatmaitan, I.M. Arias, W.B. Jakoby, Identity of Glutathione S-Transferase-B with Ligandin, a Major Binding-Protein of Liver, P Natl Acad Sci USA 71(10) (1974) 3879-3882.

[34] H. Sukardi, H.T. Chng, E.C.Y. Chan, Z. Gong, S.H. Lam, Zebrafish for drug toxicity screening: bridging the *in vitro* cell-based models and *in vivo* mammalian models, Expert Opin. Drug Metab. Toxicol. 7(5) (2011) 579-589.

[35] Z. Bencan, D. Sledge, E.D. Levin, Buspirone, chlordiazepoxide and diazepam effects in a zebrafish model of anxiety, Pharmacology, biochemistry, and behavior 94(1) (2009) 75-80.

[36] S.V. Nielsen, M. Kellner, P.G. Henriksen, H. Olsen, S.H. Hansen, E. Baatrup, The psychoactive drug Escitalopram affects swimming behaviour and increases boldness in zebrafish (*Danio rerio*), Ecotoxicology 27(4) (2018) 485-497.

[37] A. Stewart, N. Wu, J. Cachat, P. Hart, S. Gaikwad, K. Wong, E. Utterback, T. Gilder, E. Kyzar, A. Newman, D. Carlos, K. Chang, M. Hook, C. Rhymes, M. Caffery, M. Greenberg, J. Zadina, A.V. Kalueff, Pharmacological modulation of anxiety-like phenotypes in adult zebrafish behavioral models, Prog Neuropsychopharmacol Biol Psychiatry 35(6) (2011) 1421-31.

[38] M. Gehrcke, L.M. Giuliani, L.M. Ferreira, A.V. Barbieri, M.H.M. Sari, E.F. da Silveira, J.H. Azambuja, C.W. Nogueira, E. Braganhol, L. Cruz, Enhanced photostability, radical scavenging and antitumor activity of indole-3-carbinol-loaded rose hip oil nanocapsules, Mat Sci Eng C-Mater 74 (2017) 279-286.

[39] M.C. Fontana, K. Coradini, S.S. Guterres, A.R. Pohlmann, R.C.R. Beck, Nanoencapsulation as a way to control the release and to increase the photostability of clobetasol propionate: influence of the nanostructured system, J Biomed Nanotechnol 5(254-263) (2009).

[40] K.L. Aillon, Y. Xie, N. El-Gendy, C.J. Berkland, M.L. Forrest, Effects of nanomaterial physicochemical properties on *in vivo* toxicity, Adv Drug Deliv Rev 61(6) (2009) 457-66.

[41] M.H.M. Sari, L.M. Ferreira, V.A. Zborowski, P.C.O. Araujo, V.F. Cervi, C.A. Bruning, L. Cruz, C.W. Nogueira, p,p'-Methoxyl-diphenyl diselenide-loaded polymeric nanocapsules are chemically stable and do not induce toxicity in mice, Eur J Pharm Biopharm 117 (2017) 39-48.

[42] B. Halliwell, Reactive oxygen species and the central nervous system, J Neurochem 59(5) (1992) 1609-23.

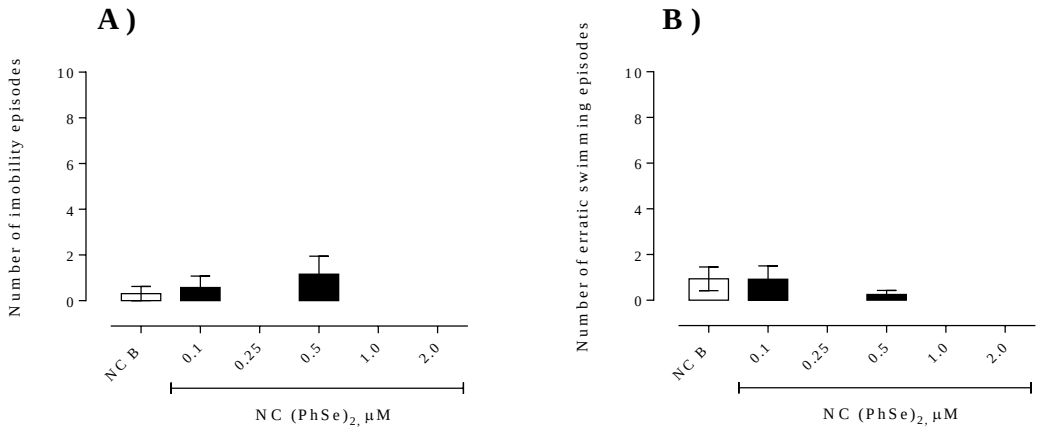

Figure 1. Immobility (A) and erratic swimming (B) of zebrafish after exposure to the NC B and NC $(PhSe)_2$. Each column represents the mean ± S.E.M. Data were analyzed by one-way ANOVA and no significant differences were detected. For notes, NC $(PhSe)_2$ means nanocapsules containing $(PhSe)_2$; NC B means nanocapsules without $(PhSe)_2$.

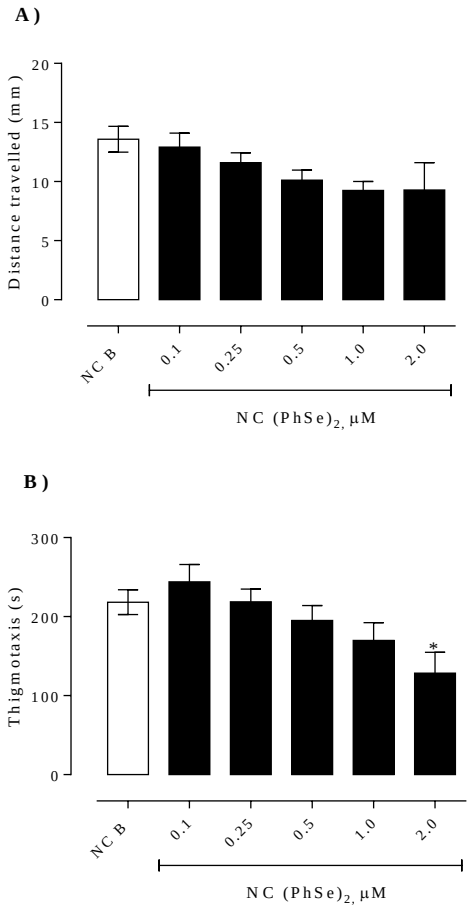

Figure 2. Effects of NC $(PhSe)_2$ on distance travelled (A) and tigmotaxis (B). Each column represents the mean ± S.E.M. Asterisks denote significant differences (* $p<0.05$) in comparison to the NC B group by one-way ANOVA, followed by Newman-Keuls post hoc test. For notes, NC $(PhSe)_2$ means nanocapsules containing $(PhSe)_2$; NC B means nanocapsules without $(PhSe)_2$.

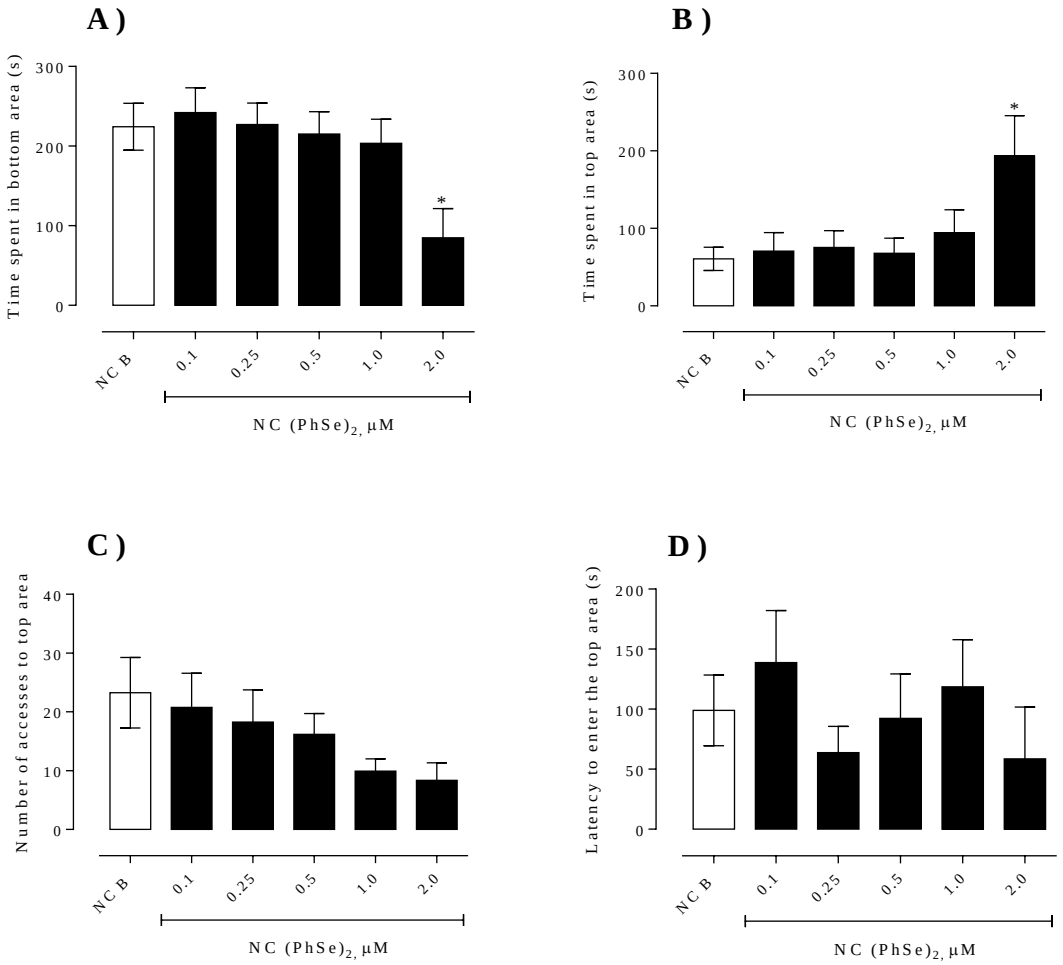

Figure 3. Effects of NC $(PhSe)_2$ on vertical exploratory parameters: Time spent in the bottom area (A), time spent in the top area (B), number of entries to the top area (C) and latency to enter to the top area (D). Each column represents the mean ± S.E.M. Asterisks denote significant differences (* $p<0.05$) in comparison to the NC B group by one-way ANOVA, followed by Newman-Keuls post hoc test. For notes, NC $(PhSe)_2$ means nanocapsules containing $(PhSe)_2$; NC B means nanocapsules without $(PhSe)_2$.

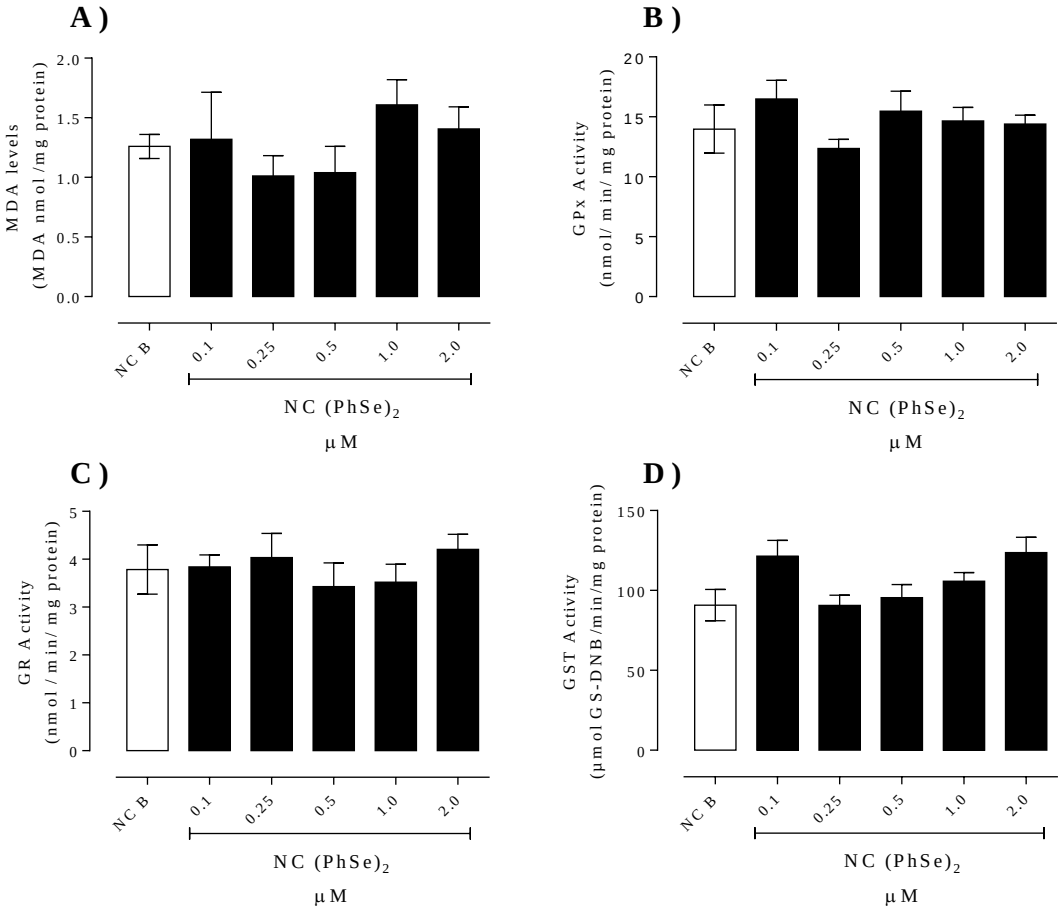

Figure 4. Oxidative status of zebrafish brain following NC $(PhSe)_2$ exposure. TBARS levels (A), glutathione peroxidase (B), glutathione reductase (C) and glutathione S-transferase (D) activities. Each column represents the mean ± S.E.M. One-way ANOVA did not reveal significant differences among groups. For notes, NC $(PhSe)_2$ means nanocapsules containing $(PhSe)_2$; NC B means nanocapsules without $(PhSe)_2$.

4.2 Manuscrito 1

Diphenyl diselenide-loaded nanocapsules suspension is effective in reducing the tumor development in an animal model of glioblastoma multiforme

Luana Mota Ferreira[a], Juliana Hofstatter Azambuja[b], Elita Ferreira da Silveira[c], Marcel Henrique Marcondes Sari[a,d], Bruna da Cruz Weber Fulco[d], Vinicius Costa Prado[d], Nicolly Espindola Gelsleichter[b], Liziane Raquel Beckenkamp[b], Marilda Fernandes da Cruz[b], Rosélia M. Spanevello[c], Marcia Rosângela Wink[b], Rita de Cassia Sant Anna Alves[e], Cristina Wayne Nogueira[d], Elizandra Braganhol[b,c], Letícia Cruz[a].

[a]Laboratório de Tecnologia Farmacêutica, Programa de Pós-graduação em Ciências Farmacêuticas, Centro de Ciências da Saúde, Universidade Federal de Santa Maria, Santa Maria, RS, Brazil.

[b]Programa de Pós-Graduação em Biociências, Universidade Federal de Ciências da Saúde, Porto Alegre, RS, Brazil.

[c]Programa de Pós-Graduação em Bioquímica e Bioprospecção, Centro de Ciências Químicas, Farmacêuticas e de Alimentos, Universidade Federal de Pelotas, Pelotas, RS, Brazil.

[d]Laboratório de Síntese, Reatividade e Avaliação Farmacológica e Toxicológica de Organocalcogênios, Centro de Ciências Naturais e Exatas, Universidade Federal de Santa Maria, Santa Maria, RS, Brazil.

[e]Departamento de Patologia e de Medicina Legal, Universidade Federal de Ciências da Saúde de Porto Alegre, Porto Alegre, RS, Brazil.

*Corresponding author

Letícia Cruz, Programa de Pós-Graduação em Ciências Farmacêuticas, Universidade Federal de Santa Maria, Santa Maria, 97105-900, Brazil.

Phone: +55 55 3220 9373

E-mail: leticiacruz@smail.ufsm.br

Abstract

Gliomas are the most aggressive malignant tumors of the central nervous system. The diphenyl diselenide $(PhSe)_2$ is an organoselenium compound that has multiple pharmacological properties, including antitumoral effect, but it exhibits physicochemical limitations, which can be circumvented by its nanoencapsulation. This way, this study was designed to evaluate the antiglioma effect of free and nanoencapsulated $(PhSe)_2$ in a gliobastoma multiform animal model as well as to test their *in vivo* toxicity. For the *in vitro* tests, rat glioma C6 cells were incubated during 48 h with free $(PhSe)_2$ or NC $(PhSe)_2$ and the cell viability (MTT assay), propidium iodide (PI) uptake and nitrite levels were determined. The glioblastoma model was induced by implantation of C6 glioma cells (1×10^6 cells) in the right striatum. Both compound forms decreased the C6 glioma cells viability without causing any effect to astrocytes cells (healthy control). The NC $(PhSe)_2$ had superior effect than its free form and also increased the nitrite content. The repeated intragastric administration of $(PhSe)_2$ or NC $(PhSe)_2$ (5 mg/kg/day during 15 days) caused neither alteration in the plasma renal and hepatic markers of function nor in the parameters of oxidative balance in brain, liver and kidneys. Independent of the $(PhSe)_2$ forms, the intragastric treatment (1mg/kg/day during 15 days) reduced brain tumor size In conclusion, the $(PhSe)_2$ nanoencapsulation improved its cytotoxic effect against C6 glioma cells and both compound forms attenuated the tumor development and caused no toxicological effects.

Keywords: Organoselenium compounds, C6 cells, polymeric nanoparticles, gliomas

1. Introduction

The gliomas are central nervous system cancer, which are characterized by aggressive neoplasms, with rapid invasiveness tissues rate and low response to treatment, presenting high mortality and morbidity [1, 2]. Among them, the glioblastoma multiforme is the ultimate grade of malignancy, in which the median overall survival of patients does not exceed a year after the diagnosis [2, 3]. Current therapy of gliomas includes combination of neurosurgical resection, radiotherapy and chemotherapy. Nevertheless, surgery is often not indicated because the tumor has high rate of recurrence and elevate capacity for proliferation and an infiltrate growth pattern. Besides, the main reason for chemotherapy failure is associated with the difficulty of drugs passing through the blood–brain barrier, which restricts the access to the central nervous system and induces therapy failure [2, 4]. Recognizing the need to improve patients' survival, the research for the new and innovative strategies for glioma treatment is very relevant.

The organoselenium compounds belong to a class of molecules with multiple pharmacological properties [5]. Among them, the diphenyl diselenide [$(PhSe)_2$] is the most studied compound because of its potent antioxidant, neuroprotective and antiinflammatory actions. Of particular importance, the $(PhSe)_2$ antitumoral effect was already reported by *in vitro* evaluations against human neuroblastoma [6], human colon adenocarcinoma [7] and human melanoma cells [8], and *in vivo* by a rodent model of mammary cancer [9]. Converging lines of evidence suggest that the molecular mechanisms of $(PhSe)_2$ antitumoral action could be attributed to the modification in the apoptotic and pro-apoptotic proteins content as well as the expression of p53 gen, which can change the cell growth cycle [7, 10]. Reinforcing this hypothesis, Melo and co workers demonstrated that $(PhSe)_2$ protected MCF-7 cells against tamoxifen-induced DNA damage without reducing its selective toxicity against tumor cells [11].

Despite the $(PhSe)_2$ pharmacological potentialities, toxic issues, such as the inhibition of some enzymes (δ-aminolevulinate enzyme dehydratase (δ-ALA-D)) [12] and oxidation of glutathione (GSH) [13] limit its therapeutic uses. In addition, the $(PhSe)_2$ is a poorly water-soluble compound [14], which leads to low oral bioavailability [15] and hinders its administration by parenteral route due to the difficulty of preparing aqueous formulations. Considering that, the $(PhSe)_2$

incorporation into polymeric nanocapsules has been studied as an alternative to optimize its toxicological and physicochemical limitations [16, 17].

The nanostructured systems have been extensively studied due to many advantages achieved by encapsulating drugs, for instance: sustained and site-specific drug delivery [18], stability improvement [19], toxicity reduction [18, 20] as well as enhancement of pharmacological effects and bioavailability [21-23], among others [24]. Despite the great number of scientific reports concerning nanocarriers development focused on cancer management, there are few FDA approved nanomedicines. The main are Abraxane (breast cancer), Doxil (ovarian cancer), Oncaspar (acute lymphoblastic leukemia), DaunoXome (Kaposis's sarcoma) and Emend for the chemotherapy-induced nauseas. The nanoparticles efficacy in cancer treatment is mainly attributed to sitespecific drug release and side effects reduction [25-27].

Some studies about $(PhSe)_2$ incorporation into polymeric nanocapsules demonstrated that this association improved its biological distribution [16] and antioxidant action without causing toxic effects [17]. Recently, our research group developed a suspension of $(PhSe)_2$-loaded polymeric nanocapsules that showed many advantages in comparison to the free compound. Despite the adequate physicochemical characteristics, the nanoencapsulation provided superior storage stability and photostability. Besides, differently from its free form, the $(PhSe)_2$-loaded nanocapsules selectively reduced the viability of A375 melanoma cells, without causing toxicity to healthy keratinocyte cells [8].

Considering the potential of $(PhSe)_2$-loaded nanocapsules for cancer treatment, the purpose of this study was to investigate the antitumor effect of $(PhSe)_2$ free and nanoencapsulated against the glioblastoma multiforme. For this, *in vitro* and *in vivo* protocols were carried out to demonstrate the possible efficacy of the treatment against C6 rat glioma cells and in an animal model of glioblastoma. Besides, an *in vivo* toxicological study was also conducted.

2. Materials and Methods

2.1 Drugs, reagents and materials

The $(PhSe)_2$ was obtained accordingly to a previously described method of Paulmier. Chemical purity of the compound (99.9 %) was assessed by gas

chromatography-mass spectrometry and high-performance liquid chromatography (Shimadzu QP2010PLUS GC/MS). The ^{1}H and ^{13}C nuclear magnetic resonance spectra were obtained at 400 MHz (Bruker AvanceTM III HD) and showed analytical and spectroscopic data in full agreement with the assigned structure.

Poly(Ɛ-caprolactone) (PCL) (MW: 80 KDa) and Span 80® (sorbitan monooleate) were acquired from Sigma Aldrich (Brazil). Tween 80® (polysorbate 80) and MCT (medium chain triglycerides) were furnished by Delaware (Brazil). Dulbecco's modified Eagle's medium (DMEM), Fungizone, penicillin/streptomycin, 0.25% trypsin/EDTA solution and fetal bovine serum (FBS) were obtained from Gibco (USA). The 3(4-5-dimethyl)-2-5diphenyl tetrazolium bromide (MTT) was acquired from Thermofisher. The glioma cell line C6 was purchased from American Type Culture Collection (USA). All other chemicals and solvents were obtained from standard commercial suppliers with analytical grade standard and were used as received.

2.2 Nanocapsule suspensions

Nanocapsules suspension containing $(PhSe)_2$ were prepared and characterized (average diameter, polydipersity index, zeta potential, pH, $(PhSe)_2$ content and encapsulation efficiency) as described in our previous study [8]. Briefly, an organic phase containing PCL (0.1 g), Span 80® (0.077 g), MCT (330 µL), acetone (27 mL), and $(PhSe)_2$ (0.05 g) was magnetically stirred at 40 °C for 60 min to solubilize the constituents, and then injected into a Tween 80® (0.077 g) aqueous dispersion (53 mL). The mixture was magnetically stirred for 10 min at room temperature and then solvent was eliminated by evaporation under reduced pressure until a 10 mL of final volume, which corresponds to a $(PhSe)_2$ concentration of 5.0 mg/mL (NC $(PhSe)_2$). For comparison purposes, formulations without $(PhSe)_2$ were also prepared (NC B).

2.3. In vitro assays

2.3.1 Glioma cultures

The C6 cells were cultured in DMEM containing 0.1% Fungizone and 100 U/L penicillin/streptomycin and supplemented with 5% (v/v) FBS. After the cultures reached confluency, the cells were released by trypsinization of the cultivation bottle

and seeded in 96 well plates, which were maintained at 37 °C in a humidified atmosphere of 5% CO_2 for 24 h. The plates containing C6 cells were incubated with NC $(PhSe)_2$ or free $(PhSe)_2$ at the concentrations 1, 2.5, 5, 10, 25, 50, 100 and 200 µM for 48h. These concentrations were selected based on our previous study about the cytotoxic effect of $(PhSe)_2$ [8]. To achieve such concentrations, 10-fold serial dilutions were made using RPMI culture medium from the $(PhSe)_2$ nanocapsules suspension or the stock solution of free $(PhSe)_2$, which was dissolved in DMSO (10 %). For comparison purposes, plates incubated with DMSO (10 %) or NC B were simultaneously performed. All observations were validated by at least three independent experiments and for each experiment the analyses were conducted in triplicate.

2.3.2 Primary astrocyte cultures

Primary astrocyte cultures were prepared as described by da Silveira and coworkers [26]. Briefly, brain cortex samples of newborn Wistar rats (1–2 days old; Ethical committee protocol number 23110009402/2016-01) were obtained, removed and mechanically homogenized in a Ca þ 2 and Mg þ 2 free balanced salt solution pH 7.4, (137 mM NaCl, 5.36 mM KCl, 0.27 mM Na_2HPO_4, 1.1 mM KH_2PO_4 and 6.1 mM glucose). After centrifugation (5 min/1000 *xg*), the pellet was suspended in DMEM supplemented with 10% FBS. The cells ($5x10^4$) were plated in poly-L-lysine-coated 96-well plates and 4 h later they were gently shaken, washed with PBS, and the medium was changed to remove neuron and microglia contaminants. Over a period of 20–25 days, the cultures grew until achieve confluence and the medium was replaced every four days. The plates containing astrocytes cells were incubated with NC $(PhSe)_2$ or free $(PhSe)_2$ at a concentration range 10, 25, 50 and 100 µM for 48 h. Cells treated with DMSO (10 %) or NC B were used for comparison purposes as described in section 2.3.1.

2.3.3 MTT assay

The MTT reduction assay was performed to determine the C6 and astrocytes viability. The test was carried out according to our previous study [8]. After the aforementioned incubations the plates were washed twice with sodium phosphate

buffer and an amount of the yellow tetrazolium salt MTT solution (1 mg/mL) was added to the plates. Following, the plates were incubated at 37 °C for 3 h, under light protection until the formation of violet formazan crystals. Later, the solution was then removed and an amount of DMSO was added to each well. The optical density of each plate was measured at 492 nm and the results were expressed by cell viability (%) in comparison to the DMEM culture medium, which was used as the negative cell death control.

2.3.4 Nitrite content determination

The Griess reaction was used to estimate the nitrite (NO_2^-) levels, as a nitric oxide (NO) marker, in the culture medium [28] after C6 incubation with $(PhSe)_2$, free and nanoencapsulated. Briefly, culture supernatant was mixed with sulfanilamide in 5% phosphoric acid, followed by an incubation at room temperature during 10 min. Then, n-1l-napthylethylenediamine (NED) 0.1% was added to the samples and incubated protected from light for 10 min. The absorbance was determined in a spectrophotometer at 540 nm. The amount of nitrite in the supernatant was determined using a sodium nitrate standard curve. Results were expressed as μM of NO_2^-.

2.3.5 Propidium iodide assay

Cell damage in C6 cells was assessed by fluorescent imaging of propidium iodide (PI) uptake. After the incubations, cells were gently washed with calcium - magnesium free (CMF) and incubated with PI (7.5 μM) for 1 h. PI fluorescence was excited at 515-560 nm using an inverted microscope (Olympus IX71, Japan) equipped with a standard rhodamine filter. The images were captured using a digital camera connected to the microscope and were qualitatively evaluated regarding the presence of PI fluorescence.

2.4 Animals

The *in vivo* experiments were carried out using male adult Wistar rats (250–350 g), which were maintained in an appropriated accommodation room under the following conditions: controlled temperature (25 ± 2 °C) and relative humidity (60%), suitable brightness, soundproofing, under a 12:12 h light/dark cycle (7 AM to 7 PM)

and with free access to water and food (GUABI, Brazil). The experimental procedures were approved by the Ethical Research Committee of Federal University of Santa Maria (toxicological evaluations - protocol number 2171170217/2017) and Ethical Research Committee of the Federal University of Pelotas (animal model of glioma - protocol number: 23110009402/2016-01) affiliated to the Council for Control of Animal Experiments (CONCEA) and in accordance with the NIH Guide for the Care and Use of Laboratory Animals.

2.5 In vivo toxicity

2.5.1 General Procedures and treatments

The animals were randomly distributed in four groups (n=5-6 animals/group). and received the treatment by intragastric route (i.g.), once a day, in a repeated administration regiment (during 15 days) and in a 1 mL/kg constant volume of body weight (figure 1A). Each administration corresponds to a $(PhSe)_2$ dose of 5 mg/Kg regardless its form. The experimental groups were the following:

I) Control - the animals received MCT (1 mL/Kg, i.g.);

II) NC B - the animals received NC B suspension (1 mL/Kg, i.g.);

III) $(PhSe)_2$ - the animals received $(PhSe)_2$ at 5 mg/kg (1 mL/Kg, i.g.);

IV) NC $(PhSe)_2$ - the animals received NC $(PhSe)_2$ at 5 mg/Kg (1 mL/kg, i.g.).

The free compound was dissolved in MCT (5 mg/mL) and the nanocapsule suspensions (NC $(PhSe)_2$ and NC B) were prepared as described in *section 2.3* and used as obtained. The animals were periodically monitored every 24 h to record mortality, behavioral pattern changes, ptosis, tremors, diarrhea, salivation, piloerection, tremors, locomotor alterations or seizures. Furthermore, before receiving the treatment, the body weight gain and food consumption were daily recorded as well.

2.5.2 Toxicological parameters

Twenty-four hours after the last treatment, the animals were slightly anesthetized prior to blood collection by heart puncture. In sequence, the blood samples were centrifuged at 2,500 *xg* during 10 min to obtain the plasma fraction, which were

used for determining biochemical markers of hepatic and renal function. After this procedure, rats were sacrificed and samples of brain, liver and kidneys were collected and*in situ* macroscopically observed based on their position, color, shape, size and consistency. Besides, the samples were accurately weighed, frozen and stored at -80ºC until the biochemical analysis.

2.5.2.1 Plasma biochemical parameters

The plasma samples were used to estimate hepatic and renal functionality using commercial kits (Labtest, Brazil). The total bilirubin levels, alanine (ALT) and aspartate aminotransferase (AST) activities were measured to evaluate hepatic function while urea and creatinine levels were used to assess renal function.

2.5.2.2 Tissue preparation and biochemical assays

The tissue samples were homogenized in 50 mM Tris HCl at pH 7.4, 1:5 (brain) or 1:10 (liver and kidneys) (w/v), and then centrifuged at 2,500 *xg* during 10 min at 4 °C to yield a low-speed supernatant fraction (S1). Freshly prepared S1 was used to estimate some parameters of oxidative status. A different protocol of homogenization was conducted to estimate the protein carbonylation level, in which no centrifugation was performed. Protein concentration was measured by the Bradford methodology [29] using bovine serum albumin (1 mg/mL) as the analytical standard.

2.5.2.2.1 Non-protein thiol levels

To determine the non-protein thiol (NPSH), an aliquot of S1 was mixed with 10% trichloroacetic acid solution (1:1, v/v) and the clear supernatant (S2) was obtained through centrifugation. The S2 contains the free thiol groups, which reacts with 5,5-dithiobis (2-nitrobenzoic acid) (DTNB) generating a yellow complex measured at 412 nm [30]. The results were expressed as nmol NPSH/g tissue.

2.5.2.2.2 Protein carbonylation

Briefly, homogenates were diluted 1:8 (v/v) and an aliquot was added to the reaction mixture containing 10 mM DNPH (prepared in 2 M HCl). The samples were protected from light during and shaken with a vortex mixer each 15 min over 1 h. Following, denaturation buffer, ethanol and hexane were added to each tube. The tubes

were shaken with a vortex mixer for 40 s and centrifuged (15 min). The supernatants were discarded and the pellets were washed twice with ethanol:ethyl acetate (1:1, v/v) and resuspended in a denaturation buffer. The sample tubes were shaken with a vortex mixer for 5 min. These samples were used to measure absorbance at 370 nm [31]. The results were reported as carbonyl content (nmol/mg protein).

2.5.2.2.3 Delta-aminolevulinic acid dehydratase (δ-ALA-D) activity

The δ-ALA-D activity was determined according to Sassa [32]. The samples were incubated at 37 °C in a medium containing 45 mM phosphate buffer, pH 6.8 and the enzymatic reaction was initiated by adding the substrate (5-aminolevulinate) to a 2.2 mM final concentration. The incubation was stopped by adding trichloroacetic acid solution (10 % TCA) with 10 mM $HgCl_2$. The reaction product, porphobilinogen, was spectrophotometrically measured at 555 nm with modified Erlich's reagent. The results are expressed as nmol of porphobilinogen /h/mg protein.

2.5.2.2.4 Superoxide dismutase (SOD) activity

SOD activity was determined as described by Misra and Fridovich [33]. Prior diluted aliquots of S1 (1:10 v/v) were added in a Na_2CO3 buffer 50 mM pH 10.3 and the enzymatic reaction was initiated by adding epinephrine. The color reaction was measured at 480 nm and the enzyme activity was expressed as U (1U decomposes 1 μmol of H_2O_2/min at pH 7 and at 25 ºC)/mg protein.

2.5.2.2.5 Glutathione-S-Transferase (GST) activity

The assay to determine the GST activity was performed based on Habig and coworkers [34]. The reaction mixture contained an aliquot of S1, 0.1 M potassium phosphate buffer pH 7.4, 100 mM GSH and as substrate 100 mM 1-chloro-2,4-dinitrobenzene (CDNB) were used. The reaction product was spectrophotometrically detected at 340 nm and the results were expressed as CDNB conjugated nmol/minute/mg protein.

2.5.2.2.6 Catalase (CAT) activity

The CAT activity was carried out by monitoring the H_2O_2 consumption at 240 nm. The enzymatic reaction was performed by adding an aliquot of S1 and the substrate (H_2O_2) at a concentration of 0.3 mM in a medium containing 50 mM phosphate buffer, pH 7.0. The enzymatic activity was expressed in units (1U decomposes 1 μmol of H_2O_2/min at pH 7 and at 25 ºC)/mg protein [35].

2.5.2.2.7 Reactive species (RS) production

The substrate 2′-7′-dichlorofluorescein diacetate (DCFH-DA) was applied to measure the intracellular formation of ROS, according to Myhre and co-workers [36]. An aliquot of S1 was mixed with DCFH-DA (1 mM) and Tris-HCl buffer (10 mM; pH 7.4) and then incubated for 60 min protected from light. The fluorescence was measured using a fluorimeter (488 nm for excitation and 525 nm for emission) and ROS levels were expressed as nmol of DCF per milligram of protein.

2.6 Pre-clinical model of glioblastoma

2.6.1 Glioma implantation

Firstly, C6 glioma cells were cultured as described at *section 2.3.1*. Then, a total of 1 x 106 cells were dispersed in DMEM/5% FBS and an aliquot (3 μL) was injected in the right striatum at a depth of 6.0 mm (coordinates regarding bregma: 0.5 mmposterior and 3.0 mm lateral) of animals, prior anesthetized with ketamine and xylazine injected by the intraperitoneal route [26]. Immediately after surgery, the animals were kept in a warm room until full recovery from the anesthesia.

2.6.2 General Procedures and treatments

Five days after glioma implantation, the rats were randomly assigned to different groups (3-5 animals/group), each one receiving the following treatments once a day, during 15 days by the intragastric route (figure 1B):

I) Control - the animals received MCT (1 mL/Kg, i.g.);

II) NC B - the animals received NC B suspension (1 mL/Kg, i.g.);

III) $(PhSe)_2$ - the animals received $(PhSe)_2$ at 1 mg/kg (1 mL/Kg, i.g.);

IV) NC $(PhSe)_2$ - the animals received NC $(PhSe)_2$ at 1 mg/Kg (1 mL/kg, i.g.).

As well as to *in vivo* toxicity, the compound in its free form was dissolved in MCT (1 mg/mL). The NC $(PhSe)_2$ and NC B were prepared as described in *section 2.3* and diluted with sterile water to achieve the desired concentration (1 mg/mL). After 20 days of glioma implantation (5 days after glioma implantation + 15 days of treatment), the rats were euthanized and the entire brain was removed, sectioned and fixed with 10% paraformaldehyde (pH 7.4).

2.6.3 Tumor size quantification

Tumor size was analyzed by the captured images with Image Tool Software. The total volume (mm3) of the tumor was computed by summing the segmented areas and by multiplication of the slice resolution.

2.7 Statistical analysis

All experimental results are presented as mean (s) ± standard error of the *n* observation means (S.E.M.). The GraphPad Prism® version 6 software was used to perform the Student's *t* test and variance analyses one-way (ANOVA) followed by post-hoc Tukey's test. Values of $p<0.05$ were considered statistically significant. The IC50 values were calculated by linear regression using the GraphPad Prism® version 6.

3. Results

3.1 In vitro assays

3.1.1 Evaluation of C6 cells viability

The preliminary *in vitro* antiglioma effect of NC $(PhSe)_2$ was investigated in C6 cell line employing MTT test (figure 2A). The free $(PhSe)_2$ significantly reduced the C6 viability at a concentration range 25 - 200 µM (73.30, 58.12, 40.27 and 38.27 %, respectively) ($p<0.05$ by One-way ANOVA followed by Tukey's test) while NC $(PhSe)_2$ had effect at lower concentrations (10 µM to 200 µM; 63.23, 53.69, 37.72, 34.66 and 25.60 %, respectively) ($p<0.05$ by One-way ANOVA followed by Tukey's test). The statistical evaluation revealed significant difference between $(PhSe)_2$ free and nanoencapsulated, indicating that NC $(PhSe)_2$ had a superior effect against C6 cell line. In agreement with these results, the free $(PhSe)_2$ presented an IC50 value of 74.83 µM,

while NC $(PhSe)_2$ was 43.40 µM. The NC B had no antitumor effect independent of the concentration tested ($p>0.05$ by One-way ANOVA).

3.1.2 Evaluation of astrocyte cells viability

The astrocytes cells were used as non-transformed cell model to assess the formulations safety and selectivity (10 – 100 µM; Figure 2B). After 48 h of incubation, no significant differences in the cell viability were observed among the experimental groups ($p>0.05$ by One-way ANOVA). All samples and concentrations tested did not significantly modify the cell viability.

3.1.3 Nitrite content determination in C6 cells

Concerning to the nitrite levels determination, our data demonstrated that the incubation with NC $(PhSe)_2$ and NC B (50, 100 and 200 µM) significantly increased the nitrite content (Figure 3; $p<0.05$ by One-way ANOVA followed by Tukey's test). Interestingly, free $(PhSe)_2$ did not modify the nitrite content ($p<0.05$ by One-way ANOVA followed by Tukey's test).

3.1.4 Propidium incorporation in C6 cells

The possible occurrence of necrosis induced by the treatment was estimated using the PI incorporation in C6 cells. Corroborating with the MTT assay, the incubation of C6 cells with free $(PhSe)_2$ and NC $(PhSe)_2$ at 100 µM caused cell morphological alterations and density reduction (Figure 4). However, few cells incorporated the PI. No modifications were observed in C6 cells incubated with NC B.

3.2 In vivo toxicity evaluations

The repeated administration schedule triggered no clinical abnormality signs or death to rats over the experimental protocol. Neither the relative body weight gain ($p<0.05$ by One-way ANOVA; Figure 5A) nor the total food consumption ($p<0.05$ by One-way ANOVA; Figure 5B) showed statistical difference between the groups that received the $(PhSe)_2$, free or nanoencapsulated, and control group (animals that received MCT oil). On the other hand, the animals treated with NC B had an increase in food consumption and consequently presented an increment in the relative body weight over

the days ($p>0.05$ by One-way ANOVA followed by Tukey's test; Figure 5A and 5B). Moreover, the samples of brain, liver and kidneys of the treated animals presented similar morphology, color, shape, size and consistency.

3.2.1 Plasma biochemical parameters

Table 1 demonstrates the results of plasma biochemical parameters of the animals that received the repeated treatment. No statistical difference was detected neither to AST and ALT activities nor to total bilirubin, creatinine and urea levels ($p<0.05$ by One-way ANOVA).

3.2.2 Parameters of oxidative status

The repeated treatment schedule did not cause alteration in NPSH, ROS, and carbonyl protein levels as well as in δ- ALA-D, SOD, GST, and CAT activities ($p>0.05$ by One-way ANOVA; Figure 6). No statistical difference was detected to any of the aforementioned parameter among the experimental groups.

3.3 Antiglioma effect in a pre-clinical protocol

The treatments effectiveness was evaluated by the analysis of tumor size (figure 7). As expected, the implanted tumors had glioblastoma characteristics and $(PhSe)_2$, free or nanoencapsulated, were effective in reducing tumor progression. By One-Way ANOVA analysis it was observed a significant difference among the groups treated with MCT oil (176.60 ± 22.91 mm^3) and with the compound (free – 13.94 ± 3.05 mm^3 or NC – 15.49 ± 5.32 mm^3) ($p<0.0001$). Interestingly, NC B had a slight antitumor effect (112.20 ± 19.93 mm^3 - $p<0.005$), which was lower than the groups that received free $(PhSe)_2$ and NC $(PhSe)_2$ ($p<0.01$).

4. Discussion

Despite the pharmacological potential of $(PhSe)_2$, its clinical use remains a challenge due to its physicochemical limitations as well as some toxic issues [12, 15]. In this sense, the incorporation of this compound into nanocapsules emerges as an advantageous alternative to improve its therapeutic index and optimize the treatment regimen by expanding the array of possible administration routes. The results obtained

in the current study demonstrated for the first time the promising effect of the $(PhSe)_2$, free and nanoencapsulated, against glioblastoma using *in vitro* and *in vivo* protocols. In addition, the repeated administration showed neither unspecific toxic effects nor oxidative balance impairment, suggesting the safeness of the treatments.

According to World Health Organization (WHO), the gliomas are classified in astrocytic tumors grade II and III, oligodendrogliomas grade II and III and glioblastomas as grade IV, which are the most aggressive kind [37]. Despite the multimodality approach to glioma treatment, the patients had survival between 3 and 16 months [38]. Considering that, the research for innovative therapies for gliomas treatment is relevant and, in such context, the nanocarrier systems can be promising alternatives [4, 26, 39, 40]. The development of nanotechnological-based therapies to glioblastoma treatment could increase the amount of drug that reaches the central nervous system because of the small size of the nanoparticles. Besides, the nanocarriers can promote a controlled release of the active, which improves its efficacy and reduces the toxic effects in other organs [40, 41].

The antiglioma effect of $(PhSe)_2$, free and nanoenapsulated, was demonstrated by a set of *in vitro* techniques. The results of MTT assay showed that both compound forms selectively reduced C6 cell viability without causing changes in astrocyte cells. Corroborating with this test, the cell density was also reduced by the treatment with the compound at 100µM. It is important to highlight that the $(PhSe)_2$ nanoencapsulation enhanced the antiglioma effect. At some concentrations in which the free compound had no action the NC $(PhSe)_2$ caused a reduction in C6 cells viability, which was further confirmed by the IC50 values. These results are in accordance with other studies that reported an improvement of *in vitro* and *in vivo* biological effects by associating active substances to nanocarrier systems [19, 42-44].

Nitric oxide (NO) is an inorganic free radical, which plays important and complex role in cancer biology. It modulates different cellular events dependent on its concentration, such as proliferation, apoptosis, angiogenesis, migration and invasion [45, 46]. In gliomas, the NO produced could increase the permeability of the tumor endothelium, enhancing the delivery of chemotherapeutic drugs [47]. In this sense, our results demonstrated an increase in NO_2^- levels at the highest NC $(PhSe)_2$ and NC B concentration tested. Of particular importance, it was already reported that the antitumor

effect of substances incorporated into nanocapsules composed by PCL and MCT seems to be connected to the NO production. Drewes and co-workers obtained an augmentation in NO_2^- levels after cells incubation with blank nanocapsules without causing toxicity to tumor cells. However, this study also demonstrated the high NO_2^- levels were linked to the acetyleugenol-loaded lipid core nanocapsules antitumor effect, suggesting that this cellular mediator has an important contribution to the final pharmacological effect [48]. In addition, other mechanisms could be associated with the antiglioma effect, such as the apoptosis and necrosis pathways. In this study, the PI incorporation assay was used to further investigate the mechanisms through $(PhSe)_2$ could exert its cytotoxicity. The late apoptotic stage and necrotic cells can be identified by the PI incorporation, because of their membrane loss the integrity, thus PI can enter, bind to nuclear DNA and stain positively the cells [49, 50]. In our study, few cells incorporated the PI, suggesting that necrosis is poorly involved in the antiglioma effect of $(PhSe)_2$, which indicated that other cell death pathways may mediate such effect. According to the literature, compounds with antiproliferative effects in tumor cells without promoting a necrotic cell death are considered good candidate as anticancer drugs [51].

Despite the attractive properties of nanosystems, there is an increasing concern about their safety. In front of this, estimating the possible biological interactions among the nanocapsule suspensions components with the body and the potential inherent risks of these carriers are critical issues [52]. Besides, depending on the vehicle and administration route, the $(PhSe)_2$ can trigger toxicological impairments, reinforcing the importance of better elucidate the possible effects [53]. The study of *in vivo* toxicity demonstrated that independent of $(PhSe)_2$ form, the repeated administration schedule did not trigger mortality or systemic toxicity. The oxidative status evaluation of different tissues (brain, liver and kidneys) showed no alterations as well as the plasma markers of hepatic and renal function in comparison to the control group. Corroborating the present results, a similar profile was reported to nanocapsules containing p,p'-methoxyl-diphenyl diselenide, an organoselenium compound counterpart of $(PhSe)_2$[22]. Therefore, these data indicate that nanocapsules suspension contaning $(PhSe)_2$ are well tolerated.

The literature reports several studies about the $(PhSe)_2$ *in vivo* pharmacological actions, including the anticancer effect [5]. However, this is the first study that evaluated the effectiveness of $(PhSe)_2$, free and nanoencapsulated, in a pre-clinical model of glioblastoma. The results showed that both $(PhSe)_2$ forms effectively mitigated the tumor growth, reducing the final volume to around 15 mm^3. The most common chemotherapeuticsused to treat gliomas are carmustine, PCV (procarbazine, lomustine, and vincristine) and the first-line temozolomide [54]. In a study using the same preclinical glioma model, the efficacy of temozolomide was demonstrated and the drug reduced the tumor size to 35 – 30 mm3 [55]. In this sense, it is possible to suggest that $(PhSe)_2$ was more effective than the therapy usually applied in the glioma clinical management, however, complementary analyses must be carried out to reinforce this hypothesis. It is important to highlight that the nanoencapsulation kept the antitumor effect of $(PhSe)_2$ without causing additional toxicity. Although the antiglioma performance is similar, the nanocapsules suspension represents a more advantageous way to administer $(PhSe)_2$ due to its aqueous and colloidal character, allowing its administration by several routes, including oral and parenteral, which is not possible in its free form.

5. Conclusion

This study reported the $(PhSe)_2$ effectiveness against glioma tumor using *in vitro* techniques and a pre-clinical glioblastoma model. The nanoencapsulation of $(PhSe)_2$ increased its *in vitro* antitumor effect, which seems to exert its selective cytotoxicity mediated at least in part by NO pathway without necrosis involvement. Furthermore, the repeated administration of both $(PhSe)_2$ forms mitigated the glioblastoma growth without causing any toxicity, but future studies are needed to better elucidate the mechanism associated to the antiglioma effect of the compound. Taken together, the $(PhSe)_2$-loaded polymeric nanocapsules arise as a promising candidate to future studies aiming at developing improved treatment to glioma.

Conflict of interest

The authors report no conflict of interest. The authors alone are responsible for the article content and writing.

Acknowledgements

L. M. Ferreira acknowledges the grant from CAPES.

References

[1] Q.T. Ostrom, L. Bauchet, F.G. Davis, I. Deltour, J.L. Fisher, C.E. Langer, M. Pekmezci, J.A. Schwartzbaum, M.C. Turner, K.M. Walsh, M.R. Wrensch, J.S. Barnholtz-Sloan, The epidemiology of glioma in adults: a "state of the science" review, Neuro-Oncology, 16 (2014) 896-913.

[2] A. Behin, K. Hoang-Xuan, A.F. Carpentier, J.Y. Delattre, Primary brain tumours in adults, Lancet, 361 (2003) 323-331.

[3] O.O. Kanu, A. Mehta, C.H. Di, N.J. Lin, K. Bortoff, D.D. Bigner, H. Yan, D.C. Adamson, Glioblastoma multiforme: a review of therapeutic targets, Expert Opin Ther Tar, 13 (2009) 701-718.

[4] R. Karim, C. Palazzo, B. Evrard, G. Piel, Nanocarriers for the treatment of glioblastoma multiforme: Current state-of-the-art, J Control Release, 227 (2016) 23-37.

[5] C.W. Nogueira, J.B.T. Rocha, Toxicology and pharmacology of selenium: emphasis on synthetic organoselenium compounds, Arch Toxicol, 85 (2011) 1313-1359.

[6] T. Posser, M.T. de Paula, J.L. Franco, R.B. Leal, J.B.T. da Rocha, Diphenyl diselenide induces apoptotic cell death and modulates ERK1/2 phosphorylation in human neuroblastoma SH-SY5Y cells, Arch Toxicol, 85 (2011) 645-651.

[7] F. Nedel, V.F. Campos, D. Alves, A.J.A. McBride, O.A. Dellagostin, T. Collares, L. Savegnago, F.K. Seixas, Substituted diaryl diselenides: Cytotoxic and apoptotic effect in human colon adenocarcinoma cells, Life Sci, 91 (2012) 345-352.

[8] L.M. Ferreira, V.F. Cervi, M.H.M. Sari, A.V. Barbieri, A.P. Ramos, P.M. Copetti, G.F. Brum, K. Nascimento, J.M. Nadal, P.V. Farago, M.R. Sagrillo, C.W. Nogueira, L. Cruz, Diphenyl diselenide loaded poly(ε-caprolactone) nanocapsules with selective antimelanoma activity: Development and cytotoxic evaluation, Mat Sci Eng C-Mater, 91 (2018) 1-9.

[9] N.B.D. Barbosa, C.W. Nogueira, T.N. Guecheva, M.D. Bellinaso, J.B.T. Rocha, Diphenyl diselenide supplementation delays the development of N-nitroso-Nmethylurea-induced mammary tumors, Arch Toxicol, 82 (2008) 655-663.

[10] M. Diaz, R. Gonzalez, D. Plano, J.A. Palop, C. Sanmartin, I. Encio, A diphenyldiselenide derivative induces autophagy via JNK in HTB-54 lung cancer cells, J Cell Mol Med, 22 (2018) 289-301.

[11] M.T. Melo, I.M. de Oliveira, I. Grivicich, T.N. Guecheva, J. Saffi, J.A.P. Henriques, R.M. Rosa, Diphenyl diselenide protects cultured MCF-7 cells against tamoxifen-induced oxidative DNA damage, Biomed Pharmacother, 67 (2013) 329-335.

[12] N.B.V. Barbosa, J.B.T. Rocha, G. Zeni, T. Emanuelli, M.C. Beque, A.L. Braga, Effect of organic forms of selenium on delta-aminolevulinate dehydratase from liver, kidney, and brain of adult rats, Toxicol Appl Pharm, 149 (1998) 243-253.

[13] R.M. Rosa, R. Roesler, A.L. Braga, J. Saffi, J.A.P. Henriques, Pharmacology and toxicology of diphenyl diselenide in several biological models, Braz J Med Biol Res, 40 (2007) 1287-1304.

[14] M. Prigol, C.W. Nogueira, G. Zeni, M.R. Bronze, L. Constantino, Physicochemical and Biochemical Profiling of Diphenyl Diselenide, Appl Biochem Biotech, 169 (2013) 885-893.

[15] M. Prigol, C.A. Bruning, F. Martini, C.W. Nogueira, Comparative Excretion and Tissue Distribution of Selenium in Mice and Rats Following Treatment with Diphenyl Diselenide, Biol Trace Elem Res, 150 (2012) 272-277.

[16] C.F.A. Giordani, D. de Souza, L. Dornelles, C.W. Nogueira, M.P. Alves, M. Prigol, O.E.D. Rodrigues, Diphenyl Diselenide-Loaded Nanocapsules: Preparation and Biological Distribution, Appl Biochem Biotech, 172 (2014) 755-766.

[17] S.T. Stefanello, F. Dobrachinski, N.R. de Carvalho, G.P. Amaral, R.P. Barcelos, V.A. Oliveira, C.S. Oliveira, C.F.A. Giordani, M.E. Pereira, O.E.D. Rodrigues, F.A.A. Soares, Free radical scavenging *in vitro* and biological activity of diphenyl diselenideloaded nanocapsules: DPDS-NCS antioxidant and toxicological effects, Int J Nanomed, 10 (2015).

[18] M.C.L. Marchiori, C. Rigon, P.M. Copetti, M.R. Sagrillo, L. Cruz, Nanoencapsulation Improves Scavenging Capacity and Decreases Cytotoxicity of Silibinin and Pomegranate Oil Association, Aaps Pharmscitech, 18 (2017) 3236-3246.

[19] M. Gehrcke, L.M. Giuliani, L.M. Ferreira, A.V. Barbieri, M.H.M. Sari, E.F. da Silveira, J.H. Azambuja, C.W. Nogueira, E. Braganhol, L. Cruz, Enhanced photostability, radical scavenging and antitumor activity of indole-3-carbinol-loaded rose hip oil nanocapsules, Mat Sci Eng C-Mater, 74 (2017) 279-286.

[20] L.M. Ferreira, V.F. Cervi, M. Gehrcke, E.F. da Silveira, J.H. Azambuja, E. Braganhol, M.H.M. Sari, V.A. Zborowski, C.W. Nogueira, L. Cruz, Ketoprofen-loaded pomegranate seed oil nanoemulsion stabilized by pullulan: Selective antiglioma formulation for intravenous administration, Colloid Surface B, 130 (2015) 272-277.
[21] M.H.M. Sari, L.M. Ferreira, V. AngonesiZborowski, P.C.O. Araujo, J.M. Nadal, P.V. Farago, L. Cruz, C.W. Nogueira, p,p '-Methoxyl-diphenyl diselenideincorporation into polymeric nanocapsules improves its antinociceptive action: Physicochemical and behavioral studies, Colloid Surface B, 157 (2017) 464-472.
[22] M.H.M. Sari, L.M. Ferreira, V.A. Zborowski, P.C.O. Araujo, V.F. Cervi, C.A. Bruning, L. Cruz, C.W. Nogueira, p,p'-Methoxyl-diphenyl diselenide-loaded polymeric nanocapsules are chemically stable and do not induce toxicity in mice, Eur J Pharm Biopharm, 117 (2017) 39-48.
[23] M. Gehrcke, M.H.M. Sari, L.M. Ferreira, A.V. Barbieri, L.M. Giuliani, V.C. Prado, J.M. Nadal, P.V. Farago, C.W. Nogueira, L. Cruz, Nanocapsules improve indole-3- carbinol photostability and prolong its antinociceptive action in acute pain animal models, Eur J Pharm Sci, 111 (2018) 133-141.
[24] L.A. Frank, R.V. Contri, R.C.R. Beck, A.R. Pohlmann, S.S. Guterres, Improving drug biological effects by encapsulation into polymeric nanocapsules, Wires Nanomed Nanobi, 7 (2015) 623-639.

[25] D.R. Nogueira, L.E. Scheeren, L.B. Macedo, A.I.P. Marcolino, M.P. Vinardell, M. Mitjans, M.R. Infante, A.A. Farooqi, C.M.B. Rolim, Inclusion of a pH-responsive amino acid-based amphiphile in methotrexate-loaded chitosan nanoparticles as a delivery strategy in cancer therapy, Amino Acids, 48 (2016) 157-168.
[26] E.F. da Silveira, J.M. Chassot, F.C. Teixeira, J.H. Azambuja, G. Debom, F.T. Beira, F.A.B. Del Pino, A. Lourenco, A.P. Horn, L. Cruz, R.M. Spanevello, E. Braganhol, Ketoprofen-loaded polymeric nanocapsules selectively inhibit cancer cell growth *in vitro* and in preclinical model of glioblastoma multiforme, Invest New Drug, 31 (2013) 1424-1435.
[27] G. Lollo, M. Vincent, G. Ullio-Gamboa, L. Lemaire, F. Franconi, D. Couez, J.P. Benoit, Development of multifunctional lipid nanocapsules for the co-delivery of

paclitaxel and CpG-ODN in the treatment of glioblastoma, Int J Pharmaceut, 495 (2015) 972-980.

[28] D.J. Stuehr, C.F. Nathan, Nitric-Oxide - a Macrophage Product Responsible for Cytostasis and Respiratory Inhibition in Tumor Target-Cells, J Exp Med, 169 (1989) 1543-1555.

[29] M.M. Bradford, A rapid and sensitive method for the quantitation of microgram quantities of protein utilizing the principle of protein-dye binding, Anal. Biochem, 79 (1976) 248-254.

[30] G.L. Ellman, Tissue Sulfhydryl Groups, Arch Biochem Biophys, 82 (1959) 70-77.

[31] A.Z. Reznick, L. Packer, Oxidative Damage to Proteins - Spectrophotometric Method for Carbonyl Assay, Method Enzymol, 233 (1994) 357-363.

[32] S. Sassa, Delta-Aminolevulinic-Acid Dehydratase Assay, Enzyme, 28 (1982) 133-143.

[33] H.P. Misra, I. Fridovich, The role of superoxide anion in the autoxidation of epinephrine and a simple assay for superoxide dismutase, J Biol Chem, 247 (1972) 3170-3175.

[34] W.H. Habig, M.J. Pabst, W.B. Jakoby, Glutathione S-Transferases - First Enzymatic Step in Mercapturic Acid Formation, J Biol Chem, 249 (1974) 7130-7139.

[35] H. Aebi, Catalase *In vitro*, Methods Enzymol., 105 (1984) 121-126.

[36] O. Myhre, J.M. Andersen, H. Aarnes, F. Fonnum, Evaluation of the probes 2 ',7 '-dichlorofluorescin diacetate, luminol, and lucigenin as indicators of reactive species formation, Biochem Pharmacol, 65 (2003) 1575-1582.

[37] D.N. Louis, A. Perry, G. Reifenberger, A. von Deimling, D. Figarella-Branger, W.K. Cavenee, H. Ohgaki, O.D. Wiestler, P. Kleihues, D.W. Ellison, The 2016 World Health Organization Classification of Tumors of the Central Nervous System: a summary, Acta Neuropathol, 131 (2016) 803-820.

[38] E.R. Laws, I.F. Parney, W. Huang, F. Anderson, A.M. Morris, A. Asher, K.O. Lillehei, M. Bernstein, H. Brem, A. Sloan, M.S. Berger, S. Chang, Survival following surgery and prognostic factors for recently diagnosed malignant glioma: data from the Glioma Outcomes Project, Journal of neurosurgery, 99 (2003) 467-473.

[39] I. Brigger, C. Dubernet, P. Couvreur, Nanoparticles in cancer therapy and diagnosis, Adv Drug Deliver Rev, 64 (2012) 24-36.

[40] F. Pourgholi, M. Hajivalili, J.N. Farhad, H.S. Kafil, M. Yousefi, Nanoparticles: Novel vehicles in treatment of Glioblastoma, Biomed Pharmacother, 77 (2016) 98-107.

[41] G. Caruso, M. Caffo, C. Alafaci, G. Raudino, D. Cafarella, S. Lucerna, F.M. Salpietro, F. Tomasello, Could nanoparticle systems have a role in the treatment of cerebral gliomas?, Nanomed-Nanotechnol, 7 (2011) 744-752.

[42] N.S. Pegoraro, J. Mattiazzi, E.F. da Silveira, J.H. Azambuja, E. Braganhol, L. Cruz, Improved photostability and cytotoxic effect of coenzyme Q10 by its association with vitamin E acetate in polymeric nanocapsules, Pharm Dev Technol, 23 (2018) 400-406.

[43] M.H.M. Sari, V.A. Zborowski, L.M. Ferreira, N.D. Jardim, P.C.O. Araujo, C.A. Bruning, L. Cruz, C.W. Nogueira, Enhanced pharmacological actions of p,p '-methoxyldiphenyl diselenide-loaded polymeric nanocapsules in a mouse model of neuropathic pain: Behavioral and molecular insights, J Trace Elem Med Bio, 46 (2018) 17-25.

[44] A. Bernardi, E. Braganhol, E. Jager, F. Figueiro, M.I. Edelweiss, A.R. Pohlmann, S.S. Guterres, A.M. Battastini, Indomethacin-loaded nanocapsules treatment reduces in vivo glioblastoma growth in a rat glioma model, Cancer letters, 281 (2009) 53-63.

[45] D. Fukumura, S. Kashiwagi, R.K. Jain, The role of nitric oxide in tumour progression, Nat Rev Cancer, 6 (2006) 521-534.

[46] M. Lechner, P. Lirk, J. Rieder, Inducible nitric oxide synthase (iNOS) in tumor biology: The two sides of the same coin., Semin Cancer Biol, 15 (2005) 277-289.

[47] D. Lam-Himlin, M.G. Espey, G. Perry, M.A. Smith, R.J. Castellani, Malignant glioma progression and nitric oxide, Neurochem Int, 49 (2006) 764-768.

[48] C.C. Drewes, L.A. Fiel, C.G. Bexiga, A.C.C. Asbahr, M.K. Uchiyama, B. Cogliati, K. Araki, S.S. Guterres, A.R. Pohlmann, S.P. Farsky, Novel therapeutic mechanisms determine the effectiveness of lipid-core nanocapsules on melanoma models, Int J Nanomed, 11 (2016) 1261-1279.

[49] D. Plesca, S. Mazumder, A. Almasan, DNA damage response and apoptosis, Methods Enzymol, 446 (2008) 107-122.

[50] G. Lollo, G. Ullio-Gamboa, E. Fuentes, K. Matha, N. Lautram, J.P. Beno, *In vitro* anti-cancer activity and pharmacokinetic evaluation of curcumin-loaded lipid nanocapsules, Mater. Sci. Eng. C, 91 (2018) 859-867.

[51] A. Bernardi, R.L. Frozza, E. Jager, F. Figueiro, L. Bavaresco, C. Salbego, A.R. Pohlmann, S.S. Guterres, A.M. Battastini, Selective cytotoxicity of indomethacin and indomethacin ethyl ester-loaded nanocapsules against glioma cell lines: an *in vitro* study, Eur J Pharmacol, 586 (2008) 24-34.

[52] S. Aula, S. Lakkireddy, K. Jamil, A. Kapley, A.V.N. Swamyd, H.R. Lakkireddy, Biophysical, biopharmaceutical and toxicological significance of biomedical nanoparticles, Rsc Adv, 5 (2015) 47830–47859.

[53] M. Prigol, R.F. Schumacher, C. WayneNogueira, G. Zeni, Convulsant effect of diphenyl diselenide in rats and mice and its relationship to plasma levels, Toxicol Lett, 189 (2009) 35-39.

[54] X.B. Wang, Y.L. Jia, P. Wang, Q.H. Liu, H.R. Zheng, Current status and future perspectives of sonodynamic therapy in glioma treatment, Ultrason Sonochem, 37 (2017) 592-599.

[55] F.B. Morrone, D.L. Oliveira, P. Gamermann, J. Stella, S. Wofchuk, M.R. Wink, L. Meurer, M.I.A. Edelweiss, G. Lenz, A.M.O. Battastini, *In vivo* glioblastoma growth is reduced by apyrase activity in a rat glioma model, BMC Cancer, 6 (2006) 1-10.

Table 1. Biochemical plasma analyses of animals submitted to the repeated treatment with $(PhSe)_2$ (5 mg/kg, i.g.), free or NC.

Biochemical parameters				
Parameter	**MCT**	**$(PhSe)_2$**	**NC $(PhSe)_2$**	**NC B**
AST (U/L)	105.30 ± 21.27	99.43 ± 22.74	98.00 ± 17.40	102.90 ± 27.45
ALT (U/L)	94.00 ± 39.22	108.00 ± 46.43	107.6 ± 39.02	145.50 ± 33.67
Total Bilirubin (mg/dL)	0.42 ± 0.22	0.40 ± 0.22	0.48 ± 0.15	0.27 ± 0.05
Creatinine (mg/dL)	0.62 ± 0.30	0.57 ± 0.19	0.52 ± 0.12	0.55 ± 0.11
Urea (mg/dL)	81.13 ± 20.11	96.92 ± 40.13	93.81 ± 29.31	85.57 ± 34.27

Values are expressed as mean ± S.E.M of 5-6 animals/group to each parameter. Data were evaluated through ordinary One-way ANOVA ($p>0.05$). Abbreviations: AST-aspartate aminotransferase; ALT - alanine aminotransferase; MCT - medium chain triglycerides.

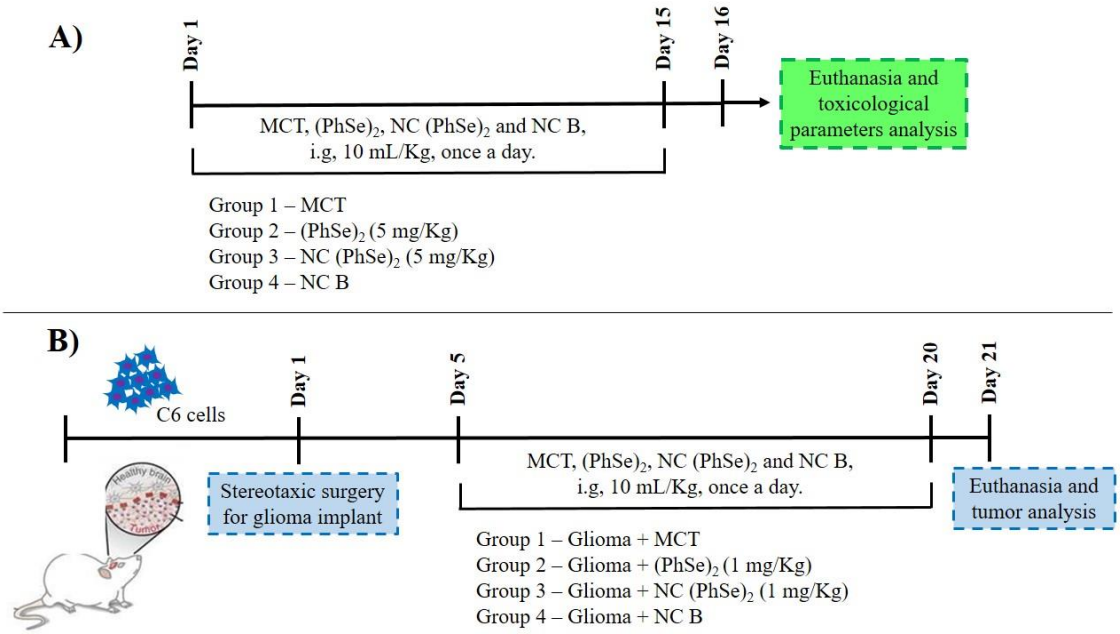

Figure 1. Schematic representation of the experimental design performed to evaluate toxicity (A) and antiglioma effect (B). The animals received during fifteen days a daily administration of $(PhSe)_2$, free or incorporated into NCs suspension, and its vehicle, MCT or NC B. For notes, i.g means intragastric route; $(PhSe)_2$ means free diphenyl diselenide; NC $(PhSe)_2$ means nanocapsules containing diphenyl diselenide; NC B means nanocapsules without diphenyl diselenide; and MCT means medium chain triglycerides.

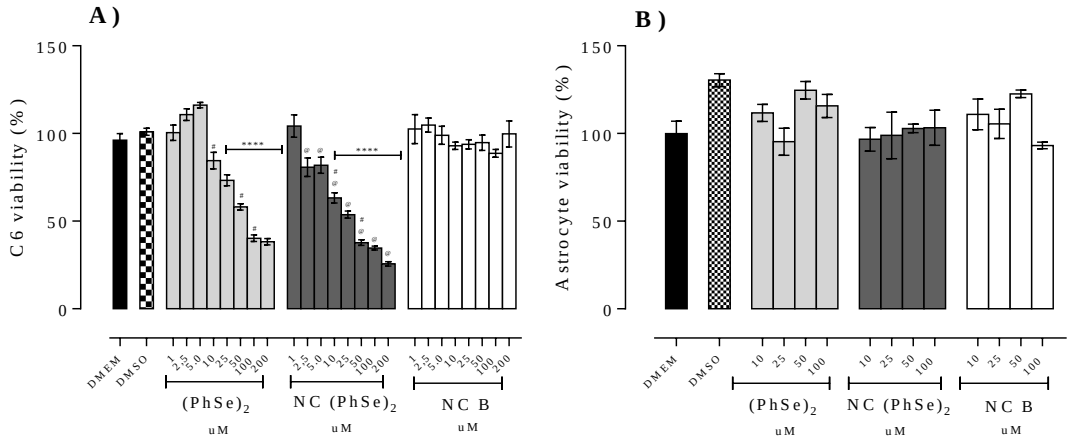

Figure 2. Cytotoxic effect of NC $(PhSe)_2$ and free $(PhSe)_2$ against glioma cell line (C6) (A) and in primary astrocyte cells (B) after 48 h of incubation assessed by MTT assay. Each column represents the mean ± S.E.M. of triplicate. Asterisks denote significant differences (**** $p<0.0001$) in comparison to the negative control group and sharps ($^{\#}$ $p<0.05$) denote significant differences among the concentrations of the same group, by one-way ANOVA, followed by Tukey's post hoc test. Arroba symbol ($^{@}$ $p<0.05$) denotes significant differences between the same concentrations of free $(PhSe)_2$ and NC $(PhSe)_2$ by Unpaired Student's *t* test.

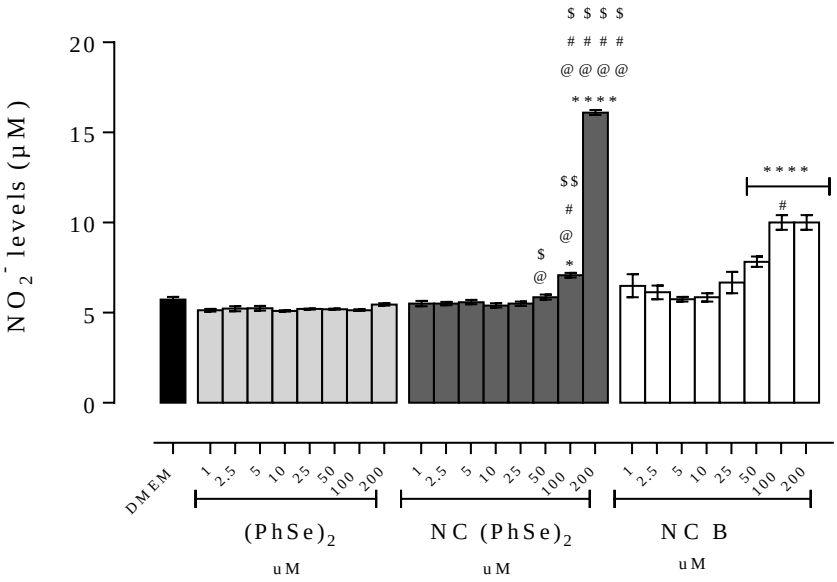

Figure 3. Nitrite (NO_2^-) levels in C6 cell cultures. Each column represents the mean ± S.E.M. of triplicate. Asterisks denote significant differences (* $p<0.005$ and **** $p<0.0001$) in comparison to the negative control group and sharps ($^{\#}$ $p<0.05$ and $^{\#\#\#\#}$ $p<0.0001$) denote the differences among the concentrations in the same group, by one-way ANOVA, followed by Tukey's post hoc test. Arroba symbol ($^{@}$ $p<0.05$ and $^{@\,@\,@\,@}$ $p<0.0001$) denotes significant differences between the same concentrations of NC $(PhSe)_2$ and $(PhSe)_2$ while cipher ($^{\$}$ $p<0.05$, $^{\$\,\$}$ $p<0.01$, and $^{\$\,\$\,\$\,\$}$ $p<0.0001$) means significant differences between the same concentrations of NC B and NC $(PhSe)_2$ by Unpaired Student's *t* test.

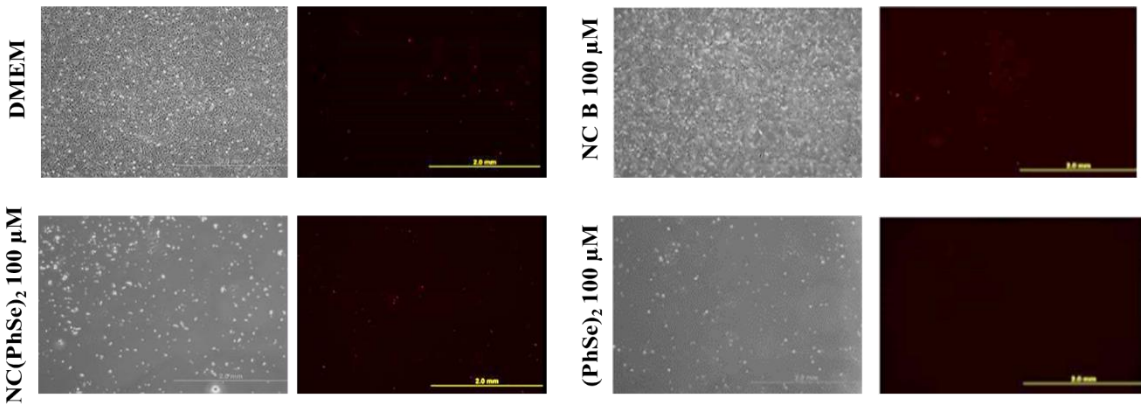

Figure 4. Propidium iodide (PI) incorporation in C6 cell following 48 h of incubation with $(PhSe)_2$, free or nanoencapsulated. DMEM and NC B were used to comparative purposes.

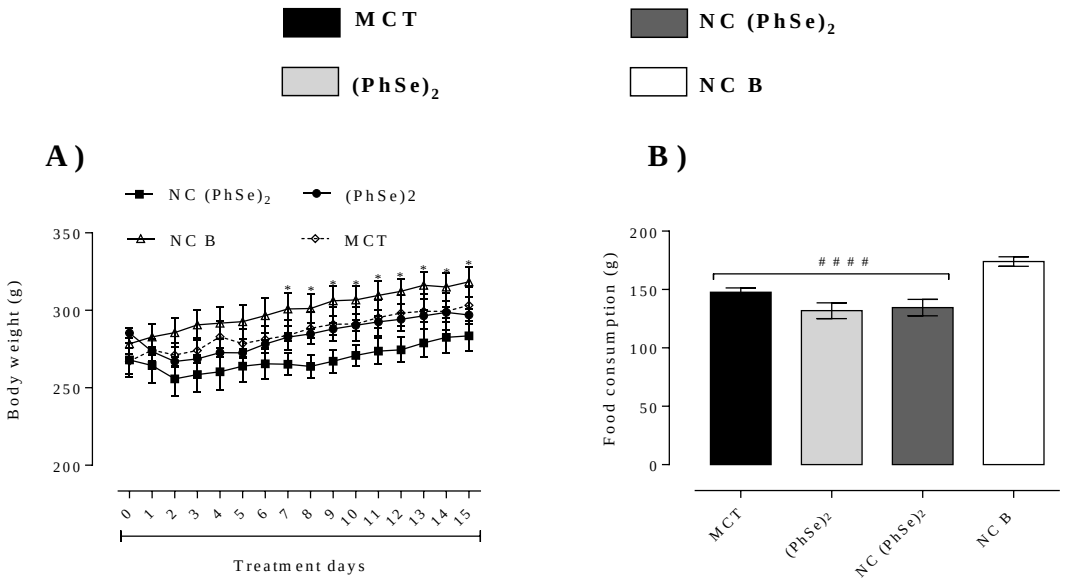

Figure 5. Effect of the repeated treatment in body weight gain **(A)** and food intake **(B)** over the experiment. Each column/point represents the mean ± S.E.M of 5-6 rats/group performed in three independent experiments. Asterisks denote significant differences (* $p<0.05$) in comparison to the negative control group and sharps ($^{\#\#\#\#}$ $p<0.0001$) denote differences between samples and NC B, by one-way ANOVA, followed by Tukey's post hoc test.

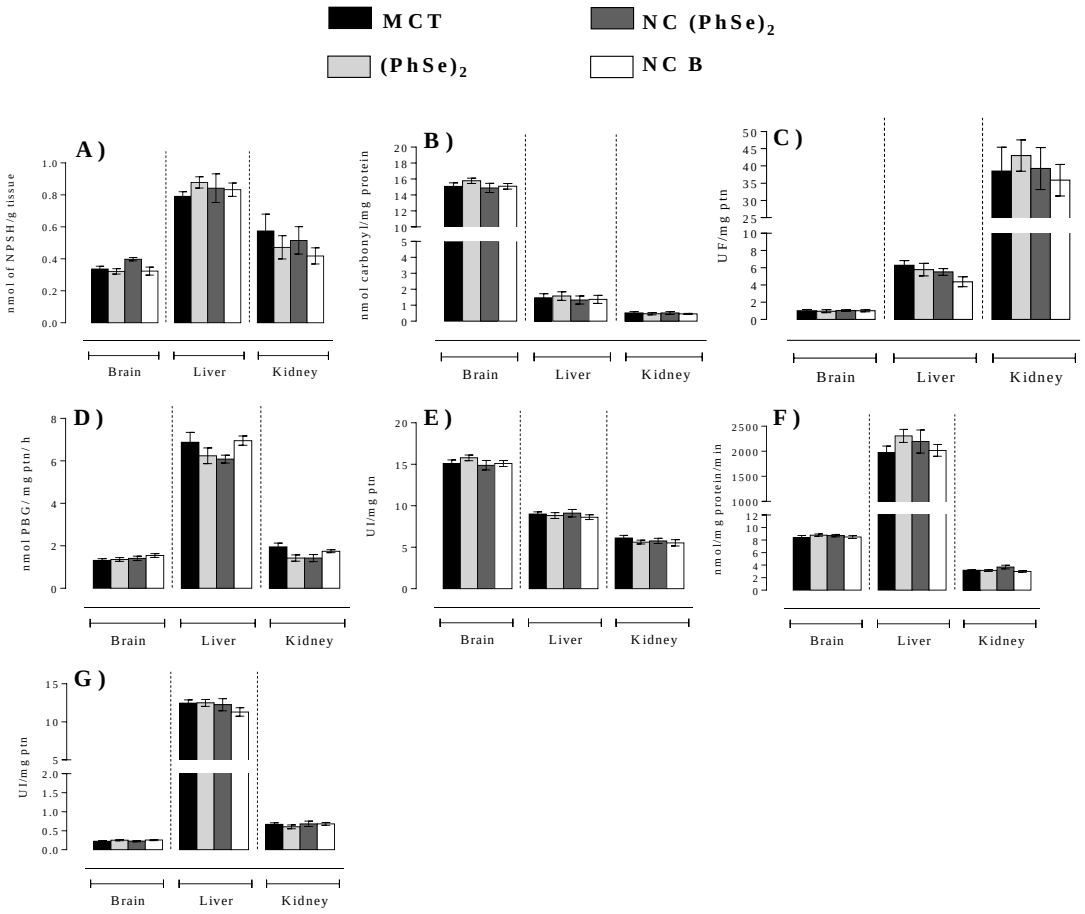

Figure 6. Effect of the repeated treatment with $(PhSe)_2$ (5 mg/kg, i.g.), free or incorporated into the NC, in the NPSH (A), Carbonyl protein (B) and ROS (C) levels and δ-ALA-D (D), SOD (E) and GST (F) and CAT (G) activity in different tissues. Each column represents the mean ± S.E.M of 5-6 rats/group. Data were analyzed by One-way ANOVA (p>0.05).

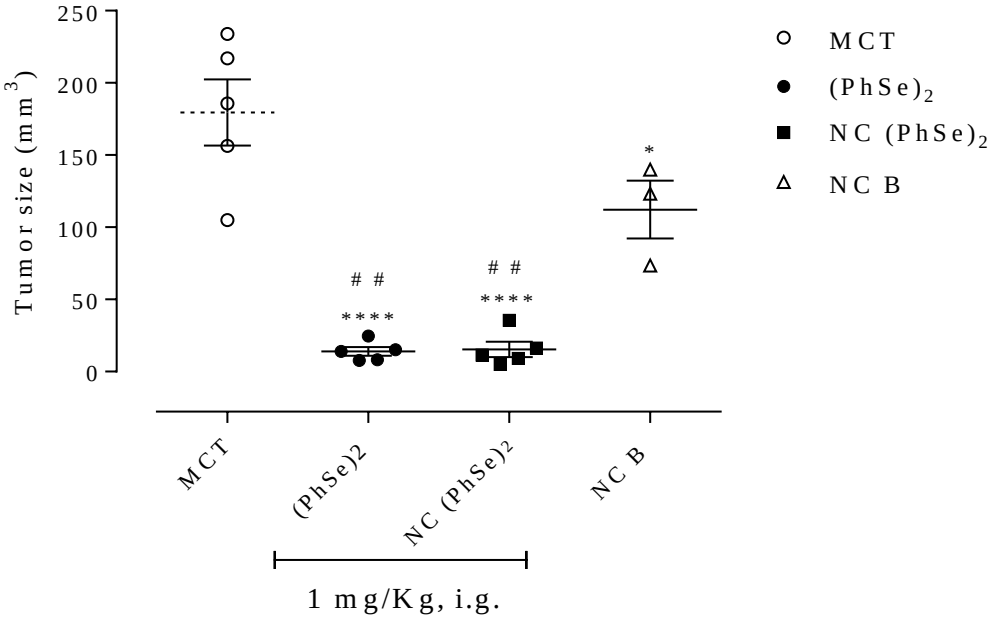

Figure 7. Evaluation of tumor size in glioma-implanted rats. Data were analyzed by one-way ANOVA, followed by Tukey's post hoc test, in which the asterisks denote significant differences (* $p<0.005$ and **** $p<0.0001$) in comparison to the negative control group and sharps ($^{\#\#}$ $p<0.01$) means significant differences between $(PhSe)_2$ or NC $(PhSe)_2$ with NC B.

DISCUSSÃO GERAL

5. Discussão geral

Giordani e colaboradores (2014) desenvolveram pela primeira vez nanocápsulas poliméricas para a incorporação do $(PhSe)_2$ (GIORDANI et al., 2014). Neste estudo, as suspensões de nanocápsulas foram desenvolvidas utilizando o PCL como polímero e o óleo de canola como núcleo oleoso, sendo este óleo empregado como veículo para dissolver o $(PhSe)_2$ na grande maioria dos trabalhos que demonstram seus efeitos farmacológicos em modelos animais (NOGUEIRA E ROCHA, 2010). Baseado nos resultados promissores do estudo de Giordani e colaboradores (2014), esta tese apresenta o desenvolvimento de nanocápsulas poliméricas para a incorporação do $(PhSe)_2$ empregando triglicerídeos de cadeia média (TCM) como núcleo oleoso das nanocápsulas. Uma vez que o óleo de canola apresenta ácido linolêico e olêico em sua composição, e estes constituintes agregam propriedades anti-inflamatórias e antioxidantes para o óleo (BORGES et al., 2014), optou-se por usar um óleo quimicamente inerte para o desenvolvimento das partículas deste estudo a fim de melhor elucidar as propriedades do composto associado ao carreador. O TCM foi um dos primeiros núcleos oleosos de nanocápsulas poliméricas, sendo bem tolerado por diversas vias de administração, incluindo a intravenosa (GUTERRES et al., 1995). No entanto, mesmo sendo um óleo comumente utilizado no preparo das nanocápsulas, é essencial que o composto tenha afinidade pelo óleo utilizado e por isso, uma avaliação da solubilidade do $(PhSe)_2$ no TCM foi realizada, como uma etapa de pré-formulação. Para isso foi realizada a adição de um excesso do $(PhSe)_2$ a 2 mL de TCM. Após agitação magnética over night foi realizada centrifugação a 3.000 rpm por 10 minutos e uma alíquota do sobrenadante foi retirada e diluída em uma mistura de acetonitrila:acetona (1:1, v/v). Na sequência, foi realizada a quantificação por cromatografia líquida de alta eficiência (CLAE), conforme o método descrito no **artigo 1**. A solubilidade do $(PhSe)_2$ foi de 18,50 ± 1,22 mg/mL de TCM, sugerindo que este óleo é adequado para compor o núcleo das nanocápsulas. Similarmente, Sari e colaboradores (2017) testaram a solubilidade do disseleneto de bis (p-metoxifenila) [$(OMePhSe)_2$], um análogo estrutural do $(PhSe)_2$, em óleo de canola e TCM, visando a preparação de nanocápsulas com este composto. Os resultados demonstraram que o $(OMePhSe)_2$ foi mais solúvel no TCM (27,07 ± 0,8 mg/mL) do que no óleo do canola (23,84 ± 0,5 mg/mL) (SARI et al., 2017), corroborando os achados desta tese.

O primeiro conjunto de resultados, apresentados no **artigo 1**, demontrou que as nanocápsulas desenvolvidas neste estudo têm características físico-químicas semelhantes às

encontradas em trabalhos que empregaram os mesmos constituintes, PCL e TCM, para compor o sistema (FONTANA et al., 2009; GEHRCKE et al., 2017; SARI et al., 2017). Para complementar a caracterização do sistema e devido à elevada lipofia do $(PhSe)_2$, estudos preliminares do perfil de liberação do $(PhSe)_2$ a partir das nanocápsulas também foram relizados empregando a técnica de sacos de diálise. Diversos meios de liberação foram testados: solução salina 0,9 % + 5% de polisorbato 80, tampão fosfato pH 7,4 + 2 % de polisorbato 80, água + 5 % polisorbato 80 + PEG 400 (60:40), água + etanol (70:30), água + etanol (50:50) e água + lauril sulfato de sódio (1, 2 e 5 %). Também foram testadas diferentes alíquotas das amostras e diferentes volumes do meio de liberação, na tentativa de encontrar condições experimentais apropriadas para realização do ensaio. O $(PhSe)_2$ foi detectado apenas nos meios de liberação que continham etanol na sua composição, porém em quantidades muito pequenas. Após 48 horas de experimento, menos de 4 % do composto havia sido liberado das nanocápsulas para o meio externo. Tais achados sugerem que a liberação do ativo a partir das nanoestruturas é bastante controlada, contudo, esses resultados não proporcionam informações suficientes para entender a liberação do composto, principalmente devido as limitações analíticas enfrentadas.

Também foi realizado um estudo de estabilidade das formulações, onde se observou apenas alterações nos valores do pH, algo que já é descrito para esse tipo de estrutura (FONTANA et al., 2009; FRIEDRICH et al., 2008; SARI et al., 2017) É interessante mencionar que este perfil de alta estabilidade parece estar bastante associado com o tipo de nanoestrutura. Antunes e colaboradores desenvolveram uma formulação de nanoesferas para incorporação do $(PhSe)_2$, empregando o polímero poli-ácido lático (PLA), e os resultados da avaliação da estabilidade (7 dias) demonstraram alterações em parâmetros como tamanho médio de partícula e IPD (ANTUNES et al., 2017). Diante disso, se reforça a hipótese de que as nanocápsulas apresentam-se como o nanosistema mais adequado para a incorporação do $(PhSe)_2$.

Uma vez que as suspensões de nanocápsulas contendo $(PhSe)_2$ apresentaram características promissoras, uma avaliação preliminar foi conduzida para a avaliar a citotoxicidade da formulação frente a queratinócitos e células sanguíneas humanas, bem como estudar o seu potencial para reduzir a viabilidade de células de melanoma humano A375. Estas avaliações foram realizadas em parceria com a Universidade Franciscana, sob orientação da Professora Drª. Michele Rorato Sagrillo.

É crescente o número de pesquisas visando avaliar a toxicidade de sistemas nanoestruturados. Para este fim, estudos empregando células de diferentes linhagens tornam-se a primeira escolha, minimizando assim o uso de animais (AULA et al., 2015). Os resultados demonstraram que a incorporação do composto às nanocápsulas evitou a redução da viabilidade dos queratinócitos, a qual, por outro lado, foi observada para o composto livre. Além disso, tanto o $(PhSe)_2$ livre, quanto sua forma nanoencapsulada, reduziram a viabilidade das células de melanoma A375. Vale ressaltar que nosso estudo é o primeiro a contemplar tais avaliações de citotoxicidade, em especial, visando uma linhagem celular de melanoma humano para este derivado de Se. Dessa forma, os resultados apresentados no **artigo 1** reforçam a hipótese que compostos orgânicos de selênio são bons candidatos para o desenvolvimento de fármacos para o tratamento do câncer e corroboram com trabalhos que relataram um efeito antitumoral do $(PhSe)_2$ frente a células de neuroblastoma humano (POSSER et al., 2011) e adenocarcinoma de cólon (NEDEL et al., 2012).

Embora iniciais, os resultados relacionados ao **artigo 1** foram fundamentais para o direcionamento desta tese, pois ampliaram a perspectiva de avaliação e fortaleceram a proposição das nanocápsulas de $(PhSe)_2$ para a terapia antitumoral. Desta forma, na sequência foi conduzido um estudo mais aprofundado com relação ao efeito do $(PhSe)_2$ e das NC $(PhSe)_2$ sobre linhagens de melanoma resistentes. A resistência das células tumorais às terapias convencionais é um dos grandes desafios que se objetiva contornar com a busca por novas alternativas para o tratamento do câncer, juntamente com a redução dos efeitos adversos causados por esses fármacos (BRIGGER et al., 2012; NOOTER e STOTER 1996). Para a avaliação do efeito do $(PhSe)_2$ e das NC $(PhSe)_2$ frente às células SK-Mel-103, um conjunto de técnicas *in vitro* foi empregado, a fim de elucidar de uma forma mais detalhada o possível mecanismo do efeito antitumoral (**manuscrito 1**). Tais experimentos foram realizados em parceria com a Universidade Federal de Ciências da Saúde de Porto Alegre, sob orientação da Professora Drª Elizandra Braganhol. Com os resultados obtidos sugere-se que as NC $(PhSe)_2$ apresentam um efeito superior frente às células de melanoma resistentes, e que esse efeito pode estar atribuído a indução da apotose e necrose, bem como através da modulação da síntese de óxido nítrico.

Visto que as suspensões de nanocápsulas contendo o $(PhSe)_2$ se mostraram promissoras para o tratamento do melanoma, foi proposto o desenvolvimento de hidrogéis contendo estas nanocápsulas, objetivando a aplicação cutânea desta formulação como terapia

adjuvante para o melanoma. Vale ressaltar que este é o primeiro trabalho visando desenvolvimento de formulação e avaliação do $(PhSe)_2$ para aplicação cutânea, o que reforça a relevância científica deste estudo e torna promissor o estudo para aplicação cutânea de outros compostos de Se. Até então, a grande maioria dos trabalhos envolvendo o composto livre foram voltados para sua administração pelas vias oral, intragástrica, intraperitoneal ou subcutânea (BARBOSA et al., 2008; BARBOSA et al., 2008; NOGUEIRA E ROCHA 2010; PRIGOL et al., 2012; PRIGOL et al., 2010).

Os hidrogéis foram desenvolvidos pelo simples e rápido espessamento das suspensões de nanocápsulas empregando um polissacarídeo natural, a goma xantana. Nosso grupo de pesquisa tem utilizado essa técnica nos últimos dois anos para desenvolver hidrogéis de goma gelana contendo nanocápsulas e têm obtido resultados promissores (MARCHIORI et al., 2017; PEGORARO et al., 2017). Nesta tese, a goma xantana foi escolhida como um novo agente espessante de suspensão de nanocápsulas poliméricas e os resultados encontrados no **manuscrito 1** nos indicaram que os hidrogéis foram desenvolvidos com sucesso e apresentaram características físico-químicas adequadas para a aplicação do $(PhSe)_2$ pela via tópica. Cabe lembrar que, além das análises que envolveram a caracterização das formulações semissólidas, um estudo de estabilidade também foi conduzido, o que não havia ainda sido feito com hidrogéis preparados a base do espessamento das suspensões com gomas naturais. Outro ponto importante é que as formulações contendo o $(PhSe)_2$, tanto na sua forma livre quanto na nanoencapsulada, não apresentaram fenômenos de instabilidade como o crescimento microbiológico observado nas formulações contendo somente os veículos. Esse achado vai de encontro a relatos anteriores sobre o $(PhSe)_2$, o qual já foi estudado na sua forma livre como agente antifúngico (ROSSETI et al., 2015), o que pode ter contribuído para a manutenção da estabilidade microbiológica e físico-química das formulações durante o período de armazenamento. No entanto, testes microbiológicos devem ser realizados para atribuir de fato esse efeito ao composto.

A avaliação de permeação cutânea *in vitro* utilizando pele humana é de extrema importância para predizer o local de ação da formulação e consequentemente sua efetividade contra as células de melanoma. No estudo de permeação cutânea *in vitro* demonstrado no **manuscrito 1** foi observado que o hidrogel contendo as NC $(PhSe)_2$ foi capaz de aumentar a permeação/penetração na pele e liberar o composto em maior quantidade na derme do que o hidrogel contendo a forma livre. Esse efeito pode ser considerado favorável, uma vez que as

células tumorais de melanoma atingem a derme ocasioando os piores prognósticos da doença. Além disso, também foi observado uma quantidade significativa do composto no estrato córneo, indicando um maior tempo de retenção da formulação na pele, o que ocasionaria a liberação controlada e consequentemente um efeito prolongado no local do tumor.

Em um estudo realizado por Prigol e colaboradores (2009) foi demonstrado que a toxicidade do composto é influenciada pela via de administração (intraperitoneal > intragástrica > subcutânea), solvente (DMSO > óleo de canola) e a espécie animal (camundongos > ratos) (PRIGOL et al., 2009). Além disso, um assunto muito discutido nos últimos anos é a nanotoxicologia, visto que o tamanho reduzido sistemas nanoestruturados pode modificar consideravelmente as propriedades físico-químicas dos materiais, assim como a interação destes com as macromoléculas no organismo (YILDIRIMER et al., 2011). Levando isso em consideração, experimentos visando melhor avaliar a toxicidade das suspensões de nanocápsulas contendo o $(PhSe)_2$ tem grande relevância. Neste âmbito, o peixe zebra tem sido bastante empregado como modelo animal para avaliar a toxicidade de sistemas nanoestruturados através de análises de mal-formação em embriões, imunotoxicidade, genotoxicidade, ruptura do sistema branquial, neurotoxicidade influência na reprodutividade e estudos comportamentais (CHAKRABORTY et al., 2016). Interessantemente, Ibrahim e colaboradores (2014) relataram que a exposição de peixa zebra ao $(PhSe)_2$ na sua forma livre causou efeito ansiolítico nos animais, no entanto, em determinadas concentrações, foram observadas alterações comportamentais preditivas de toxicidade (IBRAHIM et al., 2014). Baseado nesses resultados, o **manuscrito 2** foi conduzido no sentido de demonstrar os efeitos da exposição do peixe zebra às NC $(PhSe)_2$, fazendo um comparativo com o estudo anterior. Este estudo foi realizado em parceria com o Prof. Dr. Denis Rosemberg, da Universidade Federal de Santa Maria. Através da análise de diversos parâmetros comportamentais, observamos que a exposição dos animais às NC $(PhSe)_2$ não desencadeou modificações negativas nos comportamentos avaliados. Vale ressaltar que Ibrahim e colaboradores (2014) relataram que as concentrações de 0,5 e 1,0 µM de $(PhSe)_2$ provocaram efeitos indesejados nos peixes (IBRAHIM et al., 2014), o que não foi observado para a formulação de nanocápsulas.

Visto que as NC $(PhSe)_2$ não causaram toxicidade em peixe zebra, estudos adicionais de toxicidade foram realizados utilizando ratos como modelo animal, os quais apresentam um organismo mais complexo, através de um protocolo de administração semelhante ao que seria

usado para testar a ação antiglioma *in vivo* da formulação (**manuscrito 3**). Este protocolo foi realizado no Laboratório de Síntese, Reatividade e Avaliação Farmacológica e Toxicológica de Organocalcogênios, sob orientação da Profª Drª Cristina Wayne Nogueira, na Universidade Federal de Santa Maria. Ao longo do experimento, não foram observadas alterações no peso dos animais, nem no consumo de ração dos grupos que recebram o composto. As análises bioquímicas não revelaram alterações do estado oxidativo dos tecidos nem nos marcadores plasmáticos de função renal e hepática. No que diz respeito a estudos de toxicidade em roedores envolvendo formulações nanoestruturadas contendo o composto, Stefanello e colaboradores, em 2015, utilizaram as nanocápsulas contendo $(PhSe)_2$ desenvolvidas no trabalho de Giordani e colaboradores (2014), testaram diferentes doses da formulação contendo o composto em camundongos (3,12 mg/Kg, 15,6 mg/Kg, 31,20 mg/Kg, 156 mg/Kg, e 312 mg/Kg) pela via intraperitoneal e, após 72 horas, avaliaram a dose letal e parâmetros oxidativos (STEFANELLO et al., 2015). Diante disso, o **manuscrito 3** relata pela primeira vez um estudo de toxicidade de NC $(PhSe)_2$ após administração repetida durante 15 dias e pela via intragástrica. Protocolo semelhante a este foi realizado no estudo de Sari e colaboradores (2017), onde a administração repetida de formulação de nanocápsulas contendo o composto $(OMePhSe)_2$ (25 mg/Kg) em camundongos, durante um período de 7 dias, não causou alterações bioquímicas e nem plasmáticas (SARI et al., 2017). Diante dos poucos relatos sobre nanocápsulas contendo $(PhSe)_2$ a detalhada avaliação da toxicidade das formulações se faz importante para demonstrar a segurança da administração desses sitemas em organismos vivos.

Dando seguimento às avaliações da atividade antitumoral do $(PhSe)_2$, livre e nanoencapsulado, estudos *in vitro* foram realizados para demonstrar o efeito antiglioma das formulações, em colaboração com a Profª. Drª. Elizandra Bragranhol, na Universidade Federal de Ciências da Saúde de Porto Alegre. Para este fim foram utilizadas as mesmas técnicas do **manuscrito 1**, onde foi observado pelo teste do MTT que tanto a forma livre quanto a nanoencapsulada reduziu a viabilidade das células C6, sem causar toxicidade aos astrócitos, e que a nanoencapsulação proporcionou uma melhora no efeito *in vitro* demonstrado pelos valores de IC_{50}. Além disso, resultados semelhantes aos encontrados no **manuscrito 1** para os níveis de óxido nítrico foram observados, ou seja, um aumento nos níveis de NO_2^- nas amostras incubadas com NC B e NC $(PhSe)_2$, sugerindo que as nanocápsulas compostas por PCL e TCM podem ter uma influência sobre os compostos de

nitrogênio e, pelo menos em parte, mediar seu efeito citotóxico frete às células de melanoma e glioma. Adicionalmente, foi observado que poucas células captaram o iodeto de propídio, o que sugere que o envolvimento do processo de necrose na morte celular possa não ser tão relevante. Estudos complementares que avaliem a participação do processo de apoptose poderiam ser realizados para complementar esses resultados, mas de qualquer forma, pode-se inferir que o $(PhSe)_2$ apresenta potencial como bom candidato a fármaco quimioterápico, uma vez que o ideal é que se tenha um efeito antiproliferativo sem causar morte celular por necrose (BERNARDI et al., 2008).

Um dos grandes desafios que limita a eficácia dos tratamentos atualmente disponíveis para o glioma é a dificuldade destes fármacos em ultrapassar a barreia sangue-cérebro, requerendo assim a administração de altas doses para alcançar concentrações terapêuticas no tecido cerebral, o que paralelamente também desencadeia efeitos adversos (BEHIN et al., 2003; KARIM et al., 2016). Sendo assim, a incorporação de moléculas farmacologicamente ativas em sistemas nanoestruturados torna-se uma alternativa promissora para contornar tais limitações e alcançar uma maior eficácia terapêutica (KARIM et al., 2016). Levando em consideração a incidência de cânceres do tipo glioma e as vantagens conferidas pelos sistemas nanoestruturados para terapias voltadas para liberação de fármacos a nível cerebral, um estudo de atividade antitumoral *in vivo* foi realizado no **manuscrito 3**. Os resultados revelaram que as nanocápsulas reduziram o tamanho do tumor implantado no cérebro dos animais, assim como o composto na sua forma livre, o qual pode ter ultrapassado a barreira sangue-cérebro devido a sua elevada lipofilia. Esse efeito do $(PhSe)_2$ pode ser explicado pelos estudos prévios de Prigol e colaboradores (2012) e Giordani e colaboradores (2014), os quais quantificaram o elemento Se no cérebro dos animais após a administração do $(PhSe)_2$ e de nanocápsulas contendo $(PhSe)_2$, sugerindo que tanto o composto livre quanto o nanoencapsulado são capazes de ultrapassar a barreira sangue-cérebro. Além disso, a presença do polisorbato 80 na composição das nanocápsulas pode ter contribuído para esse efeito, uma vez que este atua como uma âncora para as apolipoproteínas (Apo), principalmente Apo A (A-I), B e E, favorecendo sua captação pelas células da barreira sangue-cérebro (KARIM et al., 2016; KREUTER 2014). Um ponto importante a ser observado é que a incorporação do $(PhSe)_2$ às nanocápsulas poliméricas manteve o efeito na redução do tamanho do tumor semelhante observado para a forma livre, porém, o desenvolvimento de uma formulação aquosa viabiliza sua administração por diferentes vias, melhorando sua solubilidade nos fluídos do trato

gastrintestinal e possibilitando sua utilização também pela via intravenosa. No entanto, deve-se considerar a hipótese de que a utilização de doses menores do composto poderia fornecer mais evidências sobre o possível impacto da nanoencapsulação frente ao efeito no modelo animal de glioma.

Por fim, diante do que foi discutido, pode-se refletir que os resultados desta tese servem como um degrau para futuros estudos mais aprofundados sobre os efeitos promissores apresentados para as nanocápsulas poliméricas contendo $(PhSe)_2$, ressaltando que essa formulação viabiliza o uso deste composto por diferentes vias de administração. A figura 9 resume os resultados encontrados nesta tese.

Figura 9. Resumo dos experimentos e resultados apresentados nesta tese

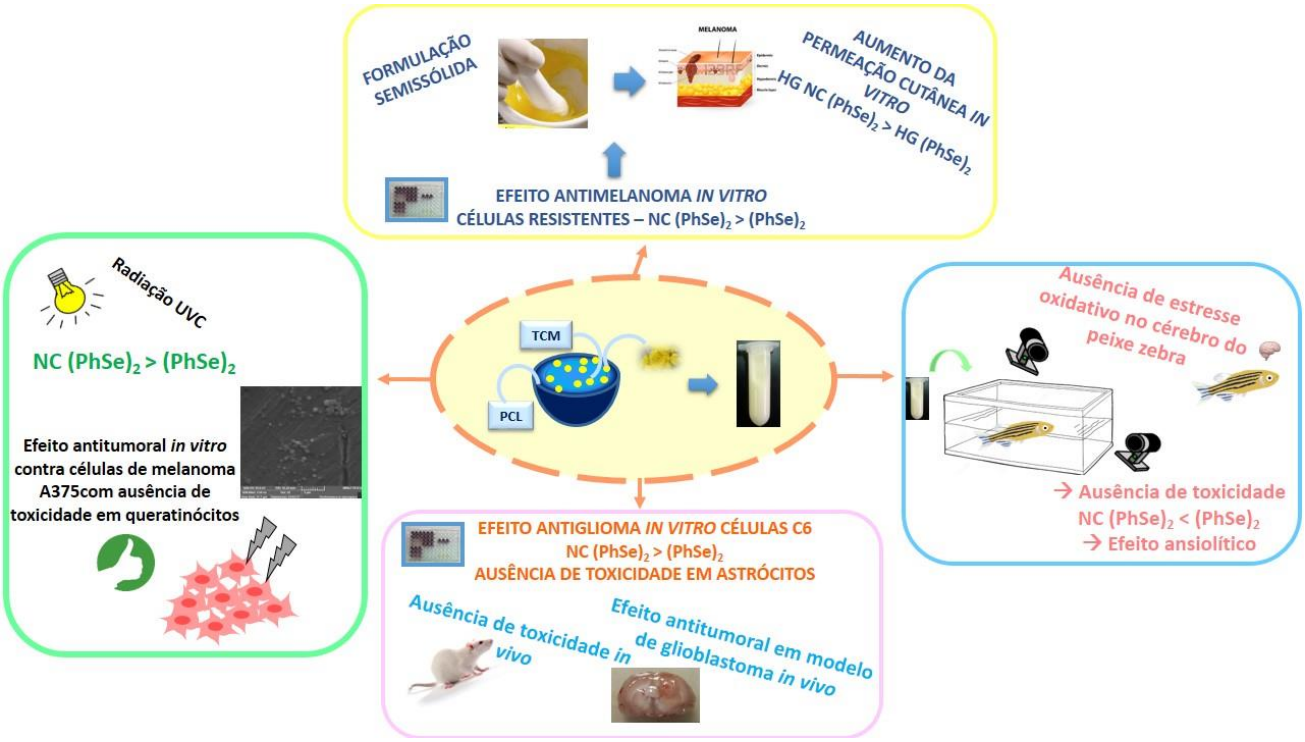

CONCLUSÃO GERAL

6. Conclusão geral

O delineamento experimental empregado neste estudo permitiu a incorporação do disselento de difenila em um sistema nanoestruturado, contornando suas limitações físico-químicas e prevenindo os efeitos indesejáveis causados pelo composto livre, viabilizando sua administração por diferentes vias de administração, incluindo a cutânea, a qual nunca havia sido explorada para o composto. Além disso, uma detalhada caracterização da toxicidade da formulação foi realizada, demonstrando sua segurança. As formulações apresentaram um potente efeito antitumoral contra dois tipos de tumores bastante agressivos, sendo que estas atividades foram demonstradas pela primeira vez para este composto. Desta forma, as nanocápsulas, tanto na forma de suspensão, quanto de hidrogel, apresentam grande potencial como nanocarreadores do $(PhSe)_2$ em sistemas biológicos visando efeito antitumoral.

6.1 Perspectivas

Com base no conjunto de resultados obtidos nesta tese sugere-se, para estudos futuros, a determinação de efeito antimelanoma em um modelo pré-clínico, avaliando a suspensão de nanocápsulas pela via intragástrica e os hidrogéis pela via cutânea. Além disso, pode-se também realizar estudos de atividade antitumoral utilizando a formulação pela via intravenosa, já que a incorporação do composto em um sistema aquoso permite sua administração por essa via. Por fim, este trabalho abre perspectivas para estudos de atividade antitumoral do composto livre e nanoencapsulado em diferentes tipos de tumores.

REFERÊNCIAS

7. Referências

ACKER, C. I., et al. Antidepressant-like effect of diphenyl diselenide on rats exposed to malathion: Involvement of Na+K+ ATPase activity. **Neuroscience Letters**, 455(3): 168-172, 2009.

ACKER, C. I. AND C. W. NOGUEIRA. Chlorpyrifos acute exposure induces hyperglycemia and hyperlipidemia in rats. **Chemosphere**, 89(5): 602-608, 2012.

ADABI, M., et al. Biocompatibility and nanostructured materials: applications in nanomedicine. **Artif Cells Nanomed Biotechnol**, 45(4): 833-842, 2017.

ALMEIDA, J. S., et al. Nanostructured Systems Containing Rutin: *In vitro* Antioxidant Activity and Photostability Studies. **Nanoscale Research Letters**, 5(10): 1603-1610, 2010.

ANTUNES, O. D., et al. Preparation, physicochemical characterization and antioxidant activity of diphenyl diselenide-loaded poly(lactic acid) nanoparticles. **Journal of Trace Elements in Medicine and Biology**, 39: 176-185, 2017.

ARAÚJO, F. A., et al. Development and characterization of parenteral nanoemulsions containing thalidomide. **European Journal of Pharmaceutical Sciences**, 42(3): 238-245, 2011.

ARSHAD, A., et al. Convection-enhanced delivery of carpoblatin PLGA nanoparticles for the treatment of glioblastoma. **Plos One**, 10(7): 1-16, 2015.

AULA, S., et al. Biophysical, biopharmaceutical and toxicological significance of biomedical nanoparticles. **Rsc Advances**, 5: 47830–47859, 2015.

BARBOSA, N. B. D., et al. Diphenyl diselenide supplementation delays the development of N-nitroso-N-methylurea-induced mammary tumors. **Archives of Toxicology**, 82(9): 655-663, 2008.

BARBOSA, N. B. V., et al. Dietary diphenyl diselenide reduces the STZ-induced toxicity. **Food and Chemical Toxicology**, 46(1): 186-194, 2008.

BARBOSA, N. B. V., et al. Diphenyl diselenide reduces temporarily hyperglycemia: Possible relationship with oxidative stress. **Chemico-Biological Interactions**, 163(3): 230-238, 2006.

BARBOSA, N. B. V., et al. Effect of organic forms of selenium on delta-aminolevulinate dehydratase from liver, kidney, and brain of adult rats. **Toxicology and Applied Pharmacology**, 149(2): 243-253, 1998.

BEBER, T. C., et al. Cationic Polymeric Nanocapsules as a Strategy to Target Dexamethasone to Viable Epidermis: Skin Penetration and Permeation Studies. **Journal of Nanoscience and Nanotechnology**, 16(2): 1331-1338, 2016.

BEHIN, A., et al. Primary brain tumours in adults. **Lancet**, 361(9354): 323-331, 2003.

BEHNE, D., et al. Identification of Type-I Iodothyronine 5'-Deiodinase as a Selenoenzyme. **Biochemical and Biophysical Research Communications**, 173(3): 1143-1149, 1990.

BERNARDI, A., et al. The antiproliferative effect of indomethacin-loaded lipid-core nanocapsules in glioma cells is mediated by cell cycle regulation, differentitaion, and the inhibition of survival pathways. **International Journal of Nanomedicine**, 8: 711-729, 2013.

BERNARDI, A., et al. Selective cytotoxicity of indomethacin and indomethacin ethyl ester-loaded nanocapsules against glioma cell lines: an *in vitro* study. **European Journal of Pharmacology**, 586(1-3): 24-34, 2008.

BORGES, L. P., et al. Protective effect of diphenyl diselenide on acute liver damage induced by 2-nitropropane in rats. **Toxicology**, 210(1): 1-8, 2005.

BORGES, M. C., et al. Ácidos graxos poli-insaturados ômega-3 e lúpus eritematoso sistêmico: o que sabemos? **Revista Brasileira de Reumatologia**, 54(6): 459-466, 2014.

BRANDES, A. A., et al. Temozolomide in patients with high grade gliomas. **Oncology**, 59(3): 181-186, 2000.

BRIGGER, I., et al. Nanoparticles in cancer therapy and diagnosis. **Advanced Drug Delivery Reviews**, 64: 24-36, 2012.

BRUNING, C. A., et al. Protective Effect of Diphenyl Diselenide on Ischemia and Reperfusion-Induced Cerebral Injury: Involvement of Oxidative Stress and ProInflammatory Cytokines. **Neurochemical Research**, 37(10): 2249-2258, 2012.

CAPANEMA, N. S. V., et al. Bioengineered carboxymethyl cellulose-doxorubicin prodrug hydrogels for topical chemotherapy of melanoma skin cancer. **Carbohydrate Polymers**, 195: 410-412, 2018.

CARLETTO, B., et al. Resveratrol-loaded nanocapsules inhibit murine melanoma tumor growth. **Colloids and Surfaces B-Biointerfaces**, 144: 65-72, 2016.

CASOLARO, M., et al. Hydrogel containing L-valine residues as a platform for cisplatin chemotherapy. **Colloids and Surfaces B-Biointerfaces**, 88(1): 389-395, 2011.

CECHELLA, J. L., et al. The impact of a diphenyl diselenide-supplemented diet and aerobic excercise on memory of middle-aged rats. **Physiology and Behavior**, 135: 125-129, 2014.

CHAKRABORTY, C., et al. Zebrafsh: A complete animal model to enumerate the nanoparticle toxicity. **Journal of Nanobiotechnology**, 14(65): 1-13, 2016.

CHASSOT, J. M., et al. Beclomethasone Dipropionate-Loaded Polymeric Nanocapsules: Development, *In vitro* Cytotoxicity, and *In vivo* Evaluation of Acute Lung Injury. **Journal of Nanoscience and Nanotechnology**, 15(1): 855-864, 2015.

CLARK, L. N., et al. Association between the anatomic distribution of melanoma and sex. **Journal of the American Academy of Dermatology**, 56(5): 768-773, 2007.

COMASSETO, J. V. Selenium and tellurium chemistry: historical background. **Journal of the Brazilian Chemical Society**, 21: 2027-2031, 2010.

COSTA, M. D., et al. Diphenyl diselenide prevents hepatic alterations induced by paraquat in rats. **Environmental Toxicology and Pharmacology**, 36(3): 750-758, 2013.

COUVREUR, P., et al. Nanocapsule technology: A review. **Critical Reviews in Therapeutic Drug Carrier Systems**, 19(2): 99-134, 2002.

COUVREUR, P., et al. Nanotechnologies for drug delivery: Application to cancer and autoimmune diseases. **Progress in Solid State Chemistry**, 34(2-4): 231-235, 2006.

COUVREUR, P. AND C. VAUTHIER. Nanotechnology: Intelligent design to trat complex disease. **Pharmaceutical Research**, 23(7): 1417-1450, 2006.

DA ROCHA, J. T., et al. Hypolipidaemic activity of orally administered diphenyl diselenide in Triton WR-1339-induced hyperlipidaemia in mice. **Journal of Pharmacy and Pharmacology**, 61(12): 1673-1679, 2009.

DA SILVEIRA, E. F., et al. Ketoprofen-loaded polymeric nanocapsules selectively inhibit cancer cell growth *in vitro* and in preclinical model of glioblastoma multiforme. **Investigational New Drugs**, 31(6): 1424-1435, 2013.

DE ANDRADE, D. F., et al. Nanoencapsulation of Clobetasol Propionate Decreases Its Penetration to Skin Layers Without Changing Its Relative Skin Distribution. **Journal of Nanoscience and Nanotechnology**, 15(1): 875-879, 2015.

DE FREITAS, A. S. AND J. B. T. ROCHA. Diphenyl diselenide and analogs are substrates of cerebral rat thioredoxin reductase: A pathway for their neuroprotective effects. **Neuroscience Letters**, 503(1): 1-5, 2011.

DE LIMA, J. A., et al. Novel Pemulen/Pullulan blended hydrogel containing clotrimazole-loaded cationic nanocapsules: Evaluation of mucoadhesion and vaginal permeation. **Materials Science & Engineering C-Materials for Biological Applications**, 79: 886-893, 2017.

DELLIS, D., et al. Physicochemical profile of nimesulide - Exploring the interplay of lipophilicity, solubility and ionization. **Journal of Pharmaceutical and Biomedical Analysis**, 44(1): 57-62, 2007.

DIAS, G. R. M., et al. Diphenyl diselenide supplemented diet reduces depressive-like behavior in hypothyroid female rats. **Physiology & Behavior**, 124: 116-122, 2014.

DIAZ, M., et al. A diphenyldiselenide derivative induces autophagy via JNK in HTB-54 lung cancer cells. **Journal of Cellular and Molecular Medicine**, 22(1): 289-301, 2018.

DIMER, F. A., et al. Impactos da nanotecnologia na saúde : produção de medicamentos. **Química Nova**, 36(10): 1520-1526, 2013.

DREWES, C. C., et al. Novel therapeutic mechanisms determine the effectiveness of lipid-core nanocapsules on melanoma models. **International Journal of Nanomedicine**, 11: 1261-1279, 2016.

EL-SAMALIGY, M. S., et al. Polyalkyl cyanoacrylate nanocapsules. **Journal of Pharmacy and Pharmacology**, 38(3): 216-218, 1986.

FANG, J., et al. The EPR effect: Unique features of tumor blood vessels for drug delivery, factors involved, and limitations and augmentation of the effect. **Advanced Drug Delivery Reviews**, 63(3): 136-151, 2011.

FAO/OMS. Report 7ª Joint FAO/OMS Expert Consultation. Bangkok. Thailand. **Human Vitamin and Mineral Requirements**, 2002.

FERREIRA, L. M., et al. Ketoprofen-loaded pomegranate seed oil nanoemulsion stabilized by pullulan: Selective antiglioma formulation for intravenous administration. **Colloids and Surfaces B-Biointerfaces**, 130: 272-277, 2015.

FERREIRA, L. M., et al. Pentamidine-Loaded Poly(epsilon-Caprolactone) Nanoparticles Show Low Acute Lung Toxicity *In vivo*. **Latin American Journal of Pharmacy**, 34(5): 1039-1042, 2015.

FERREIRA, L. M., et al. Pomegranate seed oil nanoemulsions with selective antiglioma activity: optimization and evaluation of cytotoxicity, genotoxicity and oxidative effects on mononuclear cells. **Pharmaceutical Biology**, 54(12): 2968-2977, 2016.

FESSI, H., et al. Nanocapsule Formation by Interfacial Polymer Deposition Following Solvent Displacement. **International Journal of Pharmaceutics**, 55(1): R1-R4, 1989.

FLOHÉ, L., et al. Glutathione peroxidase: a selenium enzyme. **Febs Letters**, 32: 132-134, 1973.

FLORES, F. C., et al. Hydrogels Containing Nanocapsules and Nanoemulsions of Tea Tree Oil Provide Antiedematogenic Effect and Improved Skin Wound Healing. **Journal of Nanoscience and Nanotechnology**, 15(1): 800-809, 2015.

FONTANA, M. C., et al. Nanoencapsulation as a way to control the release and to increase the photostability of clobetasol propionate: influence of the nanostructured system. **Journal of Biomedical Nanotechnology**, 5(254-263), 2009.

FONTANA, M. C., et al. Improved efficacy in the treatment of contact dermatitis in rats by a dermatological nanomedicine containing clobetasol propionate. **European Journal of Pharmaceutics and Biopharmaceutics**, 79(2): 241-249, 2011.

FRANK, L. A., et al. Improving drug biological effects by encapsulation into polymeric nanocapsules. **Wiley Interdisciplinary Reviews-Nanomedicine and Nanobiotechnology**, 7(5): 623-639, 2015.

FRIEDRICH, R. B., et al. Development and physicochemical characterization of dexamethasone-loaded polymeric nanocapsule suspensions. **Química Nova**, 31(5): 1131-1136, 2008.

GE, K. AND G. YANG. The epidemiology of selenium deficiency in the etiological study of endemic diseases in China. **American Journal of Clinical Nutrition**, 57: 259-263,1993.

GECIONI, L., et al. Stealth and nonstealth nanocapsules containing camptothecin: in vitro and *in vivo* activity on B16-F10 melanoma. **Journal of Pharmacy and Pharmacology**, 59: 1359 – 1364, 2007.

GEHRCKE, M., et al. Enhanced photostability, radical scavenging and antitumor activity of indole-3-carbinol-loaded rose hip oil nanocapsules. **Materials Science & Engineering C-Materials for Biological Applications**, 74: 279-286, 2017.

GEHRCKE, M., et al. Nanocapsules improve indole-3-carbinol photostability and prolong its antinociceptive action in acute pain animal models. **European Journal of Pharmaceutical Sciences**, 111: 133-141, 2018.

GHISLENI, G., et al. Diphenyl diselenide exerts anxiolytic-like effect in Wistar rats: Putative roles of GABAA and 5HT receptors. **Progress in NeuroPsychopharmacology & Biological Psychiatry**, 32(6): 1508-1515, 2008.

GIORDANI, C. F. A., et al. Diphenyl Diselenide-Loaded Nanocapsules: Preparation and Biological Distribution. **Applied Biochemistry and Biotechnology**, 172(2): 755-766,2014.

GROBBEN, B., et al. Rat C6 glioma as experimental model system for the study of glioblastoma growth and invasion. **Cell and Tissue Research**, 310(3): 257-270, 2002.

GROSSMAN, D. AND D. C. ALTIERI. Drug resistance in melanoma: Mechanisms, apoptosis, and new potential therapeutic targets. **Cancer and Metastasis Reviews**, 20(1-2): 3-11, 2001.

GUO, J., et al. Aptamer-functionalized PEG–PLGA nanoparticles for enhanced antiglioma drug delivery. **Biomaterials**, 32(31): 8010-8020, 2011.

GUTERRES, S. S., et al. Polymeric nanoparticles, nanospheres and nanocapsules, for cutaneous applications. **Drug Target Insights**, 2: 147-157, 2007.

GUTERRES, S. S., et al. Poly(Dl-Lactide) Nanocapsules Containing Diclofenac .1. Formulation and Stability Study. **International Journal of Pharmaceutics**, 113(1): 57-63, 1995.

HAASS, N. K., et al. Adhesion, migration and communication in melanocytes and melanoma. **Pigment Cell Research**, 18(3): 150-159, 2005.

HOLMGREN, A. Thioredoxin. **Annual Review of Biochemistry**, 54: 237-271, 1985.

HOUSEHOLDER, K. T., et al. Intravenous delivery of comptothecin-loaded PLGA nanocparticles ofr the treatment of intracranial glioma. **International Journal of Pharmaceutics**, 479: 374-380, 2015.

IARC, I. A. F. R. O. C.-. Low selenium levels linked to liver cancer development. **Press Release**, 425, 2016.

IBRAHIM, M., et al. Anxiolytic effects of diphenyl diselenide on adult zebrafish in a novelty paradigm. **Prog Neuropsychopharmacol Biol Psychiatry**, 54: 187-194, 2014.

INCA. ABC do Cancer - Abordagens Básicas para o Controle do Cancer **Instituto Nacional de Câncer José Alencar Gomes da Silva - INCA, Rio de Janeiro**, 3. ed. rev. atual.: 1-108, 2017.

INCA. ESTIMATIVA 2018. Incidência de Câncer no Brasil **Instituto Nacional de Câncer José Alencar Gomes da Silva - INCA**, Rio de Janeiro, RJ, 2018.

INCA. INSTITUTO NACIONAL DO CÂNCER, Rio de Janeiro. **Disponível em: <www. Inca.gov.br>. Acesso em: 06/18**, 2018.

INEU, R. P., et al. Diphenyl diselenide reverses gastric lesions in rats: Involvement of oxidative stress. **Food and Chemical Toxicology**, 46(9): 3023-3029, 2008.

JUNYAPRASERT, V. B., et al. Q10-loaded NLC versus nanoemulsions: Stability, rheology and *in vitro* skin permeation. **International Journal of Pharmaceutics**, 377: 207-214, 2009.

KALUEFF, A. V., et al. Zebrafish neurobehavioral phenomics for aquatic neuropharmacology and toxicology research. **Aquat Toxicol**, 170: 297-309, 2016.

KALUEFF, A. V., et al. Towards a comprehensive catalog of zebrafish behavior 1.0 and beyond. **Zebrafish**, 10(1): 70-86, 2013.

KARANEM, V., et al. Poly(Ɛ-caprolactone) nanocparticles of carboplatin: Preparation, characterization and *in vitro* cytotoxicity evaluation in U-87 MG cell lines. **Colloids and Surfaces B: Biointerfaces**, 130: 48-52, 2015.

KARIM, R., et al. Nanocarriers for the treatment of glioblastoma multiforme: Current state-of-the-art. **Journal of Controlled Release**, 227: 23-37, 2016.

KAVANAGH, D., et al. Adjuvant therapies in the treatment of stage II and III malignant melanoma. **Surgeon-Journal of the Royal Colleges of Surgeons of Edinburgh and Ireland**, 3(4): 245-256, 2005.

KHOSO, P. A., et al. Selenium Deficiency Affects Immune Function by Influencing Selenoprotein and Cytokine Expression in Chicken Spleen. **Biological Trace Element Research**, 18: 1396-1399, 2018.

KRAI, J., et al. Doxazosin nanoencapsulation improves its *in vitro* antiproliferative and anticlonogenic effects on breast cancer cells. **Biomedicine & Pharmacotherapy**, 94: 10-20, 2017.

KREUTER, J. Drug delivery to the central nervous system by polymeric nanoparticles: What do we know? **Advanced Drug Delivery Reviews**, 71: 2-14, 2014.

KUMAR, A., et al. Application of xanthan gum as polysaccharide in tissue engineering: A review. **Carbohydrate Polymers**, 180: 128-144, 2018.

LEVIN, V. A., et al. Phase II study of 6-thioguanine, procarbazine, dibromodulcitol, lomustine, and vincristine chemotherapy with radiotherapy for treating malignant glioma in children. **Neuro-Oncology**, 2(1): 22-28, 2000.

LI, G. S., et al. Keshan disease: an endemic cardiomyopathy in China. **Human Pathology**, 16(6): 602-609, 1985.

LI, J., et al. Recent advances in targeted nanoparticles drug delivery to melanoma. **Nanomedicine-Nanotechnology Biology and Medicine**, 11(3): 769-794, 2015.

LOLLO, G., et al. Development of multifunctional lipid nanocapsules for the codelivery of paclitaxel and CpG-ODN in the treatment of glioblastoma. **International Journal of Pharmaceutics**, 495(2): 972-980, 2015.

LOUIS, D. N., et al. The 2016 World Health Organization Classification of Tumors of the Central Nervous System: a summary. **Acta Neuropathologica**, 131(6): 803-820, 2016.

LUCHESE, C., et al. Diphenyl diselenide reduces inflammation in the mouse model of pleurisy induced by carrageenan: reduction of pro-inflammatory markers and reactive species levels. **Inflammation Research**, 61(10): 1117-1124, 2012.

MACIEL, E. N., et al. Diphenyl diselenide and diphenyl ditelluride differentially affect delta-aminolevulinate dehydratase from liver, kidney, and brain of mice. **Journal of Biochemical and Molecular Toxicology**, 14(6): 310-319, 2000.

MAGALHAES, N. S. S., et al. The stability and *in vitro* release kinetics of a clofibride emulsion. **International Journal of Pharmaceutics**, 76(3): 225-237, 1991.

MAGENHEIM, B. AND S. BENITA. Nanoparticles Characterization: A Comprehensive Physicochemical Approach. **S. T. P. Pharma Sciences**, 1(4): 221-241, 1991.

MARCATO, P. D. AND N. DURAN. New aspects of nanopharmaceutical delivery systems. **Journal of Nanoscience and Nanotechnology**, 8(5): 2216-2229, 2008.

MARCHIORI, M. C. L., et al. Improved tretinoin photostability in a topical nanomedicine replacing original liquid suspension with spray-dried powder with no loss of effectiveness. **Drug Development and Industrial Pharmacy**, 39(4): 579-586, 2013.

MARCHIORI, M. C. L., et al. Hydrogel containing silibinin-loaded pomegranate oil based nanocapsules exhibits anti-inflammatory effects on skin damage UVB radiationinduced in mice. **Journal of Photochemistry and Photobiology B-Biology**, 170: 25- 32, 2017.

MARCHIORI, M. C. L., et al. Nanoencapsulation Improves Scavenging Capacity and Decreases Cytotoxicity of Silibinin and Pomegranate Oil Association. **Aaps Pharmscitech**, 18(8): 3236-3246, 2017.

MATTHEOLABAKIS, G., et al. Nanodelivery strategies in cancer chemotherapy: biological rationale and pharmaceutical perspectives. **Nanomedicine**, 7(10): 1577-1590, 2012.

MEI, L., et al. Enhanced antitumor and anti-metastasis efficiency via combined treatment with CXCR4 antagonist and liposomal doxorubicin. **Journal of Controlled Release**, 196: 324-331, 2014.

MEI, L., et al. Pharmaceutical nanotechnology for oral delivery of anticancer drugs. **Advanced Drug Delivery Reviews**, 65(6): 880-890, 2013.

MELERO, A., et al. Nanoencapsulation in Lipid-Core Nanocapsules Controls Mometasone Furoate Skin Permeability Rate and Its Penetration to the Deeper Skin Layers. **Skin Pharmacology and Physiology**, 27(4): 217-228, 2014.

MELO, M. T., et al. Diphenyl diselenide protects cultured MCF-7 cells against tamoxifen-induced oxidative DNA damage. **Biomedicine & Pharmacotherapy**, 67(4): 329-335, 2013.

MISHRA, B., et al. Liranaftate loaded Xanthan gum based hydrogel for topical delivery: Physical properties and ex-vivo permeability. **International Journal of Biological Macromolecules**, 107: 1717-1723, 2018.

MORA-HUERTAS, C. E., et al. Polymer-based nanocapsules for drug delivery. **International Journal of Pharmaceutics**, 385(1-2): 113-142, 2010.

MORA-HUERTAS, C. E., et al. Nanocapsules prepared via nanoprecipitation and emulsification-diffusion methods: Comparative study. **European Journal of Pharmaceutics and Biopharmaceutics**, 80(1): 235-239, 2012.

MOUSSEAU, M., et al. A Study of the Expression of 4 Chemoresistance-Related Genes in Human Primary and Metastatic Brain-Tumors. **European Journal of Cancer**, 29A(5): 753-759, 1993.

NCI. NATIONAL CANCER INSTITUTE - About Cancer. **Disponível em: <https://www.cancer.gov/>. Acesso em: 07/18**, 2018.

NEDEL, F., et al. Substituted diaryl diselenides: Cytotoxic and apoptotic effect in human colon adenocarcinoma cells. **Life Sciences**, 91(9-10): 345-352, 2012.

NOGUEIRA, C. W., et al. Anti-inflammatory and antinociceptive activity of diphenyl diselenide. **Inflammation Research**, 52(2): 56-63, 2003.

NOGUEIRA, C. W. AND J. B. T. ROCHA. Diphenyl Diselenide a Janus-Faced Molecule. **Journal of the Brazilian Chemical Society**, 21(11): 2055-2071, 2010.

NOGUEIRA, C. W. AND J. B. T. ROCHA. Toxicology and pharmacology of selenium: emphasis on synthetic organoselenium compounds. **Archives of Toxicology**, 85(11): 1313-1359, 2011.

NOGUEIRA, C. W. AND J. B. T. ROCHA. Organoselenium and organotellurium compounds: Toxicology and pharmacology. **Chemistry of Functional Groups: The Chemistry of Organic Selenium and Tellurium Compounds**, pat 0567, 2012.

NOGUEIRA, C. W., et al. Organoselenium and organotellurium compounds: Toxicology and pharmacology. **Chemical Reviews**, 104(12): 6255-6285, 2004.

NOOTER, K. AND G. STOTER. Molecular mechanisms of multidrug resistance in câncer chemotherapy. **Pathology Research and Practice**, 192(7): 768-780, 1996.

OLIVEIRA, C. P., et al. An algorithm to determine the mechanism of drug distribution in lipid-core nanocapsule formulations. **Soft Matter**, 9(4): 1141-1150, 2013.

ORUNOGLU, M., et al. Effects of curcumin-loaded PLGA nanoparticles on the RG2 rat glioma model. **Materials Science & Engineering C-Materials for Biological Applications**, 78: 32-38, 2017.

OSTROM, Q. T., et al. The epidemiology of glioma in adults: a "state of the science" review. **Neuro-Oncology**, 16(7): 896-913, 2014.

OURIQUE, A. F., et al. Lipid-core nanocapsules as a nanomedicine for parenteral administration of tretinoin: development and *in vitro* antitumor activity on human myeloid leukaemia cells. **Journal of Biomedical Nanotechnology**, 6(3): 214-223, 2010.

OURIQUE, A. F., et al. Improved photostability and reduced skin permeation of tretinoin: Development of a semisolid nanomedicine. **European Journal of Pharmaceutics and Biopharmaceutics**, 79(1): 95-101, 2011.

PEGORARO, N. S., et al. Nanoencapsulation of coenzyme Q10 and vitamin E acetate protects against UVB radiation-induced skin injury in mice. **Colloids and Surfaces BBiointerfaces**, 150: 32-40, 2017.

PEGORARO, N. S., et al. Improved photostability and cytotoxic effect of coenzyme Q10 by its association with vitamin E acetate in polymeric nanocapsules. **Pharmaceutical Development and Technology**, 23(4): 400-406, 2018.

PEREZ-HERRERO, E. AND A. FERNANDEZ-MEDARDE. Advanced targeted therapies in cancer: Drug nanocarriers, the future of chemotherapy. **European Journal of Pharmaceutics and Biopharmaceutics**, 93: 52-79, 2015.

POON, W., et al. Targeting B16 tumors *in vivo* with peptide-conjugated gold nanoparticles. **Nanotechnology**, 26(28), 2015.

POPLE, P. V. AND K. K. SINGH. Development and evaluation of topical formulation containing solid lipid nanoparticles of vitamin A. **Aaps Pharmscitech**, 7(4), 2006.

POSSER, T., et al. Diphenyl diselenide induces apoptotic cell death and modulates ERK1/2 phosphorylation in human neuroblastoma SH-SY5Y cells. **Archives of Toxicology**, 85(6): 645-651, 2011.

POSSER, T., et al. Diphenyl diselenide confers neuroprotection against hydrigen peroxide toxicity in hippocampal slices. **Brain Research**, 199: 138-147, 2008.

POULSEN, H. E., et al. Role of oxidative DNA damage in cancer initiation and promotion. **European Journal of Cancer Prevention**, 7: 9-16, 1998.

PRADOS, M. D. AND V. LEVIN. Biology and treatment of malignant glioma. **Seminars in Oncology**, 27(3): S1-S10, 2000.

PRAJAPATI, V. D., et al. Pharmaceutical applications of various natural gums, mucilages and their modified forms. **Carbohydrate Polymers**, 92(2): 1685-1699, 2013.

PRIGOL, M., et al. Comparative Excretion and Tissue Distribution of Selenium in Mice and Rats Following Treatment with Diphenyl Diselenide. **Biological Trace Element Research**, 150(1-3): 272-277, 2012.

PRIGOL, M., et al. Diphenyl diselenide induces anxiolytic-like and sedative effects on the chick social separation-stress behavior. **Neuroscience Letters**, 495(2): 140-143, 2011.

PRIGOL, M., et al. *In vitro* metabolism of diphenyl diselenide in rat liver fractions. Conjugation with GSH and binding to thiol groups. **Chemico-Biological Interactions**, 200(2-3): 65-72, 2012.

PRIGOL, M., et al. Physicochemical and Biochemical Profiling of Diphenyl Diselenide. **Applied Biochemistry and Biotechnology**, 169(3): 885-893, 2013.

PRIGOL, M., et al. Convulsant action of diphenyl diselenide in rat pups: measurement and correlation with plasma, liver and brain levels of compound. **Archives of Toxicology**, 84(5): 373-378, 2010.

PRIGOL, M., et al. Convulsant effect of diphenyl diselenide in rats and mice and its relationship to plasma levels. **Toxicology Letters**, 189(1): 35-39, 2009.

PUND, S., et al. Transcutaneous delivery of leflunomide nanoemulgel: Mechanistic investigation into physicomechanical characteristics, *in vitro* anti-psoriatic and antimelanoma activity. **International Journal of Pharmaceutics**, 487(1-2): 148-156, 2015.

REDPATH, M., et al. Ibuprofen and hydrogel-released ibuprofen in the reduction of inflammation-induced migration in melanoma cells. **British Journal of Dermatology**, 161(1): 25-33, 2009.

RESNIER, P., et al. Efficient ferrocifen anticancer drug and Bcl-2 gene therapy using lipid nanocapsules on human melanoma xenograft in mouse. **Pharmacological Research**, 126: 54-65, 2017.

RIGO, L. A., et al. Nanoencapsulation of rice bran oil increases its protective effects against UVB radiation-induced skin injury in mice. **European Journal of Pharmaceutics and Biopharmaceutics**, 93: 11-17, 2015.

RIGON, R. B., et al. Nanotechnology-Based Drug Delivery Systems for Melanoma Antitumoral Therapy: A Review. **Biomed Research International**, 2015.

ROBERTS, M. S., et al. Topical and cutaneous delivery using nanosystems. **Journal of Controlled Release**, 247: 86-105, 2017.

ROCHA, J. T., et al. Effects of diphenyl diselenide on depressive-like behavior in ovariectomized mice sumitted to subchronic stress : involvement of the serotonergic systems. **Psychopharmacology**, 222: 709-719, 2012.

ROSA, R. M., et al. Pro-oxidant action of diphenyl diselenide in the yeast Saccharomyces cerevisiae exposed to ROS-generating conditions. **Life Sciences**, 77(19): 2398-2411, 2005.

ROSA, R. M., et al. Cytotoxic, genotoxic, and mutagenic effects of diphenyl diselenide in Chinese hamster lung fibroblasts. **Mutation Research-Genetic Toxicology and Environmental Mutagenesis**, 628(2): 87-98, 2007.

ROSA, R. M., et al. Pharmacology and toxicology of diphenyl diselenide in several biological models. **Brazilian Journal of Medical and Biological Research**, 40(10): 1287-1304, 2007.

ROSSETI, I. B., et al. Diphenyl diselenide (PhSe)(2) inhibits biofilm formation by Candida albicans, increasing both ROS production and membrane permeability. **Journal of Trace Elements in Medicine and Biology**, 29: 289-295, 2015.

RUEL-GARIEPY, E., et al. A thermosensitive chitosan-based hydrogel for the local delivery of paclitaxel. **European Journal of Pharmaceutics and Biopharmaceutics**, 57(1): 53-63, 2004.

SANMARTIN, C., et al. Selenium compounds and apoptotic modulation: A new perspective in cancer therapy. **Mini-Reviews in Medicinal Chemistry**, 8(10): 1020-1031, 2008.

SANTOS, S. S., et al. Clotrimazole-loaded Eudragit® RS100 nanocapsules: Preparation, characterization and *in vitro* evaluation of antifungal activity against Candida species. **Materials Science and Engineering: C**, 33(3): 1389-1394, 2013.

SANTOS, S. S., et al. Formulation and *in vitro* evaluation of coconut oil-core cationic nanocapsules intended for vaginal delivery of clotrimazole. **Colloids and Surfaces B: Biointerfaces**, 116: 270-276, 2014.

SARI, M. H. M., et al. p,p'-Methoxyl-diphenyl diselenide-loaded polymeric nanocapsules are chemically stable and do not induce toxicity in mice. **European Journal of Pharmaceutics and Biopharmaceutics**, 117: 39-48, 2017.

SAVEGNAGO, L., et al. Diphenyl diselenide exerts antidepressant-like and anxiolyticlike effects in mice: Involvement of L-arginine-nitric oxide-soluble guanylate cyclase pathway in its antidepressant-like action. **Pharmacology Biochemistry and Behavior**, 88(4): 418-426, 2008.

SAVEGNAGO, L., et al. Mechanisms involved in the antinociceptive effect caused by diphenyl diselenide in the formalin test. **Journal of Pharmacy and Pharmacology**, 60(12): 1679-1686, 2008.

SAVEGNAGO, L., et al. Antisecretory and antiulcer effects of diphenyl diselenide. **Environmental Toxicology and Pharmacology**, 21(1): 86-92, 2006.

SCHAFFAZICK, S. R., et al. CARACTERIZAÇÃO E ESTABILIDADE FÍSICOQUÍMICA DE SISTEMAS POLIMÉRICOS NANOPARTICULADOS PARA ADMINISTRAÇÃO DE FÁRMACOS. **Química Nova**, 26(5): 726-737, 2003.

SCHREIBER, S., et al. Immunotherapy of metastatic malignant melanoma by a vaccine consisting of autologous interleukin 2 transfected cancer cells: Outcome of a phase I study. **Human Gene Therapy**, 10(6): 983-993, 1999.

SHAH, K. A., et al. Solid lipid nanoparticles (SLN) of tretinoin: Potential in topical delivery. **International Journal of Pharmaceutics**, 345(1-2): 163-171, 2007.

SHI, J. J., et al. Nanotechnology in Drug Delivery and Tissue Engineering: From Discovery to Applications. **Nano Letters**, 10(9): 3223-3230, 2010.

SHI, S. J., et al. Dual drugs (microRNA-34a and paclitaxel)-loaded functional solid lipid nanoparticles for synergistic cancer cell suppression. **Journal of Controlled Release**, 194: 228-237, 2014.

SIEGEL, R. L., et al. Cancer Statistics, 2018. **Ca-a Cancer Journal for Clinicians**, 68(1): 7-30, 2018.

SINGH, S., et al. Towards therapeutic advances in melanoma management: An overview. **Life Sciences**, 174: 50-58, 2017.

SISTI, A., et al. Topical treatment of melanoma skin metastases with Imiquimod: a review. **Dermatology Online Journal**, 21(2): 1-9, 2015.

STEFANELLO, S. T., et al. Free radical scavenging *in vitro* and biological activity of diphenyl diselenide-loaded nanocapsules: DPDS-NCS antioxidant and toxicological effects. **International Journal of Nanomedicine**, 10, 2015.

STEIN, G. S. AND A. B. PARDEE. Cell Cycle and Growth Control: Biomolecular Regulation and Cancer. **Springer**, 2004.

TAKEI, T., et al. Injectable and biodegradable sugar beet pectin/gelatin hydrogels for biomedical applications. **Journal of Biomaterials Science-Polymer Edition**, 24(11): 1333-1342, 2013.

VERMA, P., et al. Development,*in vitro*and*in vivo*characterization of Eudragit RL 100 nanoparticles for improved ocular bioavailability of acetazolamide. **Drug Delivery**, 20(7): 269-276, 2013.

WANG, S. Q., et al. Ultraviolet A and melanoma: A review. **Journal of the American Academy of Dermatology**, 44(5): 837-846, 2001.

WANG, X. B., et al. Current status and future perspectives of sonodynamic therapy in glioma treatment. **Ultrasonics Sonochemistry**, 37: 592-599, 2017.

WEBER, J., et al. Association of Borage Oil and Betamethasone Dipropionate in LipidCore Nanocapsules: Characterization, Photostability and *In vitro* Irritation Test. **Journal of Nanoscience and Nanotechnology**, 16(2): 1354-1362, 2016.

WILHELM, E. A., et al. Evidence of the involvement of K plus channels and PPAR gamma receptors in the antidepressant-like activity of diphenyl diselenide in mice. **Journal of Pharmacy and Pharmacology**, 62(9): 1121-1127, 2010.

YANG, L., et al. Hyaluronic acid/chitosan nanoparticles for delivery of curcuminoid and its *in vitro* evaluation in glioma cells. **International Journal of Biological Macromolecules**, 72: 1391-1401, 2015.

YILDIRIMER, L., et al. Toxicological considerations of clinically applicable nanoparticles. **Nano Today**, 6(6): 585-607, 2011.

YOO, J.-W., et al. pH-sensitive Eudragit nanoparticles for mucosal drug delivery. **International Journal of Pharmaceutics**, 403(1-2): 262-267, 2011.

ZASSO, F. B., et al. On the mechanisms involved in antinociception induced by diphenyl diselenide. **Environmental Toxicology and Pharmacology**, 19(2): 283-289, 2005.

ANEXOS

8. Anexos

ANEXO A: Carta de aprovação do projeto de pesquisa pela Comissão de Ética em Pesquisa – Plataforma Brasil para a realização do experimento de permeação cutânea do **manuscrito 1.**

UNIVERSIDADE FEDERAL DE SANTA MARIA/ PRÓ-REITORIA DE PÓS-GRADUAÇÃO E

PARECER CONSUBSTANCIADO DO CEP

DADOS DO PROJETO DE PESQUISA

Título da Pesquisa: DESENVOLVIMENTO DE FORMULAÇÕES SEMISSÓLIDAS DE BASE NANOTECNOLÓGICA PARA AUMENTO DA PERMEAÇÃO CUTÂNEA DE ATIVOS ANTITUMORAIS E ANTI-INFLAMATÓRIOS

Pesquisador: Letícia Cruz

Área Temática:

Versão: 2

CAAE: 55220016.3.0000.5346

Instituição Proponente: Universidade Federal de Santa Maria/ Pró-Reitoria de Pós-Graduação e

Patrocinador Principal: Financiamento Próprio

DADOS DO PARECER

Número do Parecer: 1.632.595

Apresentação do Projeto:

É um projeto de doutorado sobre o desenvolvimento de formulações semissólidas de base nanotecnológica para aplicação tópica de diferentes ativos, tanto de origem natural como sintética, com potencialidades antitumorais e anti-inflamatórias, para o tratamento de desordens da pele, sendo delineado no sentido de preparar e caracterizar os sistemas nanoestruturados contendo ativos de origem natural e sintética, visando a aplicação tópica. Além disso, pretende-se estudar o perfil de permeação/retenção cutânea dos fármacos empregando pele humana a qual tem sido selecionada como membrana biológica em diversos trabalhos na tentativa de predizer o comportamento da formulação in vivo. Serão utilizadas as moléculas ativas silibinina, indol-3-carbinol, di-indol metano, ubiquinona, cetoprofeno, disselento de difenila e disseleneto (PhSe)2 de p,p'-metoxiladifenila(p-OMePhSe)2, selecionadas devido as suas potencialidades antitumoral e anti-inflamatória sobre a pele. Cabe mencionar, que esta via de administração de fármacos é de fácil aplicação, agradável para o paciente e favorece a efetiva adesão ao tratamento. Desta forma, as formulações de base nanotecnológica que se pretende desenvolver podem ser alternativas terapêuticas ou profiláticas importantes para o manejo dos principais tipos de tumores de pele e de lesões inflamatórias relacionadas. As peles para o experimento serão doadas pelo Médico Cirurgião Plástico Celso André de Souza (CRM 21896).

Endereço: Av. Roraima, 1000 - prédio da Reitoria - 2° andar
Bairro: Camobi **CEP:** 97.105-970
UF: RS **Município:** SANTA MARIA
Telefone: (55)3220-9362 **E-mail:** cep.ufsm@gmail.com

SANTA MARIA, 12 de Julho de 2016

Assinado por:
CLAUDEMIR DE QUADROS
(Coordenador)

Endereço: Av. Roraima, 1000 - prédio da Reitoria - 2° andar
Bairro: Camobi **CEP:** 97.105-970
UF: RS **Município:** SANTA MARIA
Telefone: (55)3220-9362 **E-mail:** cep.ufsm@gmail.com

ANEXO B: Carta de aprovação do projeto de pesquisa pela Comissão de Ética no Uso de Animais da Universidade Federal de Santa Maria (UFSM) para a realização dos experimentos em peixe-zebra do **manuscrito 2.**

Comissão de Ética no Uso de Animais
da
Universidade Federal de Santa Maria

CERTIFICADO

Certificamos que a proposta intitulada "Avaliação da exposição aguda as nanocápsulas contendo disseleneto de difenila sobre efeitos comportamentais e bioquímicos em peixe zebra (Danio rerio)", protocolada sob o CEUA nº 2301271116, sob a responsabilidade de **Letícia Cruz** *e equipe; Luana Mota Ferreira; Charlene Menezes; Cristina Wayne Nogueira; Denis Broock Rosemberg; Luíz Vinícius Costa da Rosa; Marcel Henrique Marcondes Sari; Talise Ellwanger Müller* - que envolve a produção, manutenção e/ou utilização de animais pertencentes ao filo Chordata, subfilo Vertebrata (exceto o homem), para fins de pesquisa científica ou ensino - está de acordo com os preceitos da Lei 11.794 de 8 de outubro de 2008, com o Decreto 6.899 de 15 de julho de 2009, bem como com as normas editadas pelo Conselho Nacional de Controle da Experimentação Animal (CONCEA), e foi **aprovada** pela Comissão de Ética no Uso de Animais da Universidade Federal de Santa Maria (CEUA/UFSM) na reunião de 19/01/2017.

We certify that the proposal "Acute exposure evaluation to diphenyl diselenete nanocapsules on behavioral and biochemical effects in zebrafish (Danio rerio)", utilizing 384 Fishes (males and females), protocol number CEUA 2301271116, under the responsibility of **Letícia Cruz** *and team; Luana Mota Ferreira; Charlene Menezes; Cristina Wayne Nogueira; Denis Broock Rosemberg; Luíz Vinícius Costa da Rosa; Marcel Henrique Marcondes Sari; Talise Ellwanger Müller* - which involves the production, maintenance and/or use of animals belonging to the phylum Chordata, subphylum Vertebrata (except human beings), for scientific research purposes or teaching - is in accordance with Law 11.794 of October 8, 2008, Decree 6899 of July 15, 2009, as well as with the rules issued by the National Council for Control of Animal Experimentation (CONCEA), and was **approved** by the Ethic Committee on Animal Use of the Federal University of Santa Maria (CEUA/UFSM) in the meeting of 01/19/2017.

Finalidade da Proposta: Pesquisa (Acadêmica)

Vigência da Proposta: de 01/2017 a 12/2108 Área: Farmácia Industrial

Origem:	Não aplicável biotério						
Espécie:	Peixes	sexo:	Machos e Fêmeas	idade:	60 a 60 dias	N:	384
Linhagem:	Peixe Zebra (Danio rerio)			Peso:	04 a 06 g		

Resumo: O disseleneto de difenila é um composto orgânico de selênio conhecido por suas diversas atividades farmacológicas já relatadas. No entanto, o disseleneto de difenila apresenta efeitos tóxicos, por oxidar grupos tióis, e elevada lipofilia, o que limita sua biodisponibilidade oral e dificulta o preparo de soluções de uso parenteral. Diante das limitações relatadas para o uso do disseleneto de difenila na terapêutica, torna-se relevante a pesquisa por novas formulações para a administração deste composto, uma vez que o mesmo apresenta-se como um forte candidato a fármaco pela sua potencialidade farmacológica. Nesse sentido, nanocápsulas poliméricas são uma alternativa promissora para a administração do composto. Esses sistemas apresentam tamanho na faixa nanométrica e são capazes de reduzir efeitos tóxicos, melhorar a atividade biológica, proteger compostos lábeis da degradação e modificar o perfil de liberação e consequentemente aumentar a biodisponibilidade. Dessa forma, levando em consideração que o peixe zebra (Danio rerio) é um modelo experimental de baixo custo e apresenta sistema nervoso central funcionalmente semelhante ao humano, o objetivo deste projeto é avaliar o efeito da exposição aguda de nanocápsulas poliméricas contendo disseleneto de difenila sobre efeitos neurotóxicos e bioquímicos nos animais em questão. Tais efeitos serão estudados através da avaliação de parâmetros motores e não motores do tipo ansiedade, além de dosagens bioquímicas no cérebro dos animais.

Local do experimento: Os animais serão mantidos no Biotério de experimentação do Laboratório de Fisiologia de Peixes (LAFIPE) ▯ UFSM ▯ CCS ▯ Departamento de Farmacologia e Fisiologia, durante os períodos de aclimatação e experimentação, cujos responsáveis são os professores Dr. Bernardo Baldisserotto e Vania Lucia Loro.

Santa Maria, 19 de janeiro de 2017

Avenida Roraima, 1000, Reitoria, 2º andar - CEP 97105-900 Santa Maria, RS - tel: 55 (55) 3220-9362 / fax:
Horário de atendimento: das 8:30 ás 12h e 14h ás 17hs : e-mail: ceua.ufsm@gmail.com
CEUA N 2301271116

Comissão de Ética no Uso de Animais
da
Universidade Federal de Santa Maria

Profa. Dra. Daniela Bitencourt Rosa Leal
Coordenadora da Comissão de Ética no Uso de Animais
Universidade Federal de Santa Maria

Prof. Dr. Denis Broock Rosemberg
Vice-Coordenador da Comissão de Ética no Uso de Animais
Universidade Federal de Santa Maria

Avenida Roraima, 1000, Reitoria, 2º andar - CEP 97105-900 Santa Maria, RS - tel: 55 (55) 3220-9362 / fax:
Horário de atendimento: das 8:30 ás 12h e 14h ás 17hs : e-mail: ceua.ufsm@gmail.com
CEUA N 2301271116

ANEXO C: Carta de aprovação do projeto de pesquisa pela Comissão de Ética no Uso de Animais da Universidade Federal de Santa Maria (UFSM) para a realização dos experimentos de toxicidade m ratos do **manuscrito 3.**

Comissão de Ética no Uso de Animais
da
Universidade Federal de Santa Maria

CERTIFICADO

Certificamos que a proposta intitulada "Avaliação da influência da via de administração na distribuição tecidual e nos efeitos toxicológicos de nanocápsulas de poli-?-caprolactona contendo polietilenoglicol para incorporação de disseleneto de difenila", protocolada sob o CEUA nº 2171170217, sob a responsabilidade de **Letícia Cruz** *e equipe; Luana Mota Ferreira; Cristina Wayne Nogueira; Marcel Henrique Marcondes Sari; Sydney Hartz Alves* - que envolve a produção, manutenção e/ou utilização de animais pertencentes ao filo Chordata, subfilo Vertebrata (exceto o homem), para fins de pesquisa científica ou ensino - está de acordo com os preceitos da Lei 11.794 de 8 de outubro de 2008, com o Decreto 6.899 de 15 de julho de 2009, bem como com as normas editadas pelo Conselho Nacional de Controle da Experimentação Animal (CONCEA), e foi **aprovada** pela Comissão de Ética no Uso de Animais da Universidade Federal de Santa Maria (CEUA/UFSM) na reunião de 27/04/2017.

We certify that the proposal "Evaluation of the administration route influence on the tissue distribution and toxicological effects of poly-?-caprolactone nanocapsules containing polyethyleneglycol for the diphenyl diselenide incorporation", utilizing 60 Heterogenics rats (60 males), protocol number CEUA 2171170217, under the responsibility of **Letícia Cruz** *and team; Luana Mota Ferreira; Cristina Wayne Nogueira; Marcel Henrique Marcondes Sari; Sydney Hartz Alves* - which involves the production, maintenance and/or use of animals belonging to the phylum Chordata, subphylum Vertebrata (except human beings), for scientific research purposes or teaching - is in accordance with Law 11.794 of October 8, 2008, Decree 6899 of July 15, 2009, as well as with the rules issued by the National Council for Control of Animal Experimentation (CONCEA), and was **approved** by the Ethic Committee on Animal Use of the Federal University of Santa Maria (CEUA/UFSM) in the meeting of 04/27/2017.

Finalidade da Proposta: Pesquisa (Acadêmica)

Vigência da Proposta: de 04/2017 a 12/2017 Área: Farmácia Industrial

Origem:	Biotério Central UFSM						
Espécie:	Ratos heterogênicos	sexo:	Machos	idade:	60 a 60 dias	N:	60
Linhagem:	Wistar			Peso:	250 a 300 g		

Resumo: Esse projeto propõe estudar a influência das vias de administração intragástrica e intraperitoneal na biodistribuição tecidual e nos efeitos tóxicos do disseleneto de difenila incorporado as nanocápsulas poliméricas revestidas polietilenoglicol. Para tanto, será realizado um protocolo de administração repetida, pelo período de 15 dias e, após o tratamento, os animais serão eutanasiados e então será estimada a biodistribuição tecidual da molécula ou seus metabólitos através da quantificação do átomo de selênio presente em diferentes amostras como gordura, rim, pulmão, fígado, cérebro, eritrócitos, urina e fezes. A quantificação do Selênio será feita por espectroscopia de plasma simultâneo. Além disso, baseado no fato de que a via de administração e o veículo de administração pode modificar o perfil toxicológico, também serão avaliados parâmetros referentes ao balanço oxidativo, hemograma completo e marcadores de dano renal e hepático.

Local do experimento: Os experimentos serão realizados no Laboratório de Síntese, Reatividade e Avaliação Farmacológica e Toxicológica de Organocalcogênios sob orientação da Professora Doutora Cristina W. Nogueira.

Santa Maria, 21 de julho de 2018

Prof. Dr. Denis Broock Rosemberg
Coordenador da Comissão de Ética no Uso de Animais
Universidade Federal de Santa Maria

Prof. Dr. Saulo Tadeu Lemos Pinto Filho
Vice-Coordenador da Comissão de Ética no Uso de Animais
Universidade Federal de Santa Maria

Avenida Roraima, 1000, Reitoria, 2º andar - CEP 97105-900 Santa Maria, RS - tel: 55 (55) 3220-9362 / fax:
Horário de atendimento: das 8:30 ás 12h e 14h ás 17hs : e-mail: ceua.ufsm@gmail.com
CEUA N 2171170217

ANEXO D: Carta de aprovação do projeto de pesquisa pela Comissão de Ética no Uso de Animais da Universidade Federal de Pelotas (UFPel) para a realização dos experimentos do modelos pré-clínico de glioblastoma do **manuscrito 3.**

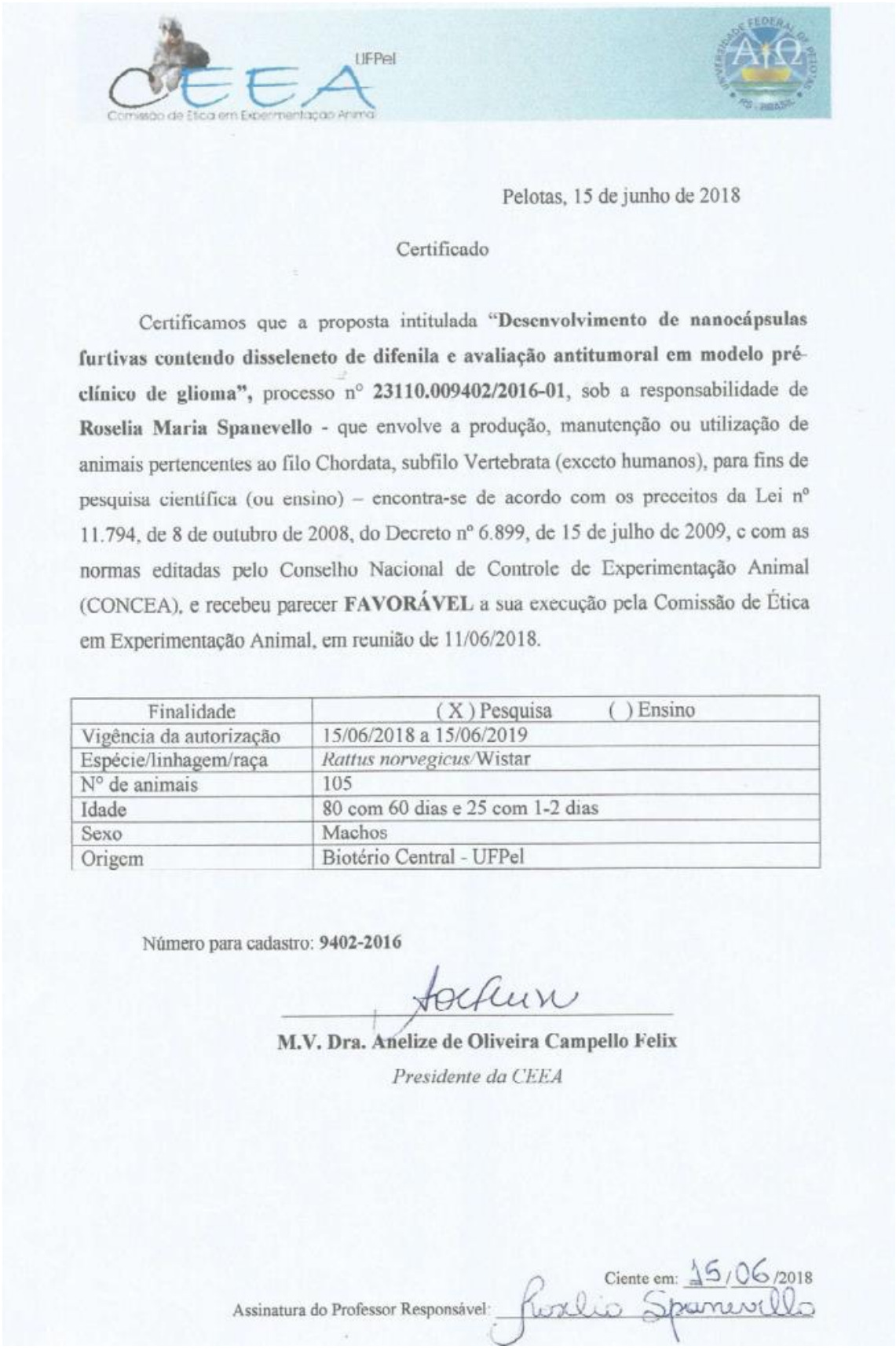

UFPel
CEEA
Comissão de Ética em Experimentação Animal

Pelotas, 15 de junho de 2018

Certificado

Certificamos que a proposta intitulada "**Desenvolvimento de nanocápsulas furtivas contendo disseleneto de difenila e avaliação antitumoral em modelo pré-clínico de glioma",** processo nº **23110.009402/2016-01**, sob a responsabilidade de **Roselia Maria Spanevello** - que envolve a produção, manutenção ou utilização de animais pertencentes ao filo Chordata, subfilo Vertebrata (exceto humanos), para fins de pesquisa científica (ou ensino) – encontra-se de acordo com os preceitos da Lei nº 11.794, de 8 de outubro de 2008, do Decreto nº 6.899, de 15 de julho de 2009, e com as normas editadas pelo Conselho Nacional de Controle de Experimentação Animal (CONCEA), e recebeu parecer **FAVORÁVEL** a sua execução pela Comissão de Ética em Experimentação Animal, em reunião de 11/06/2018.

Finalidade	(X) Pesquisa ( ) Ensino
Vigência da autorização	15/06/2018 a 15/06/2019
Espécie/linhagem/raça	*Rattus norvegicus*/Wistar
N° de animais	105
Idade	80 com 60 dias e 25 com 1-2 dias
Sexo	Machos
Origem	Biotério Central - UFPel

Número para cadastro: **9402-2016**

M.V. Dra. Anelize de Oliveira Campello Felix
Presidente da CEEA

Ciente em: 15/06/2018
Assinatura do Professor Responsável: Roselia Spanevello

ANEXO E: Autorização para reprodução do artigo científico “Diphenyl diselenide loaded poly(ε-caprolactone) nanocapsules with selective antimelanoma activity: Development and cytotoxic evaluation” publicado na Materials Science and Engineering C, volume 91, páginas 1-9, 2018.